Acta Montanistica Slovaca
ISSN 1335-1788
actamont.tuke.sk

Contents

Aleksei LIPANOV, Andrei LESCHEV, Pavel OVCHARENKO, Daynier Rolando DELGADO SOBRINO, Lyudmila KOLESNIKOVA and **Konstantin STERKHOV:** Selection of optimal modes of obtaining broad fractions of light hydrocarbons from oil-associated gas at oil production sites **1**

Vladislav SVIATSKII, Witold BIALY, Kirill SENTYAKOV and **Alexandr REPKO:** Estimation of Quality Indicators of Ecological Thermoplastic Fiber Materials **14**

Michał SIEGMUND, Dominik BAŁAGA, Dagmar JANÁČOVÁ and **Marek KALITA:** Comparison of spraying nozzles operational parameters of different design **24**

Maryna KYSLYTSYNA, Pavel RASCHMAN, Ľuboš POPOVIČ and **Gabriel SUČIK:** Kinetic analysis of the dissolution of natural magnesite in nitric acid **35**

Marinko ŠKARE, Daniel TOMIĆ and **Saša STJEPANOVIĆ:** Energy Consumption and Green GDP in Europe: A Panel Cointegration Analysis 2008 - 2016 **46**

Sarfaraz A. BHUTTO, Rizwan Raheem AHMED, Dalia STREIMIKIENE, Saifullah SHAIKH and **Justas STREIMIKIS:** Portfolio Investment diversification at Global stock market: A Cointegration Analysis of Emerging BRICS(P) Group **57**

Alexey KHORESHOK, Kirill ANANIEV, Alexander ERMAKOV, Dilshad KUZIEV and **Alexander BABARYKIN:** Determination of the Rational Number of Cutters on the Outer Cutting Drums of Geokhod **70**

Łukasz BOŁOZ: Interpretation of the results of mechanical rock properties testing with respect to mining methods **81**

Grzegorz STOPKA: Laboratory research on the influence of selected technological parameters on cutting forces during hard rock mining with asymmetric disc tools **94**

Lucia BEDNÁROVÁ, Jana DŽUKOVÁ, Roland GROSOŠ, Marián GOMORY and **Miloš PETRÁŠ:** Legislative instruments and their use in the management of raw materials in the Slovak Republic **105**

Csaba SIDOR, Branislav KRŠÁK, Ľubomír ŠTRBA, Ján GAJDOŠ, Adriana ŠEBEŠOVÁ and **Jana KOLAČKOVSKÁ:** Examples of secondary online data for raising awareness about geo and mining heritage **116**

Miroslav LAŠŠÁK, Katarína DRAGANOVÁ, Monika BLIŠŤANOVÁ, Gabriel KALAPOŠ and **Juraj MIKLOŠ:** Small UAV Camera Gimbal Stabilization Using Digital Filters and Enhanced Control Algorithms for Aerial Survey and Monitoring **127**

Acta Montanistica Slovaca
ISSN 1335-1788
actamont.tuke.sk

Selection of optimal modes of obtaining broad fractions of light hydrocarbons from oil-associated gas at oil production sites

Aleksei LIPANOV[1], Andrei LESCHEV[2], Pavel OVCHARENKO[2], Daynier Rolando DELGADO SOBRINO[3*], Lyudmila KOLESNIKOVA[4] *and* ***Konstantin STERKHOV[4]***

Authors' affiliations and addresses:
[1] Keldysh Institute of Applied Mathematics, Russian Academy of Sciences (RAS), Russia, Moscow, Miusskaya Sq., 4,
e-mail: aml35@yandex.ru

[2] Udmurt Federal Research Center, UrD, RAS, Russia, Udmurt Republic, Izhevsk, T. Baramzina St., 34,
e-mail: l130758@yandex.ru
e-mail: ovcpg@yandex.ru

[3]Institute of Production Technologies, Faculty of Materials Science and Technology in Trnava, Slovak University of Technology in Bratislava, Jána Bottu 25, 917 24, Slovakia
tel: + 421 908 674 132,
e-mail: daynier_sobrino@stuba.sk

[4] Kalashnikov Izhevsk State Technical University, Russia, Udmurt Republic, Izhevsk, Studencheskaya St., 7
e-mail: klusian@yandex.ru
e-mail: skvdw@mail.ru

***Correspondence:**
Daynier Rolando DELGADO SOBRINO, Institute of Production Technologies, Faculty of Materials Science and Technology in Trnava, Slovak University of Technology in Bratislava, Jána Bottu 25, 917 24, Slovakia
tel: + 421 908 674 132
e-mail: daynier_sobrino@stuba.sk

How to cite this article:
Lipanov, A., Leschev, A., Ovcharenko, P., Delgado Sobrino, D.R., Kolesnikova, L. and Sterkhov, K. (2020). Selection of optimal modes of obtaining broad fractions of light hydrocarbons from oil-associated gas at oil production sites. *Acta Montanistica Slovaca*, Volume 25 (1), 1-13

DOI:
https://doi.org/10.46544/AMS.v25i1.1

Abstract
Decreasing pollution and increasing oil fields profitability are key goals of the proper extraction of hydrocarbons from oil-associated gas (OAG). Despite the potential of a proper OAG utilization, oil companies often struggle with an increase in the overall gas cost and possible unprofitability of its treatment though conventional methods (Igitkhanyan et al., 2014). These cost-related issues have been mentioned before by authors like Braginskii and Chernavskiito (2011) and Arutyunov et al. (2017). This paper introduces a novel method for OAG separation and the subsequent obtention of the Broad Fraction of Light Hydrocarbons (BFLH) that relies on compression followed by the cooling. The proposal is implemented on a mobile laboratory unit developed to define power expenditures and optimize the modes of obtaining broad fractions of hydrocarbons from OAG at oil fields with low gas factor and caloricity due to high nitrogen content. The experiments of the paper contributed validating the proposed method and the mobile unit, and this, among others, by determining optimal modes for the obtention of the BFLH from AOG with different initial compositions of hydrocarbons components and harmful admixtures, and also by determining concrete values for the dependence of the OAG compression pressure on temperature.

Keywords
Oil-associated gas, compression, broad fractions, light hydrocarbons, mobile laboratory unit, oil fields

Introduction and Background Information

During the process of extraction, delivery and processing of oil, the OAG is produced. The OAG is a natural hydrocarbon gas diluted in oil or being in the "caps" of oil and gas-condensate fields. The amount of OAG in one ton of oil can vary from one, two up to several thousand cubic meters (Semenova et al., 2016; Ivanova et al., 2018). In contrast to natural gas, OAG contains, apart from methane and ethane, a large share of propane, butane and heavier hydrocarbons (RIA Novosti). One of the main and subsequent procedures of OAG utilization lies on its splitting into separate components. This treatment process allows obtaining dry stripped gas and a broad fraction of light hydrocarbons (BFLH). This BFLH can be further used as raw material for petrochemical productions, as ecologically pure fuel for heating, used in the same oil preparation process chain right at the oil filed, and there are even recent studies analyzing its theoretical use for power generation in gas-piston engines thus significantly decreasing its flaring (Arutyunov et al., 2020).

World volumes of OAG extracted together with oil are rather significant (Baranov et al., 2017). Half a century ago OAG was just burnt at flare facilities, thus doing significant harm to ecology and this because when burning OAG, carbon dioxide and active soot are released into the atmosphere. Today, however, even where there are still other pollution problems associated to oil and gas production, see Atoufi and Lampert (2020), this associated product of oil extraction, i.e. OAG, is more frequently caught and used, among others, for heating technical premises and producing electrical power. This is an approach that allows industrial enterprises to solve their own power problems without needing power supply from outside what in many cases leads to cost savings if the gas is obtained efficiently and properly (Škvareková et al., 2019). Besides, OAG is also a valuable raw material for the chemical industry. This altogether allows, not only to qualitatively utilize OAG preserving the ecology but also to obtain profit from it in petrochemistry.

Over the last years, the main problem of OAG has been widely discussed all over the globe, including Russia. In Russia, especially after the governmental decrees on increasing the payment for limit-excessing burning of OAG came into effect and after the activation of investment programs of oil-and-gas companies, the qualitative changes in this sphere have started to occur. Thus, the recent and expected production growth of light hydrocarbon raw material in Russia for further use in the petrochemical industry is directly connected with OAG processing growth (Kiryushin et al., 2013).

Oil-associated gas can be both a valuable and dangerous associated component during oil extraction. Usually, there is no constant ratio of OAG components, and thus there can be a completely different proportion of OAG components at different oil fields. The OAG contains the following components: methane (CH4), ethane (C2H6), propane (C3H8), butane (C4H10), pentane (C5H12), hexane (C6H14), carbon dioxide (CO2), nitrogen (N2), oxygen (O2) and hydrogen sulfide (H2S) (GOST R 55598), Kuppusamy et al. (2020). These components can be conventionally divided into **foamy** – hydrocarbons (methane, ethane, propane, butane, pentane, hexane), **inert** (hydrogen, carbon dioxide), and **harmful or dangerous** – hydrogen sulfide, carbon dioxide. The content of hydrocarbons at different oil fields varies in a very broad range. Thus, at some oil fields OAG can contain over 80% of hydrocarbons, while at others, usually old ones, the content of hydrocarbons does not exceed 6 or 7 % (Speight, 2012; Kayukova et al., 2009).

Generally, OAG extracted from wells is unstable by its component composition and volume. As mentioned, at different oil fields usually OAG with different compositions will be extracted. Even in fields located close to each other, the OAG composition can significantly differ. Besides, the gas composition also changes with the field depletion. In this particular case, inert components, such as, first of all, nitrogen, prevail in the OAG composition. Similarly, the volume of extracted OAG depends on the good recovery given that with the increase in the oil field operation time, both the oil and OAG volume extraction usually goes down. In turn, OAG hydrocarbons can be divided as follows:

- gas – components of group C1, C2 (methane, ethane) being only in a gaseous state under the conditions close to atmospheric ones (pressure and temperature). They are slightly diluted in liquids;
- unstable components of group C3, C4 (propane, butane) – gases, become liquids at low temperature or under elevated pressure (1.6 MPa);
- and stable C5, C6 (pentane, hexane).

Gas components are distinguished by the fact that they are converted into the liquid state at very low temperatures or under very high pressures. Unstable hydrocarbons can be in a gaseous state at normal temperature, and in a liquid state under the pressure of 0.16 MPa. On the other hand, stable hydrocarbons are liquids.

As for the use of the gases, these can be used only either at the extraction site or transported by a gas pipeline transport which has been preliminarily prepared, i.e. dried and purified. On the other hand, in liquid state OAG components can be used either on-site or transported by automobile transport. Components in a liquid state can be used as:

- solvents when repairing wells;

- fuels at oil fields and with insufficient amount of own OAG;
- to return pentane-hexane group into marketable oil.

At the oil fields in the operation of the Russian Udmurt Republic, the extracted oil is characterized by the low gas factor ranging from 4.5 to 35 m^3/t. Besides, OAG here contains a lot of nitrogen – from 30 up to 90%, and consequently, it has low caloricity – from 1200 up to 6600 kcal/m^3. Also, at the majority of oil fields in the area OAG contains a significant amount of hydrogen sulfide 0.2 – 0.5% (up to 2%) by volume, and, consequently, OAG is practically useless for domestic purposes.

The OAG complexity lies on more careful preparation in contrast to the natural gas. The preparation comprises its separation from heavier hydrocarbons and water. During the phases of transportation and use in pipelines, these components can be condensed and form liquid plugs, and also clogs that leads to damage in the gas equipment (Rafa et al., 2014). The OAG can be transported only by pipeline transport or by its compression. In both cases, it is a quite expensive process. Therefore, while working with small volumes of OAG, it is advisable to use it only for technological purposes at oil fields for oil preparation, namely, for its heating.

One of the main tasks and ways for decreasing environmental pollution and increasing the profitability of oil fields is precisely the extraction of unstable and stable hydrocarbons from OAG. In this case, the liquid fraction can be obtained, which can be transported by mobile means of transportation.

All the existing methods of OAG processing can be split into three main groups: physic-energy; thermal-chemical and chemical-catalytic. In this regard, three main technologies have been developed based on these methods: cryogenic technologies (low-temperature separation, condensation, rectification); membrane technology and adsorption technology (Vorobiev et al., 2018). Despite the existence of these well-known methods, in the actual practice of oil fields, only some methods of OAG processing are applied. The main and most used method is usually OAG utilization by its separation into components. This process allows obtaining dry stripped gas which, by its essence, is the same natural gas and also the BFLH. The BFLH can be further used, for example, as raw material for petrochemical productions.

It is well-known in the states of the art and practice, see for example Igitkhanyan et al. (2014) that the most suitable and effective approach of OAG utilization is its treatment at the same gas processing plants. This is explained by the fact that for faraway oil fields, OAG transportation to such utilization plants is very costly, and, in some cases, is either complicated or even impossible from the technical side. In such cases, it is advisable to realize the OAG processing at the same oil fields, which is by far a more profitable option, especially for those cases where the oil field operation time or its life cycle are quite limited.

However, the real difficulties arise when implementing any possible utilization method for the later use OAG for manufacturing or commercial purposes, which are conditioned by the features of this type of raw material, and this, as it is necessary to perform the whole set of works for OAG preparation, i.e. removal of mechanical admixtures and drying, and stripping, desulfurization, laying gas pipelines to distant oil fields, see Karch et al. (2018), construction of gas collecting facilities to just cite the most important ones.

In each particular case, the types and volume of works differ, since they are defined by the same OAG features, distances and conditions of transportation and ultimately by the requirements of the gas consumer. In any case, the fulfilment of any volume of such preparatory measures results in oil gas cost increase and possible unprofitability of OAG treatment for oil companies (Bako and Božek, 2016), what at the end also leads to further negative impact for the environment and a lost chance for the involved companies in the generation of some extra profits.

In this regard and as mentioned above, from the perspective of economic feasibility, it is preferable to treat OAG directly at the oil field obtaining the liquid fraction (BFLH), as liquid BFLH is more convenient and cost-effective to transport to chemical enterprises and besides, it can be more effectively used for own purposes as producing heat or electric power, and this because the BFLH has higher caloric value than oil-associated gas (Mullakhmetova et al., 2015).

Based on all described background information, problematic issues and gaps in the states of the art and practice, the present paper introduces a small-sized mobile laboratory unit “LURPNG” for obtaining the BFLH from OAG. The unit has been developed and produced by Izhevsk specialists from UdmFRC UrD RAS together with teachers and students of Kalashnikov Izhevsk State Technical University under the supervision of Academician of RAS, Doctor of Science in Engineering, Prof. A.M. Lipanov. The main goals behind the design and development of this unit have been: 1) to offer the possibility of experimental determination of the BFLH obtention from OAG on certain oil fields and 2) to provide a more flexible BFLH obtention by being able to transport the proposed unit by a wide scale of means of transportation, especially to those oil fields located far from the main transport arteries. The solution of the problem set up addressed with the proposed unit and within the paper is topical for distant oil fields with a low rate, which besides lack gas pipeline systems, thus, the OAG is utilized by burning.

Material and Methods

A synthesized description of the proposed laboratory unit for oil-associated gas separation "LURPNG"

The Laboratory unit "LURPNG" is intended for defining power losses and optimizing the modes for obtaining the BFLH from OAG at oil fields with low gas factor and low caloricity due to high nitrogen content, see Fig. 1.

Fig. 1. Laboratory unit for OAG separation "LURPNG. Source: Self-elaboration.

In the particular case of the proposed unit, the compression method of gas mixture separation is used to obtain the BFLH from the OAG (Zaitsev et al., 2017). This laboratory unit is equipped with a refrigeration machine, which allows significantly lowering the costs for the BFLH condensation, thus, making it attractive from the point of power costs. The small unit size allows effectively using it on smaller distant oil fields, specifically the ones with low rate. The technology of compression separation is based on different elasticities of saturated vapours and the difference in condensation pressures of separate components of the mixture. When the temperature or pressure in a two-phase system (vapour - liquid) change, its equilibrium is disrupted and immediately renovated due to the change in the mass ratio of the phases. For example, at a constant temperature, the vapour phase compression results in the condensation of the part of vapours, and with the volume increase, the part of the liquid is evaporated. In both cases, the vapour phase pressure, corresponding to the given temperature, does not change (Lipanov et al., 2016).

However, with the compression method, the extraction degree of heavy hydrocarbons is lower, as only a part of hydrocarbon vapours is condensed, the second part stays in the vapour phase to maintain the phase equilibrium. The transition degree is defined by the initial composition, i.e. by the content of heavy hydrocarbons and pressure elevation degree (Leschev et al., 2009).

The pressure of the gas mixture p is calculated by the following Eq. 1:

$$p = \sum_{i=1}^{N} p_i, \tag{1}$$

Where:

$p_i = x_i p$ – the partial pressure of i-gas in the mixture composition;

N – number of gases in the mixture;

xi – molar concentration of the i-gas in the mixture.

The bond of the partial pressures, volume and mass of the gas is defined by the following Eq. 2.

$$p_i = \frac{m_i}{\mu_i} \cdot \frac{RT}{V} = \mu_i \frac{RT}{V} \tag{2}$$

Where:

m_i – mass of the i-gas of the mixture;

μ_i – the molar mass of the i-gas;

R – gas constant;

T – the temperature of the gas mixture;

V – the volume of the gas mixture.

On the other hand, with the OAG compression, the pressure of all its components increases proportionally, and part of the gases, whose pressure exceeded the vapour pressure, is condensed. The Antoine equation (Eq. 3) that appears next can be used to calculate the pressure of saturated vapours of gases in a pressure range up to 0,2 - 0,3 mPa (Khafizov et al., 2012).

$$\ln(P_s) = \frac{A-B}{T+C} \tag{3}$$

Where:

A, B, C – empirical coefficients (Skaftymov, 2012), T – temperature in K, Ps – saturated vapour pressure in mm Hg.

The following Tab. 1 displays the pressure data of saturated OAG vapour components depending on the temperature (Blyablyas et al., 2017).

Tab. 1. Saturated OAG vapour components pressure values under different temperatures

Substance	Boiling temperature, [°K]	The pressure of saturated vapour at different temperatures of OAG, [MPa]				
		253 [°K]	263 [°K]	273 [°K]	283 [°K]	293 [°K]
Propane	231.1	0.2397	0.3387	0.4653	0.6238	0.8180
Isobutane	261.3	0.0711	0.1063	0.1537	0.2158	0.2951
n-Butane	272.7	0.0443	0.0682	0.1013	0.1457	0.2037
n-Pentane	309.2	0.0088	0.0149	0.0240	0.0371	0.0555
n-Hexane	341.9	0.0018	0.0034	0.0059	0.0099	0.0159
Hydrogen sulfide	212.8	0.5350	0.7433	1.0057	1.3290	1.7200

From Tab. 1, it can be seen that heavier hydrocarbons are condensed under low pressure. It can also be concluded that, in terms of the OAG condensation, as the temperature increases, the pressure of saturated vapours increases as well. Consequently, the expenditures of OAG components condensation go up. In the considered pressure and temperature ranges of Tab. 1, hydrogen sulfide condensation takes place under higher pressure and at a lower temperature. In this regard, it is also possible to come to the conclusion that having selected the optimal pressure and temperature modes during OAG condensation, it is possible to exclude or minimize hydrogen sulfide penetration into the condensate. The optimal selection of such modes is one of the important elements the present paper highlights, and at the same time, something that the proposed method and the mobile unit designed and developed take into account.

Based on these facts and with the aim of practically verify them, the mobile laboratory unit "LURPNG" has been designed, produced and tested at oil fields of the Udmurt Republic and Samara region to solve the problem of optimal mode selection of OAG condensation at particular places of oil extraction with different chemical compositions. The following Fig. 2 shows the block diagram of the developed laboratory unit.

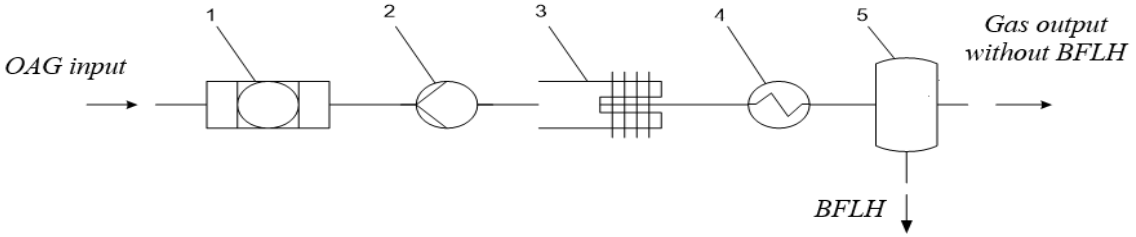

Fig. 2. Block Diagram of the proposed unit. 1 – Filter, 2 – Compressor, 3 – Air heat exchanger, 4 – Evaporator of the refrigeration machine, 5 – Separator. Source: Self-elaboration.

On the other hand, Tab. 2 displays technical characteristics and parameters of the mobile laboratory unit for OAG separation "LURPNG".

Tab. 2. Key technical characteristics and parameters of the unit "LURPNG"

Designation	Parameter value
Rated capacity of the unit for OAG, [m^3/hr]	2.0 – 3.0
Input power, [kW]	0.5 – 1.50
Control volume of BFLH filling, [ml/m^3]	100/0.0001
Supply voltage, [V]	220
The unit is equipped with sensors	Input gas consumption Output gas consumption Electrical power consumption
Maximum weight of the unit, [kg]	60
Overall dimensions (LxWxH), [m]	0.81x0.51x0.54

As can be seen in Fig. 2, in brief, the general functioning of the laboratory unit for OAG separation starts with its connection to the gas pipe using a high-pressure hose. Inside the unit, the gas gets into the filter (1) where it is cleaned from water and oil drops, then it gets into the gas counter and compressor (2). The heated gas is cooled down to the ambient temperature by the air heat exchanger (3) and then to 40 °C by the tubular heat exchanger. The heat exchanger is in the refrigeration evaporator chamber (4), where the freon gas from the refrigeration machine is supplied. A controller sets the condensation cooling temperature of the gas products. Subsequently, from the tubular heat exchanger, the gas flows into the separator (5) upper part. The porous body is the centre of the condensate drop formation; the condensate is collected in the same separator lower part. When the ball valves are open, the condensate is collected in a transparent measured sampler for the BFLH connected to same separator 5. The sampler is a 100-ml measuring glass bottle.

On the other hand, the pressure in the separator is set by a membrane valve consisting of two cavities – the lower one connected to the separator, and the upper one connected to the LNG container (Leschev et al., 2009). The liquefied gas in the container is in the equilibrium state, i.e. depending on the temperature, it will be under certain pressure, which defines the condensation of light hydrocarbon vapours, which are in it, and also the heavier ones. In the case of the container being filled with propane, all the gases, including it, are condensed in the separator. All lighter gases, for instance, from hydrocarbons – methane, ethane, from the inert gases – nitrogen, inert gases, carbon dioxide, etc. flow through a membrane valve to the atmosphere via the gas meter. The elastic membrane divides two-valve cavities – the upper one, which is a reference with the filled gas, and the lower one which is the working one. When the gas pressure in the working cavity exceeds the pressure in the reference one (condensation pressure, vapour pressure), the membrane bends and the gas flows through holes being subsequently discharged into the atmosphere. When the pressure in the valve working cavity goes down, the membrane closes the holes, and the discharge stops. The pressure in the separator (condensation pressure of the BFLH vapours) is controlled by the manometer. Finally, when the reference volume of the transparent measured vessel is filled, the unit is switched off, the data of the meters are recorded, the ball valves are closed, and the sampler with the BFLH is disconnected from the unit.

The laboratory unit proposed by the authors in this paper has been successfully tested at some oil fields of the Udmurt Republic and Samar region as it will be detailed further in the experimental part of this paper. The main aims have been, among others, to evaluate the possibility of extracting the BFLH from OAG at different oil fields, and to assess the operational efficiency of the mobile laboratory unit "LURPNG" at different oil fields and under different conditions, see Fig. 3. When tested, the laboratory unit has demonstrated itself as workable and simple in operation.

Fig. 3. Testing of the mobile laboratory unit "LURPNG" at an oil filed in the Udmurt Republic. Source: Self-elaboration.

Results and Discussion

Analysis of the experiment results for obtaining the BFLH from OAG with different chemical compositions.

The experiment presented here is mainly aimed at defining the optimal condensation temperature, at which the electrical power consumption to obtain the BFLH liquid phase will be minimal. This experiment is realized using the designed and developed mobile laboratory unit "LURPNG based on the compression method. During the experiment, the amounts of input and output gas were measured. The parameters of the input gas (OAG) used to obtain the BFLH are given in Tab. 3.

The obtained BFLH was discharged into the transparent measured 100 ml vessel (0.0001 m^3); the vessel filling time was measured with a stopwatch. When the transparent vessel was filled up to 100 ml, the unit was switched off, and the recordings of the inlet gas volume meters, outlet gas volume meters and electric power meter were taken. The recordings of the gas volume meters were related to normal conditions. For this particular experiment, the normal conditions were assumed as those of a pressure of 101, 325 Pa (1 atm., 760 mm Hg) and a temperature of 293.15 K, i.e. the so-called "room" temperature of 20 °C (Physical encyclopedia).

Tab. 3. Chemical composition of the input gas (OAG)

No	Index designation	Test results, measurement units [%]	Extended uncertainty of the test results (P=0.95) [%]
1.	Helium molar fraction	0.088	± 0.008
2.	Helium volumetric fraction	0.088	± 0.009
3.	Hydrogen molar fraction	0.0262	± 0.0025
4.	Hydrogen volumetric fraction	0.0264	± 0.0027
5.	Oxygen molar fraction	0.033	± 0.004
6.	Oxygen volumetric fraction	0.034	± 0.004
7.	Nitrogen molar fraction	54.8	± 1.1
8.	Nitrogen volumetric fraction	55.2	± 1.4
9.	Carbon dioxide molar fraction	1.36	±0.11
10.	Carbon dioxide volumetric fraction	1.36	±0.12
11.	Methane molar fraction	12.4	± 0.6
12.	Methane volumetric fraction	12.5	± 0.7
13.	Ethane molar fraction	6.2	± 0.6
14.	Ethane volumetric fraction	6.2	± 0.6
15.	Propane molar fraction	14.4	± 0.6
16.	Propane volumetric fraction	14.3	± 0.7
17.	i-Butane molar fraction	2.56	±0.15
18.	i-Butane volumetric fraction	2.51	±0.16
19.	n-Butane molar fraction	5.5	± 0.3
20.	n-Butane volumetric fraction	5,3	± 0,3
21.	i-Pentane molar fraction	1.26	±0.13
22.	i-Pentane volumetric fraction	1.21	±0.13
23.	n-Pentane molar fraction	1.01	±0.10
24.	n-Pentane volumetric fraction	0.96	±0.10
25.	Hexane molar fraction	0.43	± 0.04
26.	Hexane volumetric fraction	0.40	± 0.04
27.	Hydrogen sulfide molar fraction	under 0.01	-
28.	Hydrogen sulfide volumetric fraction	under 0.01	-

On the other hand, in the previous Tab. 3, it can be seen that OAG contains over 50% of inert gas nitrogen, this means that the work for condensing this nitrogen is useless, since after the OAG treatment nitrogen is released into the atmosphere. Consequently, the pressure elevation for OAG components condensation is unfeasible.

The unit was tested at the ambient temperature of +20°C, and two test samples were taken at different conditions of condensation temperature. The test sample 1 was obtained at the condensation temperature in the separator of +4°C, while the test sample 2 was obtained at the temperature of +20°C. The selection of the condensation temperature (+4°C and +20°C) was conditioned by the fact that at a condensation temperature below +4°C ice crystals can be formed in the condensate and clog the pipeline, while at high condensation temperature the process proceeds under high pressure, resulting in increased power expenditures (Skaftymov, 2012). The liquefied gas container, setting the condensation pressure in the separator with the membrane valve, was also at the ambient temperature of +20°C when taking test samples 1 and 2. As a result of the tests, the BFLH liquids with the diluted gases were obtained, see Tab. 4.

Tab. 4. Component composition and volumetric concentration of the BFLH gas phase

Component concentration of test sample 1				Component concentration of test sample 2			
Name	Molar [%]	Volume [%]	Mass [%]	Name	Molar [%]	Volume [%]	Mass [%]
Helium	0.005483	0.005545	0.0006828	Helium	0.01075	0.01086	0.001368
Hydrogen	0.02613	0.02643	0.00168	Hydrogen	0.02908	0.02937	0.00182
Oxygen	0.1388	0.1402	0.1382	Oxygen	1.799	1.815	1.829
Carbon dioxide	8.938	8.986	12.23	Carbon dioxide	8.392	8.427	11.73
Nitrogen	2.618	2.645	2.281	Nitrogen	8.982	9.065	7.993
Methane	44.11	44.50	22.01	Methane	41.72	42.04	21.26
Ethane	11.76	11.79	11.00	Ethane	10.57	10.59	10.10
Propane	19.31	19.19	26.48	Propane	16.98	16.86	23.78
i-Butane	3.052	2.995	5.517	i-Butane	2.665	2.612	4.920
n-Butane	6.098	5.968	11.02	n-Butane	5.328	5.208	9.838
i-Pentane	1.661	1.600	3.728	i-Pentane	1.452	1.397	3.328
n-Pentane	1.224	1.170	2.748	n-Pentane	1.055	1.007	2.419
Hexane	1.060	0.9847	2.841	Hexane	1.020	0.9463	2.792

Once the dissolved gases were removed from the BFLH (Tab. 4), a stable BFLH with the following percentage of components was obtained:

propane-butane part – 46.0 %
pentane-hexane part – 51.8 %
diluted gases – 2.2%

Based on the results of the obtained BFLH that appear in Tab. 4, it is also possible to see that when the temperature goes down to +4°C, a lot of diluted gases such as methane, ethane, propane, butane are observed in the BFLH. This way, the gas is easily condensed, but at the same time, the BFLH becomes less stable. When the condensation temperature is elevated up to +20°C, then heavier fractions are liquefied (pentane, hexane).

The results of the test also demonstrated that the power losses for obtaining fixed volume (100 ml) of the BFLH are similar for both cases, and the deviations are within the measurement error.

Influence of the hydrogen sulfide and carbon dioxide in the OAG on the chemical composition of the BFLH obtained by the compression method.

It is well-known that hydrocarbon gases contain a significant amount of acid gas components – hydrogen sulfide and carbon dioxide (CO_2 and H_2S), also water vapours. In the presence of acid components, water vapours cause the emergence of active corrosion processes. The availability of hydrogen sulfide and carbon dioxide in the gas composition also increases the content of such water vapours.

The OAG contains this hydrogen sulfide and carbon dioxide, which according to the standards (GOST R 52087-2018) are inadmissible admixtures in combustion gas, and therefore, it becomes necessary to investigate their removal from the BFLH. For these purposes, the OAG is usually purified to extract these acid gases (CO_2 and H_2S) from it, and as a result, the output gas meets the requirements of GOST.

Based upon these facts, several investigations were also realized using the proposed mobile laboratory unit "LURPNG" for determining and analyzing the amount of hydrogen sulfide and carbon dioxide in the BFLH obtained by compression, and this as a consequence of their presence and concentrations in the very initial OAG the BFLH was to be obtained from. The experiments were conducted at two oil fields where the OAG contained a lot of hydrogen sulfide and carbon dioxide so as to be able to draw more robust conclusions on the efficacy of the unit and its working principle and method. The chemical compositions of the inlet gas (OAG) and outlet gas (after processing) are given in Tab. 5.

Tab. 5. Chemical composition of the inlet gas (OAG) and outlet gas after the BFLH separation

Component composition, molar fraction, [%]:	Oil field 1, test sample 1		Oil field 2, test sample 2	
	inlet gas	outlet gas	inlet gas	outlet gas
Oxygen	Under 0.0100	Under 0.0100	Under 0.0100	Under 0.0100
Nitrogen	41.4927	47.5814	44.1051	47.2568
Helium	0.0633	0.0775	0.0678	0.0746
Hydrogen	0.0157	0.0195	0.019	0.0173
Hydrogen dioxide	**10.8218**	**12.0546**	**11.5929**	**12.221**
Methane	11.4837	13.8878	11.8629	13.1098
Ethane	5.4244	5.7081	6.2227	6.3293
Propane	8.0524	7.6568	8.6778	7.939
i-Butane	2.6805	1.7967	2.4952	1.9645
n-Butane	6.4392	3.1647	5.0647	3.6696
neo-Pentane	0.0124	0.004	0.008	0.0054
i-Pentane	5.3228	1.2818	2.6507	1.3978
n-Pentane	3.0656	0.7835	1.6108	0.7057
Hexane	1.9801	0.7188	2.347	0.4491
Benzene	0.0326	0.0121	0.0686	0.0096
Heptane	0.1174	0.0505	0.3938	0.0536
Toluene	0.0091	0.0035	0.0016	0.0053
Octane	0.0087	0.0097	0.0353	0.0088
Hydrogen sulfide	**2.9575**	**5.1732**	**2.7581**	**4.7661**
Carbonyl sulfide	0.0057	0.0057	0.0056	0.0056
Methyl mercamptan	0.0044	0.0051	0.0049	0.006
Ethyl mercamptan	0.003	0.0018	0.0025	0.0021
Carbon disulfide	0.0002	Under 0.0001	0.0002	0.0002
Propyl mercamptan-2	0.0045	0.0019	0.0027	0.0015
2-Methylpropyl mercamptan-1	0.0007	0.0005	0.0006	0.0005
Propyl mercamptan-1	0.0004	0.0003	0.0003	0.0002
Methylethylsulfide	0.0002	Under 0.0001	0.0002	0.0002
Butyl mercamptan-2	0.0005	0.0003	0.0005	0.0003
Methylpropylsulfide	0.0001	Under 0.0001	0.0001	Under 0.0001
Dimethylsulfide	0.0004	0.0002	0.0003	0.0002

Similarly, Tab. 6 presents the chemical compositions of the BFLH obtained from the OAG (Tab. 5) after being processed at the laboratory unit "LURPNG". The analysis of the results obtained indicates that the presence of hydrogen sulfide in the outlet gas increases after separation (Tab. 5), and the presence of hydrogen sulfide becomes minimal at its solubility level in the BFLH (Tab. 6). The authors also come to the conclusion that the stable liquid fraction of the BFLH is obtained ecologically clean, i.e. purified from hydrogen sulfide and carbon dioxide admixtures, ad this using the designed and developed unit and the proposed compression method.

Tab. 6. BFLH composition (test sample 1, test sample 2)

Oil field 1, test sample 1		Oil field 2, test sample 2	
Designation of indexes	Test result	Designation of indexes	Test result
1. Mass fraction of hydrocarbon components, [%]:		**1. Mass fraction of hydrocarbon components, [%]:**	
Methane	**0.0585**	**Methane**	**0.0233**
Ethane	**1.2272**	**Ethane**	**0.4491**
Propane	**11.4468**	**Propane**	**4.2402**
i-Butane	7.9451	i-Butane	3.7227
n-Butane	**20.2540**	**n-Butane**	**11.0980**
2.2-dimethylpropane	0.0297	2.2-dimethylpropane	0.0246

Dimethylcyclopropane	0.0090
i-Pentane	16.0666
n-Pentane	**10.5830**
Isomers C_6	12.8021
Naphtenes C_6	2.0781
n-Hexane	**5.1581**
Benzene	0.0569
Isomers C_7	3.4676
Naphtenes C_7	2.0124
n-Heptane	**1.7317**
Toluene	0.0571
Isomers C_8	1.1619
Naphtenes C_8	0.8221
n-Octane	**0.3992**
Aromatic hydrocarbons C_8	0.0556
Isomers C_9	0.3521
Naphtenes C_9	0.1142
n-Nonane	**0.0105**
Aromatic hydrocarbons C_9	0.0190
Isomers C_{10}	0.0424
Naphtenes C_{10}	0.0168
Aromatic hydrocarbons C_{10}	0.0039
n-Decane	**0.0105**
Isomers C_{11}	0.0052
Naphtenes C_{11}	0.0012
n-Undecane	**0.0038**
n-Dodecane	**0.0016**
Indanes	0.0003
2. Mass fraction of carbon dioxide	**0.7661**
3. Mass fraction of hydrogen sulfide	**1.1799**
4. Mass fraction of sulfur containing components:	
Mercamptans:	
Methyl mercamptan	0.0050
Ethyl mercamptan	0.0076
Propyl mercamptan-2	0.0161
2-Methylpropyl mercamptan-2	0.0009
Propyl mercamptan-1	0.0012
Butyl mercamptan-2	0.0044
2-Methylpropyl mercamptan-1	0.0003
Butyl mercamptan-1	0.0003
Sulfides:	
Dimethylsulfide	0.0007
Methylethylsulfide	0.0007
Methylisopropylsulfide	Less than 0.0001
Diethylsulfide	0.0001
Methylpropylsulfide	0.0007
Disulfides:	
Methylpropylsulfide	0.0001
Methylisopropylsulfide	Less than 0.0001
Diethylsulfide	Less than 0.0001

Dimethylcyclopropane	0.0050
i-Pentane	14.1624
n-Pentane	**9.8088**
Isomers C_6	18.5359
Naphtenes C_6	3.4136
Hexenes	0.0006
n-Hexane	**7.5244**
Benzene	0.0600
Isomers C_7	7.8591
Naphtenes C_7	4.0051
n-Heptane	**4.4016**
Toluene	0.0893
Isomers C_8	3.5402
Naphtenes C_8	2.2649
n-Octane	**1.4203**
Aromatic hydrocarbons C_8	0.2189
Isomers C_9	1.2427
Naphtenes C_9	0.5460
n-Nonane	**0.2841**
Aromatic hydrocarbons C_9	0.0717
Isomers C_{10}	0.1968
Naphtenes C_{10}	0.0557
Aromatic hydrocarbons C_{10}	0.0137
n-Decane	**0.0303**
Isomers C_{11}	0.0181
Naphtenes C_{11}	0.0046
Aromatic hydrocarbons C_{11}	0.0012
n-Undecane	**0.0093**
Isomers C_{12}	0.0005
Naphtenes C_{12}	0.0005
Aromatic hydrocarbons C_{12}	0.0004
n-Dodecane	**0.0084**
Indanes	0.0054
Total of C_{13+}	0.0064
2. Mass fraction of carbon dioxide, %	**0.2899**
3. Mass fraction of hydrogen sulfide , %	**0.2862**
4. Mass fraction of sulfur containing components, %:	
Mercamptans:	
Methyl mercamptan	0.0035
Ethyl mercamptan	0.0077
Propyl mercamptan-2	0.0206
2-Methylpropyl mercamptan-2	0.0009
Propyl mercamptan-1	0.0019
Butyl mercamptan-2	0.0085
2-Methylpropyl mercamptan-1	0.0003
Butyl mercamptan-1	0.0003
Sulfides:	
Dimethylsulfide	0.0008
Methylethylsulfide	0.0005
Methylisopropylsulfide	0.0003

Methylpropylsulfide	Less than 0.0001	Diethylsulfide	0.0001
Carbonyl sulfide	**0.0057**	Methylpropylsulfide	0.0011
Carbon disulfide	**0.0050**	**Disulfides:**	
Not identified sulfur containing compounds	**0.0009**	Methylpropylsulfide	0.0001
		Methylisopropylsulfide	0.0001
		Diethylsulfide	0.0001
		Methylpropylsulfide	0.0001
		Carbonyl sulfide	**0.0032**
		Carbon disulfide	**0.0080**
		Not identified sulfur containing compounds	**0.0020**

On the other hand, the experiment results obtained and appearing in Tab. 5 and 6 confirm the calculation values of the parameters given in Tab. 1 and that hydrogen sulfide is not condensed within the considered range of temperatures and pressures. Thus, the liquefied gas purified from harmful admixtures (BFLH) is obtained directly on small-rate oil fields with minimum power losses. The method proposed within this paper for the OAG compression separation using a refrigeration machine is new for the units of such type. The method working capacity and efficacy is also proved by the experiments carried out. Both the proposed method of OAG compression separation and the mobile laboratory unit "LURPNG" based on it are recommended for use on distant oil fields with a low rate, for which the pipeline installation is economically impractical and unfeasible. The results of the experiments show that an ecologically clean stable liquid fraction of BFLH purified from hydrogen sulfide and carbon dioxide admixtures is obtained using the proposed method and unit. The resulting product can be further delivered for further treatment to produce petrochemical products, to be pumped into the wells as a solvent for repairs or even to be used as fuel at the oil fields with insufficient amount of own OAG.

Conclusions and Further research

The present paper presented a mobile laboratory unit named "LURPNG" that allows obtaining the BFLH directly at small-rate faraway oil fields where there are poor or non-existing piping systems and/or are away from major transport infrastructure. These oil fields are characterized by having a low gas factor and caloricity due to high nitrogen content. The presented mobile unit is mainly characterized by its ability to obtain the BFLH using a compression approach or method, which is also a contribution and added value of this paper.

A series of experiments were realized using the proposed mobile unit where it was possible to define optimal modes for the obtention of the BFLH from AOG with different initial compositions of hydrocarbons components and harmful admixtures, such as hydrogen sulfide and carbon dioxide. The study also experimentally confirmed concrete values for the dependence of the OAG compression pressure on the temperature. In this regard, it was possible to conclude that when the condensation temperature goes up, the liquid fraction of the BFLH becomes more stable, since it contains fewer volatile fractions and does not contain the admixtures of hydrogen sulfide and carbon dioxide. On the other hand, it was also demonstrated that at low condensation temperatures the gas solubility increases, subsequently the caloricity of the BFLH liquid fraction goes up, and thus it can be used as fuel for technological purposes at oil fields or to heat technical premises.

The BFLH obtained in the experiments proved to be a valuable power product without hydrogen sulfide admixtures, despite the fact that this was obtained from OAG with high hydrogen sulfide content. Besides, the compression method of OAG separation proposed by the authors allows flexibly obtaining the liquid fraction of the BFLH depending on its further application, i.e. for pumping it into wells as a solvent during maintenance, for the transportation by mobile transport as an ecologically pure fuel. The experiments also allowed obtaining important results related to the quantitative and qualitative composition of the BFLH for certain small-rate oil fields. Future research aims at experimentally examining low oil fields in specific regions in order to determine the presence of wells for which the utilization of the LURPNG mobile laboratory facility is convenient and cost-effective in term of OAG utilization. The small size and mobility of the proposed unit will allow these works to be performed for all fields, regardless of their remoteness.

References

Arutyunov, V. S.; Savchenko, V. I.; Sedov, V. I.; Nikitin, A. V.; Troshin, K. Y.; Borisov, A. A.; Fokin, I. G.; Makaryan, I. A. and Strekova, L. N. (2017). New Potentialities for Utilization of Associated Petroleum Gases in Power Generation and Chemicals Production. Eurasian Chemico-Technological Journal, 19, pp. 265-271, DOI: http://doi.org/10.18321/ectj662.

Arutyunov, V.; Troshin, K.; Nikitin, A.; Belyaev, A.; Arutyunov, A.; Kiryushin, A. and Strekova, L. (2020). Selective oxycracking of associated petroleum gas into energy fuel in the light of new data on self-ignition delays of methane-alkane compositions. Chemical Engineering Journal, 381, DOI: https://doi.org/10.1016/j.cej.2019.122706.

Atoufi, H. D. and Lampert, D. J. (2020). Impacts of Oil and Gas Production on Contaminant Levels in Sediments. Current Pollution Reports, DOI: https://doi.org/10.1007/s40726-020-00137-5.

Bako, B. and Božek, P. (2016). Trends in simulation and planning of manufacturing companies. Procedia Engineering [online]. Proccedings of the International Conference on Manufacturing Engineering and Materials, ICMEM 2016, 6. - 10. June 2016, Nový Smokovec, Slovakia, 149, pp. 571-575.

Baranov, M. N.; Božek, P.; Prajová, V.; Ivanova, T. N.; Novokshonov, D. N.; Korshunov, A. I. (2017). Constructing and calculating of multistage sucker rod string according to reduced stress. Acta Montanistica Slovaca, 22 (2), pp. 107-115.

Blyablyas, A. N. and Korepanov, M. A. (2017). Technology of compressor-absorption purification as the method of to increase the efficiency of OAG application. Journal Exposition, Oil, Gas, 1 (54).

Braginskii, O. B. and Chernavskii, S.Y. (2010). Utilization of Associated Petroleum Gas: Economic Issues. Rossiiskii Khimicheskii Zhurnal, 54(5), pp. 19–22.

GOST R 52087-2018. Gas and hydrocarbons.

GOST R 55598. Oil-associated gas, classification criteria.

Igitkhanyan, I. A. and Bogak , T. V. (2014). Efficiency of oil-associated gas processing methods in Russia. Bulletin of Tomsk State Pedagogic University, (TSPU Bulletin), 8(149).

Ivanova, T. N.; Korshunov, A. I. and Koretckiy, V. P. (2018). Dual Completion Petroleum Production Engineering for Several Oil Formations. Management Systems in Production Engineering. Gliwice 2018, 26(4), pp. 133-136, DOI: 10.1515/mspe-2018-0035.

Karch, L.; Škvareková, E. and Kawicki A. (2018). Environmental and geological impact assessment within a project of the NorthSouth Gas Interconnections in Central Eastern Europe. Acta Montanistica Slovaca, 23 (1), pp. 26-38.

Kayukova, G.P.; Romanov, G. V.; Lukianova, R.G. and Sharipova. N.S. (2009). Organic geochemistry of sedimentary strata and foundation of Tatarstan territory, M.: GEOS, 487 p., with illustrations.

Khafizov, F.S. and Krasnov, A. V. (2012). Pressure of saturated vapors for oil products. Electronic scientific journal Oil and gas engineering, Iss.3, pp. 406-412.

Kiryushin, P. A.; Knizhnikov, A. Y. ; Kochi, K. V.; Puzanov, T. A. and Uvarov, S.A. (2013). Oil-associated gas in Russia: prohibited to burn, must be processed! Analytical report on economic and ecological expenditures of burning oil-associated gas in Russia. World Wildlife Fund (WWF), Moscow, 2013.

Kuppusamy, S.; Maddela, N. R.; Megharaj, M. and Venkateswarlu, K. (2020). An Overview of Total Petroleum Hydrocarbons. Total Petroleum Hydrocarbons. Springer, Cham, pp. 1-27, DOI: https://doi.org/10.1007/978-3-030-24035-6_1.

Lipanov, A. M.; Yu, A.; Leschev, M. A.; Korepanov, P. G.; Ovcharenko, I. and Zaitsev, N. (2016). Unit for oil-associated gas separation at the oil fields of Udmurt Republic. Proceedings of All-Russian scientific-practical conference dedicated to the 85th anniversary of V.I. Kudinov, Doctor of Science in Engineering, Professor, Academician of RANS “Modern technologies of oil and gas extraction. Perspectives of the development of mineral and raw material complex (Russian and world experience)”, May 26-27, 2016. — Izhevsk: Publishing Center “Udmurt University”, pp. 231-236.

Mullakhmetova, L. I. and Cherkasova, E. I. (2015). Oil-associated gas: preparation, transportation and processing. Bulletin of Technological University. 18 (19), pp. 83-90.

Physical encyclopedia (2019) – Normal conditions. Available at: http://femto.com.ua/articles/part_2/2520.html.

Rafa, V.; Borzan, M. and Teuţan, E. (2014). Determination of occurring of sealing damages in transport of hydrocarbons, detection of accidental leakes of natural gases. In: ACTA TECHNICA NAPOCENSIS, Series: Applied Mathematics and Mechanics and Engineering, 57(2), pp.287-290.

RIA Novosti (2019). Oil-associated gases. Available at: https://ria.ru/20100201/206673791.html.

Semenova, S. A. and Abrzhina, L. L. (2016) Methods of decreasing the harmful effect of burning oil-associated gas by its utilization. Available at: http://elar.urfu.ru/bitstream/10995/74233/1/sueb_2016_028.pdf.

Skaftymov, N. A. (2012). Basics of gas supply. Reprinted edition of 1975. — M.: ECOLIT, 2012. — 344 p.

Škvareková, E.; Tomašková, M.; Wittenberger, G.; Zelenák, Š. (2019). Analysis of Risk Factors for Underground Coal Gasification. Management Systems in Production Engineering. Gliwice 2019, 27(4), pp. 227-235, DOI: 10.1515/mspe-2019-0036.

Speight, J. (2012). Oil analysis. Reference book: translated from English under the editorship of L.G. Nekhamkina, E.A. Novikova. - SPb. - "Profession", 480 p., with illustrations.

Vorobiev, A. E. and Zhang L. (2018). Applied innovative technologies for processing of associated gas in China. The Eurasian Scientific Journal, [online] 2(10). Available at: https://esj.today/PDF/11NZVN218.pdf.

Yu, A.; Leschev, M.; Kurguzkin, G.; Lipanov, A. M.; Yu, S.; Popov, D. Zorin, M. (2009). Device for biogas separation into methane and carbon dioxide. Patent RU (11) 2 424 478 (13) C2.

Zaitsev, I. N.; Korepanov, M. A.; Leschev, A. Y.; Lipanov, A.M.; Ovcharenko, P. G. (2017). Methods of oil-associated gas separation at the oil field. Industrial and ecological safety, labor protection, Iss.1, pp.20-21.

Acta Montanistica Slovaca
ISSN 1335-1788
actamont.tuke.sk

Estimation of Quality Indicators of Ecological Thermoplastic Fiber Materials

***Vladislav SVIATSKII*[1*], *Witold BIALY*[2], *Kirill SENTYAKOV*[1] *and* *Alexandr REPKO*[1]**

Authors' affiliations and addresses:
[1] Technology of Mechanical Engineering and Instrument Making, Votkinsk Branch of Kalashnikov Izhevsk State Technical University, Russia
e-mail: svlad-2000@yandex.ru
e-mail: la1030@mail.ru
e-mail: aleksrepko@gmail.com

[2] Politechnika Śląska, Wydział Organizacji i Zarządzania, Instytut Inżynierii Produkcji ul. Roosevelta 26, 41-800 Zabrze, Polska
e-mail: Witold.Bialy@polsl.pl

[3] Slovak University of Technology in Bratislava, Faculty of Materials Science and Technology, 917 24 Trnava, Slovakia
e-mail: pavol.bozek@stuba.sk

***Correspondence:**
Vladislav Sviatskii, Technology of Mechanical Engineering and Instrument Making, Votkinsk Branch of Kalashnikov Izhevsk State Technical University, Russia
e-mail: svlad-2000@yandex.ru

Funding information:
FSBEI
13.04.03/18BBYA

Acknowledgement:
The research is funded by researchers' grant FSBEI of Higher Education "Kalashnikov ISTU" 13.04.03/18BBYA.

How to cite this article:
Sviatskii. V., Bialy, W., Sentyakov, K. and Repko, A. (2020). Estimation of Quality Indicators of Ecological Thermoplastic Fiber Materials. *Acta Montanistica Slovaca*, Volume 25 (1), 14-23

DOI:
https://doi.org/10.46544/AMS.v25i1.2

Abstract
The article discusses the process of obtaining fibrous material from a thermoplastic by blowing methods, and also provides a method for calculating the average diameter d_f and length l_f of elementary fibers. According to the presented calculations, the average elementary fibers' diameter value d_f depends on the airflow speed from the blow head in the fiber formation zone. The greater the air velocity V_p, the smaller the diameter of the elementary fibers. The elementary fibers' length lf depends on their diameter d_f and variable angle γ of the blowing head diffuser. The smaller the diameter of the elementary fibers d_f and the larger the variable angle γ, the smaller the length of the elementary fibers. At γ = 0 degrees, the fiber is obtained, with an increase in the angle γ, the fiber length becomes fixed. The average elementary fibers' diameter d_f varies depending on the speed of the airflow flowing from the blowing head in the fiber formation zone. The greater the air velocity V_p, the smaller the diameter of the elementary fibers. The discrepancy between the calculating results of the average fiber diameter with their real values does not exceed 13%, which, according to the process complexity, can be considered satisfactory. The elementary fibers' length lf depends on the elementary fibers' diameter d_f and a variable angle γ. The smaller the diameter of the elementary fibers d_f and the larger the variable angle γ, the smaller the length of the elementary fibers. At γ = 0 deg, the infinite length fiber is obtained, and with an increase in the angle γ, the fiber length becomes fixed.

Keywords
recycled thermoplastic raw materials; vertical and horizontal method of blowing a melting jet; fiber formation; methodology for calculating the average diameter and length of elementary fibers.

Introduction and Basic Information

Among the promising technologies for the production of the fibrous materials from secondary thermoplastics, one can attribute the blowing method, the essence of which is to inflate the thermoplastic stream jet flowing from the melting unit with a stream of compressed air. In this case, the melting unit can be of any type, for example, hydrostatic or extrusion (Sviatskii et al., 2015; Sviatskii et al., 2018).

The technological process for producing fibrous materials by the blowing method from recycled thermoplastics consists of stages (Fig. 1).

At the first stage, the preparation of feedstock is carried out. Primary or secondary granular PET material, as well as flexes (flakes) obtained after the crushing of used plastic containers, can be used as the raw material for the production of the fibrous materials (Sentyakov et al., 2014; Sentyakov et al., 2016). Judging by the experience of obtaining such products by vertical blowing method, the use of flexes as a feedstock significantly reduces the production cost. The preparation of the feedstock is following: - it is careful sorting because it should exclude the presence of metal or other refractory objects that could lead to an equipment malfunction; - raw materials drying in order to remove moisture from it, which can lead to a noticeable decrease in the finished product quality.

Worldwide growth in polymer waste ranges from 5 to 10% annually. In 2018, according to the European Statistical Agency (Eurostat), polymer waste amounted to almost 30 million tons. In the structure of polymeric wastes, 34% are polyethylene wastes; 30% PET; 14% - PP; 8% - Polystyrene and other materials. Of the total amount of polymer waste, up to 50% is plastic packaging, containers made of PET materials [2].

Processing of polymer waste into secondary raw materials, which can be used as a new resource base, is one of the most dynamically developing areas.

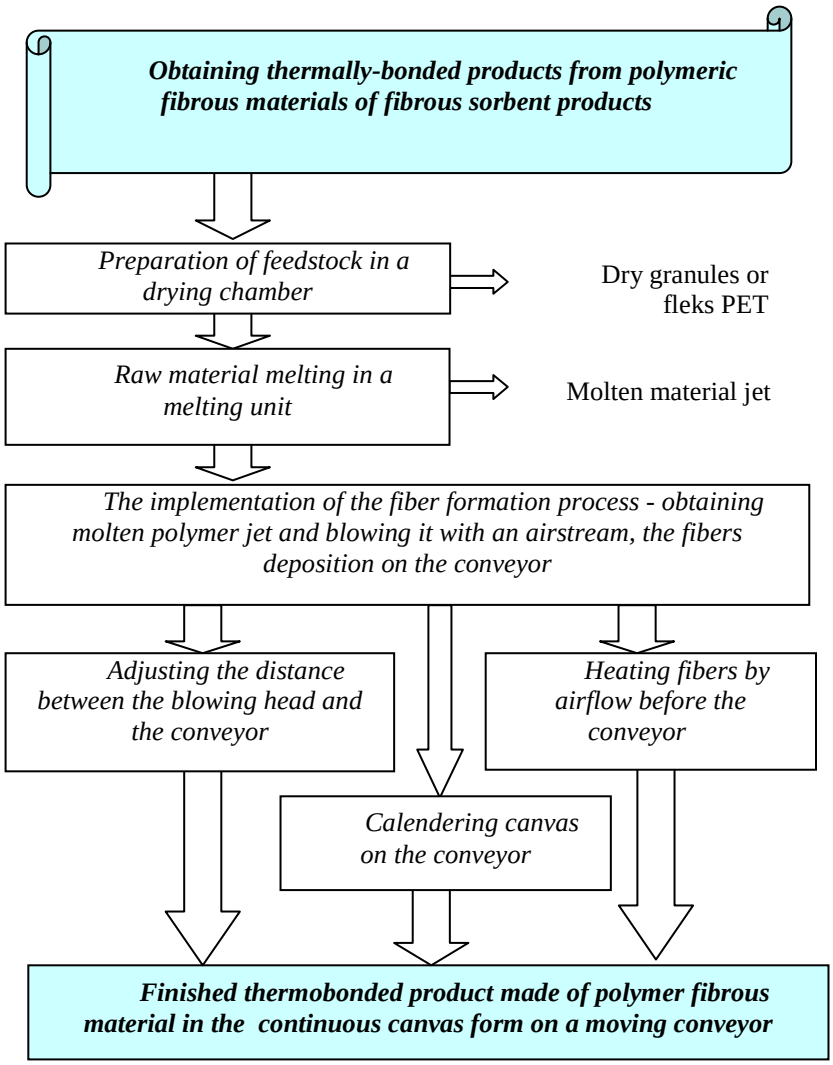

Fig. 1. The technological scheme of obtaining thermally-bonded products from polymeric fibrous materials

Literature review

The nomenclature of manufactured structural and building materials is currently quite extensive. A separate place in it is occupied by fibrous materials from mineral and synthetic raw, which are widely used in engineering, construction, heat power, and light industry (Baranov et al., 2017). The use of such materials as various composite materials production basis and as sorbents for environment purification from oil and oil products pollution is promising (Yim et al., 2018).

Of dual interest to the national economy are fibrous materials products based on recycled synthetic raw. The point of such dual interest is that the use of recycled raw materials can significantly reduce the cost of the finished products, and the extraction of such raw materials from the environment can solve one of the environmental problems – to prevent environmental pollution with synthetic household and industrial waste.

Processing of polymer wastes into fibrous materials is difficult due to the lack of an appropriate level of wastes sorting and treatment that are not homogeneous in chemical composition and contain inclusions. In addition, as a rule, the waste has a lower molecular weight compared to standard primary thermoplastic raw materials. As a result, secondary thermoplastics have a lower melt viscosity and melting point, as well as low mechanical characteristics that do not allow the use of classical (spunbond) technologies for the production of the fibrous materials.

Methodology

In the second stage, it is necessary to meet the feedstock and get a molten material stream with the given parameters: the primary diametrical size and the initial flow rate.

To implement this stage, equipment for processing various plastic materials is used - a screw extruder or a melting unit with the molten material outflow under the influence of hydrostatic pressure in the form of a cylinder with external electric heating elements.

The screw extruder has a complicated shape (Beno et al., 2013; Buransky et al., 2013). At present, it is possible to use modern production technologies such as 5-axis machining (Kovac and Peterka, 2014; Pokorný et al., 2012), CAD/CAM/CNC and IT technology (Nemeth et al., 2019), and modern cutting tools (Peterka and Pokorny, 2014), mostly coated (Chaus et al., 2018), to produce a screw extruder. These technologies ensure a high match of complex shape (Vopat et al., 2014) and dimensional accuracy (Peterka et al., 2008) and satisfactory roughness of the machined surface (Peterka, 2004; Vopat et al., 2015).

In the third stage, it is necessary to implement the fiber formation process, acting on the molten material stream with a compressed air stream, to obtain elementary staple fibers with an average diameter of 10 ... 150 microns and a length of 50 to 500 mm.

At the fourth stage, it is necessary to perform the preliminary formation of a given geometric shape of the product. Regardless of what geometric shape the finished product will have (flat napkins, pillows or sheets), the primary product for their further formation is a canvas. Such a canvas is a non-woven fibrous product in which elementary staple fibers intertwined with each other are held together by natural cohesion forces. In cross-section, the canvas can be made with a thickness of 20 to 100 mm and a width of 500 to 1200 mm. The canvas is formed during the deposition of elementary staple fibers emerging from the blowing head on the conveyor belt, so its length is not fixed (Smirnov et al., 2018; Kobeticova et al., 2017).

The fifth, final stage of the technological scheme for producing thermally-bonded products involves the thermal treatment of the primary canvas formed from elementary polymer fibers, and as shown in Fig. 1 has three embodiments.

The first option of the final stage is to reduce the distance from the fiberizing device to the receiving conveyor when the elementary fibers moving together with the airflow have not yet entered the solid phase. In this case, the fibers' thermal bonding occurs due to their adhesion to each other. The number of such bonded fibers, the strength, and the conditional density of the resulting product is inversely proportional to the distance indicated above. To ensure the stability of the finished product properties across the conveyor width, it is necessary that the blowing head of the fiberizing device oscillates in the horizontal plane. When implementing this option, it will be necessary to stabilize the surrounding space temperature (Bako and Bozek, 2016).

The second option of the final stage is heating the fibers, for example, with an electric hairdryer to maintain the temperature of the elementary fibers at the beginning of their deposition process on a conveyor close to the melting temperature. When using PET fiber to obtain thermally-bonded products, the airflow temperature acting on the primary canvas should be in the range 220 ... 250 °C. In this case, it is necessary to ensure uniform temperature distribution across the canvas width, for example, using several hairdryers placed at the same distance along the nozzle width or one hair dryer that performs transverse vibrations using a special mechanism with an amplitude equal to the width of the canvas.

The third version of the final stage is the calendaring process implementation. In this case, the primary canvas is passed between two cylindrical rollers heated to a temperature close to the polymer melting temperature. In this case, on the canvas surface, it is possible to obtain a thin layer of elementary fibers that are soldered together, increasing the strength of such a thermally bonded product. It is possible to make such an

option with one calendering roller - in this case, the thermal bonding of the fibers will occur only on one surface of the canvas deposited on the conveyor. Naturally, canvas strength is reduced. However, it becomes possible to use it, for example, for oil products sorption from the surface of the water. Then its conditional density should be less.

Materials and methods

In the course of research and development work to develop a technology for manufacturing products from fibrous materials based on secondary PET, a block diagram of the machines and assemblies interaction was developed (Fig. 2), which contains two technological machines: M1 - a machine for the production of the fibrous materials based on secondary raw materials with a hydrostatic melting unit type and M2 - a machine for the production of the fibrous materials based on secondary raw materials with an extrusion melting unit type.

In the secondary raw materials preparation, most of the units that make up the M1 and M2 machines are universal - they can be used in other similar machines for processing secondary synthetic raw materials. Such universal aggregates are aggregates for the feedstock preparation: A11 - aggregate for feedstock crushing; A12 - unit for drying the source and granular raw materials; A13 - unit for granulating raw materials; A14 - unit for the dosed supply of source and granular raw materials. The functioning of these units is accompanied by the following processes: P11 - the process of secondary raw materials crushing- in the considered technology - used plastic bottles of polyethylene terephthalate with the fleks formation no larger than 5 mm; P12 - the secondary raw materials drying process before granulation, which may be preceded by the process of cleaning the obtained flexes from paper and other foreign inclusions; P13 - the process of granulating raw materials, which is not elementary and includes the processes of melting flexes in an extruder, the formation and cooling of a system of molten raw materials jets with their subsequent crushing and the formation of the granules with a diameter of 1.5 ... 2 mm and a length of 3 . 4 mm; P14 - the raw materials (granules) drying process before melting to remove moisture, the presence of which significantly reduces the quality of the finished products (Bozek and Pivarciova, 2013; Bozek and Pokorny, 2014). Note that the presence of the A13 aggregate for granulating the feedstock is not a prerequisite for the operability of the M1 and M2 machines - not granules, but flexes can be used as raw materials. However, the quality of the products can change for the worse due to difficulties in the melt homogenization process.

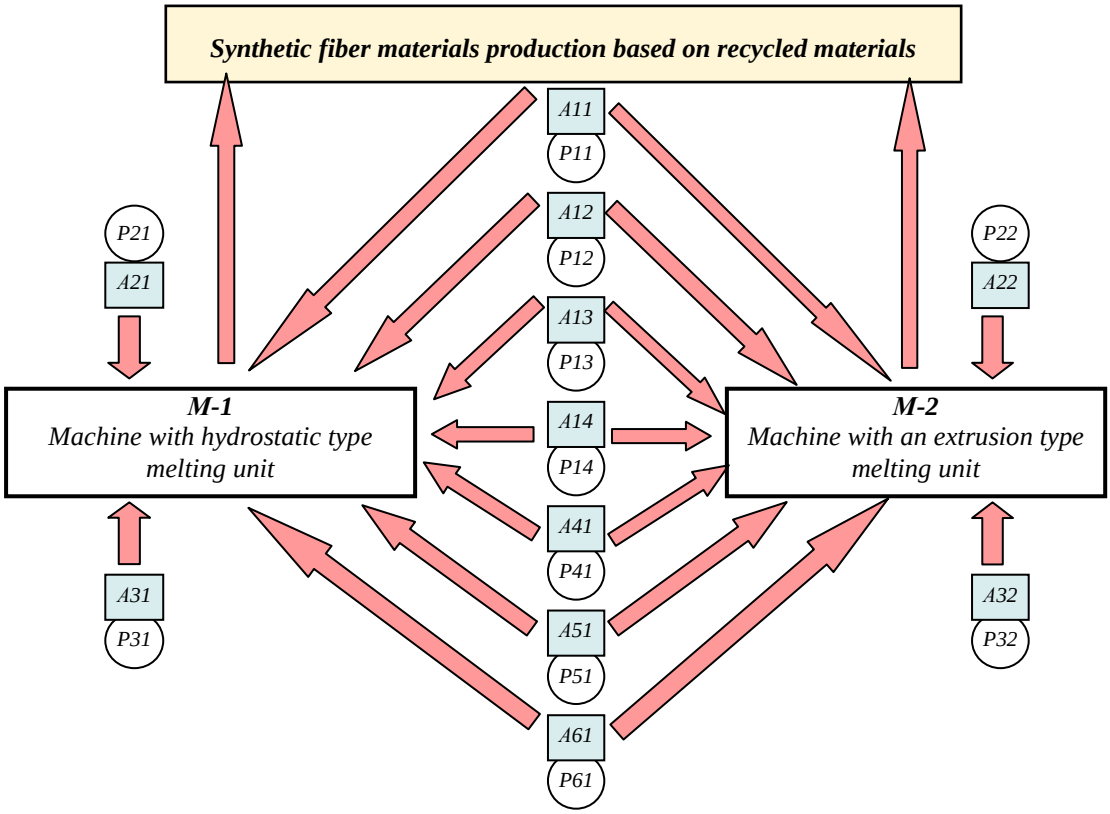

Fig. 2. The structural diagram of machinery and equipment interaction that implements the production of the fibrous materials by blowing from thermoplastics, including secondary ones.

In the production of the fibrous materials, not all aggregates and the corresponding processes in machines M1 and M2 are completely interchangeable (Yankov, 2006). The main structural difference between the machines M1 and M2 is due to the fact that they use fundamentally different melting units, respectively, in the first - the hydrostatic type melting unit A21, and in the second - the extrusion type melting unit A22. They also differ in jet-forming units: in a machine M1 - a jet-forming unit A31 of vertical design, and in a machine M2 - a jet-forming unit A32 of horizontal design. Accordingly, the processes that determine the functioning patterns of these units are different: P21 - the process of melting raw materials in a hydrostatic type melting unit, P22 - the process of melting raw materials in an extruder-type melting unit and P31 - the formation process of molten raw materials jet during vertical flow, P32 - the formation process of molten raw materials jets during the horizontal flow.

The following three machines units under consideration realizing the production of products from fibrous materials based on secondary thermoplastic raw materials are also interchangeable and can be used in similar machines not only developed by the authors M1 and M2, but also in other possible options, these are: A41 and P41 - aggregates and processes fiber formation. A51 and P51 - aggregates and processes of canvas formation. A61 and P61 - aggregates and processes of thermal bonding.

When designing industrial equipment for the fibrous material production from thermoplastics by blowing method, the task is to determine the geometric and energy parameters of the technological process at which the production of fibrous materials with specified quality indicators is provided (Domnina and Repko, 2017). And, first of all, the production of fibrous materials with the required average diameter d_f and length l_f of elementary fibers.

In the vertical-blowing method (Fig. 3), the process of converting a molten thermoplastic, flowing out of a melting unit under hydrostatic pressure, into a fiber is based on the assumption that the airflow generated in the blowing head with an annular nozzle has a double role: stretching the melt jet due to surface friction forces and its separation. According to the first hypothesis - due to aerodynamic forces in turbulent flow, according to the second hypothesis - due to the surface friction forces. Downstream of the airflow, the further movement of elementary fibers occurs under the influence of turbulent airflow, in which, as a result of cooling the fibers, the temperature decreases below the melting point of the material, and the fiber formation process stops.

In the extrusion-blowing method (Fig. 4), the process of obtaining elementary fibers from thermoplastics during horizontal blowing involves the melting and transportation of the feedstock by extrusion. In this case, the melting stream from the die extends horizontally. Due to gravity, the melting stream assumes a shape curved in the vertical plane and also increases by 15 ... 25% in the transverse direction due to a decrease in the flow velocity, and then, due to the viscous flowing state of the melt, the jet diameter gradually decreases. An air stream flowing out of the blowing head slotted nozzle affects the melting stream in the plastic state zone, deforming it, as a result of which it bends, stretches, and bursts into elementary fibers due to the surface friction forces. Further movement of elementary fibers occurs under the influence of turbulent airflow, as a result of their cooling, the process of fiber formation stops.

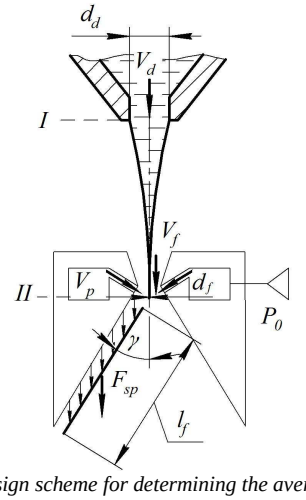

Fig.3. The design scheme for determining the average diameter d_f and length l_f of elementary fibers for the vertical-blowing method

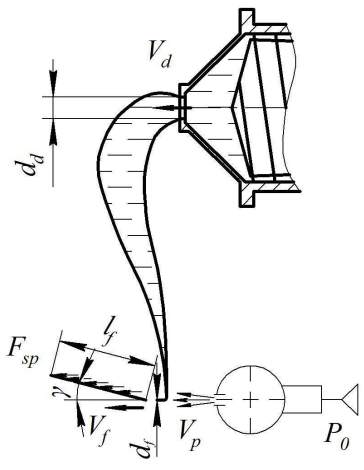

Fig.4. The design scheme for determining the average diameter d_f and length l_f of elementary fibers for the extrusion-blowing method

A theoretical study of the melt flow process shown in Figures 3 and 4 showed that the nature of the melting flow depends on many factors that affect the quality of the resulting fiber, and is a function:

$$d_f, l_f = f\left(V_d, V_p, V_f\right) \tag{1}$$

where V_d is the melt flow speed through the die, m.s^{-1}; V_p – the airflow speed at the blowing head outlet, m.s^{-1}; V_f – the fiber moving speed at the moment of separation, m.s^{-1}.

The design scheme for producing fibrous material by the vertical blowing of a molten thermoplastic jet flowing out under hydrostatic pressure is shown in Fig. 3. A stream of molten thermoplastic flows out of the melting unit, then this stream enters into interaction with a stream of compressed air flowing out of the blowing head. The diameter of a single filament, which is formed by the interaction of an airstream with a molten material stream, can be determined using the continuity equation:

$$Q_I = Q_{II}$$

We determine the volumetric flow rate of the melt jet in sections *I* and *II*, where Q_I is the flow rate at the die section, and Q_{II} is the flow rate in the stretch zone until the jet breaks off by shear.

$$Q_I = V_d \frac{\pi d_d^2}{4}, \tag{2}$$

$$Q_{II} = V_f \frac{\pi d_f^2}{4}, \tag{3}$$

where V_d is the melt flow rate through the die, m.s^{-1}; V_f - fiber speed at the moment of separation, m.s^{-1}; d_d - the die diameter, m; d_f - average diameter of elementary fibers, m.

The fiber velocity at the moment of separation V_{sp} depends on the average speed of the airflow V_p flowing out of the blowing head. It can be assumed that the fiber velocity V_f will be less than the airflow velocity V_p; this decrease can be taken into account by the coefficient K_t.

$$V_f = V_p K_t \tag{4}$$

We take the melting jet flow rate in two sections equal to $Q_I = Q_{II}$, and the coefficient $K_t < 1$ depends on the forces required to burst a solid jet of molten material, as well as on the geometric shape of the blowing head nozzle and the conditions for the formation of the elementary fibers. Then the continuity equation can be written as:

$$V_d \frac{\pi d_d^2}{4} = V_P K_t \frac{\pi d_f^2}{4} \tag{5}$$

Therefore, from equation (5), one can determine the elementary fiber average diameter:

$$d_f = \sqrt{\frac{V_d}{V_P K_t}} d_d \tag{6}$$

Since the fiber velocity depends on the airflow speed, from the formula (6) we can deduce the coefficient K_t:

$$K_t = \frac{V_d d_d^2}{V_p d_f^2} \tag{7}$$

The airflow velocity V_p in the elementary fibers formation zone in the blowing head was investigated and determined in workpieces.

The flow rate of the melt from the melting unit V_d can be determined by the formula:

$$V_d = \frac{G}{\rho_p S} \tag{8}$$

where ρ_p is the molten PET material density, (ρ_p = 1300 kg / m^3) S is the die area, which is determined by: $S = \pi d_f^2 / 4$, m^3; G - volumetric capacity of the melting unit, kg.s^{-1}. The methodology for determining the

volumetric productivity of a hydrostatic type melting unit is presented in the workpiece (Qazizada and Pivarčiová, 2018).

The results of calculating the coefficient K_t are presented in Table 1.

Table 1 - Results of calculating the fiber diameter dв and the coefficient K_t

The blowing head characteristics		The melting unit characteristics		Characteristics calculation results		
P_0, kPa	V_p, m/s	d_d, m	V_d, m/s	d_f, m	V_f, m/s	K_t
50	81	0,0025	0,014	0,000094	32,4	0,4
		0,0035	0,017	0,000140	32,4	0,4
100	163	0,0025	0,014	0,000024	144	0,90
		0,0035	0,017	0,000038	144	0,90
150	258	0,0025	0,014	0,000017	254,8	0,98
		0,0035	0,017	0,000028	254,8	0,98

In addition to pulling the filament from the polymer melt and changing its diameter due to the airflow in the blowing head, there is also a separation force F_{sp}, due to which elementary fibers are formed, *H*.

$$F_{sp} = C_x S \frac{\rho_f V_{av}^2 (\mathrm{tg}\,\gamma)}{2}, \tag{9}$$

where C_x is the thread drag coefficient; V_{av} - the average airflow rate at the outlet of the blowing head annular gap, m.s^{-1}; *S* is the elementary fiber area, m^2, which is defined as: $S = d_f l_f$; ρ_f - gas density, kg / m^3; tg γ is a variable angle that affects the polymer fiber formation along the length lf.

Knowing the separation force F_{sp}, we write down the strength conditions of this elementary thread (Elbakian et al., 2018).

According to the first hypothesis, the separation of elementary fibers occurs due to aerodynamic forces in a turbulent flow, where the tensile stress is defined as the ratio of the separation force F_{sp} to the cross-sectional area of the elementary fiber (Kalentev et al., 2017).

$$\sigma_p = \frac{4F_{sp}}{\pi d_f^2}. \tag{10}$$

Thus, substituting equation (9) into (10), we obtain the general structure of the formula:

$$\sigma_p = \frac{4C_x l_f \rho V_{av}^2 (tg\gamma)}{2\pi d_f}. \tag{11}$$

At the moment of elementary fibers separation, the tensile stress of the thread must be greater or equal to the allowable stress: $\sigma_p \geq [\sigma_p]$. Formula 11 explains how to calculate the elementary fiber length l_f:

$$l_f = \frac{[\sigma_p] 2\pi d_f}{4C_x \rho V_{av}^2 (tg\gamma)}. \tag{12}$$

From formula (12) it follows that the larger the fiber diameter d_f, the more the fiber length l_f increases with an increase in airflow V_{av} at the exit from the blowing head annular gap.

To determine the fiber length lf we take the tensile strength at the time of elementary fibers separation from polyethylene terephthalate σ_p = 49 ... 59 MPa; thread drag coefficient C_x = 0,026. In (Elbakian et al., 2018) were investigated seven diffusers designs with an angle β = 0; 3; 5; 8; 10; 12; 14 deg.

Results of research

The calculations results of fiber length lf depending on a variable angle γ and fiber diameter d_f are presented in Table 2.

From the calculations, it is seen that at an angle $\gamma = 0$ deg. an infinite polymer monofilament is formed, but the larger the angle γ, the polymer fibers in the process of blowing them with air become of a fixed length l_f.

As a result of field tests of the fibrous material obtaining process using secondary polyethylene terephthalate, it was shown that when the melt expires with a temperature $t = 270 \div 280$ ° C through a die with a diameter of d_d = 0,0025 m and airflow affects the resulting monofilament in the blow head working area at P_0 = 50 kPa, fibrous material is formed with an average diameter d_f from 0,000080 to 0,000107 m and a length l_f from 0,1 to 0,5 m at an angle γ = 12 degrees. At d_d = 0,0035 m, an angle of γ = 12 deg and P_0 = 50 kPa, the average fiber diameter d_f was from 0,000097 to 0.000128 m and a length l_f from 0,3 to 0,7 m. After increasing the air pressure in the blowing head to P_0 = 100 kPa, the average fiber diameters at d_d = 0,0025 m, d_f from 0,000010 to 0,000027 m; at d_d = 0,0035 m, respectively, d_f is from 0,000015 to 0,000034 m. In the case of the last two options, the fiber length l_f was from 0,004 to 0,1 m at an angle γ = 12 degrees.

Detailed experimental studies of the blowing head with an annular converging nozzle and the process of fiber formation are presented in workpieces (Straka et al., 2014).

Table 2 - The calculations results of fiber length l_f

P_0, kPa	d_f, m	γ, deg	Fiber length l_f, m	d_f, m	Fiber length l_f, m
50	9.4×10^{-5}	0	Thread goes to ∞	1.4×10^{-4}	∞
		1	1,902		4.101
		3	0,664		1,374
		5	0,382		0,821
		8	0,236		0,506
		10	0,186		0,406
		12	0,156		0,336
		14	0,133		0,281
100	2.4×10^{-5}	0	∞	3.8×10^{-5}	∞
		1	0,0319		0,0533
		3	0,0102		0,0178
		5	0,0061		0,0106
		8	0,0038		0,0066
		10	0,0030		0,0052
		12	0,0025		0,0043
		14	0,0021		0,0037
150	0.000017	0	∞	0,000028	∞
		1	0,0060		0,0166
		3	0,0021		0,0056
		5	0,0012		0,0033
		8	0,00077		0,0021
		10	0,00061		0,0016
		12	0,00051		0,0014
		14	0,00043		0,0012

Conclusion

Despite its low efficiency (compared to material and raw material recycling), the energy recovery of plastic waste is the only suitable recovery method for highly contaminated plastic packaging (agriculture, construction) and for hardly separable plastic waste (multilayer plastic packaging and foils) (Zhang et al., 2014). For the second potential group of plastic waste, for worn tires, the possibilities of material recycling are limited due to their volume. For example, in the US, there is about 10 kg of used tires per capita every year; in the EU, it is about 7 kg. Advantages of energy recycling compared to material recycling:

Waste reduction up to 90%

harmful substances reduction (controlled detoxification)

the possibility of further use of inorganic fractions

Possibility of recovery of contaminated and heavily contaminated plastic waste

the possibility of effective recovery of waste that cannot be recovered through a material or raw material recycling.

The choice of the best plastic waste recycling process depends on several factors. In addition to material characteristics (chemical composition, degree of contamination, the content of inorganic impurities, degree of degradation) and economic indicators (costs of removal, identification, cleaning, sorting), the possibilities of their further application in practice and the environmental impact must be carefully considered.

Thus, the above structural diagram of the technological complex for machines and units interaction that implements the double principle of producing fibrous materials from thermoplastics, which allows solving the problems of their improvement and creating new designs taking into account the peculiarities of the functioning of these processes, and the synthesis of new machines for this purpose (Molenda, 2019).

Also, the article presents methods for calculating the average diameter d_f and length l_f of the fiber when producing fibrous materials by the vertical-blowing method.

References

Bako B., Bozek P.: Trends in Simulation and Planning of Manufacturing Companies. ICMEM 2016, Procedia Engineering, Volume: 149, pp. 571-575.

Baranov M., Bozek P., Prajova V., Ivanova T., Novokshonov D., Korshunov A.: Constructing and calculating of multistage sucker rod string according to reduced stress. Acta Montanistica Slovaca. 2017, Vol. 22, Issue: 2, pp. 107-115.

Beno M., Zvoncan M., Kovac M. Peterka, J.: Circular interpolation and positioning accuracy deviation measurement on five axis machine tools with different structures. In Tehnicki vjesnik-technical gazette. Vol 20 Rel 3, pp 479-484, 2013.

Bozek P., Pivarciova E.: Flexible manufacturing system with automatic control of product quality. In Strojarstvo, Volume 55, Issue 3, April 2013, pp. 211-221.

Bozek P., Pokorný P.: Analysis and evaluation of differences dimensional products of production system. In Applied Mechanics and Materials, Volume 611, 2014, pp. 339-345.

Buransky, I., Morovic, L., Peterka, J. Application of Reverse Engineering for Redesigning and Manufacturing of a Printer Spare Part. Conference: 4th International Conference on Manufacturing Science and Engineering (ICMSE 2013) Location: Dalian, PEOPLES R CHINA Date: MAR 30-31, 2013 Sponsor(s): NE Univ; Harbin Inst Technol; Jilin Univ. MATERIAL DESIGN, PROCESSING AND APPLICATIONS, PARTS 1-4 Book Series: Advanced Materials Research. Published: 2013. Vol 690-693, pp. 2708-2712.

Chaus, A.S., Pokorny, P., Caplovic, E., Sitkevich. MV., Peterka, J.: Complex fine-scale diffusion coating formed at low temperature on high-speed steel substrate. In 2nd International Conference on Applied Surface Science (ICASS) Location: Dalian, PEOPLES R CHINA Date: JUN 12-15, 2017. APPLIED SURFACE SCIENCE. Published: 2018. Vol 437, pp. 257-270.

Domnina K., Repko V.: About the application of computational experiment in the theory of fibro-foam concrete. Bulletin of BSTU. V.G. Shukhov. No.10, 2017, pp. 90-93.

Elbakian A., Sentyakov B., Božek P., Kuric I., Sentyakov K.: Automated Separation of Basalt Fiber and Other Earth Resources by the Means of Acoustic Vibrations. Acta Montanistica Slovaca. Vol. 23, No 3, 2018, pp. 271-281.

Environ. Sci. Technol, 46, 2012, pp. 6431–6437.

Kalentev E., Václav S., Božek P., Korshun;ov A., Tarasov V.: Numerical analysis of the stress-strain state of a rope strand with linear contact under tension and torsion loading conditions. In Advances in Science and Technology Research Journal. Vol. 11, Issue 2, pp. 231-239.

Kobeticova H., Sviatskii, V., Gerulová, K., Wachter, I., Nikitin, Y., Blinová, L. Soldán, M.: The use of waste from bauxite ore in sorption of 3,5-dichlorophenol from waste water. Acta Montanistica Slovaca, Vol. 22, No 4, 2017 pp. 404-411.

Kovac, M. Peterka, J.: Selected 5-axis Strategies for High-speed milling of Thin-walled Parts. In International Conference on Materials Science and Mechanical Engineering (ICMSME 2013) Location: Kuala Lumpur, MALAYSIA Date: OCT 27-28, 2013. MATERIALS SCIENCE AND MECHANICAL ENGINEERING Book Series: Applied Mechanics and Materials. 2014. Vol 467, pp. 466-469.

Molenda M.: Quality Study and Improvement of Logistic Processes on the Example of a Chosen Enterprise. Management Systems in Production Engineering, Volume 27: Issue 1, Published online: 28 Mar 2019, pp. 18–22.

Nemeth, M., Nemethova, A., Michalconok, G.: Determination Issues of Data Mining Process of Failures in the Production Systems. In 8th Computer Science On-Line Conference (CSOC) Location: CZECH REPUBLIC Date: APR 24-27, 2019. ARTIFICIAL INTELLIGENCE METHODS IN INTELLIGENT ALGORITHMS Book Series: Advances in Intelligent Systems and Computing. 2019. Vol 985, pp. 200-207.

Papkov S.: Theoretical foundations of the production of chemical fi bers. Moscow: Chemistry, 1988, 272 pp.

Qazizada E Pivarčiová E.: Reliability of parallel and serial centrifugal pumps for dewatering in mining process. Acta Montanistica Slovaca, Vol. 23, No 2, 2018 pp. 141-152.

Peterka J.: A new approach to calculating the arithmetical mean deviation of a profile during copy milling. In Strojniski vestnik-journal of mechanical engineering. 2004. Vol 50 Rel 12, pp. 594-597.

Peterka, J., Pokorny, P., Vaclav, S.: CAM strategies and surface accuracy. In Annals of DAAAM and Proceedings of the International DAAAM Symposium2008. Annals of DAAAM for 2008 and 19th International DAAAM Symposium", "Intelligent Manufacturing and Automation: Focus on Next Generation of Intelligent Systems and Solutions"; Trnava; Slovakia; 22 October 2008 through 25 October 2008; Code 106299. pp.1061-1062.

Peterka, J., Pokorný, P.: Influence of lead angle from the vertical axis milling on effective radius of the cutter. In Key Engineering Materials. 7th International Congress of Precision Machining, ICPM 2013; Miskolc; Hungary; 3 October 2013 through 5 October 2013; Code 103401. Vol 581, 2014, pp. 44-49.

Pokorný P., Peterka J., Vaclav S., The task of 5-axis milling. In Tehnicki vjesnik-technical gazette. Vol 19, Rel 1, pp 147-150, 2012.

Sentyakov B., Shirobokov K., Sviatskii V.: Processes of obtaining and practical use of polyethylene terephthalate fiber from secondary raw materials. Stary Oskol: Publishing house «TNT», 2014 , 162 pp.

Sentyakov B., Repko A., Sviatskii M., Soldan M., Nikitin Y.: Simulation of oil products separation from fibrous sorbent material centrifugally. Acta Montanistica Slovaca, Vol.21(2016), No 3, pp. 238-246.

Straka M., Bindzár P., Kaduková A.: Utilization of the multicriteria decision-making methods for the needs of mining industry. Acta Montanistica Slovaca, 2014, 19(4). pp. 199-206.

Sviatskii V., Sentyakov B., Sviatskii M., Sentyakov K., Garayev S.: Simulation of the process of fabrication canvas with fibrous materials. In Vestnik ISTU, No. 2, Izhevsk, 2015, pp.17-20.

Sviatskii V., Božek P., Sokolov M.: Determination of melting unit productivity when producing synthetic fibrous materials by vertical blowing method. Acta Technologica Agriculturalurae. Vol. 21, No 4, 2018, pp 139-143.

Sviatskii V., Sentyakov B., Sviatskii M., Sentyakov K., Garayev S.: Simulation of the process of fabrication canvas with fibrous materials. Vestnik ISTU, No. 2., Izhevsk 2015, 2015, pp.17-20.

Smirnov V., Repko A.: Workpiece Temperature Variations During Flat Peripheral Grinding. Management Systems in Production Engineering, Volume 26: Issue 2, Published online: 22 May 2018, pp. 93–98.

Vopat T., Peterka J., Kovac M., Buransky I.: The wear measurement process of ball nose end mill in the copy milling operations. 24th DAAAM International Symposium on Intelligent Manufacturing and Automation; Zadar; Croatia; 23 October 2013 through 26 October 2013; Code 104678 Volume 69, 2014, Pages 1038-10472013

Vopat T., Peterka J., Šimna V.: The influence of different types of copy milling on the surface roughness and tool life of end mills. In 25th DAAAM international symposium on intelligent manufacturing and automation, 2014. procedia engineering Vol 100, pp 868-876, 2015

Yankov V.: Processing of fiber-forming polymers." Moscow-Izhevsk: Research Center "Regular and chaotic dynamics. 2006. 452 pp .

Yim U., Kim M., Ha S., Kim S., Shim W.: Oil Spill Environmental Forensics: the Hebei Spirit Oil Spill Case, 2018, pp.145 – 168.

Zhang S., Wang P., Fu X., Chung, T.: Sustainable water recovery from oily wastewater via forward osmosismembrane distillation (FO-MD), Water Res., 52, 2014, pp. 112–121.

Acta Montanistica Slovaca
ISSN 1335-1788
actamont.tuke.sk

Comparison of spraying nozzles operational parameters of different design

Michał SIEGMUND[1], *Dominik BAŁAGA*[2], *Dagmar JANÁČOVÁ*[3*] *and* *Marek KALITA*[4]

Authors' affiliations and addresses:
[1] KOMAG Institute of Mining Technology, Pszczyńska 37, 44-101 Gliwice, Poland
e-mail: msiegmund@komag.eu

[2] KOMAG Institute of Mining Technology, Pszczyńska 37, 44-101 Gliwice, Poland
e-mail: dbalaga@komag.eu

[3] Tomas Bata University in Zlin, Faculty of Applied Informatics, Nam. T.G.Masaryka 5555, 76001 Zlin, Czech Republic
e-mail: janacova@utb.cz

[4] KOMAG Institute of Mining Technology, Pszczyńska 37, 44-101 Gliwice, Poland
e-mail: mkalita@komag.eu

***Correspondence:**
Dagmar Janáčová, Tomas Bata University in Zlin, Faculty of Applied Informatics, Nam. T.G.Masaryka 5555, 76001 Zlin, Czech Republic
e-mail: janacova@utb.cz

Funding information:
European Regional Development Fund under the project CEBIA-Tech No. CZ.1.05/2.1.00/03.0089

Acknowledgment:
This work was supported by the European Regional Development Fund under the project CEBIA-Tech No. CZ.1.05/2.1.00/03.0089

How to cite this article:
Siegmund, M., Bałaga, D., Janáčová, D. and Kalita, M. (2020). Comparison of spraying nozzles operational parameters of different design. *Acta Montanistica Slovaca*, Volume 25 (1), 24-34

DOI:
https://doi.org/10.46544/AMS.v25i1.3

Abstract
A general methodology for assessing the spraying nozzles in the aspect of dust control efficiency is presented. The testing process, as well as test results analysis, is described on the example of two designs of spraying nozzles (the author solution and the commercial one). Both nozzle designs are discussed with regard to their structure and principle of operation. Parameters describing the absorption surface area in relation to time and working media flowrate are used for analyses of test results.

Keywords
dust, spraying system, optimization, coal

Introduction

Many design solutions of spraying nozzles for dust control, especially in underground hard coal mines (Prostański & Vargová, 2018; Bałaga, 2019; Prostański, 2017a; Bałaga, Kalita, Siegmund & Klimek, 2019; Prostański, 2018) were developed and successfully implemented as well as tools for modelling the dust propagation in mine workings (Prostański, 2015; Prostański, 2017b) were designed in the KOMAG Institute. KOMAG's knowledge is used for the development of new solutions of air-water spraying nozzles. When using the compressed air, the water stream can be atomized to droplets of diameter equal to a dozen or so micrometres. In KOMAG Institute, the STK air-water spraying nozzle with an internal mixing of both agents was developed and implemented (Prostański, 2017a; Prostański, 2013; Prostański, 2012). Spraying systems developed in KOMAG are equipped both with author's designs of spraying nozzles as well as with the nozzles available on the market. Their operational parameters are tested in the KOMAG's laboratory to select their proper type and nozzle diameter. To increase the effectiveness of bonding the dust particles with water droplets, the surface area of dust absorption, i.e. the total surface area of all water drops, should be maximally increased without changing the total volume of the water stream.

Analysis of droplets fraction distribution in a spraying water stream should be used for selection of a proper spraying stream type for the dust control system. Droplets in the atomized water stream make a typical heterogeneous (polydisperse) system, which is characterized by high scatter of drops diameter. Due to the big differentiation in drops sizes of the water stream, the stream is described by the mean drop diameters (Semião, Andrade, Graça Carvalho, 1996). Mean diameter is a representative value, which characterizes a set of the same droplets representing the real drops population. Mean diameter can be different, depending on the parameter of droplets set used for the calculation such as drops number, their diameters, surface areas. It is the parameter used to assess the quality of water dispersion (Chaussonnet, Braun, Dauch, Keller, Sänger, Jakobs, Koch, Kolb, & Bauer, 2019.; Wang, Tan, Zhang, Li & Liu, 2019).

Due to the planned application of the developed nozzle design, i.e. to airborne dust control, volumetric Sauter mean diameter D32 was used in part concerning the test results analyses. This diameter is a diameter of a homogenous representative set of the volume of the same drops and the same total surface area as in the real drops set (Orzechowski & Prywer, 1991; Bałaga, Kalita & Siegmund, 2019; Chidambaram, Arunachalam & Vijayaraghavan, 2015).

The generated absorption surface area can be determined for a time unit or for flow intensity of the spraying medium. In (Bałaga, Kalita & Siegmund, 2019) the authors suggested using the parameter describing the spraying stream in the form of the following absorption surface area of the generated droplets:

- PA/T – Absorption surface area of all droplets in a spraying stream produced within time T equal to 1 min.
- PA/W - Absorption surface area of all droplets in a spraying stream produced after dispersing 1 dm^3 of water.
- PA/P - Absorption surface area of all droplets in a spraying stream produced using compressed air of volume equal to 1 Nm^3.

Testing the operational parameters of the spraying nozzles

In the KOMAG Institute of Mining Technology, both author's spraying nozzle design and that one available on the market were used in the spraying installations. These spraying nozzles, before their installation in the industrial objects, were tested in the KOMAG laboratory regarding their fractional distribution of droplets and spraying media consumption versus their supply pressure. Comparative tests of the following two designs of spraying nozzles:

the air-water spraying nozzle of flat stream manufactured by BETE, type PF250 (Fig. 1).
author’s design solution of STK spraying nozzle, producing the flat stream (Fig. 2),
will be presented.

Two designs of nozzle generating a flat water stream enabling comparison of nozzle operational parameters were used. Tests of water stream parameters for the commercial PF250 spraying nozzle generating a flat stream were conducted within the realization of the doctoral thesis (Bałaga, 2015). Testing the STK type nozzles was realized within the statutory KOMAG's project entitled: Young scientist - Virtual prototyping of spraying nozzles using the additive manufacture technology" (Siegmund, 2016).

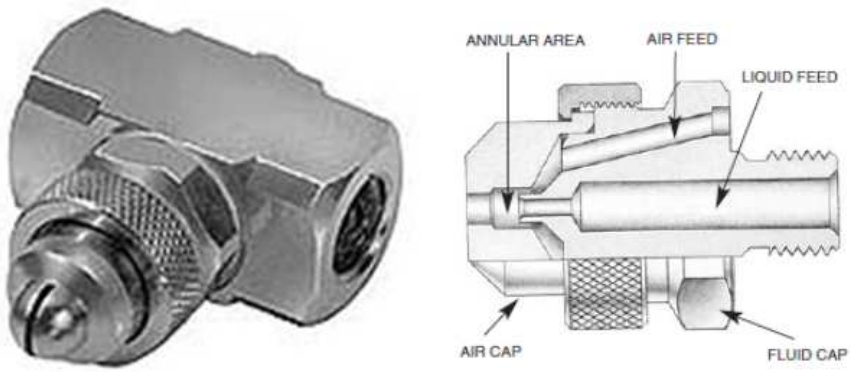

Fig. 1. Design of PF250 nozzle, made by BETE [BETE catalogue]

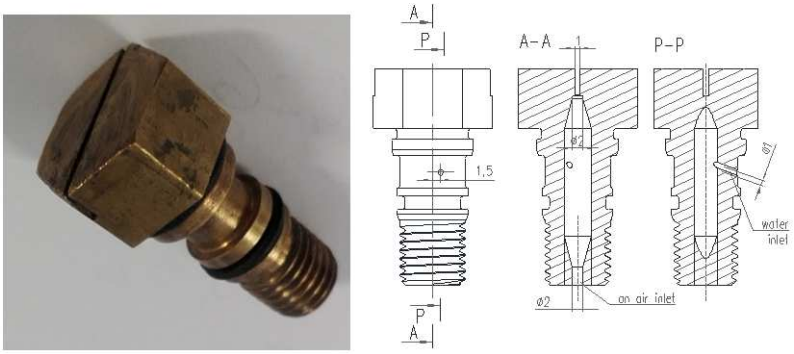

Fig. 2. Design of STK nozzle [Siegmund, 2016]

Testing the nozzles operational parameters consisted of measurements of water flow rate as well as the fractional distribution of droplets in a spraying stream in each nozzle depending on water and compressed air pressures.

Schematic diagram of the test stand is shown in Fig. 3.

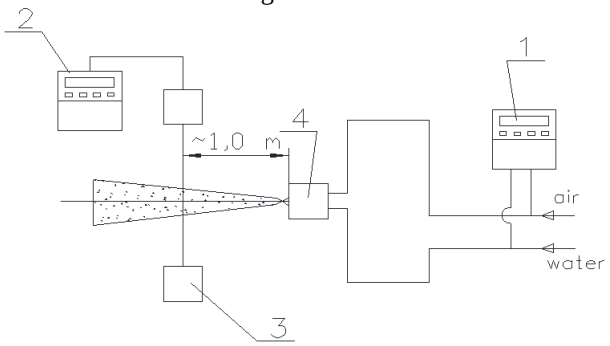

Fig. 3. Schematic diagram of the test stand (Bałaga, 2015; Bałaga & Jaszczuk, 2016): 1- media measuring unit (water and air), 2 - drops analyzer recording device, 3 - drops analyzer, 4 - air-water nozzle with a fixing body.

During the tests, the following parameters were recorded using the special testing infrastructure (Fig . 4):

- distribution of particles diameter in a sprayed stream of liquid,
- supplying pressure and volumetric airflow rate in air mains supplying the nozzle,
- supplying pressure and volumetric water flowrate in water mains supplying the nozzle.

Tests of drops fractional distribution in a spraying stream generated by PF250 nozzle were conducted for 25 combinations of water and air pressures, which were changed every 0.1 MPa within a range from 0.3 to 0.7 MPa. The sample stream generated by PF250 nozzle during the test is given in Fig. 4.

Fig. 4. The test stand during measurements of the distribution of drops diameters in a stream generated by PF250 nozzle (Bałaga, 2015)

For the STK nozzle designed by authors, the measurements were taken for the same pressure of water and air, i.e. 0.3; 0.4; 0.5 or 0.6 MPa. The same pressures of supply water and air were required by the nozzle design to secure proper operation of the nozzle. The sample stream generated by PF250 nozzle during the test is given in Fig. 5.

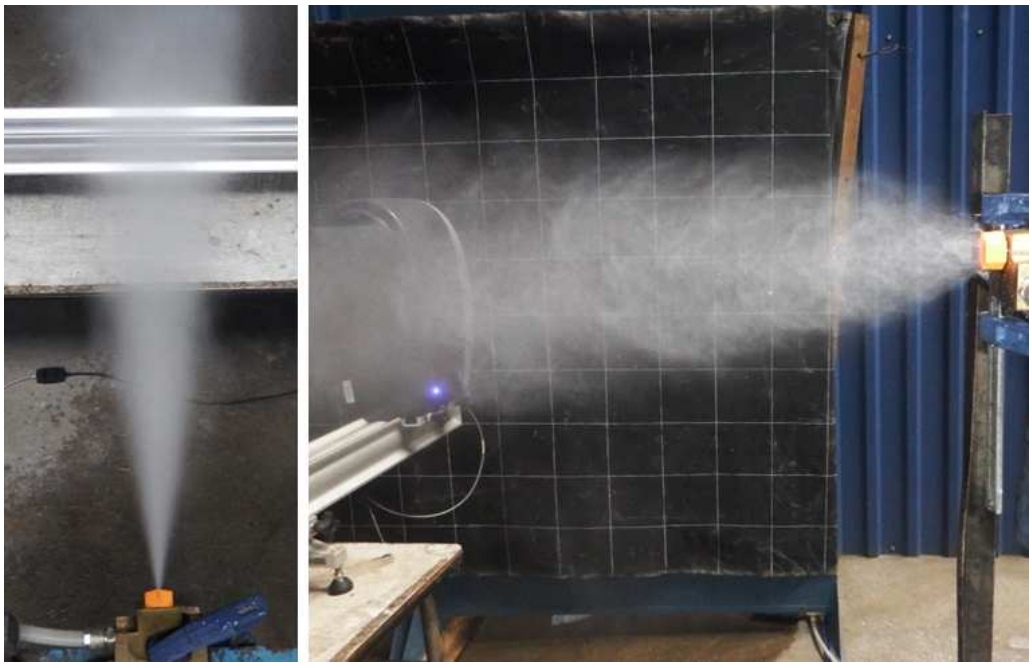

Fig. 5. Flat stream generated by the tested STK nozzle (Siegmund, 2016)

Test results

The results from testing the parameters of the spraying stream for each combination of water and compressed air pressures for the commercial solution of PF250 nozzle are presented in Table 1. Due to the sensitivity of the measuring device, some of the air flowrate results are not given. On the basis of the measured water and compressed air flow rate, as well as D32 Sauter, mean diameter, absorption surface area of the generated water streams was calculated. Due to lack of complete values of compressed air flowrates for PF250 nozzle, it is not possible to create the diagram of air output and absorption surface area in relation to this output (PA/T).

Tab. 1. Results from testing the water stream for different combinations of water and compressed air supply pressures for PF250 nozzle (Bałaga, 2015)

Water supply pressure [MPa]	*Air supply pressure [MPa]*	*Water flowrate [dm^3/min]*	*Air flow rate [Nm^3/min]*	*Mean diameter D (32) [µm]*	*Absorption surface area PA/T [m^2]*	*Absorption surface area PA/W [m^2]*
	0.3	1.5	lack	109.2	82.4	54.9
	0.4	1.2	0.242	63.49	113.4	94.5
0.3	**0.5**	1.3	0.239	29.32	266.0	204.6
	0.6	0.9	0.305	24.78	217.9	242.1
	0.7	0.6	0.337	19.14	188.1	313.5
	0.3	1.7	lack	134.1	76.1	44.7
	0.4	1.5	lack	99.9	90.1	60.1
0.4	**0.5**	1.7	0.264	56.81	179.5	105.6
	0.6	1.3	0.267	44.19	176.5	135.8
	0.7	1.2	0.313	26.43	272.4	227.0
	0.3	2.1	lack	138.9	90.7	43.2
	0.4	2.0	lack	118.6	101.2	50.6
0.5	**0.5**	2.0	0.264	82.39	145.6	72.8
	0.6	1.6	0.301	60.48	158.7	99.2
	0.7	1.5	0.331	37.87	237.7	158.4
	0.3	2.2	lack	129	102.3	46.5
	0.4	2.1	lack	113.6	110.9	52.8
0.6	**0.5**	2.0	lack	97.88	122.6	61.3
	0.6	1.8	0.252	79.75	135.4	75.2
	0.7	1.5	0.301	48.5	185.6	123.7
	0.3	2.2	lack	126.9	104.0	47.3
	0.4	2.2	lack	117.8	112.1	50.9
0.7	**0.5**	2.1	0.238	106.3	118.5	56.4
	0.6	2.0	0.301	93.43	128.4	64.2
	0.7	1.8	0.324	75.41	143.2	79.6

The results from testing the parameters of the spraying stream for different water and compressed air pressures for STK nozzle are presented in Table 2.

Tab. 2. Results from testing the parameters of spraying stream for different water and compressed air pressures for STK nozzle (Siegmund, 2016)

Water supply pressure [MPa]	Air supply pressure [MPa]	Water flowrate [dm^3/min]	Air flow rate [Nm3/min]	Mean diameter D (32) [µm]	Absorption surface area PA/T [m^2]	Absorption surface area PA/W [m^2]	Absorption surface area PA/P [m^2]
0.3	**0.3**	0.20	0.06	25.5	44.7	139.5	1063.1
0.4	**0.4**	0.14	0.101	23.4	35.7	87.0	575.0
0.5	**0.5**	0.16	0.107	19.3	73.2	146.3	101.6
0.6	**0.6**	0.36	0.12	32.5	63.5	99.2	783.6

On the basis of data from Tables 1 and 2, the comparative diagrams for all the tested combinations of the nozzles supply pressures are created. They are presented in Fig. 6 to 14.

In Fig. 6, diagram of water flowrate changes versus pressures of media supplying the PF250 nozzle is given. Water flowrate is equiproportional to its supply pressure and inverse proportional to the compressed air supply pressure.

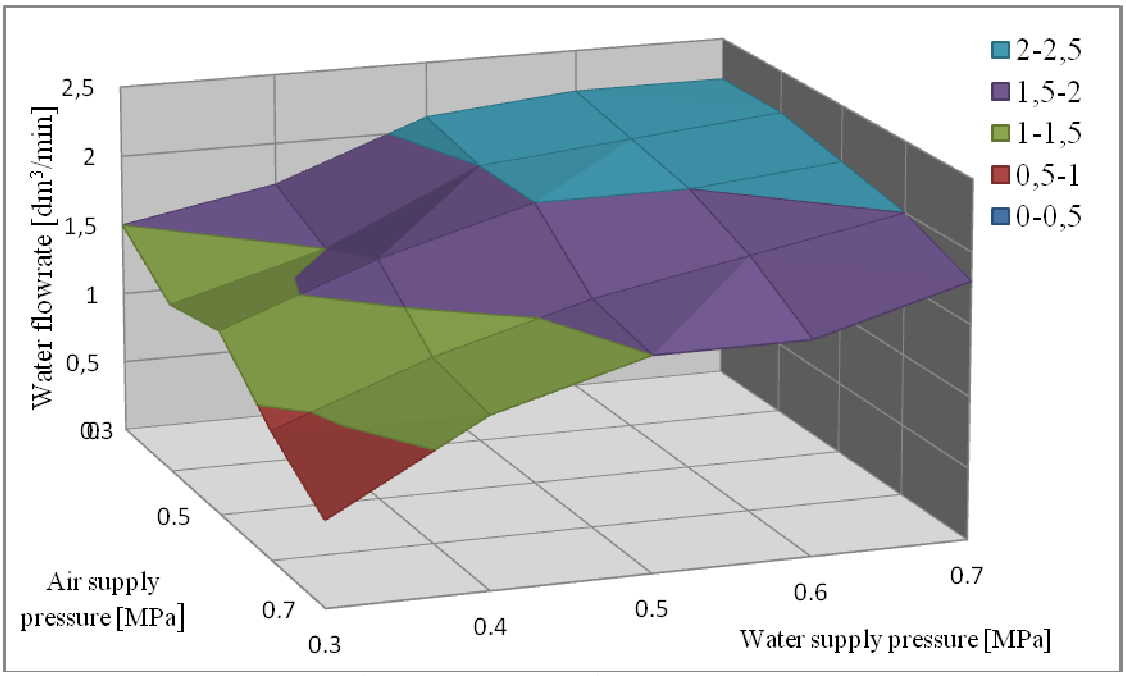

Fig. 6. Water flowrate versus pressures of supplying media in PF250 nozzle

Water flowrate in the case of STK nozzle was significantly lower, and it is given in Fig. 7, where a diagram of water flowrate for PF250 nozzle, when the supply pressure of both media is the same is also given. STK nozzle consumed significantly less water for generation of spraying stream (by about 5 times) than PF250 nozzle.

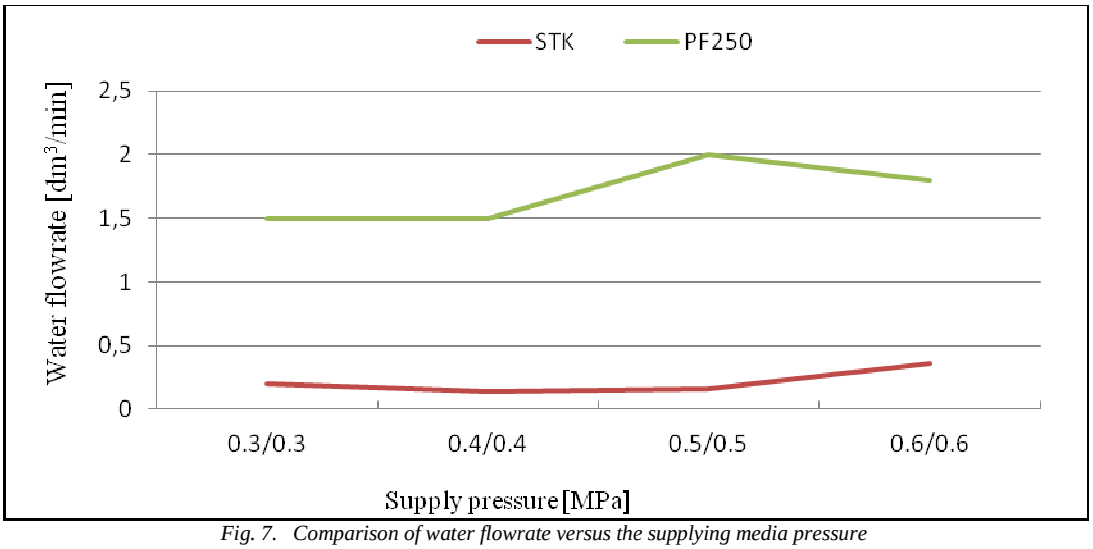

Fig. 7. Comparison of water flowrate versus the supplying media pressure

In Fig. 8, diagram of changes in D(32) Sauter mean diameter, which is the main parameter of the spraying nozzle, versus pressure of media supplying the PF250, is shown. D(32) mean diameter is smallest for the extremely low water pressure and maximum compressed air pressure. In the case of compressed air pressure drop to a minimum, D(32) mean diameter is about 3 times bigger.

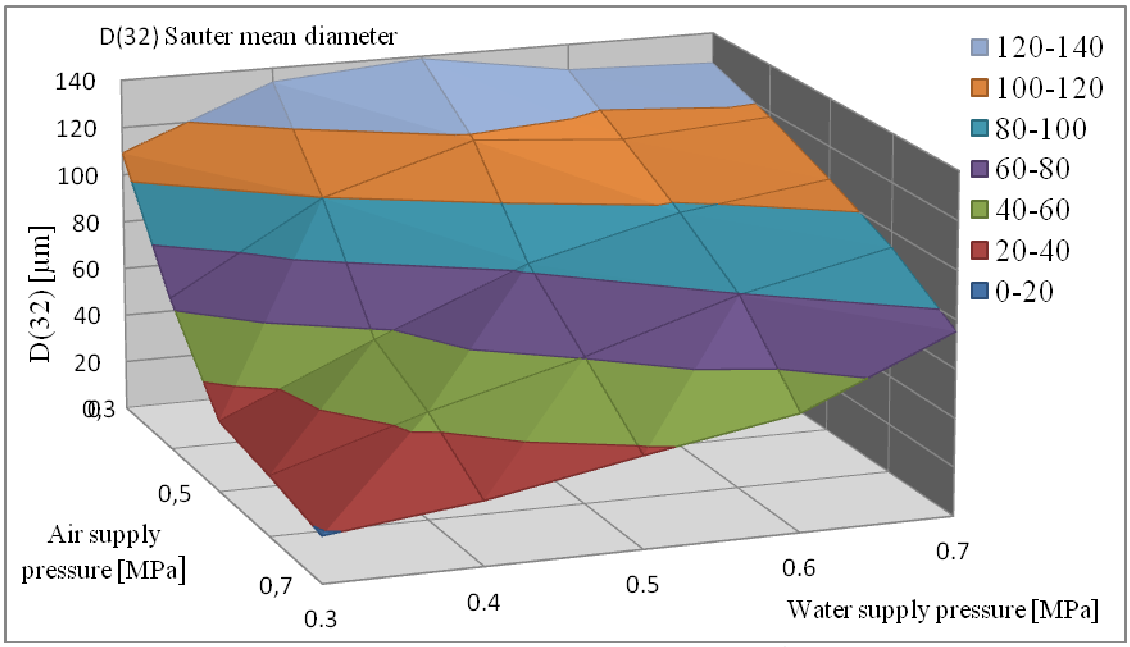

Fig. 8. D(32) mean diameter versus the supplying media pressure for PF250 nozzle

Comparison of D(32) Sauter mean diameter for both nozzles at the same supply pressure of both media is given in Fig. 9. Significantly bigger (by about 3 times) mean diameter in the case of PF250 nozzle can be observed.

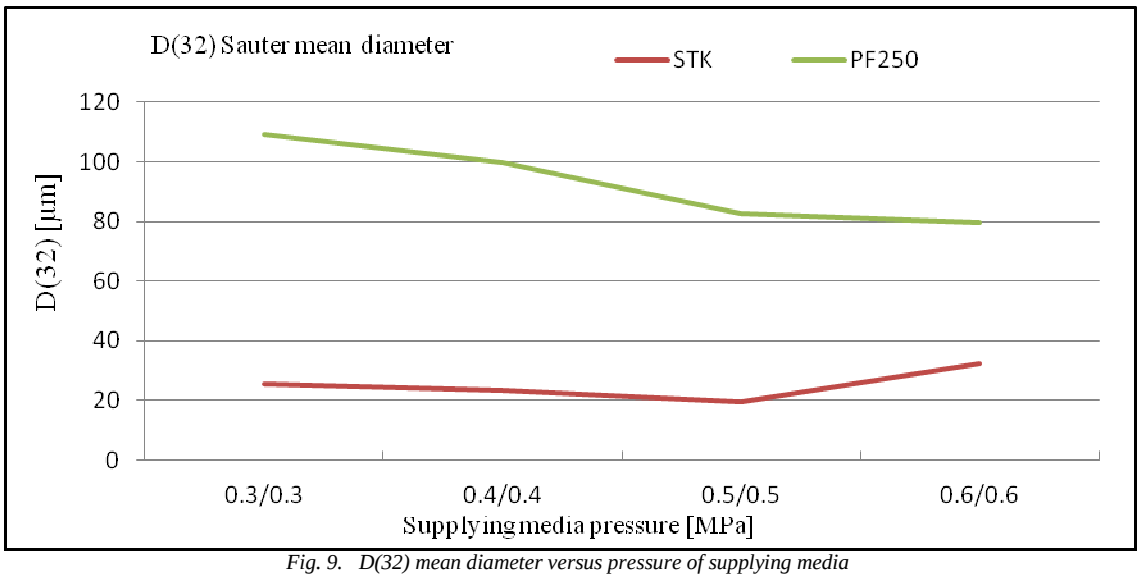

Fig. 9. D(32) mean diameter versus pressure of supplying media

For the analysis of the generated absorption surface area, the diagram of changes in the absorption surface area PA/T versus the combination of supplying media pressure for PF250 nozzle is given in Fig. 9. The best results regarding the surface area, which can be produced within 1 minute are obtained for the combination of air pressure 0.5 MPa and water pressure 0.3 MPa as well as for air pressure 0.7 MPa and water pressure 0.4 MPa.

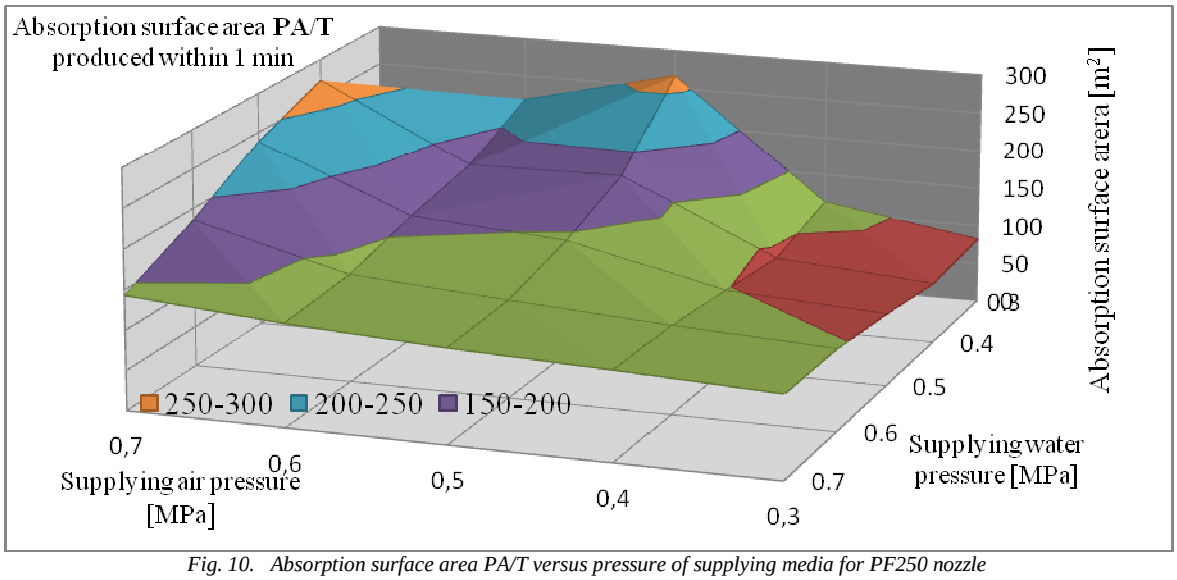

Fig. 10. Absorption surface area PA/T versus pressure of supplying media for PF250 nozzle

Comparison of absorption surface area generated within 1 min by both nozzles is given in Fig. 11. It can be noticed that PF250 nozzle produced an absorption surface area by about 2-2.5 times greater than STK nozzle.

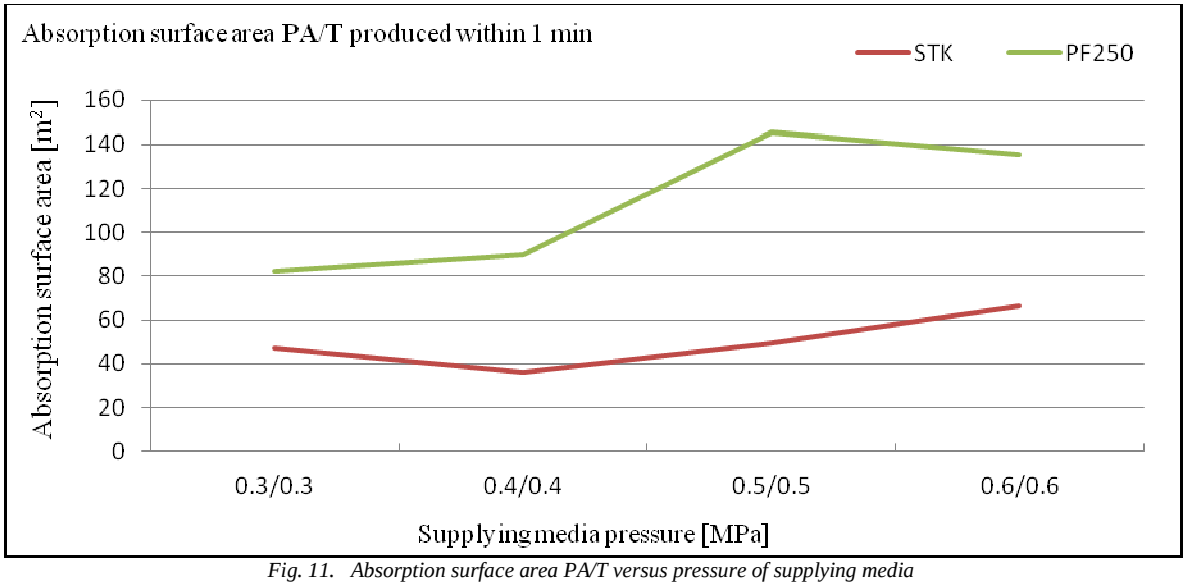

Fig. 11. Absorption surface area PA/T versus pressure of supplying media

In Fig. 12, absorption surface area PA/W changes versus the combination of supplying media pressures for PF250 nozzle is presented. Comparing absorption surface areas produced from 1 dm^3 of water, an increase of PA/W with a decrease in water pressure and increase of compressed air pressure can be observed.

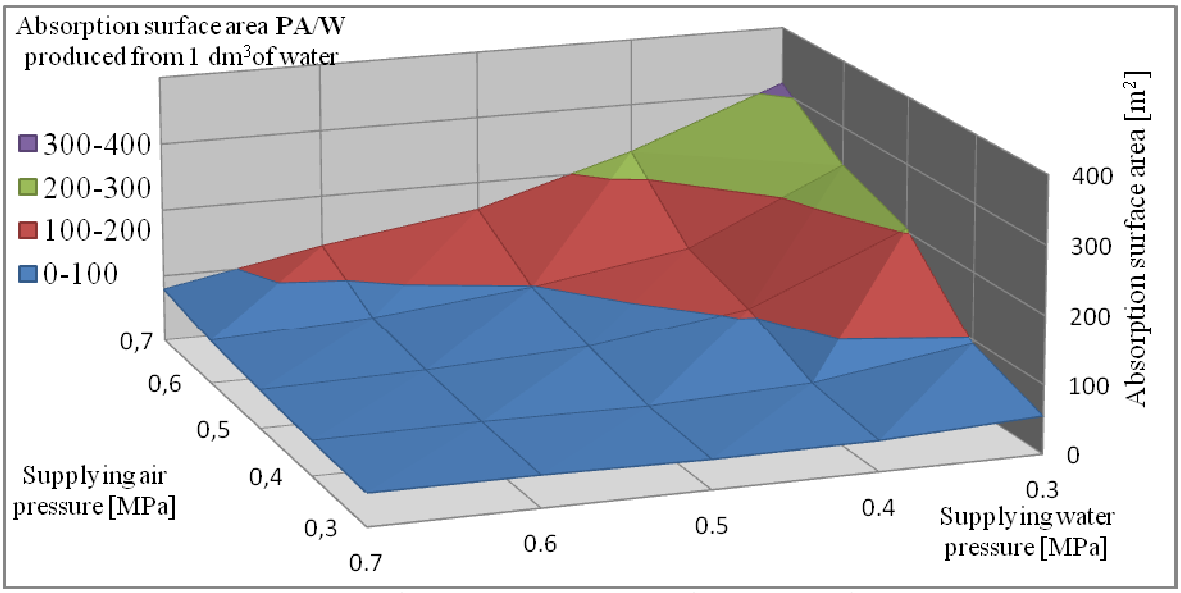

Fig. 12. Absorption surface area PA/T versus pressures of supplying media for PF250 nozzle

Comparison of absorption surface area produced from 1 dm^3 of water for both nozzles is presented in Fig. 13. STK nozzle produced 3 times greater surface area than PF250 nozzle.

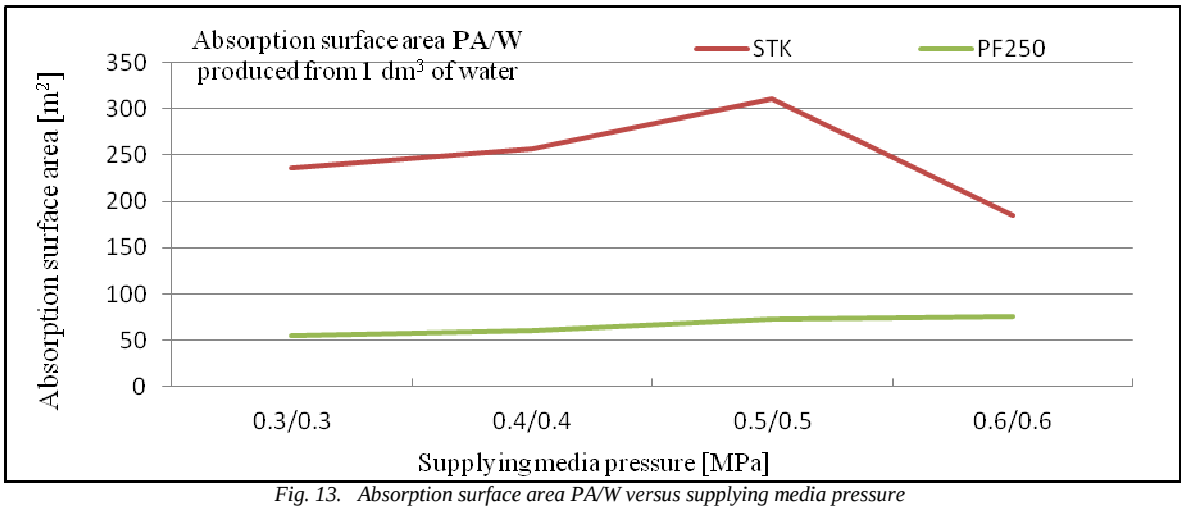

Fig. 13. Absorption surface area PA/W versus supplying media pressure

In Fig. 14 a diagram of changes in absorption surface area PA/P versus supplying media pressure for both nozzles is given. For PF250 nozzle, due to lack of all the data, the diagram is presented only for supply pressures 0.5 and 0.6 MPa.

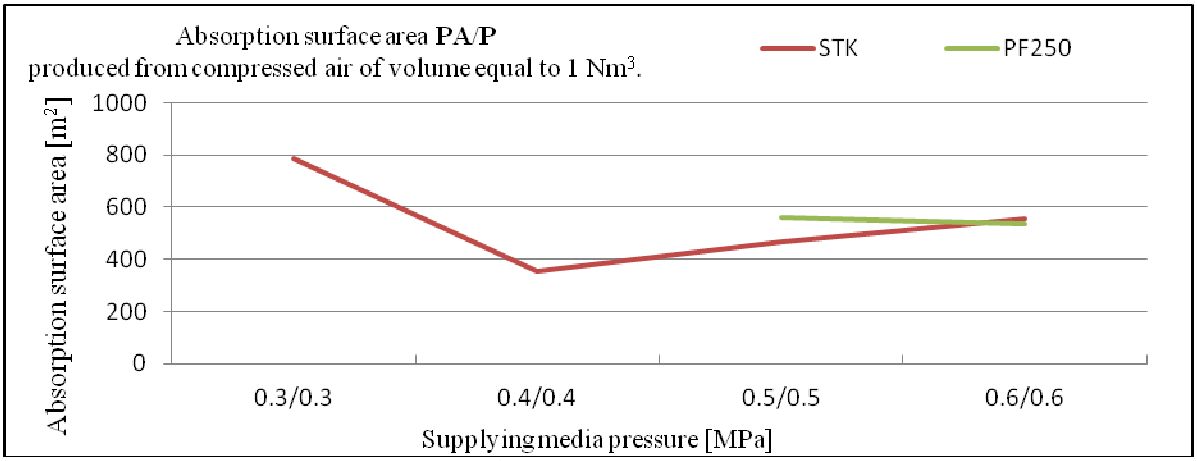

Fig. 14. Absorption surface area PA/P versus supplying media pressure

Conclusions

Research projects, realized at KOMAG and focused on development and implementation of the systems for airborne dust control, require correct selection of nozzle type and its diameter. Depending on the place characteristics as well as parameters of available supplying media, the spraying systems should be equipped with the spraying nozzles, adapted as much as possible to the operational conditions. Bearing in mind that increase of dust control efficiency is equiproportional to a reduction of the drop mean diameter in the spraying water stream, type of nozzle should be selected in a way enabling to generate the drops of diameters as small as possible. At the same time, other assumed operational parameters such as range or media flowrate should be followed. Measurements of stream parameters should be taken in a few points within the effective range of the stream to assess stream homogeneity and repeatability of its parameters.

On the basis of the results from testing the PF250 nozzle at different combinations of supplying media pressures, it can be concluded that:

- Change in the pressure of one medium changes the flowrate of both media.
- The smallest D(32) mean diameter was obtained for the combination of extreme pressures of water (0.3 MPa) and air (0.7 MPa).
- The biggest absorption surface area of a stream generated within 1 min is obtained for compressed air pressure higher than water pressure by 0.2-0.3 MPa.

Comparison of two spraying nozzles of different design enables to conclude that:

- STK nozzle consumes about 5 times less water.
- D(32) Sauter mean diameter for PF250 nozzle was about 4 times bigger than STK nozzle.
- Absorption surface area of a stream generated by PF250 nozzle at the same time was 2.0 – 2.5 times bigger than the surface area generated by the STK nozzle.
- Taking into account absorption surface area produced from 1 dm^3 of water, STK nozzle is 5 times more efficient.
- There are no significant differences in compressed air consumption regarding the absorption surface area within a similar range.

References

Bałaga, D. (2015) Wpływ parametrów strumienia zraszającego na redukcję zapylenia generowanego przez kombajn ścianowy. [Impact of spraying stream parameters on a reduction of dust generated by a longwall shearer]. Doctoral thesis. Gliwice, Poland. (not published).

Bałaga, D. (2019). Assessment of efficiency in reduction of dust concentration in mineral processing plants using the state-of-the-art technical measures. *New Trends In Production Engineering*, *2*(1), 11-19. doi: 10.2478/ntpe-2019-0001

Bałaga, D., & Jaszczuk, M. (2016) Wpływ parametrów strumienia zraszającego na redukcję zapylenia generowanego przez kombajn ścianowy. [Impact of spraying stream parameters on a reduction of dust generated by a longwall shearer]. Scientific Projects- KOMAG Monographs. KOMAG Institute of Mining Technology No. 47

Bałaga, D., Kalita, M., & Siegmund, M. (2019). Analysis of fraction distribution of the water drops stream generated by the spraying nozzles of new KOMAG design. Paper presented at the *IOP Conference Series: Materials Science and Engineering, , 545*(1) doi:10.1088/1757-899X/545/1/012010

Bałaga, D., Kalita, M., Siegmund, M., & Klimek, Z. (2019). Measurements of dust concentration at workplaces in a hard coal mine processing plants after installation of the NEPTUN spraying system. Paper presented at the *IOP Conference Series: Materials Science and Engineering*, *545*(1) doi:10.1088/1757-899X/545/1/012005

Chaussonnet, G., Braun, S., Dauch, T., Keller, M., Sänger, A., Jakobs, T., Koch, R., Kolb, T., & Bauer, H. -. (2019). Toward the development of a virtual spray test-rig using the smoothed particle hydrodynamics method. *Computers and Fluids, 180*, 68-81. doi:10.1016/j.compfluid.2019.01.010

Chidambaram E.L., Arunachalam N., & Vijayaraghavan L. (2015), Analytical Model to Predict Sauter Mean Diameter in Air Assisted Atomizers for MQL in Machining Application. *Procedia CIRP*,37, pp. 117-121. doi.org/10.1016/j.procir.2015.09.007.

Orzechowski, Z., & Prywer, J. (1991). Rozpylanie cieczy. [Spraying of liquid.] Warszawa, Poland: Wydawnictwo Naukowo Techniczne, ISBN 83-204-1378-8

Prostański, D. (2012). Dust control with use of air-water spraying system. *Archives of Mining Sciences*, *57*(4), 975-990. doi:10.2478/v10267-012-0065-7

Prostański, D. (2013). Use of air-and-water spraying systems for improving dust control in mines. Journal of Sustainable Mining, 12(2), 29-34. doi:10.7424/jsm130204

Prostański, D. (2015). Experimental study of coal dust deposition in mine workings with the use of empirical models. *Journal of Sustainable Mining, 14*(2), 108-114. doi:10.1016/j.jsm.2015.08.015

Prostański, D. (2017a) Zraszanie powietrzno-wodne jako metoda ograniczenia zagrożenia zapłonem metanu i wybuchem pyłu węglowego oraz redukcji zapylenia powietrza. [Air-and-water spraying as a method of reducing hazards of methane ignition and coal dust explosion and a reduction of dust inthe air]. Scientific Projects- KOMAG Monographs. KOMAG Institute of Mining Technology No. 51. ISBN 978-83-65593-07-8.

Prostański, D. (2017b). Empirical models of zones protecting against coal dust explosion. Archives of Mining Sciences, 62(3), 611-619. doi:10.1515/amsc-2017-0044

Prostański, D. (2018). Development of research work in the air-water spraying area for reduction of methane and coal dust explosion hazard as well as for dust control in the Polish mining industry. Paper presented at the *IOP Conference Series: Materials Science and Engineering, 427*(1) doi:10.1088/1757-899X/427/1/012026

Prostański, D., & Vargová, M. (2018). Installation optimization of air-and-water sprinklers at belt conveyor transfer points in the aspect of ventilation air dust reduction efficiency. *Acta Montanistica Slovaca, 23*(4), 422-432.

Semião, V., Andrade, P. & Graça Carvalho M., (1996). Spray characterization: Numerical prediction of Sauter mean diameter and droplet size distribution. *Fuel,* 75, pp. 1707-1714 doi.org/10.1016/S0016-2361(96)00163-9.

Siegmund, M. (2016) Młody naukowiec. Wirtualne prototypowanie konstrukcji dysz zraszających wykorzystujące technologię druku 3D. [Young Scientist. Virtual prototyping of spraying nozzles using 3D print technology]. Report on the work realization. Gliwice, Poland. (not published).

Wang, P., Tan, X., Zhang, L., Li, Y. & Liu, R., (2019). Influence of particle diameter on the wettability of coal dust and the dust suppression efficiency via spraying. *Process Safety and Environmental Protection*, 132, pp. 189-199. doi.org/10.1016/j.psep.2019.09.031

Acta Montanistica Slovaca
ISSN 1335-1788
actamont.tuke.sk

Kinetic analysis of the dissolution of natural magnesite in nitric acid

Maryna KYSLYTSYNA[1], Pavel RASCHMAN[2], Ľuboš POPOVIČ[3] and Gabriel SUČIK[4]*

Authors' affiliations and addresses:
[1] Faculty of Materials, Metallurgy and Recycling, Technical University of Košice, Slovakia,
e-mail: maryna.kyslytsyna@tuke.sk

[2] Faculty of Materials, Metallurgy and Recycling, Technical University of Košice, Slovakia,
e-mail: pavel.raschman@tuke.sk

[3] Faculty of Materials, Metallurgy and Recycling, Technical University of Košice, Slovakia,
e-mail: lubos.popovic@tuke.sk

[4] Faculty of Materials, Metallurgy and Recycling, Technical University of Košice, Slovakia,
e-mail: gabriel.sucik@tuke.sk

***Correspondence:**
Maryna Kyslytsyna, Faculty of Materials, Metallurgy and Recycling, Technical University of Košice, Slovakia,
tel: +421 55 602 2560
e-mail: maryna.kyslytsyna@tuke.sk

Funding information:
Agency of the Ministry of Education, Science, Research and Sport of the Slovak Republic for the Structural Funds of EU 26220220131

Acknowledgement:
This work was supported by the Agency of the Ministry of Education, Science, Research and Sport of the Slovak Republic for the Structural Funds of EU, Operational Programme Research and Development, funded by the European Regional Development Fund (Grant ID: 26220220131, project "Advanced Technologies for a Mining Company of the 21st Century").

How to cite this article:
Kyslytsyna, M., Raschman, P., Popovič, P. and Sučik, G. (2020). Kinetic analysis of the dissolution of natural magnesite in nitric acid. *Acta Montanistica Slovaca*, Volume 25 (1), 35-45

DOI:
https://doi.org/10.46544/AMS.v25i1.4

Abstract
Leaching kinetics of natural magnesite with nitric acid was investigated, and the results of a detailed critical analysis are presented. The reaction system $MgCO_3$-HNO_3-H_2O has been studied with special regard to the production of pure magnesium salts. The generalised non-porous shrinking particle model considering the n-th order liquid-solid reaction was fitted to the measured kinetic data and the values of apparent activation energy, E_A, and reaction order, n, were calculated. Relatively high values of E_A (43.7 and 58.5 kJ mol^{-1}) obtained for both "low" (0.01-0.1 M) and "high" (1-6 M) concentrations of HNO_3, respectively, lay within the range of values presented by other authors and indicate that the overall process is controlled by the chemical reaction in the whole range of reaction conditions considered (temperature from 70 to 100°C and concentration of HNO_3 from 0.01 to 6M). This hypothesis has been confirmed by the calculated values of n, which considerably differ from 1. Until now, it has been assumed in the literature that n=1 and no attention has been paid to the actual mechanism of the intrinsic chemical reaction. In this work, the value of n=0.22 was calculated for the solutions with "low" HNO_3 concentration, and n=0.05 was obtained for the concentrated HNO_3 solutions. These values of n are considerably lower than the value of n=0.5, predicted by the theory. It is hypothesised that the decrease in n with increased acid concentration might be related to the formation of CO_2 and its transfer from the liquid to the gaseous phase.

Keywords
Leaching, shrinking particle model – verification, reaction order, activation energy, rate-determining step.

Introduction

Although magnesium is found in over 60 minerals, only *magnesite* and other five industrial minerals (dolomite, carnallite, serpentine, brucite and olivine), alongside seawater and brines, are commercially important natural sources of this element (Roskill 2013; USGS, 2019). Formally known as *magnesium carbonate* ($MgCO_3$), magnesite is found around the world (predominantly in Australia, Austria, Brazil, Canada, China, Greece, India, North Korea, Russia, Serbia, Slovakia, Spain and Turkey (Roskill, 2013, EC, 2015)), and its properties make it an invaluable raw-material in numerous fields.

Traditional products made from magnesite are refractory materials, mainly for producing steel, cement and nonferrous metals. More than 99% of mined and beneficiated magnesite is heat-treated to obtain *magnesia* (magnesium oxide, MgO) – similarly to the production of quicklime from limestone. There are three grades of magnesia available in the market: fused magnesia (FM), dead burned magnesia (DBM) and caustic calcined magnesia (CCM). While the DBM and FM are consumed in the production of refractory materials, CCM is mostly used in chemical-based applications such as fertilisers and livestock feed, pulp and paper, hydrometallurgy and waste-water treatment (Merchant, 2019; Roskill, 2013). However, the producers of magnesite in Europe, the United States, Russia, and other regions have permanently been forced to develop new products and look for new applications – there are at least three major reasons (IHS Markit, 2017; Merchant, 2019; Roskill, 2013): (a) never-ending effort of the steelmakers and cement producers to reduce the specific consumption of refractories; (b) limited growth of global steel and cement production, which has not been able to compensate the corresponding slackening in demand for refractory materials; and (c) huge China's exports of cheaper refractory grade magnesia during last decade. Thus, over the past three decades, the use of magnesite products has spread to agriculture, chemical, pharmaceutics and construction industries, and environmental protection (Roskill, 2013; Shand, 2006). Unlike FM and DBM, demand is foreseen to increase in many end uses; acquisitions take place in the market, and new capacities are appearing (Merchant, 2019; Roskill, 2013). New perspective applications are CCM, lightweight aluminium-magnesium alloys for structural components of automobiles and machinery, and *pure magnesium compounds*, especially the hydroxide and salts of various inorganic and organic acids (Merchant, 2019; Roskill, 2013; Shand, 2006).

The present work is related to the chemical processing of magnesite into pure magnesium salts. Though the added cost of chemical processing (as compared to the beneficiation of rich ores by physical methods) restricts its use in general, the relative scarcity of high-quality magnesite deposits means in certain circumstances it can be viable to upgrade magnesite via chemical route. Moreover, in mining and beneficiation of magnesite, individual operations can (and normally do!) produce low-grade magnesite which is in traditional manufacturing actually of no use; such a less-valuable, secondary magnesite raw material can advantageously be used as a feed-stock for the chemical processing. Thus, the chemical production of pure magnesium salts seems to be one way how to expand the portfolio of high value-added products, make full use of the extracted magnesite and achieve desired economic effectiveness even with smaller volumes of mined magnesite.

Like a typical hydrometallurgical process (Crundwell 2014; Habashi 2005) and many important processes in inorganic chemical technology (such as the production of alumina (Habashi, 2005), magnesia (Shand, 2006) or titanium dioxide (Bedinger, 2018)), the chemical production of pure magnesium salts from magnesite includes three main stages: (a) *leaching* of the raw-materials, (b) *purification* of the leachate, and (c) *separation* of the valuable substance in the form of a saleable product. The leaching stage requires special interest because it determines the technological demands and thus economic viability of the whole process.

The leaching generally involves a rather complex set of elementary steps represented by the transport phenomena and intrinsic chemical reaction(s). It is well known that (Sohn, 1979): (a) Under certain conditions, some of these elementary steps may become the *rate-determining step (RDS)* of the overall process; (b) the RDS can change depending upon reaction conditions, and thus rate information obtained under a given set of conditions may not be applicable under another set of conditions; (c) frequently there may not be a single rate-controlling step because several steps may have more or less equal effects on determining the overall rate. The relative importance of these steps could also change in the course of the reaction. Thus, understanding how the individual reaction steps interact with each other is important in determining not only the RDS under given reaction conditions but also whether more than a single step must be considered in expressing the overall rate (Sohn, 1979).

While certain generalisations can be made for heat and mass transfer, and pore diffusion, the adsorption and chemical reaction(s) are highly specific to the nature of the substances involved (Sohn, 1979). With special regard to the manufacturing of pure magnesium salts from magnesite using chemical methods, a number of papers have recently been published to study the leaching kinetics of magnesite in solutions of inorganic and organic acids (Abali et al., 2006; Bakan et al., 2006; Bayrak et al., 2006; Hoşgün and Kurama, 2012; Köse, 2012; Laçin et al., 2005; Özbek et al., 1999; Raza et al., 2013, 2014, 2015, 2016; Rutto and Enweremadu, 2011). However, only the temperature dependence of the leaching rate was examined, and no attention has been paid to the concentration dependence of the intrinsic kinetics, at all.

The aim of this work is a detailed kinetic analysis of the nitric acid leaching of magnesite, and the paper breakdown is as follows:

1. Formulation of a suitable simulation model to describe the leaching behaviour of the studied reaction system.
2. Model fitting to the results of kinetic leaching experiments and calculating the apparent reaction order (n) and activation energy (E_A).
3. Determination the RDS of the nitric acid leaching of natural magnesite, based on both n and E_A.

Theoretical

Simulation model of the leaching process. Let us consider an agitated tank leaching, where the ground raw magnesite with a known content of magnesium carbonate (designated as the solid substance B) undergoes a chemical reaction in the leach solution with hydrogen cations (designated as the species A), and soluble magnesium salt (for example, nitrate), carbon dioxide and water are formed. The overall process involves three steps in a series, which are as follows:

1. Mass transfer of the hydrogen cations from the bulk leach solution to the surface of magnesite particles.
2. The chemical reaction between the reactants A and B at the phase interface, according to Eq. (1),

$$B(s) + aA(aq.) \rightarrow soluble\ products \tag{1}$$

3. Mass transfer of the dissolved products from the surface of the solid particles into the main body of the lixiviant.

For the kinetic regime of leaching, when chemical reaction controls the overall rate of the process, Raschman et al. (2019) derived a generalised non-porous shrinking particle model (NSPM) which can be written in a shortened form using Eq. (2),

$$\frac{dx_B}{dt} = \frac{\frac{3}{R}}{\rho_S}\frac{\rho_L^0}{c_{Ab}^0}\frac{\phi}{\sigma} r_A^0 F(x_B), \tag{2}$$

where:

x_B = fraction of species B reacted (degree of conversion of species B);

t = reaction time;

R = initial radius of magnesite particles (i.e., the radius at $t=0$);

ρ_S = density of magnesite particles;

ρ_L^0 = initial density of the lixiviant (leach solution);

c_{Ab}^0 = initial concentration of hydrogen cations in the lixiviant: strong acids such as the nitric or hydrochloric acid are strong electrolytes and are practically fully ionised in water, c_{Ab}^0 is therefore assumed to be equal to the initial concentration of the acid;

ϕ = *reduced* A/B molar ratio, $\phi = n_A^0/(an_B^0)$;

n_A^0 and n_B^0 = initial total amount (in moles) of the species A and B, respectively;

a = stoichiometric coefficient for the species A in Eq. (1);

σ = *liquid-to-solid (L/S) mass ratio*, $\sigma = m_L^0/m_S^0$;

m_L^0 and m_S^0 = initial mass of the lixiviant and magnesite feed-stock, respectively;

r_A^0 = initial rate of the chemical reaction (1) defined by Eq. (3),

$$r_A^0 = k\gamma_A^n (c_{Ab}^0)^n = k_0 exp\left(-\frac{E_A}{R_G T}\right)\gamma_A^n (c_{Ab}^0)^n; \tag{3}$$

k = rate-constant for the reaction (1), n-th order in A;

T = temperature;

γ_A = activity coefficient of the species A in the leach solution;

n = order of chemical reaction (1) with respect to reagent A;

k_0, E_A and R_G = constants ("frequency factor", apparent activation energy of reaction (1) and gas constant, respectively) in Arrhenius´ equation $k = k_0 \exp\left(-\frac{E_A}{R_G T}\right)$;

$F(x_B)$ = function of the fraction of species B reacted, x_B, defined as follows:

$$F(x_B) = \left(1 - \frac{x_B}{\phi}\right)^n (1 - x_B)^{\frac{2}{3}}. \tag{4}$$

Unlike the commonly used *"simple"* NSPM (see, for example, Levenspiel (1999), Sohn (1979) or Wadsworth (1979)), the *generalised* NSPM assumes $n-th$ *order chemical reaction*, the influence of the *L/S ratio* and *non-ideal behaviour* of the leach solution.

For mathematical simplicity, in a kinetic analysis, it is advantageous to apply a *simplified form* of the NSPM. The *simplified* NSPM represents the solution of Eqs. (2) to (4) based on the assumption that $n = n$, $\boldsymbol{\phi} \gg \mathbf{1}$ and $\gamma_A = f(c_{Ab}^0)$ – it can be written in the form of Eqs. (5) and (6) (Raschman et al. 2019):

$$1-(1-x_B)^{\frac{1}{3}} = \frac{t}{t_R}, \tag{5}$$

$$t_R = \frac{a n_B^0 \rho_S R}{m_S^0 k_0 exp\left(-\frac{E_A}{R_G T}\right) \gamma_A^n (c_{Ab}^0)^n} \quad . \tag{6}$$

where: t_R = the time required for the complete conversion of a particle of the original raw material.

Sometimes, for practical purposes, the *reaction half-time, $t_{0.5}$* (i.e. the time required under certain reaction conditions to dissolve one half of the amount of the valuable substance B initially present in the raw materials), is used as the characteristic time of the leaching process; in such a case $t_{0.5} = 0.2063 t_R$ and Eq. (5) can be modified to Eq. (7) (Raschman et al., 2019):

$$1-(1-x_B)^{\frac{1}{3}} = 0.2063 \frac{t}{t_{0.5}}. \tag{7}$$

Material and Methods

Materials. The bulk natural raw magnesite (RM) from the SMZ Jelšava plant, Slovakia, was used in the leaching experiments. The fraction +80-125 μm was prepared by dry mill-grinding, wet-screening, washing by deionised water and drying. The physico-chemical characteristics of the RM sample are given in Table 1. The sample was analysed by wet chemical methods combined with the ICP analysis. Thermal and X-ray powder diffraction analysis proved a ferroan variety of magnesite (breunnerite) to be the prevailing phase, accompanied by small amounts of dolomite and calcite – the results are summarised in Fig. 1. The specific surface area sA < 0.1 m2 g-1 was determined by the B.E.T. nitrogen adsorption technique. Analytical reagent grade chemicals and deionised water were used in all experiments.

Table 1. Physico-chemical characteristics of used raw magnesite (RM)

Particle diameter [10^{-6} m]	Specific surface area [10^3 m^2 kg^{-1}]	Chemical elemental analysis [wt.%]						Qualitative X-ray phase analysis 1)			
		Mg	Fe	Ca	Si	Al	Cinorg.	M (B)	S	D	C
80-125	<0.1	25.3	2.91	2.13	0.26	0.05	13.7	+++	–	++	+

[1)] M (B) = ferroan magnesite (breunnerite); S = siderite; D = dolomite; C = calcite. "+" = phase detected; "–" = phase not detected.

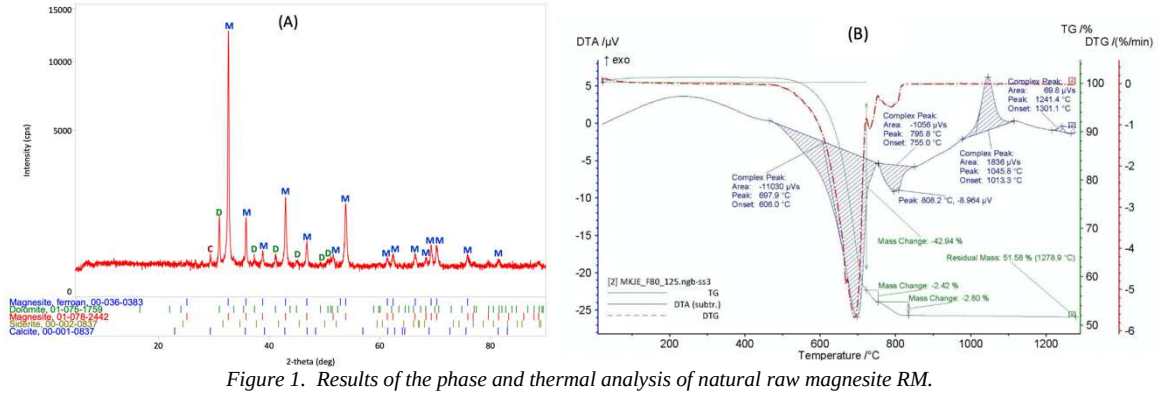

Figure 1. Results of the phase and thermal analysis of natural raw magnesite RM.
(A) X-ray diffractogram; M = ferroan magnesite (breunnerite), D = dolomite, C = calcite. (X-ray powder diffractometer Rigaku MiniFlex 600, Bragg-Brentano goniometer, CuKα radiation, Ni-filter, working voltage 40 kV, current 15 mA.).
(B) Plot of TG, DTG and DTA curves. (Simultaneous thermal analyser Netzsch STA 449 F3 Jupiter, corundum crucible, air atmosphere, temperature rate 10 K min^{-1}.)

Leaching procedure and measuring kinetic data. For the process studied, the overall chemical reaction can be written in the form of equation (8):

$$MgCO_3(s) + 2\,HNO_3(aq.) \rightarrow Mg(NO_3)_2(aq.) + CO_2(g) + H_2O(l). \quad (8)$$

The leaching behaviour of the RM in nitric acid was tested in a 0.7 l isothermal well-mixed glass batch reactor with intermittent withdrawal and analysis of the leachate samples. The reactor was equipped with a hot plate magnetic stirrer, insulating jacket and a reflux condenser. The mixing speed varied from 500 to 700 rpm and had been proved to have no observable effect on the course of leaching, under the reaction conditions considered in the present work. The temperature was maintained to within 2 K. The initial volume of nitric acid was 0.5 l in all experiments. In each test, the appropriate L/S ratio was set by the calculated amount of the RM (0.020-3.0 g). The RM sample was added to HNO_3 when the desired temperature had been reached in the reactor. The reaction suspension volume has not been affected by evaporation. The 20 ml leachate samples were withdrawn from the reaction mixture at predetermined time intervals, filtered and analysed for the magnesium and calcium by the EDTA and ICP methods. The leaching experiments were carried out under the reaction conditions, which were: temperature from 70 to 100°C, the concentration of HNO_3 from 0.01 to 6 M.

Results

Proposed simulation model. In most work on the leaching of magnesite with concentrated solutions of acids, practically no attention has been paid to the concentration dependence of the intrinsic kinetics. A simple first-order rate expression has been assumed, for mathematical simplicity rather than for valid reasons. In many practical cases, fluid-solid reactions can indeed be approximated as first-order reactions; in general, however, the concentration dependence is much more complex (Sohn, 1979). Crundwell (2013; 2014) emphasised the need to derive the value of n on the basis of a suitable mathematical model of the chemical dissolution of the solid substance B and verify it by experiment. Use of the relationship (3) enables to experimentally determine the (apparent) reaction order, n, compare it with theory and thus to identify the RDS of the overall leaching process with higher reliability, as compared to the commonly used NSPM.

A preliminary parametric study using the *generalised* non-porous shrinking particle model of leaching has shown that the values of parameters n and ϕ can alter the leaching behaviour qualitatively. In contrast, the activity coefficient of a strong acid just slightly modifies the shape of the kinetic curves but does not change the overall picture. Thus, for simplicity, it has been further assumed that $\gamma_A \cong 1$.

During the reaction of magnesite with acids, CO_2 is formed and released in a gaseous form from the reaction mixture into the atmosphere. So far, no consideration has been given to the effect of the occurrence of CO_2 on the overall leaching rate. The suitability of the proposed simulation model also for description of a reaction systems with the evolving gaseous product has, therefore, to be verified first, by comparing the model prediction with the experiment.

Experimental results. The leaching behaviour of the RM was studied in a *large excess* of nitric acid. An overview of the leaching tests carried out is given in Table 2. The measured fraction of magnesium dissolved, x_B, vs. time, t, dependencies are illustrated by some typical examples shown in Figure 2. The results of all leaching tests were used to verify the proposed simulation model and to calculate the values of kinetic model parameters.

Table 2. Reaction conditions set in individual leaching tests [1)]

Temperature [K/°C]	Initial concentration of nitric acid [M]										
	"low" [2)]					"high" [2)]					
	0.01	0.02	0.04	0.06	0.1	1	2	3	4	5	6
343 / 70						+				+	
353 / 80	+				+						
358 / 85						+				+	
363 / 90	+				+						
373 / 100	+	+++	++	++	++	++	++	++	++	++	++

1) Each "+" represents one leaching test carried out ("++…" denotes repeated tests).
2) The initial concentration of HNO3 is declared to be "low" or "high" only with respect to Fig. 3 and further discussion.

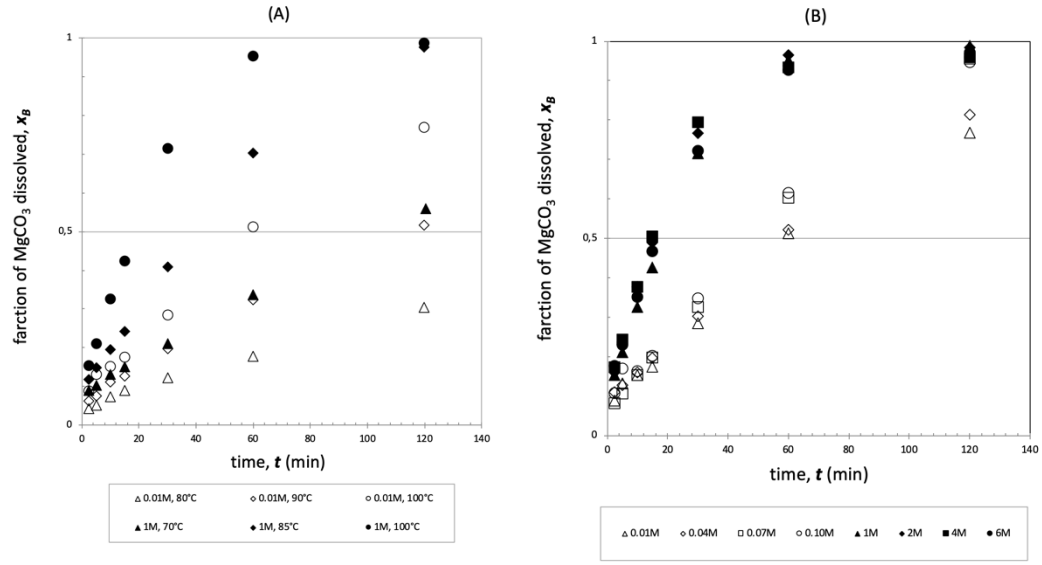

Figure 2. Examples of measured conversion (x_B) vs. time (t) kinetic curves: (A) effect of reaction temperature ($c^0_{HNO_3}$= 0.01 and 1 M); (B) effect of nitric acid concentration (T=373 K / 100°C).

Discussion

Comparison model – experiment. A number of papers have been published to study the leaching kinetics of magnesite in solutions of inorganic and organic acids (Abali et al., 2006; Bakan et al., 2006; Bayrak et al., 2006; Hoşgün and Kurama, 2012; Köse, 2012; Laçin et al., 2005; Özbek et al., 1999; Raza et al., 2013, 2014, 2015, 2016; Rutto and Enweremadu, 2011). A thorough analysis of these studies has revealed that:

1. The leaching rate is very sensitive to *temperature* – this fact is reflected in high calculated values of the apparent activation energy, E_A (42 kJ mol^{-1} < E_A < 78 kJ mol^{-1}), and, based on these results, the intrinsic chemical reaction has been identified to be the RDS.
2. No attention has been paid to the concentration dependence of the intrinsic kinetics. The *shrinking particle model* derived for the *first-order fluid-solid reaction* has exclusively been fitted to the experimental results, despite the fact that the data often had shown large deviations from the first-order reaction behaviour (distinct already by a preliminary visual assessment of the data!). Typical examples are schematically illustrated in Fig. 3: the *leaching rate* vs. *acid concentration (c_A)* dependences were first growing at a certain concentration interval $\langle c_{A,1};\ c_{A,2}\rangle$, but further either (a) indicated a weakening effect of the acid concentration in more concentrated solutions (i.e. in solutions with $c_A > c_{A,2}$) (Köse, 2012; Raza et al., 2013, 2014) – Fig. 3a; or (b) passed the maximum at $c_{A,M}$ and then even declined for $c_A > c_{A,M}$ (Bakan et al., 2006; Bayrak et al., 2006; Laçin et al., 2005) – Fig. 3b.

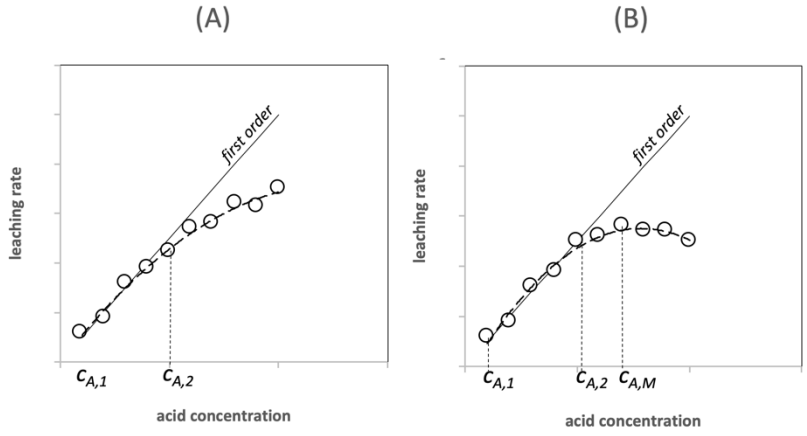

Figure 3. Schematic illustration of the leaching rate vs. acid concentration dependences obtained by some of the previous authors for the acid leaching of natural magnesite – two types of deviations from the first-order model are shown: (A) relative slow-down of the leaching (as compared to the first-order reaction); (B) absolute slow-down of the leaching process in concentrated solutions of acids.
Points = measured data, solid line = the course of leaching assuming the first-order reaction.

As discussed at the end of the theoretical section, at high L/S ratio when the condition $\phi \gg 1$ (or $(1 - x_A) \approx 1$) is fulfilled, a *simplified* NSPM in the form of Eqs. (5) and (6) should fit to the measured dependences x_B vs. t/t_R and x_B vs. $t/t_{0.5}$, respectively. Thus, the nitric acid leaching of the RM was studied in a large excess of the acid when the condition $\phi \gg 1$ was fulfilled. At first, a series of leaching tests characterised by the value of parameter $\phi \geq 10$ (which represents at least the 10-fold excess of HNO_3 if compared to stoichiometry) were carried out; the actual set up values of ϕ reached up to 48 (in 6 M HNO_3). Then, the applicability of Eq. (6) was checked using graphical analysis. To construct a scatter diagram, the *half-time* of reaction, $t_{0.5}$, has been preferred to t_R, because it is straightforward to determine $t_{0.5}$ for each run simply by interpolating the measured x_B-t data. The scatter diagram shown in Fig. 4 revealed that there is a very good correlation between the simulation model used and experiment (full and open triangles). This fact proved that the simplified NSPM is able to describe the course of leaching in the studied reaction system with acceptable accuracy.

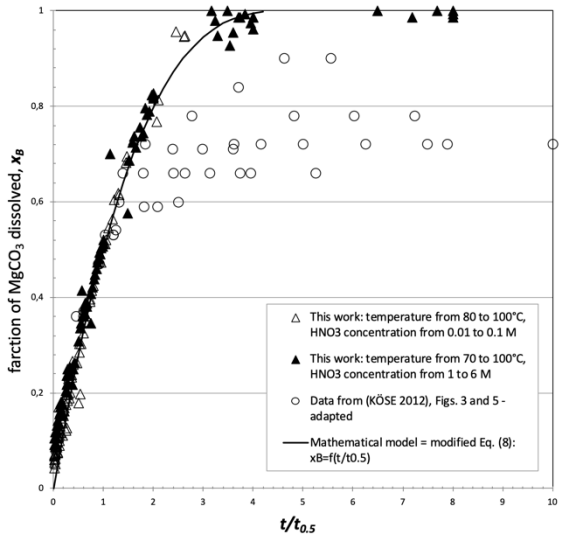

Figure 4. Conversion (x_B) vs. reduced time ($t/t_{0.5}$) dependence – comparison of a mathematical model with experiment. Points = measured data, solid line = modified Eq. (7): $x_B = 1 - (1 - 0.2063\, t/t_{0.5})^3$.

Determining the values of model kinetic parameters. For determining the values of model kinetic parameters, first (assuming for simplicity that $\gamma_A \cong 1$), Eq. (6) has been modified to express the half-time of reaction, $t_{0.5}$:

$$t_{0.5} = 0.2063 t_R = 0.2063 \frac{a n_B^0 \rho_S R}{m_S^0 k_0 exp\left(-\frac{E_A}{R_G T}\right)\left(c_{Ab}^0\right)^n} \quad . \tag{9}$$

Then, the values of n and E_A were calculated by linear regression using Eqs. (10) and (11), respectively,

$$ln\, t_{0.5} = -n\, ln\, c_{Ab}^0 + const1 \quad , \tag{10}$$

$$ln\, t_{0.5} = \frac{E_A}{R_G}\frac{1}{T} + const2 \quad . \tag{11}$$

and are summarised in Table 3.

Table 3. Kinetic parameters of the simulation model fitted by experiments

	This work		Ref. Köse (2012)
Country of the origin of the magnesite tested	Slovakia	Slovakia	Turkey
T (K / °C)	353-373 (80-100)	343-373 (70-100)	303-333 (30-60)
c_{HNO3}^0 (10^3 mol m^{-3})	0.01-0.1 (“low”)	1-6 (“high”)	1-3
R (10^{-6} m)	80-125	80-125	90-150
$\boldsymbol{E_A}$ (10^3 J mol^{-1})	43.7	58.5	3.2
$\boldsymbol{n}$ (-)	0.22	0.05	–

The values of apparent activation energy obtained in this work, both at low and high concentrations of HNO_3 (43.7 a 58.5 kJ mol^{-1}, respectively), are in good agreement with the values presented by other authors for the natural magnesite leaching with solutions of inorganic and organic acids (42 kJ mol^{-1} < E_A < 78 kJ mol^{-1} (Bakan et al., 2006; Bayrak et al., 2006; Hoşgün and Kurama, 2012; Laçin et al., 2005; Raza et al., 2013, 2014, 2015, 2016; Rutto and Enweremadu, 2011)), except a markedly lower value presented by Köse (2012) – see Table 3, for comparison. Köse (2012) investigated the same reaction system (i.e., $MgCO_3$-HNO_3-H_2O); his experimental results were therefore analysed in more detail. Since the values of ϕ used in his experiments (from 12 to 20) were high enough and the effect of the HNO_3:$MgCO_3$ ratio may have been excluded, to find an explanation for such a big difference, the original experimental results published by Köse were depicted in a modified form in Figure 4 (open rings), alongside our data (triangles).

A thorough view of all the experimental points in the graph in Figure 4 revealed a considerable difference between the layout of both sets of results. The data points of Köse (a) significantly depart from the model prediction at $x_B \geq 0.6$, and (b) indicate that the magnesium dissolution may have been finished by reaching the limit (maximum) value of x_B lying between 0.7 and 0.9.

The dissolution far from equilibrium was studied in both cases, and magnesite was expected to be fully dissolved at the end of the leaching process. The differences observed were therefore attributed either to (a) the presence of a magnesium bearing phase other than magnesite, which did not dissolve in HNO_3 at all or exhibited only a limited solubility (this seems unlikely!) or to (b) the errors in chemical analyses and/or calculations. In the sample RM, the total content of mineral phases other than "chemically soluble" carbonates was less than 1 wt. %. Hence, the maximum conversions of magnesium carbonate higher than 99 rel. % may, therefore, have been expected in the present work. This assumption was confirmed by experiment: in the leaching tests where, based on the results of chemical analyses, the carbonates were practically fully dissolved, the experimentally determined undissolved residuals represented less than 2 wt. % of the original RM sample. In the magnesite sample used by Köse, the total content of magnesium and calcium carbonate was even higher, his maximum conversions observed seem therefore to be unrealistically low. Moreover, an inconsistency between the measured data and the mathematical model used to calculate E_A is evident from Figure 4, which significantly reduces the reliability of the estimate of E_A. Thus, with respect to the above facts, the value published by Köse (2012) has been considered to be an outlier.

In the previous research on the leaching of natural magnesite with concentrated solutions of acids, to analyse the overall process, mathematical models having implicitly assumed that $n = 1$ were used and the authors paid no further attention to the actual mechanism of the intrinsic chemical reaction (1). However, Crundwell (2013, 2014, 2015) clearly explained how important physically correct proposal of the mechanism and the related values of kinetic parameters (i.e., apparent activation energy, but *especially* reaction order) are in finding out the rate-determining step of the overall leaching process. For the far from equilibrium dissolution of $CaCO_3$ in acidic solutions, Crundwell (2015) theoretically derived the value of $n = 0.5$ – this theoretical value is twice that calculated in this work for the solutions with "low" HNO_3 concentration ($n = 0.22$), and by order of magnitude higher than the value of *n* obtained for concentrated solutions ($n = 0.05$). For further discussion, due to the lack of relevant data, the experimental results recently published by Artamonova et al. (2017) for the magnesite dissolution kinetics in acidic (KCl+HCl) solutions at pH 1 to 5 have also been taken into account - an overview of all the above results is shown in Figure 5.

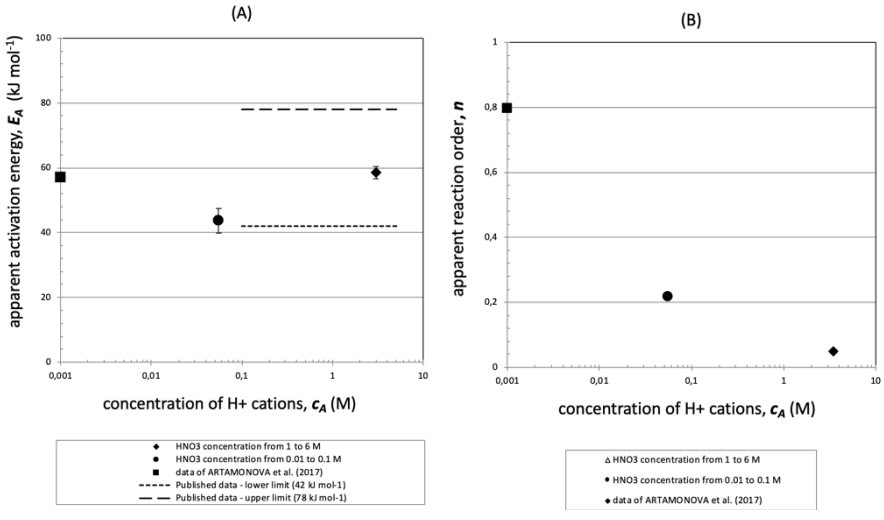

Figure 5. Comparison of the values of kinetic parameters obtained in this work with those found in the literature: (A) apparent activation energy; (B) apparent reaction order in H^+ ions.

Jordan et al. (2007) observed a negligible effect of most common organic and inorganic ligands on $MgCO_3$ dissolution in acidic saline solutions, which makes the comparison illustrated in Figs. 5ab feasible. It revealed that:

a) The E_A values obtained in this work are lying within the range of the values found by all other previous authors who have studied the leaching of natural magnesite with acid solutions.
b) Critical evaluation of the available values of *n* indicates that the value of *n* decreases with increasing acid concentration. This may be related to the formation of CO_2 and its transfer from the liquid to the gaseous phase. Since, until now, no consideration has been given to this aspect of the leaching process, and the available data is very limited, the effect of evolved gas should be addressed in more detail in the future.
c) Relatively high calculated values of the activation energy indicate that the overall process of leaching is controlled by the intrinsic chemical reaction (1) in the whole range of temperature and HNO_3 concentration studied. This hypothesis has been confirmed by the calculated values of the reaction order, which significantly differ from 1.

Conclusions

Kinetics of the leaching of natural magnesite with nitric acid was studied using both mathematical modelling and experiment. The reaction system $MgCO_3$-HNO_3-H_2O has been chosen with special regard to the production of pure magnesium salts. The results of a detailed critical analysis are summarised as follows:

1. The generalised non-porous shrinking particle model considering *the n-th order liquid-solid reaction* was fitted to the measured kinetic data and the values of apparent activation energy, E_A, and reaction order, *n*, were calculated.
2. Relatively high values of E_A (43.7 and 58.5 kJ mol^{-1}) obtained in this work for both "low" (0.01-0.1 M) and "high" (1-6 M) concentrations of HNO_3, respectively, lay within the range of values presented by other authors and indicate that the overall process of leaching is controlled by the intrinsic chemical reaction (1) in the whole range of reaction conditions considered.
3. This hypothesis has been confirmed by the calculated values of *n*, which (especially in concentrated HNO_3) considerably differ from 1. Until now, no attention has been paid to the actual mechanism of the intrinsic chemical reaction. In this work, the value of $n = 0.22$ was calculated for the solutions with "low" HNO_3 concentration, and $n = 0.05$ was obtained for concentrated HNO_3 solutions. These results enable a deeper insight not only into the reaction system studied but into the acid leaching of magnesite in general. The calculated values of *n* seem to be considerably lower than the value predicted by the theory, and it is hypothesised that the decrease in *n* with increased acid concentration might be related to the formation of CO_2 and its transfer from the liquid to the gaseous phase.

Notation

a	stoichiometric coefficient for species *A* in Eq. (1)
A	H+ ions
B	$MgCO_3$
c_{Ab}^0	initial concentration of H+ ions in bulk lixiviant
EA	apparent activation energy of reaction (1)
$F(x_B)$	function defined by Eq. (4)
k	rate-constant for reaction (1), *n*-th order in *A*;
k_0	constant ("frequency factor") in Arrhenius´ equation;
K	process parameter defined by Eq. (3)
m_L^0	initial mass of acid leach solution
m_S^0	initial mass of magnesite
n	apparent reaction order for H+ ions
n_A^0	initial total amount (in moles) of species A in lixiviant
n_B^0	initial total amount (in moles) of $MgCO_3$ in magnesite
r_A^0	initial reaction rate defined by Eq. (3);
R	initial radius of magnesite particles
R_G	gas constant = 8.314 J mol-1 K-1
t	reaction (leaching) time
$t_{0.5}$	reaction half-time
t_R	time required for complete conversion of magnesite particle
T	temperature in K
x_B	fraction of $MgCO_3$ dissolved

Greek letters

γ_A	activity coefficient of H+ ions in leach solution
ρ_L^0	initial lixiviant density
ρ_S	raw magnesite density
σ	liquid-to-solid (L/S) mass ratio (= m_L^0 / m_S^0)
ϕ	reduced A/B molar ratio (= $n_A^0/(an_B^0)$)

References

Abali, Y., Çopur, M., Yavuz, M. (2006). Determination of the optimum conditions for the dissolution of magnesite with H2SO4 solutions. Indian Journal of Chemical Technology 13, 391-397.

Artamonova, I.V., Gorichev, I.G., Kramer, S.M. (2017). Comparative analysis of dissolution kinetics of Ca, Mg, Fe, and Mn carbonates. Vestnik of the State University of Nizhni Novgorod (Lobachevsky University) №5 (103), 57–61 (in Russian).

Bakan, F., Laçin, O., Bayrak, B., Saraç, H. (2006). Dissolution kinetics of natural magnesite in lactic acid solutions. Int. J. Miner. Process. 80, 27–34.

Bayrak, B., Laçin, O., Bakan, F. Saraç, H. (2006). Investigation of dissolution kinetics of natural magnesite in gluconic acid solutions. Chemical Engineering Journal 117, 109–115.

Bedinger, G.M. (2018). 2015 Minerals Yearbook –Titanium [Advance Release]. U.S. Geological Survey.

Crundwell, F.K. (2013). The dissolution and leaching of minerals – Mechanisms, myths and misunderstandings. Hydrometallurgy 139, 132-148.

Crundwell, F.K. (2014). The mechanism of dissolution of minerals in acidic and alkaline solutions: Part I – A new theory of non-oxidation dissolution. Hydrometallurgy 149, 252-264.

Crundwell, F.K. (2015). The mechanism of dissolution of minerals in acidic and alkaline solutions: Part IV – Equilibrium and near-equilibrium behaviour. Hydrometallurgy 153, 46-57.

European Commission (2015). Critical Raw Materials Profiles, Report on critical raw materials for the EU. European Commission, Ref. Ares(2015)3396873 - 14/08/2015.

Habashi, F. (2005). A short history of hydrometallurgy. Hydrometallurgy 79, 15-22.

Habashi, F. (2007). A generalised kinetic model for hydrometallurgical processes. Chemical Product and Process Modeling 2, Iss. 1, Art. 1.

Hoşgün, H.L., Kurama, H. (2012). Dissolution kinetics of magnesite waste in HCl solution. Ind. Eng. Chem. Res. 51, 1087-1092.

IHS Markit Chemical Expert (2017). Chemical Economics Handbook - Magnesium Oxide and Other Magnesium Chemicals.

Jordan, G., Pokrovsky, O.S., Guichet, X., Schmahl, W.W. (2007). Organic and inorganic ligand effects on magnesite dissolution at 100 °C and pH=5 to 10. Chemical Geology 242, 484–496.

Köse, T.E. (2012). Dissolution of magnesium from natural magnesite ore by nitric acid leaching. Journal of Engineering and Architecture Faculty of Eskişehir Osmangazi University XXV (2), 43–55.

Laçin, O., Dönmez, B., Demir, F. (2005). Dissolution kinetics of natural magnesite in acetic acid solutions. Int. J. Miner. Process. 75, 91– 99.

Levenspiel, O. (1999). Chemical Reaction Engineering (3-rd edition). John Wiley & Sons, New York.

Merchant Research and Consulting Ltd. (2019). Magnesium and Compounds: 2019 World Market Review and Forecast to 2028.

Özbek, H., Abali, Y., Çolak, S., Ceyhun, I., Karagölge, Z. (1999). Dissolution kinetics of magnesite mineral in water saturated by chlorine gas. Hydrometallurgy 51, 173–185.

Raschman, P., Popovič, Ľ., Fedoročková, A., Kyslytsyna, M., Sučik, G. (2019). Non-porous shrinking particle model of leaching at low liquid-to-solid ratio. Hydrometallurgy 190 – in press. https://doi.org/10.1016/j.hydromet.2019.105151.

Raza, N., Zafar, Z.I., Najam-ul-Haq, M. (2013). An analytical model approach for the dissolution kinetics of magnesite ore using ascorbic acid as leaching agent. International Journal of metals 2013, Article ID 352496.

Raza, N., Zafar, Z.I., Najam-ul-Haq, M. (2014). Utilisation of formic acid solutions in leaching reaction kinetics of natural magnesite ores. Hydrometallurgy 149, 183–188.

Raza, N., Zafar, Z.I., Najam-ul-Haq, M., Kumar, R.V. (2015). Leaching of natural magnesite ore in succinic acid solutions. Int. J. Miner. Process. 139, 25-30.

Raza, N., Raza, W., Asif, M. (2016). Reaction kinetics of magnesite ore in dilute ethanoic acid. Russian Journal of Nonferrous Metals 57 (4), 308-315.

Roskill Information Services Ltd. (2013). Magnesium Compounds and Chemicals: Global Industry Markets and Outlook (12th ed.).

Rutto, H.L., Enweremadu, Ch. (2011). The dissolution study of a South African magnesium-based material from different sources using a pH-stat. Chemical Industry and Chemical Engineering Quarterly 17 (4), 459-468.

Shand, M.A. (2006). The Chemistry and Technology of Magnesia. John Wiley & Sons, Hoboken, New Jersey.

Sohn, H.Y. (1979). Fundamentals of the Kinetics of Heterogeneous Reaction Systems in Extractive Metallurgy. In: Sohn H.Y. and Wadsworth M.E. (Editors): Rate Processes of Extractive Metallurgy. Plenum Press, New York, pp. 1-51.

U. S. Geological Survey (2019). Mineral Commodity Summaries – Magnesium Compounds.

Wadsworth, M.E. (1979). Hydrometallurgical Processes – Principles of Leaching. In: Sohn H.Y. and Wadsworth M.E. (Editors): Rate Processes of Extractive Metallurgy. Plenum Press, New York, pp. 133-186.

Acta Montanistica Slovaca
ISSN 1335-1788
actamont.tuke.sk

Energy Consumption and Green GDP in Europe: A Panel Cointegration Analysis 2008 - 2016

Marinko ŠKARE[1], Daniel TOMIĆ[2] and Saša STJEPANOVIĆ[3]*

Authors' affiliations and addresses:
[1] Juraj Dobrila University of Pula, Faculty of Economics and Tourism "Dr.Mijo Mirković, Preradovićeva 1/1,52100 Pula, Croatia
e-mail: mskare@unipu.hr

[2] Juraj Dobrila University of Pula, Faculty of Economics and Tourism "Dr.Mijo Mirković, Preradovićeva 1/1,52100 Pula, Croatia
e-mail: dtomic@unipu.hr

[3] Juraj Dobrila University of Pula, Faculty of Economics and Tourism "Dr.Mijo Mirković, Preradovićeva 1/1,52100 Pula, Croatia
e-mail: sstjepan@unipu.hr

***Correspondence:**
Marinko Škare, Juraj Dobrila University of Pula, Faculty of Economics and Tourism "Dr.Mijo Mirković, Preradovićeva 1/1,52100 Pula, Croatia
Tel:+385 52 377 057
e-mail: mskare@unipu.hr

Acknowledgement:
This paper is a result of scientific – research projects "Accounting for the Future, Big Data and Economic Measurement" and "The Determinants and Challenges of Competitiveness" supported by the Faculty of Economics and Tourism "Dr. Mijo Mirković", Juraj Dobrila University of Pula. Any opinions, findings, and conclusions or recommendations expressed in this paper are those of the author and do not necessarily reflect the views of the Faculty of Economics and Tourism "Dr. Mijo Mirković", Pula.

How to cite this article:
Škare, M., Tomić, D. and Stjepanović, S. (2020). Energy Consumption and Green GDP in Europe: A Panel Cointegration Analysis 2008 - 2016. *Acta Montanistica Slovaca*, Volume 25 (1), 46-56

DOI:
https://doi.org/10.46544/AMS.v25i1.5

Abstract
The paper analyzes the relationship between energy consumption and green GDP as increased energy consumption could cause an increase in GDP. In order to evaluate how and to what extent the increase in energy consumption affects the size and movement of the green GDP, the aim of this paper is to confirm the existence of a strong link between energy consumption and green GDP. Having a large number of papers linking energy consumption and GDP, through this paper, we want to emphasize an even greater role of green GDP in energy consumption by linking the impact of the consumption of different energy sources with the movements in green GDP. Namely, how much different energy sources affect the gap between green GDP and GDP. Within the empirical analysis, we use a panel cointegration technique to examine long-term relationships among integrated variables. The data analyzed in this model cover 36 countries for the period from 2008 to 2016. These 36 countries include the EU28 countries and potential candidates for accession in the European Union. The results of our analysis follow the theory as we found that an increase in energy consumption causes an increase in GDP, hence the green GDP. However, the second part of the analysis suggests that an increase in consumption of energy in sectors that are environmentally more damaging emphasize the gap between the GDP and green GDP, but that an increase in more environmentally cleaner energy consumption curtails that gap.

Keywords
Green GDP, Panel cointegration, EU28, energy consumption.

Introduction

This paper presents the relationship between energy consumption, GDP, and green GDP. Theoretically, any increase in energy consumption leads to an automatic increase in GDP. Based on a scarce number of papers related to green GDP – energy nexus, we analyze how much and in what way this energy consumption affects the movement of green GDP. Green GDP consists of several observed variables that negatively affect GDP and reduce it in a certain amount (Stjepanović, Tomić and Škare, 2019). It is usually calculated as traditional GDP minus the costs of environmental pollution and depletion of natural resources. Stjepanović, Tomić and Škare, (2017) provided us with a new green GDP measure that which was initially presented as a growth rate which makes it much easier to compare with traditional indicators. What makes this calculation of indicator stand out is that the authors carefully took and calculated the actual costs of environmental pollution and opportunity costs, and thus presented certain aspects of social costs. The result of this research brought us an alternative version of GDP that consisted of the variable waste production, CO2 emissions into the atmosphere, and consumption of natural resources. All these variables separately affect GDP and reduce it in a particular value as serious damage to the environment that will come to charge once. Through our paper, we want to analyze the true nature of the relationship between energy consumption from specific sources, like solid fuels or natural gas and green GDP. We expect that "greener" the energy source is, the smaller the negative impact on GDP should be, i.e., we should have a higher green GDP and vice versa. Our analysis, therefore, emphasizes various energy sources within today's high levels of pollution that has a huge impact on people as the environment is becoming a key economic issue. The shortcomings of GDP as a measure of a country's economic prosperity are pronounced today more than ever. One complaint is that GDP as a measure does not contain precise environmental components, and in that way only represents a deferred payment that will be paid by new generations. Therefore, it is necessary to include variables in the presentation of a country's economic progress and assess its impact on GDP, which are, in fact, related to the environment and sustainable development. Only then can we have a more objective measure that will evaluate economic progress from a different angle and on which we can assess better the efficiency and success of a country's economic system. After the introduction, we present a summary of the energy consumption and growth research.

The goal of this paper is to study the relationship between green GDP and GDP, using the energy consumption variables. Although there are papers that have dealt with similar topics, but only for one country, the emphasis of this paper is to study the European countries. By analyzing these countries, we will come to a conclusion about the impact of separate energy sources on green GDP. The gap between green GDP should be smaller in those countries that use less harmful energy sources for the environment, and larger for those countries that use more harmful energy sources. Particular emphasis is placed on renewable energy sources and their impact on Green GDP. In our analysis, we use annual panel data covering the period 2008-2016 for 36 European countries. Countries involved in the analysis are EU 28 countries plus other European countries (Iceland, Norway, Montenegro, North Macedonia, Albania, Serbia, Turkey, and Moldova). Hence, our presumption about homogenous data sample suggests that the panel data approach should be an appropriate method for analyzing this relationship. We explain the data and methods in the next section and discuss the results of the study in the results section. Finally, we conclude by giving a summary of remarks and facts in conclusion.

Literature Review

The motive of this paper is to extend previous researches on this or similar topics. Here are some papers that tried to link energy consumption and green GDP. One such paper that seeks to reveal the background of the relationship between energy consumption growth and green GDP growth for China is a paper (Hongxian, 2018), entitled "Influence energy consumption has on green GDP growth in China". In this paper, the author analyzes the direct and indirect impact on the growth rate of green GDP, which affects several ratios of energy consumption as well as the relationship between different energy sources. Likewise, (Al-mulali, 2014), in his paper, describes the association of GDP growth with energy consumption. The purpose of this paper was to investigate the relationship between gross domestic product growth and renewable and independent energy consumption in 82 developing countries. One of the papers that analyzed the relationship between green GDP and sustainable development is the paper (Vaghefi, Siwar, and Aziz, 2015), which provides evidence of the usefulness of alternative measures of GDP, i.e., green GDP. The authors calculated green GDP for Malaysia and indicated the important role of depleted natural resources and environmental damage within the country's sustainable development perspective. The problem of calculating green GDP is also studied by Wang, He and Zheng (2014), who describe the way in which the Green GDP system was designed and developed for China. The results suggested that China has not achieved 'clean 'economic growth, due to excessive pollution and too high utilization of natural resources. The authors concluded that this research confirm the *status quo* of China's

current economic development. Similar papers as that of the authors (Harnphatananusorn, Santipolvut, and Sonthi, 2019), speak of correction of GDP - for the amount it produces for air pollution and water pollution.

Strong global growth we see in the 20th and 21st century demands significant energy consumption. Energy is considered a complementary growth factor to the physical factor. According to the study by Malaczewski (2018), there is an optimal (golden point) of energy consumption proportional to the optimal combination between human and physical capital. Energy production and innovation are directly linked to carbon dioxide emissions (CO2e). Present economic growth models show over-dependency on carbon-intensive energy consumption (Rahman et al., 2019). Renewable energy use demands large support schemes to develop an efficient bio market, leading to an increase in investment efficiency and energy transformation (Gavurova et al., 2016).

World energy demand constantly increases and by 2050 is expected to reach 600-1500 EJ. year^{-1} and peak in 2100 with 900-3600 EJ. year $^{-1}$ (Kovács, 2007). Speeding urbanization is causing upward pressure to the energy consumption, and thus CO2 emission requires to re-evaluate current economic growth models if the upward trend of urbanization continues (Yazdi and Dariani, 2019). Study of Katarína et al., (2014) suggests that investments in renewable energy sources register higher efficiency and are limited by political, economic, administrative and legal constraints. Transformation to green economic growth models require significant public support since investments in renewable energy sources will remain unattractive for many years to come (Sokolovska and Kešeljević, 2019).

Transition to green economic growth models is possible and feasible. It demands strong public support schemes accompanied by consistent energy conservation policy assuring endogenous growth in the future (Faisal et al., 2018). There is a strong need to explore the link between energy consumption and future economic growth models.

Data and Methodology

Annual panel data, covering the period 2008-2016 for 36 European countries, are taken from the Eurostat database. The data for green GDP are from the study Stjepanović, Tomić and Škare (2019) using an alternative approach in measuring the green GDP (Stjepanović, Tomić and Škare, 2017). Data are expressed in logarithms and presented as lnGGDP as the logarithm of the green GDP indicator, lnGAP as the logarithm of the gap from green GDP to standard GDP measure, lnENERG as the logarithm of total energy consumption, lnFFUEL as the logarithm of solid fossil fuel consumption, lnNGAS as the logarithm of natural gas consumption, lnOIL as the logarithm of oil and petroleum consumption and lnRENEW as the logarithm of renewable and biofuel consumption, so that the energy consumption variables are expressed as a thousand tonnes of oil equivalent (TOE). Countries involved in the analysis are EU 28 countries (UK was still a part of the EU) plus other European countries (Iceland, Norway, Montenegro, North Macedonia, Albania, Serbia, Turkey, and Moldova). The logical presumption about homogeneity among European countries suggests that the panel data approach should be an appropriate method for replying to our research question; thus, this presumption will be evaluated through the results.

Cointegration analysis with panel data usually consists of unit root tests, cointegration tests, and the estimation of long-run (and short-run) relationship. For that purpose, we applied research logic and explanations from the paper from Škare, Benazić, and Tomić (2016). The panel analysis begins with panel unit root tests to avoid possible spurious results. If the series are non-stationary, the analysis continues with testing for the panel cointegration. Following the panel, unit root tests are used in this research: LLC test (Levin, Lin and Chu, 2002), Breitung test (Breitung, 2000), IPS test (Im, Pesaran and Shin, 2003), Fisher-type tests using ADF and PP tests (Maddala and Wu, 1999 and Choi, 2001) and Hadri test (Hadri, 2000).

Next, we evaluated panel cointegration tests, according to Pedroni (1999, 2004), Kao (1999) and Maddala and Wu (1999). Pedroni and Kao extend the two-step Engle-Granger (1987) framework to tests involving panel data. Pedroni introduced several tests for cointegration that allow for heterogeneous intercepts and trend coefficients across cross-sections. The Kao test follows the same approach but indicates cross-section specific intercepts and homogeneous coefficients on the first-stage regressors. Maddala and Wu (1999) applied Fisher's combined test that uses the results of the individual independent tests and Johansen's test methodology as an alternative approach that combines the tests from individual cross-sections in order to obtain test statistics for the full panel.

The long-run relationship is estimated using the pooled Panel Fully Modified Least Squares (FMOLS), pooled Panel Dynamic Least Squares (DOLS) and Pooled Mean Group/AR Distributed Lag (PMG/ARDL) estimation methods. Since FMOLS and DOLS provide only long-run estimates, for the short-run estimation, PMG/ARDL is used. Phillips and Moon (1999), Pedroni (2000), and Kao and Chiang (2000) proposed extensions of the Phillips and Hansen (1990) FMOLS estimator to panel settings while Kao and Chiang (2000), and Pedroni (2001) propose extensions of the Saikkonen (1992) and Stock and Watson (1993) DOLS estimator. FMOLS and DOLS estimation methods for panel settings allow the estimation of panel cointegrating regression

equation for non-stationary data by correcting the standard pooled OLS for serial correlation and endogeneity of regressors that are usually present in long-run relationships. The PMG/ARDL (Pesaran, Shin and Smith, 1999) takes the cointegration form of the simple ARDL model and adapts it for a panel setting by allowing the intercepts, short-run coefficients and cointegrating terms to differ across cross-sections.

To comprehend the influence of energy consumption towards the green GDP, we divide our analysis into two parts; one is dealing with the direct nexus between the green GDP and total energy consumption and the other dealing with an indirect link between the green GDP and the elements of energy consumption that comprise the total energy consumption. The direct effect is, analyzed in a twofold manner; (1) by observing the direct influence of the energy consumption on the green GDP indicator (as we expect that the rise in energy consumption should drive the standard GDP, hence the green GDP) and (2) by observing the direct influence of the energy consumption on the gap GDP indicator as the measure that reveals the bias of the standard GDP towards the green GDP (we expect that the rise in energy consumption should increase the difference between two measures). Two equations can represent these effects:

$$\ln GGDP_{it} = \alpha_{0i} + \beta_{1i}\ln ENERG_{it} + u_{it}, \quad i = 1, 2, K, N, \ t = 1, 2, K, T \tag{1}$$

$$\ln GAP_{it} = \alpha_{0i} + \beta_{1i}\ln ENERG_{it} + u_{it}, \quad i = 1, 2, K, N, \ t = 1, 2, K, T \tag{2}$$

where $\ln GGDP_{it}$ represents the logarithm of green GDP at time t, $\ln GAP_{it}$ represents the logarithm of the gap between the green GDP and standard GDP indicator at time t, $\ln ENERG_{it}$ stands for total energy consumption at time t, and uit is the error term while i and t denote country and time respectively.

Since the energy consumption variable is expected to increase the green GDP indicator, through indirect effect, we are trying to grasp the background of that relationship by observing how some parts, which the energy consumption indicator is composed of, influence the green GDP, i.e. do specific parts of the energy consumption deepen or curtail the difference between the GDP measure and the green GDP measure. This bond can be, therefore expressed as:

$$\ln GAP_{it} = \alpha_0 i + \beta_{1i}\ln FFUEL_{it} + \beta_{2i}\ln NGAS_{it} + \beta_{3i}\ln OIL_{it} + \beta_{4i}\ln RENEW_{it} + u_{it}, \quad i = 1, 2, K, N, \ t = 1, 2, K, T \tag{3}$$

where $\ln GAP_{it}$ again represents the logarithm of the gap between the green GDP and standard GDP indicator at time t, $\ln FFUEL_{it}$ stands for fossil fuel consumption at time t, $\ln NGAS_{it}$ stands for natural gas consumption at time t, $\ln OIL_{it}$ stands for oil and petroleum consumption at time t, $\ln RENEW_{it}$ stands for renewable and biofuel consumption at time t, and u_{it} is the error term while i and t denote country and time respectively.

Panel cointegration results

Regarding the order of integration of our time series, unit root tests indicated that the variables are integrated, i.e. they are non-stationary in level and stationary in first differences (results available upon request). Therefore, a panel cointegration test can be implemented. The following tables present the results of both the direct and indirect effect of energy consumption on the green GDP.

a) direct effect

The results from Pedroni's, Kao's and Johansen Fisher's panel cointegration tests were evaluated for both, equation 1 and equation 2, suggesting that there indeed exists a long-term (direct) relationship between the green GDP and energy consumption as well as between the gap GDP and energy consumption.

In both cases, with only intercept and again when intercept and trend are included, most of the Pedroni's statistics reject the null hypothesis of no cointegration between variables indicating the existence of long-run panel cointegration relationship between the observed variables (Table 1). Thus, it can be concluded that there exists a long-run relationship. Kao's panel cointegration test also strongly rejects the null hypothesis of no cointegration between variables indicating the existence of a long-run panel cointegration relationship between the observed variables (Table 2).

Table 1: Pedroni residual cointegration test

Variables: l**nGGDP**, l**nENERG**								
	Intercept				Intercept and trend			
	Statistic	Prob.	Weighted Statistic	Prob.	Statistic	Prob.	Weighted Statistic	Prob.
Panel v-Statistic	0.47	0.32	-1.66	0.95	-3.39	0.99	-5.81	1.00
Panel rho-Statistic	-1.39	0.08	-1.89	0.03	1.43	0.92	-1.30	0.90
Panel PP-Statistic	-4.90	0.00	-6.56	0.00	-6.71	0.00	-8.69	0.00
Panel ADF-Statistic	-4.80	0.00	-5.01	0.00	-5.25	0.00	5.67	0.00
Group rho-Statistic	1.45	0.93			3.53	0.99		
Group PP-Statistic	-6.99	0.00			-15.22	0.00		
Group ADF-Statistic	-5.58	0.00			-8.25	0.00		
Variables: **lnGAP**, **lnENERG**								
	Intercept				Intercept and trend			
	Statistic	Prob.	Weighted Statistic	Prob.	Statistic	Prob.	Weighted Statistic	Prob.
Panel v-Statistic	- 0.08	0.53	-1.29	0.90	-3.29	0.99	-5.21	1.00
Panel rho-Statistic	0.24	0.60	0.15	0.56	3.80	0.99	3.44	0.99
Panel PP-Statistic	-2.09	0.02	-3.47	0.00	-1.87	0.03	-4.88	0.00
Panel ADF-Statistic	-4.81	0.00	-6.79	0.00	-7.27	0.00	-8.31	0.00
Group rho-Statistic	2.97	0.99			5.25	1.00		
Group PP-Statistic	-4.19	0.00			-6.51	0.00		
Group ADF-Statistic	-8.80	0.00			-8.15	0.00		

Source: Authors' calculations.

Table 2: Kao residual cointegration test (individual intercept)

Variables	ADF	
	t-Statistic	Prob.
lnGGDP, lnENERG	-0.62	0.27
lnGAP, lnENERG	-2.43	0.01

Source: Authors' calculations.

Finally, Johansen Fisher trace and maximum eigenvalue cointegration tests reject the null hypothesis of no cointegration between variables indicating the existence of long-run panel cointegration relationship between the green GDP and energy consumption, and gap GDP variable and energy consumption (Table 3). According to these results, energy consumption could affect both green GDP variables in the long-run. Individual cross-section results (available upon request) suggest that one cointegration relation is present in almost all countries, either in the case with restricted or unrestricted constant.

Table 3: Johansen Fisher panel cointegration test (Trace and Maximum Eigenvalue)

*Variables: l**nGGDP**, l**nENERG***								
Hypothesized No. of CE (s)	*No deterministic trend (restricted constant)*				*Linear deterministic trend (unrestricted constant)*			
	*Fisher Stat.**	*Prob.*	*Fisher Stat.***	*Prob.*	*Fisher Stat.**	*Prob.*	*Fisher Stat.***	*Prob.*
None	443.90	0.00	448.50	0.00	4478.00	0.00	623.10	0.00
At most 1	117.80	0.00	115.2	0.00	166.60	0.00	166.60	0.00
*Variables: **lnGAP**, **lnENERG***								
Hypothesized No. of CE (s)	*No deterministic trend (restricted constant)*				*Linear deterministic trend (unrestricted constant)*			
	*Fisher Stat.**	*Prob.*	*Fisher Stat.***	*Prob.*	*Fisher Stat.**	*Prob.*	*Fisher Stat.***	*Prob.*
None	565.10	0.00	515.90	0.00	4478.00	0.00	623.10	0.00
At most 1	192.00	0.00	192.00	0.00	293.30	0.00	293.30	0.00

Source: Authors' calculations.

The following tables present the panel cointegration results from FMOLS, DOLS and PMG/ARDL estimation methods between the observed variables, testing the validity long-run linear cointegration relations.

Table 4: Panel cointegration results (Pooled estimation) – lnGGDP, lnENERG

Panel Fully Modified Least Squares (FMOLS)								
Variable	Constant				Constant and trend			
	Coefficient	Std. Error	t-Statistic	Prob.	Coefficient	Std. Error	t-Statistic	Prob.
lnENERG	0.12	0.04	3.48	0.00	0.07	0.03	2.05	0.04
Panel Dynamic Least Squares (DOLS)								
Variable	Constant (1,1)				Constant and trend (0,0)			
	Coefficient	Std. Error	t-Statistic	Prob.	Coefficient	Std. Error	t-Statistic	Prob.
lnENERG	0.70	0.17	4.11	0.00	0.13	0.03	3.92	0.00
PMG/ARDL (Pooled Mean Group/AR Distributed Lag) – ARDL (1,1)								
Variable	Restricted constant				Unrestricted constant			
	Coefficient	Std. Error	t-Statistic	Prob.	Coefficient	Std. Error	t-Statistic	Prob.
	Long Run Equation							
lnENERG	0.82	0.09	9.38	0.00	-0.24	0.05	-4.41	0.00
	Short Run Equation							
COINTEQ01	-0.83	0.05	-15.82	0.00	-1.24	0.08	-16.47	0.00
D(* lnENERG*)	-0.58	0.15	-3.94	0.00	-0.46	0.10	-4.47	0.00
C	14.93	0.94	15.88	0.00	34.70	2.14	16.20	0.00
@TREND					-0.01	0.01	-0.75	0.45

Source: Authors' calculations.

Table 5: Panel cointegration results (Pooled estimation) – lnGAP, lnENERG

Panel Fully Modified Least Squares (FMOLS)								
Variable	Constant				Constant and trend			
	Coefficient	Std. Error	t-Statistic	Prob.	Coefficient	Std. Error	t-Statistic	Prob.
lnENERG	0.05	0.06	0.89	0.37	-0.02	0.06	-0.43	0.67
Panel Dynamic Least Squares (DOLS)								
Variable	Constant (1,1)				Constant and trend (1,1)			
	Coefficient	Std. Error	t-Statistic	Prob.	Coefficient	Std. Error	t-Statistic	Prob.
lnENERG	0.88	0.39	2.27	0.03	5.89	1.74	3.38	0.00
PMG/ARDL (Pooled Mean Group/AR Distributed Lag) – ARDL (1,1)								
Variable	Restricted constant				Unrestricted constant			
	Coefficient	Std. Error	t-Statistic	Prob.	Coefficient	Std. Error	t-Statistic	Prob.
	Long Run Equation							
lnENERG	0.72	0.14	5.27	0.00	-0.09	0.03	-2.84	0.01
	Short Run Equation							
COINTEQ01	-0.66	0.06	-10.88	0.00	-0.82	0.04	-18.39	0.00
D(lnENERG)	0.48	0.23	2.09	0.04	-0.88	0.21	4.24	0.00
C	-4.42	0.38	-11.55	0.00	0.64	0.12	5.58	0.00
@TREND					-0.01	0.01	-2.38	0.02

Source: Authors' calculations.

Results of (pooled) estimation methods indicate that long-run coefficients are statistically significant with positive signs, as we theoretically expect. Results from the equation (1) with standard GDP measure (Table 4) indicate that the long-run coefficients obtained from all estimation methods are positive and strongly significant, varying from 0.70 to 0.82 in the case with constant (only FMOLS providing low positive impact), but are low in the case for constant with trend varying from 0.07 to 0.13 (with PMG/ARDL providing significant negative effect). Hence, it can be concluded that a rise in energy consumption leads to an increase in the green GDP, the coefficients suggesting the relationship that is rather inelastic. The increase of total energy consumption over time did not hamper the growth of green GDP. Zero restrictions on the long-run parameters are tested using the Wald test (available upon request), confirming their statistical significance. Short-run evidence from the PMG/ARDL model is consistent with the long-run relationship (available upon request), which indirectly confirms the homogeneity of the sample.

Results from the equation (2) with gap GDP measure (Table 5) also indicate the long-run coefficients obtained from estimation methods are positive and strongly significant, varying from 0.72 to 0.87 in the case with constant (again FMOLS providing limited positive impact), however, with the results that are unconvincing in the case for constant with a trend for only DOLS suggesting a significant positive relation of 5.89 (two other methods indicating either insignificant and/or negative impact). Analogously, it can be concluded that a rise in energy consumption leads to a rise in gap GDP measure, i.e. a widening of the gap between the traditional GDP indicator and the green GDP. Once more, zero restrictions on the long-run parameters are tested using the Wald test (available upon request), confirming their statistical significance. Short-run evidence from the PMG/ARDL model is consistent with the long-run relationship, however when scrutinizing on the individual short-run cross-section results (available upon request), we find mixed results regarding the signs of the coefficients, but with error correction coefficients are statistically significant for almost all countries suggesting a slow to moderate speed of convergence.

b) indirect effect

The results from Pedroni's and Kao's panel cointegration tests (Table 6), from an equation 3, strongly reject the null hypothesis of no cointegration between variables, implicating that there also exists a long-term (indirect) relationship between the green GDP and energy consumption, which can be captured by evaluating how different elements of energy consumption affect the gap between the traditional GDP and the green GDP. Johansen Fisher panel cointegration results varied due to numbers of lags used or due to insufficient data for estimation, thus we could not obtain prudent conclusions.

Table 6: Cointegration tests – lnGAP vs. energy consumption by products

Variables: lnGAP, lnFFUEL, lnNGAS, lnOIL, lnRENEW								
Pedroni residual cointegration test	Intercept				Intercept and trend			
	Statistic	Prob.	Weighted Statistic	Prob.	Statistic	Prob.	Weighted Statistic	Prob.
Panel v-Statistic	-1.85	0.97	-3.29	0.99	-2.69	0.99	-5.15	1.00
Panel rho-Statistic	5.10	1.00	5.05	1.00	7.02	1.00	6.94	1.00
Panel PP-Statistic	-2.47	0.01	-7.63	0.00	-0.69	0.24	-10.25	0.00
Panel ADF-Statistic	-2.61	0.01	-5.58	0.00	-	-	-	-
Group rho-Statistic	7.52	1.00			8.55	1.00		
Group PP-Statistic	-11.52	0.00			-18.54	0.00		
Group ADF-Statistic	-4.69	0.00			-	-		
Kao residual cointegration test	t-Statistic				Prob.			
ADF	-3.34				0.00			

Source: Authors' calculations.

The following table presents the panel cointegration results from FMOLS and DOLS estimation methods between the green GDP and selected factors of energy consumption (by products), testing the characteristics of the long-run linear cointegration relations. Reasonable PMG/ARDL estimations could not be obtained; therefore, we opted not to apply this method.

Table 7: Panel cointegration results (Pooled estimation) – lnGAP vs. energy consumption by products

Panel Fully Modified Least Squares (FMOLS)								
Variable	No constant no trend				Constant and trend			
	Coefficient	Std. Error	t-Statistic	Prob.	Coefficient	Std. Error	t-Statistic	Prob.
lnFFUEL	0.16	0.05	3.13	0.00	0.08	0.06	1.37	0.17
lnNGAS	-0.29	0.05	-5.70	0.00	0.26	0.11	2.33	0.02
lnOIL	-0.09	0.09	-1.03	0.31	0.09	0.22	0.41	0.68
lnRENEW	0.24	0.09	2.85	0.01	0.03	0.14	0.21	0.84
Panel Dynamic Least Squares (DOLS)								
Variable	No constant no trend (0,0)				Constant and trend (0,0)			
	Coefficient	Std. Error	t-Statistic	Prob.	Coefficient	Std. Error	t-Statistic	Prob.
lnFFUEL	0.12	0.05	2.11	0.04	0.32	0.09	3.67	0.00

lnNGAS	-0.25	0.06	-4.01	0.00	-0.11	0.16	-0.74	0.47
lnOIL	-0.03	0.11	-0.26	0.79	-0.09	0.83	0.24	0.00
lnRENEW	0.17	0.11	1.50	0.14	0.18	0.17	1.07	0.29

Source: Authors' calculations.

Results from the equation (3) that captures the indirect effect (Table 7) indicate long-run coefficients that are most significant with expected signs. Solid fossil fuel coefficients are positive and strongly significant (except in the case with constant and trend within FMOLS where it is statistically insignificant), varying from 0.8 to 0.32 suggesting that an increase in fossil fuel consumption widens the gap between the GDP indicator and Green GDP. Such results are expected for the consumption of fossil fuels that could be the drivers of traditional GDP measures. However, their environmental implications could be a limiting factor for green GDP growth. However, natural gas coefficients are negative and strongly significant (except in the case with constant and trend within FMOLS where it is positive) varying from -0.11 to -0.29, implying that an increase in natural gas consumption decreases the gap GDP measure. Since natural gas consumption generates less environmental pollution, it can be represented as a strong driver of green GDP development. Oil and petroleum coefficients are mostly statistically insignificant. However, its high positive correlation with green GDP and moderate negative correlation with gap GDP measure suggests that the rise of oil and petroleum consumption could be increasing the difference between the traditional and green GDP (see correlation matrix and scatter diagram in the Appendix). The same problem arises when observing renewable and biofuel consumption, which displays positive and insignificant coefficients, but with high positive correlation with green GDP and weak negative correlation with gap GDP measure (with an inconclusive display from the scatter diagram), it could have an opposite implication, therefore curtailing that gap.

Our empirical models provide valuable insight into the background and the relationship between the green GDP and energy consumption for European countries, suggesting that an increase in total energy consumption leads to an increase in green GDP variables (as it also consists of standard factors of economic growth). However, it also deepens the difference between the traditional GDP measure and green GDP measure (implying that it hampers the green development of an economy). When decomposing total energy consumption in its integral elements (consumption by product) we find that an increase in consumption of energy in sectors that are environmentally more damaging (like solid fossil fuels and oil and petroleum) emphasize the gap between the traditional and green GDP, but that an increase in more environmentally 'friendly' consumption (like natural gas and renewables and biofuels) curtails and alleviate that gap. These models illustrate when it comes to green GDP, green growth and green economy, the contribution of natural gas consumption should have a greater role in promoting economic growth for European countries and that this consumption of, for example, fossil fuels and oil, which bring a substantial proportion of the green cost, should be incorporated with sound environmental strategy.

Conclusion

In our analysis, we used two models to observe the effect of energy consumption on GDP and green GDP. In one model, we look at the relationship between total energy consumption and GDP growth, hence the green GDP, while in the other model, we concentrated on separate variables related to different energy sources, from which we then analyzed their individual impacts on the difference between GDP and green GDP.

The results confirm theoretical expectations as we provided evidence that an increase in energy consumption affects an increase in GDP and green GDP. However, the second part of the analysis confirmed that solid fuels and oil have a much greater impact on the difference between green GDP and GDP than renewable resources and natural gas, which are a much cleaner form of energy source. These results coincide with the results of other research related to green GDP, including (Al-mulali, 2014), that displayed a clear link between GDP growth and energy consumption. Other studies that provided similar results, like (Vaghefi, Siwar, and Aziz, 2015 or Wang, He and Zeng, 2014), also provided similar thoughts on the structure and system of designing research patterns on green GDP.

In general, we can accept the main hypothesis as we provide enough evidence to show that energy consumption has an important effect on green GDP development. Though the paper deals with relatively short time series (data (un)availability is a major obstacle in achieving more (time) extensive research on a cross-country base for which most of the data needed for calculation of the green GDP are published irregularly) and basic empirical modeling (without a strong background in theory), we are of the thought that future research endeavors should include reassessments of the influence of specific elements of energy consumption on green growth and economic sustainability. Our approach and deductions made above present only our research logic and could/should be subject to revision in the future. Future research patterns related to this topic should be pointed towards expanding the definition of green GDP with new variables, which will take in detail all types of pollution produced by the economic system or the economy of a country, and all forms of consumption of

natural resources, and calculate the negative impact on the health of the inhabitants of a particular country, which then represents an indirect or direct cost to that economy.

References

Al-mulali, U. (2014). GDP growth – energy consumption relationship: Revisited. *International Journal of Energy Sector Management*. 8(3).

Breitung, J. (2000). The Local Power of Some Unit Root Tests for Panel Data. In B. Baltagi (ed.), *Advances in Econometrics*, Vol. 15: Non-stationary Panels, Panel Cointegration, and Dynamic Panels, Elsevier Science Inc.

Breitung, J. and Pesaran, H. M. (2005). Unit Roots and Cointegration in Panels. *CESIFO Working Paper No. 1565*, CESifo Group Munich.

Choi, I. (2001). Unit Root Tests for Panel Data. *Journal of International Money and Finance*, 20(2), pp. 249–272.

Di Lorio, F. and Fachin, S. (2011) A Panel Cointegration study of the long-run relationship between Savings and Investments in the OECD economies, 1970-2007. *Working Paper No. 3, Department of Treasury of the Italian Ministry of Economy and Finance*.

Eurostat (2020). Available at: https://ec.europa.eu/info/departments/eurostat-european-statistics_en.

Faisal, F., Tursoy, T., Resatoglu, N.G. & Berk, N. (2018). Electricity consumption, economic growth, urbanization and trade nexus: empirical evidence from Iceland, *Economic Research-Ekonomska Istraživanja*, 31(1), 664-680, https://doi.org/10.1080/1331677X.2018.1438907.

Gavurova, B., Perzelova, I. and Bencoova, B., (2016). Economic aspects of renewable energy use-application of support schemes based on a particular biogas plant in Slovakia. Acta Montanistica Slovaca, 21(3).

Harnphatananusorn, S., Santipolvut, S. and Sonthi, C. (2019). Concepts and empirical calculation of the green GDP for Thailand. *International Journal of Green Economics*, 13(1), p.68.

Hongxian, X. 2018. Influences Energy Consumption has on Green GDP Growth in China. *IOP Conference Series: Earth and Environmental Science*. 113(1).

Im, K., Pesaran, M. and Shin, Y., (2003). Testing for unit roots in heterogeneous panels. Journal of Econometrics, 115(1), pp.53-74.

Kao, C., (1999). Spurious regression and residual-based tests for cointegration in panel data. Journal of Econometrics, 90(1), pp.1-44.

Kao, C. and Chiang, M-H. (2000). On the Estimation and Inference of a Cointegrated Regression in Panel Data. In B. Baltagi (ed.), *Advances in Econometrics, Vol. 15: Non-stationary Panels, Panel Cointegration, and Dynamic Panels*, Elsevier Science Inc.

Kovács, F. (2007). World energy demands and coal reserves. Acta Montanistica Slovaca Rocník, 12(3), 276-283.

Levin, A., Lin, C. and James Chu, C. (2002). Unit root tests in panel data: asymptotic and finite-sample properties. Journal of Econometrics, 108(1), pp.1-24.

Maddala, G. and Wu, S. (1999). A Comparative Study of Unit Root Tests with Panel Data and a New Simple Test. Oxford Bulletin of Economics and Statistics, 61(S1), pp.631-652.

Malaczewski, M. (2018). Complementarity between energy and physical capital in a simple model of economic growth, *Economic Research-Ekonomska Istraživanja*, 31(1), 1169-1184, https://doi.org/10.1080/1331677X.2018.1456353

Pedroni, P., 1999. Critical Values for Cointegration Tests in Heterogeneous Panels with Multiple Regressors. Oxford Bulletin of Economics and Statistics, 61(s1), pp.653-670.

Pedroni, P. (2000). Fully Modified OLS for Heterogeneous Cointegrated Panels In B. Baltagi (ed.), *Advances in Econometrics, Vol. 15: Non-stationary Panels, Panel Cointegration*, and Dynamic Panels, Elsevier Science Inc.

Pedroni, P. (2001). Purchasing Power Parity Tests in Cointegrated Panels. Review of Economics and Statistics, 83(4), pp.727-731.

Pedroni, P. (2004). Panel cointegration: asymptotic and finite sample properties of pooled time series tests with an application to the ppp hypothesis. Econometric Theory, 20(03).

Pesaran, M., Shin, Y. and Smith, R. (1999). Pooled Mean Group Estimation of Dynamic Heterogeneous Panels. Journal of the American Statistical Association, 94(446), pp.621-634.

Phillips, P. and Hansen, B. (1990). Statistical Inference in Instrumental Variables Regression with I(1) Processes. The Review of Economic Studies, 57(1), p.99.

Phillips, P. and Moon, H. (1999). Linear Regression Limit Theory for Nonstationary Panel Data. Econometrica, 67(5), pp.1057-1111.

Rahman, Z. U., Cai, H., Khattak, SI, & Hasan, M.M. (2019). Energy production-income-carbon emissions nexus in the perspective of NAFTA and BRIC nations: a dynamic panel data approach, *Economic Research-Ekonomska Istraživanja*, 32(1), 3384-3397, https://doi.org/10.1080/1331677X.2019.1660201.

Saikkonen, P. (1992). Estimation and Testing of Cointegrated Systems by an Autoregressive Approximation. Econometric Theory, 8(01), pp.1-27.

Sokolovska, I., & Kešeljević, A. (2019). Does sustainability pay off? A multi-factor analysis on regional DJSI and renewable stock indices, *Economic Research-Ekonomska Istraživanja*, 32(1), 423-439, https://doi.org/10.1080/1331677X.2018.1550002

Stjepanović, S., Tomić, D. and Škare, M. (2019). Green GDP: an analysis for developing and developed countries. E+M Ekonomie a Management, 22(4), pp.4-17.

Stjepanović, S. Tomić, D. and Škare, M. (2017). A new approach to measuring Green GDP: A Cross-country analysis. *Enterpreneurship and Sustainability Issues*, 4(4).

Stock, J.H. and Watson, M. (1993). A Simple Estimator Of Cointegrating Vectors In Higher Order Integrated Systems. *Econometrica*, 61(4), pp. 783-820.

Škare, M., Benazić, M. and Tomić, D. (2016). On the neutrality of money in CEE (EU member) states: A panel cointegration analysis. *Acta Oeconomica*, 66(3), pp. 393-418.

Tomić, D. (2020). The perspective of Green GDP in growth modelling. *52nd International Scientific Conference on Economic and Social Development*. Porto, Portugal, April 16-17.

Vaghefi, N., Siwar, C. and Aziz, S. (2015). Green GDP and Sustainable Development in Malaysia. *Current World Environment*, 10(1), pp.01-08.

Wang, W., He, E. and Zheng, X. (2014). Construction of Green GDP Accounting System. Advanced Materials Research, 971-973, pp.2301-2304.

Yazdi, S.K., & Dariani, A.G. (2019). CO2 emissions, urbanization and economic growth: evidence from Asian countries, *Economic Research-Ekonomska Istraživanja*, 32(1), 510-530, https://doi.org/ 10.1080/1331677X.2018.1556107

Appendix

Table 8. Correlation matrix

Correlations	**lnGGDP**	**lnGAP**	**lnFFUEL**	**lnNGAS**	**lnOIL**	**lnRENEW**
lnGGDP	1	-0.45	0.60	0.83	0.97	0.78
lnGAP	-0.45	1	-0.09	-0.49	-0.46	-0.23
lnFFUEL	0.60	-0.09	1	0.61	0.66	0.60
lnNGAS	0.83	-0.49	0.61	1	0.84	0.69
lnOIL	0.97	-0.46	0.66	0.84	1	0.80
lnRENEW	0.78	-0.23	0.60	0.69	0.80	1

Source: Authors' calculations.

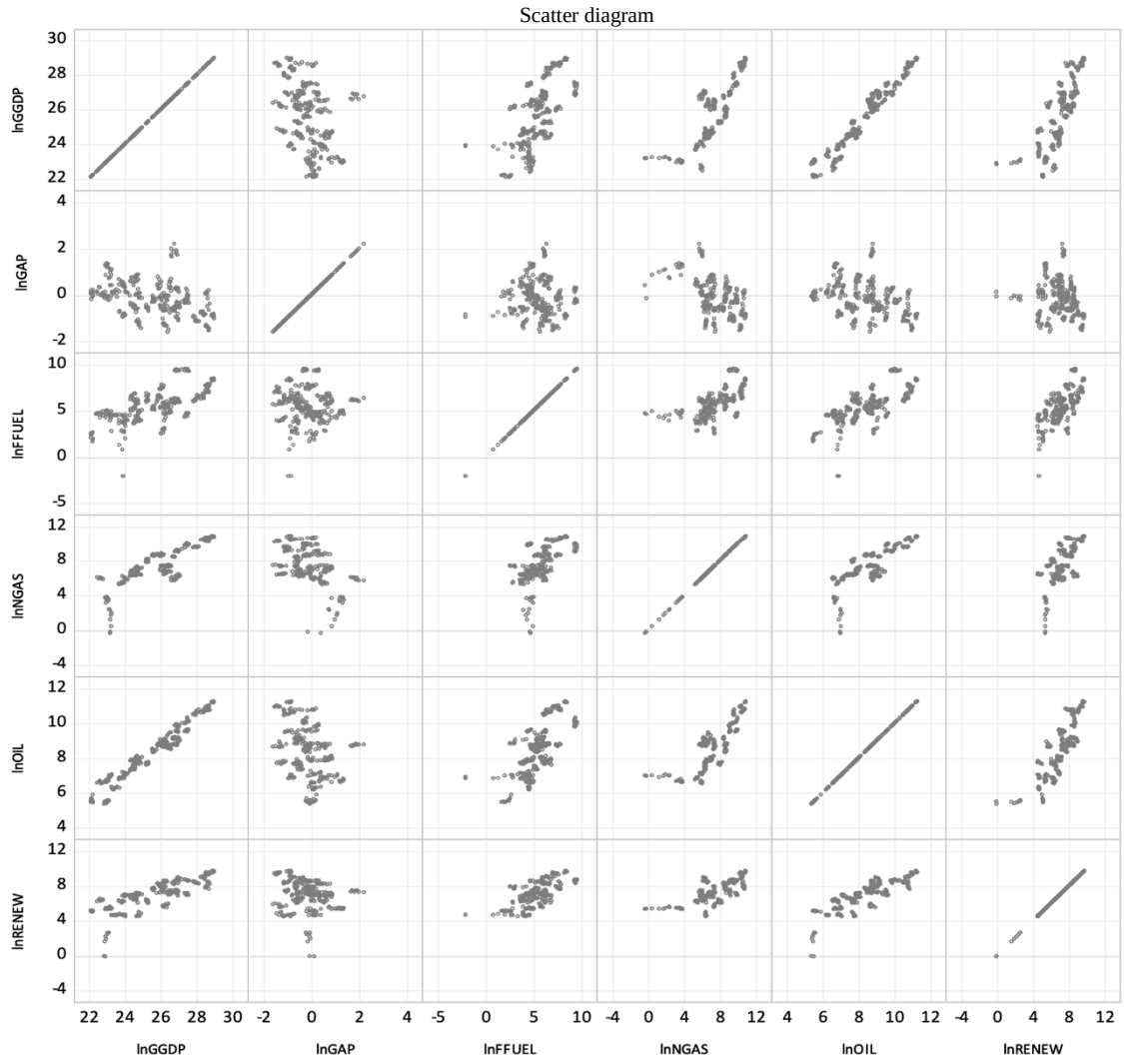

Source: Authors' calculations.

Acta Montanistica Slovaca
ISSN 1335-1788
actamont.tuke.sk

Portfolio Investment diversification at Global stock market: A Cointegration Analysis of Emerging BRICS(P) Group

***Sarfaraz A. BHUTTO*[1], *Rizwan Raheem AHMED*[2], *Dalia STREIMIKIENE*[3]*, *Saifullah SHAIKH*[4] *and* *Justas STREIMIKIS*[5, 6]**

Authors' affiliations and addresses:
[1] Institute of Commerce, Shah Abdul Latif University, Khairpur, Sindh, Pakistan
e-mail: sarfaraz_ahmed0333@yahoo.com

[2] Faculty of Management Sciences, Indus University, Block-17, Gulshan, Karachi-75300, Pakistan
e-mail: rizwanraheemahmed@gmail.com

[3] Institute of Sport Science and Innovations, Lithuanian Sports University, Sporto str. 6, LT-4422, Lithuania
e-mail: dalia.streimikiene@lsu.lt

[4] Institute of Commerce, Shah Abdul Latif University, Khairpur, Sindh, Pakistan
e-mail: saifullah.shaikh@salu.edu.pk

[5] Lithuanian Institute of Agrarian Economics, Vivulskio g. 4A-13, Vilnius, Lithuania.
[6] The University of Economics and Human Science in Warsaw, Okopowa 59, 01-043 Warsaw, Poland
e-mail: jutas.streimikis@gmail.com

***Correspondence:**
Dalia Streimikiene, Institute of Sport Science and Innovations, Lithuanian Sports University, Sporto str. 6, LT-4422, Lithuania
e-mail: dalia.streimikiene@lsu.lt

How to cite this article:
Bhutto, S. A., Ahmed, R. R., Streimikiene, S., Shaikh, S. and Streimikis, S. (2020). Portfolio Investment diversification at Global stock market: A Cointegration Analysis of Emerging BRICS(P) Group. *Acta Montanistica Slovaca*, Volume 25 (1), 57-69

DOI:
https://doi.org/10.46544/AMS.v25i1.6

Abstract
This study investigates the outcomes of emerging BRICS(P) groups at the global stock market. The Emergence of this Group helps the investors in the diversification of international portfolio funds. However, economic and financial globalization assimilated the world's leading economies to provide an interdependent investment portfolio structure for investors and savings in the transformation and allocation of funds. The diversification of the international stock market may bounce the investors of BRICS(P) Group to maximize the expected returns along with a certain level of risk placement. This study prefers to use Auto-Regressive Distributed Lag (A.R.D.L.) method to evaluate the outcomes of investment diversification and to investigate the short-term and long-term changing patterns of the sampled stock exchange markets in the BRICS(P) nations. The findings of this study show that a significant investment portfolio diversification may originate benefits if the funds become merged among the B.R.I.C.S. (Brazil, Russia, India, China, and South Africa) nations. Moreover, this study made a separate point of view for the investment funds of India and Pakistan. The study investigates that the funds of these two nations are assimilated, and the appropriate diversification of investment may exist through the assimilation of these two economies. The results would suggest the international and native investors merge their investment proposals among these economies and to construct a well-diversified portfolio because a shared value of risk protects the investors. It gives opportunities to earn desirable returns. The study has implications on all sectors of the economy, including mining as well as natural resource prices.

Keywords
Portfolio diversification, emerging BRICS(P) group, financial globalization, global stock markets, A.R.D.L. method

Introduction

In the context of portfolio investment, the modern theories of portfolio support the investors (native/international) to minimize the portfolio risk and maximize the investment return. The global framework of portfolio investment gives more provision for investors in several dimensions of risk and return (Opoku-Mensah et al., 2019; Lekovic, 2018; Bahlous & Yusof, 2014). Most of the countries are not consistent with economic prosperity. They face quick upswings and downturns in the economic cycle, though; international investment diversification reduces the volatility of investor's returns. The preliminary research studies on the global investment found a nonlinear relationship between foreign financial and instinctive/domestic financial securities due to the non-diversification of investment funds. Grubel (1968), Levy and Sarnat (1970), and Salisu and Oloko (2015) are the pioneer researchers for these empirical studies. Contrary, it is found that this nonlinear relationship may convert to linearity if we assess international investment diversification (Mei & McNown, 2019; Cosset & Suret, 1995).

Moreover, they suggested that the structure of emerging financial markets would become beneficial for investors as well as for economies. If we say that all the stock markets (National/International) are Volatile, that would not be wrong. However, the portfolio investment theories propose, "Stock markets are volatile, a good speculator may forecast well by observing the ongoing trends of the financial market." A country contains several economic and non-economic risks that push the investor to diversify the investment to other countries, like low G.D.P., devaluation of the currency, increasing interest rate, political and market risks (Okwu et al., 2020; Bahlous & Yusof, 2014; Grubel, 1968). Therefore, the globalization of financial markets gives opportunities to hold a well-diversified international portfolio. The prospect of foreign portfolio investment cantered the speculators on investing in global financial assets, which leads them to earn suitable returns and a minimal level of risk (Ozturk & Karabulut, 2020; Li, Sarkar, & Wang, 2003). However, the trade policies of several economies have become substantial to crop a liberal financial integration at the international financial market. This is the reason for the growth in financial-economic and technological globalization. Investors are risk-averse due to this behaviour. They derive benefits from the international investment diversification to speculate best in risk and return portfolio. In a study, it was investigated that with time, the investors may derive fewer benefits from investment diversification due to the increasing interdependence of financial markets (Huang & Fang, 2019; Longin & Solnik, 1995).

Moreover, some previous studies support that the volatile nature of stock markets may increase risk factors in the scenario of the financial crisis (Wang, 2019; Batareddy, Gopalaswamy, & Huang, 2012; Guidi & Ugur, 2014; Levy & Sarnat, 1970). The interdependence of financial markets set a barrier for an active investor to diversify fund. On the other hand, in the long run, it is difficult for an inactive investor to reap a maximum return in a different financial environment. In the last decade, the developed economies assimilated with the developing economies. This Emergence from the developed world to the developing world tends speculators to invest in the new emerging financial market (Ahmad et al., 2016).

Moreover, the integration of developed economies inclines the confidence of investors to maximize return with a certain level of risk. In this regard, BRICS (Brazil, Russia, India, China, and South Africa) Group has made a significant contribution among the emerging economies (Huang & Fang, 2019). It is a leading emerging Group in the international economic forum, which is potentially high for investment. The statistics of the World Economic Forum (W.E.F.) shows that China has beaten the economy of Japan (Country of Qualitative Products). Nowadays, China has become the world's 2nd largest economy, contributing a significant role in the world economy (Rao & Padhi, 2020).

Moreover, the economies of Brazil, Russia, and India have taken a specific potion in the G7 Group, particularly; Italy is affected by the G7 economies. In our observation, the BRICS Group is a rising start for investors because of two reasons. First, the BRICS Group has become a centralized unit to captivate the aggregate investment in the international market (Rao & Padhi, 2020). Secondly, these countries are also categorized as the largest consumers of goods due to the high population. Though, the growing demand for products and services exist, like India and China. The BRICS group tends to develop Social Overhead Capital (S.O.C.) to captivate the international flow of funds. The development in Social overhead capital includes the infrastructure of the country like Better Transportation ways (Freight, Carriage), Suitable Security Plans, and fast communication (Sivarethinamohan & Sujatha, 2019). A smooth Social Overhead capital attracts the international and domestic investors, and it works as a supplement in the trade and development cycle of an economy. Some other factors also bring these emerging economies as a central hub for investment like it captures more than one-fourth area of the Globe (Huang et al., 2019; Ahmad et al., 2016).

Moreover, a high level of the population, which covers 40% of the world's population, influences these areas. It contributes fifteen percent in the world's Gross Domestic Product (G.D.P.) rate. It is predicted by Goldman Sachs, that the BRIC (Brazil, Russia, India, China except for South Africa) economies are expected to achieve the target of $128 trillion in their nominal G.D.P. rate by 2050. However, the G7 economies would reach only 66 trillion dollars at that time. BRIC economies may take up 41% of the world's stock exchange market by

2030 (Huang et al., 2019). Furthermore, China is one of the leading nations among BRICS Group, though it is expected that soon the Chinese stock market would become the world's largest stock hub, and the U.S.A. capital market may have been crushed (Rao & Padhi, 2020; Zonouzi et al., 2014). A massive change is seen in several economies after the price hit in the oil market; some economies have drawn benefits and others sacrificed. I.M.F. (International Monetary Fund) and W.E.F. (World Economic Forum) suggests, "The recent change in the oil price put a good scratch at the economy of Pakistan." It is observed that Pakistan is accompanying some major economic transformation Like C.P.E.C. (China Pakistan Economic Corridor), though China's associated commercial projects bring Pakistan at financial Brink (Ghauri et al., 2020; Ahmed et al., 2018b). The economy has emerged to an international market with an index of M.S.C.I. (Morgan Stanley Capital Market). The Pakistan Stock Exchange (P.S.E.) performing well at the KSE-100 index, and according to Bloomberg KSE-100, the M.S.C.I. ranked as a 5th best stock exchange in the world. Moreover, this Emergence of Stock Markets is considered best in Asian Equity Market (Fatima & Shamim, 2020).

The above-stated facts stipulate to investigate the advantages of portfolio investment in these emerging economies and benefits associated with a well-diversified portfolio. However, it is articulated in the previous studies that portfolio diversification gives opportunities to maximize the return on investment with a certain level of risk, though; investment diversification sinks the benefits of the exchange rate, upswings at the international equity market. Diversification based on SWOT analyses of several firms, and variation in the economic policies, etc. (Ghauri et al., 2020; Guidi & Ugur, 2014; Mobarek & Li, 2014; Salisu & Oloko, 2015; Sukumaran, Gupta, & Jithendranathan, 2015). Therefore, this study tends to find the outcomes of portfolio investment diversification among the BRICS(P) Group. Moreover, this study raises the following questions to answer.

- What benefits of investment diversification can be drawn by an investor with the Emergence of stock Markets in BRICS(P) Group?
- What could be the short-run and long-run relationship among the stock markets of BRICS(P) Group?

The answers to the above-stated questions tend to enlighten and educate international investors to draw maximum benefits by investing in a portfolio. It also gives remedies to minimize portfolio-associated risk. Investors may feel satisfaction from such provisions of portfolio diversification, which would give them maximum returns, though, these analyses would help the investors to figure out an optimal and well-diversified investment portfolio among the BRICS(P) Group. This study is based on secondary data; Therefore, Time series patterns have used to comprehend short and long-term investment forces among BRICS(P) Group. Furthermore, the linear relationship among BRICS(P) Group is observed by the A.R.D.L. approach and correlation.

This study has outlined five parts; the 1st part was related to the introduction of the study topic. Moreover, 2nd part would explain a detailed review of the literature, and some evidence from past studies on the international portfolio diversification and 3rd part centres the data set and methodology, which we used to know the outcomes of the study. The study results would be explained in the 4th part. Finally, the last and 5th part of this study would summarize the study findings as to the conclusion and future research suggestions, and implications would also be included.

Substantiation from previous literature

The concept of Portfolio Investment was primarily introduced by (Markowitz, 1952) and some supporting keystones of C.A.P. (Capital Assets Pricing) Model was founded by (Lintner, 1975; Sharpe, 1964). The Markowitz Portfolio theory explains the real theme of a financial asset. It suggests the way to select financial security, which holds some unique characteristics. Moreover, at the same time, it gives analyses of implicit/explicit factors of a portfolio, which can uplift the aggregate value of investment profitable with a minimal level of risk. Furthermore, the CAPM approach includes three key elements that help estimate the expected return on financial security; these three elements such as 1) the risk-free rate of return, 2) Market risk Premium and 3) Beta values (Ozturk & Karabulut, 2020).

The first two elements assess non-diversifiable risk and beta measure the risk relevancy of individual financial security. The covariance of financial securities measures the composition of a well-diversified portfolio. In simple words, it measures the real phenomena of the ongoing market to predict the expected return with a specific portion of the risk. In a nutshell, Portfolio theory refers to the improving behaviour of investors in a portfolio context (Wang, 2019). At the same time, the CAMP approach depicts an equilibrium point of aggregate economic practice in which every investor tends to invest with a relevant percentage of risk. The above theories conclude that all investors behave rationally to make an appropriate portfolio structure, and the risk-averse nature pushes investors to build a well-diversified investment portfolio (Parveen et al., 2020). In this regard, the international portfolio gives investors more provision to circulate their investment in several economies by enjoying maximum returns with minimum risk. Therefore, the foreign portfolio investment is more dominated than the domestic one (Tsagkanos et al., 2019; Boubaker & Jouini, 2014).

Many empirical studies have focused on the benefits derived from international diversification of funds at emerging financial markets. One of the significant studies on international diversification of investment was investigated in recent years (Ahmed et al., 2018; Mobarek & Li, 2014). They found that cointegration among BRICS economies is irregular or asymmetry, and it is affected by the financial crises which have taken place in the financial market of the U.S.A. Though, newer financial and economic policies of the U.S.A. have become failed to hit financial damage at BRICS Group (Okwu et al., 2020). A regression technique was used to find the results. Previously, some supporting studies were conducted by Laurenceson and Chai (2003), and Patev et al. (2006), they had the view that no long-run relationship is expected between two broad financial markets, the American financial market and Central Eastern Europe Financial market (C.E.E.F.M.). They pointed out the declining rate of investment diversification due to the financial crisis. However, they state that investors may drive minimal provision from diversification in the period of the financial crisis and may gain short-run benefits after the financial crisis. Another study gives the opposite view of the C.E.E.F.M. role in the international part (Sivarethinamohan & Sujatha, 2019). It suggests that there is a high tendency of C.E.E.F.M. to the developed Southeastern EU markets. They are highly correlated and interdependent in the diversification of funds, especially during economic shock. The maximum benefits may drive investors at prevailing market returns and certain risk percentages (Tsagkanos et al., 2019; Guidi & Ugur, 2014).

The economic shock in the Japanese Stock Market and the American stock market affect Asian countries' financial markets (Batareddy et al., 2012). Moreover, it is investigated that the World Equity market has integrated with emerging and developed financial markets (Johnson & Soenen, 2009). The past studies have significantly stated the advantages of international investment diversification. It is stated that the financial market (Stock Market) of the U.S.A. is dominated over the Asian Financial Markets (Stock Market), these are interdependent or cointegrated (Mei & McNown, 2019; Dhanaraj, Gopalaswamy, & Babu, 2013). Moreover, they stated that the economy of the U.S.A. is declared as the world's largest economy. Though, being a large economy, they are rich in industries and major supplier of advanced technological products to Asian countries, the benefits are mutually exclusive for both US and Asian economies. Therefore, many investors are willing to invest in these cointegrated financial markets to enjoy the mutual benefits of investment diversification. However, the Economic shock or financial crisis that may take place into Asian Economies may affect the US financial market (Dhanaraj et al., 2013). A comparative study between EMU and MU is conducted by Dunis et al. (2013). They were of the view that new EMU members build a certain degree of economic acceleration over the EU Contrary, the same degree of economic acceleration in not observed in EMU. In the context of international investment diversification, the Islamic way of financing tends to be the maximum provision to invest in the selected Islamic-ruled economies (Bhoi, 2019; Bahlous & Yusof, 2014).

A comparative study was conducted to observe the co-moment of stock markets in the U.S.A., UK, Germany, and Japan. The study found the outcomes of the Japanese stock market, making a relatively lower degree of co-moment with the stock markets of the U.S.A., UK, and Germany. In contrast, a high degree is observed in the German stock market with the U.S. and UK (Rua & Nunes, 2009). According to Mobarek and Li (2014), the Association of Southeast Asian Nations (ASEAN) would not pin the benefits for international investors (No-native). However, Portfolio Diversification would not be benefited to them. Contrary, the benefits may drive from emerging economies (Ahmad et al., 2016). The maximum provision of return and minimization of risk are the key benefits of international diversification of Portfolio Investment, particularly in emerging financial markets (Ahmed et al., 2018a; Zonouzi et al., 2014). The World Equity market has reduced a little portion of portfolio diversification benefits, and it is due to the interdependence of financial markets. Moreover, the benefits of Portfolio diversification may increases if investors of emerging economies put a short sell barrier to move forward for the US stock market (Li et al., 2003). One of the significant studies is carried out on the emerging economies of South Asian Markets, and it considered three leading countries like India, Srilanka, and Pakistan.

The results of this show a significant relationship among all three countries, and they may drive portfolio diversification (Sukumaran et al., 2015). The geographical location and economic conditions may push investors to reap maximum benefits from Portfolio diversification with minimal risk (Fatima & Shamim, 2020; Valadkhani, Salisu & Oloko, 2015; Chancharat, & Harvie, 2008). According to Hoque (2007), a week correlation is observed between Bangladeshi and the Japanese Stock Market. However, the stock markets of the U.S.A. and Bangladesh are highly correlated. They were of the view that due to the similarity between stock markets, not much benefit could be derived from portfolio diversification. Emerging economies refer to frontier economies, an intermediate economic channel for an investor to diversify their funds from developed economies to developing economies. It can be done in both the short- and long run. The quick upswing and consistency prompt the expectations of investors to forecast maximum return with a small percentage of risk (Opoku-Mensah et al., 2019; Tsagkanos et al., 2019; Sukumaran et al., 2015).

Material and Methods

Data sources. This study aims to investigate the short and long-run investment relationship between the BRICS-(P) Group. To achieve the oriented object of this study, we collected secondary data from Yahoo Finance, which is an authentic source to collect refined financial data of several stock indices. This study includes seven indices only. Linking the BRICS-(P) Group, we cover the sampled countries of Brazil, Russia, India, China, South Africa, and Pakistan, which is suitable to represent the concept of emerging economies at a global level. This study induced to collect Monthly data from November-2012 to October-2018. We eliminated the data of the Dividends of firms, this was carried out by Lekovic (2018), and Bahlous and Yusof (2014) studied. The primary purpose of this study is to explore the benefits of international portfolio diversification. Though, there is no need to enter the data of dividends because it influences the intrinsic policies of an individual firm.

Estimation techniques. This study induces to analyze the short-term and long-term relationship among BRICS-(P) group by using the Auto-Regressive Distributed Lag (A.R.D.L.) approach (Fatima & Shamim, 2020; Pesaran, Shin, & Smith, 1996). It is considered as a regression model that includes appropriate numbers of lags for each independent variable (Ghauri et al., 2020; Laurenceson & Chai, 2003). Furthermore, the A.R.D.L. model includes I (1) and I (0) (But not I (2)) to ensure the past and past and present values of chosen variables. The A.R.D.L. approach supports the non-stationary data set. Moreover, it estimates the appropriate cointegration for short-term and long-term coefficient, and it is not necessary to have a unique integration level among study variables. Still, it would be fine in their efficiency and unbiasedness (Narayan P.K. & Narayan S., 2006). We have used the following six A.R.D.L. models shown by Eq. (1) to Eq. (6) as follows:

Model 1.

$$Pakista\eta_t = \alpha_0 + \alpha_1 Brazil + \alpha_2 Russia_t + \alpha_3 India_t + \alpha_4 China_t + \alpha_5 SouthAfrica_t + \alpha_6 USA(S\ \&\ P500)_t + \varepsilon_t \quad (1)$$

Model 2.

$$Brazil_t = \alpha_0 + \alpha_1 Pakista\eta_t + \alpha_2 Russia_t + \alpha_3 India_t + \alpha_4 China_t + \alpha_5 SouthAfrica_t + \alpha_6 USA(S\ \&\ P500)_t + \varepsilon_t \quad (2)$$

Model 3.

$$Russia_t = \alpha_0 + \alpha_1 Brazil + \alpha_2 Pakista\eta_t + \alpha_3 India_t + \alpha_4 China_t + \alpha_5 SouthAfrica_t + \alpha_6 USA(S\ \&\ P500)_t + \varepsilon_t \quad (3)$$

Model 4.

$$India_t = \alpha_0 + \alpha_1 Brazil + \alpha_2 Russia_t + \alpha_3 Pakista\eta_t + \alpha_4 China_t + \alpha_5 SouthAfrica_t + \alpha_6 USA(S\ \&\ P500)_t + \varepsilon_t \quad (4)$$

Model 5.

$$China_t = \alpha_0 + \alpha_1 Brazil + \alpha_2 Russia_t + \alpha_3 India_t + \alpha_4 Pakista\eta_t + \alpha_5 SouthAfrica_t + \alpha_6 USA(S\ \&\ P500)_t + \varepsilon_t \quad (5)$$

Model 6.

$$SouthAfrica_t = \alpha_0 + \alpha_1 Brazil + \alpha_2 Russia_t + \alpha_3 India_t + \alpha_4 China_t + \alpha_5 Pakista\eta_t + \alpha_6 USA(S\ \&\ P500)_t + \varepsilon_t \quad (6)$$

The study chooses seven indices. Table 1 exhibited the list of the selected indices of BRICS-(P) Group.

Tab. 1. BRIC– (P) Group indices

Country	Index
Brazil	IBOVESPA
Russia	M.I.C.E.X.
India	BSE SENSEX
China	S.S.E.
South Africa	E.Z.A.
Pakistan	KSE-100
USA	S&P500

The first six indices concern with the emerging BRICS(P) Group, and the last index measures the combined financial performance of emerging economies at the global level. Furthermore, we have used the Error correction model to assess the short-term relationship of investment portfolio diversification. The E.C.M. may extract from the A.R.D.L. model by simple linearity if the model specification is unbiased (Fatima & Shamim, 2020; Cosset & Suret, 1995). Moreover, without having a change in long-term information, we can drive short-term results by using E.C.M. (Batareddy et al., 2012). The following models from Eq. (7) to Eq. (12) specify the E.C.M.s for selected variables of the study.

Model 7.

$$\begin{aligned}\Delta \ln Pakista\eta_t &= \alpha_0 + \sum_{j=1}^{k1} b_j \Delta \ln Brazil_{t-j} + \sum_{j=0}^{k2} c_j \Delta \ln Russia_{t-j} + \sum_{j=0}^{k3} d_j \Delta \ln India_{t-j} \\ &+ \sum_{j=0}^{k4} e_j \Delta \ln China_{t-j} + \sum_{j=0}^{k5} f_j \Delta \ln SouthAfrica_{t-j} + \sum_{j=0}^{k6} g_j \Delta \ln USA(S\ \&\ P500)_{t-j} \\ &+ n_1 \ln Pakista\eta_{t-1} + n_2 \ln Brazil_{t-1} + n_3 \ln Russia_{t-1} + n_4 \ln India_{t-1} \\ &+ n_5 \ln China_{t-1} + n_6 \ln SouthAfrica_{t-1} + n_7 \ln USA(S\ \&\ P500);\end{aligned} \tag{7}$$

Model 8.

$$\begin{aligned}\Delta \ln Brazil_t &= \alpha_0 + \sum_{j=1}^{k1} b_j \Delta \ln Pakista\eta_{t-j} + \sum_{j=0}^{k2} c_j \Delta \ln Russia_{t-j} + \sum_{j=0}^{k3} d_j \Delta \ln India_{t-j} \\ &+ \sum_{j=0}^{k4} e_j \Delta \ln China_{t-j} + \sum_{j=0}^{k5} f_j \Delta \ln SouthAfrica_{t-j} + \sum_{j=0}^{k6} g_j \Delta \ln USA(S\ \&\ P500)_{t-j} \\ &+ n_1 \ln Pakista\eta_{t-1} + n_2 \ln Brazil_{t-1} + n_3 \ln Russia_{t-1} + n_4 \ln India_{t-1} \\ &+ n_5 \ln China_{t-1} + n_6 \ln SouthAfrica_{t-1} + n_7 \ln USA(S\ \&\ P500)\end{aligned} \tag{8}$$

Model 9.

$$\begin{aligned}\Delta \ln Russia_t &= \alpha_0 + \sum_{j=1}^{k1} b_j \Delta \ln Brazil_{t-j} + \sum_{j=0}^{k2} c_j \Delta \ln Pakista\eta_{t-j} + \sum_{j=0}^{k3} d_j \Delta \ln India_{t-j} \\ &+ \sum_{j=0}^{k4} e_j \Delta \ln China_{t-j} + \sum_{j=0}^{k5} f_j \Delta \ln SouthAfrica_{t-j} + \sum_{j=0}^{k6} g_j \Delta \ln USA(S\ \&\ P500)_{t-j} \\ &+ n_1 \ln Pakista\eta_{t-1} + n_2 \ln Brazil_{t-1} + n_3 \ln Russia_{t-1} + n_4 \ln India_{t-1} \\ &+ n_5 \ln China_{t-1} + n_6 \ln SouthAfrica_{t-1} + n_7 \ln USA(S\ \&\ P500)\end{aligned} \tag{9}$$

Model 10.

$$\begin{aligned}\Delta \ln India_t &= \alpha_0 + \sum_{j=1}^{k1} b_j \Delta \ln Brazil_{t-j} + \sum_{j=0}^{k2} c_j \Delta \ln Russia_{t-j} + \sum_{j=0}^{k3} d_j \Delta \ln Pakista\eta_{t-j} \\ &+ \sum_{j=0}^{k4} e_j \Delta \ln China_{t-j} + \sum_{j=0}^{k5} f_j \Delta \ln SouthAfrica_{t-j} + \sum_{j=0}^{k6} g_j \Delta \ln USA(S\ \&\ P500)_{t-j} \\ &+ n_1 \ln Pakista\eta_{t-1} + n_2 \ln Brazil_{t-1} + n_3 \ln Russia_{t-1} + n_4 \ln India_{t-1} \\ &+ n_5 \ln China_{t-1} + n_6 \ln SouthAfrica_{t-1} + n_7 \ln USA(S\ \&\ P500)\end{aligned} \tag{10}$$

Model 11.

$$\Delta \ln China_t = \alpha_0 + \sum_{j=1}^{k1} b_j \Delta \ln Brazil_{t-j} + \sum_{j=0}^{k2} c_j \Delta \ln Russia_{t-j} + \sum_{j=0}^{k3} d_j \Delta \ln India_{t-j}$$
$$+ \sum_{j=0}^{k4} e_j \Delta \ln Pakista\eta_{t-j} + \sum_{j=0}^{k5} f_j \Delta \ln SouthAfrica_{t-j} + \sum_{j=0}^{k6} g_j \Delta \ln USA(S\ \&\ P500)_{t-j} \quad (11)$$
$$+ n_1 \ln Pakista\eta_{t-1} + n_2 \ln Brazil_{t-1} + n_3 \ln Russia_{t-1} + n_4 \ln India_{t-1}$$
$$+ n_5 \ln China_{t-1} + n_6 \ln SouthAfrica_{t-1} + n_7 \ln USA(S\ \&\ P500)$$

Model 12.

$$\Delta \ln SouthAfrica_t = \alpha_0 + \sum_{j=1}^{k1} b_j \Delta \ln Brazil_{t-j} + \sum_{j=0}^{k2} c_j \Delta \ln Russia_{t-j} + \sum_{j=0}^{k3} d_j \Delta \ln India_{t-j}$$
$$+ \sum_{j=0}^{k4} e_j \Delta \ln China_{t-j} + \sum_{j=0}^{k5} f_j \Delta \ln Pakista\eta_{t-j} + \sum_{j=0}^{k6} g_j \Delta \ln USA(S\ \&\ P500)_{t-j} \quad (12)$$
$$+ n_1 \ln Pakista\eta_{t-1} + n_2 \ln Brazil_{t-1} + n_3 \ln Russia_{t-1} + n_4 \ln India_{t-1}$$
$$+ n_5 \ln China_{t-1} + n_6 \ln SouthAfrica_{t-1} + n_7 \ln USA(S\ \&\ P500)$$

The above specifications of Error Correction Models show several signs of summation, which are termed to signify E.C.M.s. Moreover, to understand the long-term relationship, the term n_s is expressed in the E.C.M.s. To identify the null-hypotheses for long-term relationship (No Cointegration) is postured as:

$H_0 = n_1 = n_2 = n_3 = n_s = 0$. If $H_0 \neq 0$, so it associates with alternative hypotheses mean

$H_1 = n_s 6 = 0$

It is performed through the F-test, where the critical values have elasticity or variation among the variable, expressed as I (0) or I (1). The hypothesis acceptance and rejection are based on upper and lower bound levels of F-statistics. The rejection region of the null hypothesis falls if the upper bound level is less than the calculated F-statistics. On the contrary, if the lower bound level is higher than the calculated F-statistics, then it is impossible to reject the null-hypotheses. If the results would influence the first aspect, then we say that there is no evidence of cointegration among study variables. If results fall in the second aspect, then we may state cointegration evidence among study variables. There might be uniqueness in results if the calculated f-stat falls in between lower and upper bound levels, though, it ensures that the results are convincing (Pesaran et al., 1996). To estimate the relative quality of the A.R.D.L. model for a given set of data, we have used the Akaike Information Criterion (A.I.C.). Moreover, A.I.C. estimates the mean of selected models, or it gives the trade-off point between the goodness of fit and simplicity of the study model.

Results

Descriptive analysis. Table 2 summarises the whole data set in the descriptive statistics. The descriptive statistics show some exciting elements in the dataset, which would influence our further chosen statistical models. The highest volatility is observed in the Russian stock market, and this stock market deviates by 0.031, which is relatively high compared to others. Contrary, the Pakistani stock exchange, particularly the KSE-100 index, is relatively less volatile; it deviates by 0.016.

Moreover, it shows completely different results compared to other countries' stock markets. The std. deviation of India shows 0.019 and -0.112, 0.14 as a minimum and maximum values. China and South Africa are relatively high volatile compared to Pakistan, India, and Brazil, showing 0.021 and 0.029 deviations.

Tab. 2. Descriptive Statistics

Variables	Minimum	Maximum	Mean	Std. Deviation
Pakistan	-0.04	0.078	0.00067	0.016
Brazil	-0.117	0.127	0.00031	0.020
Russia	-0.49	0.598	0.00042	0.031
India	-0.112	0.14	0.00049	0.019
China	-0.086	0.26	0.00016	0.021
South Africa	-0.692	0.198	-0.00005	0.029

Results of A.R.D.L. (Long-term and Short-term). As we mentioned that the A.R.D.L. approach removes the issue of unit root of data set and stationarity at the level. However, we have input the data series, which includes the log-returns of stocks. Furthermore, we have estimated the E.C.M.s by using appropriate lag length. The estimations of A.R.D.L. models are represented in Table 3, having both long-term and short-term outcomes for all the prescribes models of the study. Table 3 is categorized into three panels. Panel-A includes the long-term relationship among study variables, Panel-B refers to short-term dynamics, and finally, Panel-C depicts lower and upper Bound test.

Moreover, in the long-term dynamics, Panel-A directs to the lagged values of study variables, which gives the forecast about endogenous index in the prescribed model—taking the example of the Brazilian stock market, which is at negative endogenous index with Indian stock market. This endogenous index is handy for speculators (native and international) to predict and derive the quick maximum advantage from the portfolio diversification.

LT represents the long-term, and ST signifies the short-term. The Panel-A includes extensive evidence to forecast the future value of related indices. This forecasting is based on the lagged value and variable results. Moreover, the study chooses the endogenous index for each variable, like for Pakistan; KSE-100 is taken as an endogenous index. The results may help managers of mutual fund companies or fund managers for each member of the BRICS(P) group.

Results from Model-7. In the long-run relationship (Panel-A), it is found that the Pakistani stock market with South Africa earns no benefit of investment diversification because both stock markets move simultaneously. The relationship between both economies is statistically significant, with a positive relationship. Moreover, Panel-A shows irrelevant results of Pakistan's Stock Market with the U.S.A., India, Russia, and China. Therefore, investors of Pakistan may enjoy diversification gains by merging their portfolio investment with these growing economies (U.S.A., India, Russia, China).

Results from Model-8. In the long-run relationship (Panel-A), it is investigated that, Brazilian stock market is negatively correlated with the Indian stock market, and it is statistically significant. Moreover, it is observed that the speculators of Brazil could have investment diversifications benefits in the stock markets of Pakistan and China. The statistical results show that given economies are correlated insignificantly, the USA S&P500 has the same position as Brazil. On the other hand, Brazilian investors may not enjoy the diversification gains in Russia and South Africa. A positive correlation of the Brazilian stock market is associated with Russian and South African stock markets.

Results from Model-9. In the long-run relationship (Panel-A), It is observed that the Russian investors can secure investment diversification benefits in the stock markets of Pakistan, India, and Russia. An insignificant relationship exists in the given economies. Moreover, a significant link is found in South Africa and US S&P500 with Brazil, which means that there is no benefit of investment diversification for Russian investors.

Results from Model-10. In the long-run relationship (Panel-A), it is examined that the Indian stock market is statistically insignificant and negatively correlated with Pakistani, South African, US S&P500, and Brazilian Stock markets, which refers to the portfolio investors of India can derive benefits from investment diversification.

Results from Model-11. In the long-run relationship (Panel-A), it is found that China has an insignificant relationship with US SP500, Pakistan, Russia, and Brazil. The correlation among given economies encourages the investors of china to earn diversification gains by investing portfolios in US S&P500, Pakistan, Russia, and Brazil.

Results from Model-12. In the long-run relationship (Panel-A), it is investigated that the South African stock market has an insignificant correlation with the stock markets of Russia, Pakistan, Brazil, US S&P500, and India. Therefore, investors can invest their portfolios in the given stock markets to reap the benefits of investment diversification.

Furthermore, a short-run relationship is observed in Panel-B. It is observed that the cointegration is significant, as the E.C.M.s Models from Eq. (7) to Eq. (12) is found statistically significant. Following is the interpretation of the short-run relationship among the BRIC(P) group.

Results from Model -7 (E.C.M.). In the short run relationship (Panel-B), it is observed that the investors of the Pakistani stock market earn no short-run benefits over all the stock markets of BRICS. The E.C.M. results are statistically significant.

Results from Model-8 (E.C.M.). The short-run relationship (Panel-B) found that the Brazilian stock market has a short-term impact on US S&P500 and Russian stock markets. However, Brazil consists of no short-run effect on the rest of the other stock markets in the Group.

Results from Model-9 (E.C.M.). In the short run relationship (Panel-B), it is investigated that the Russian stock market is affected in the short run with the Indian stock market and the Brazilian stock market. However, the case is unaffected rest of the other members of the Group.

Results from Model-10 (E.C.M.). In the short run relationship, it is explored that Russian and Chinese funds have centred short-run effects on the Indian market. Moreover, the short-run effect is far from other members of the Group.

Results from Model-11 (E.C.M.). The short-run relationship shows that the Chinese Stock market has a short-term effect on the stock markets of South Africa and India. No short-run effect is found from other economies in China.

Results from Model-12 (E.C.M.). In the short run relationship (Panel-B), it is observed that the stock market of South Africa is affected if short-run volatility exists in the Chinese stock market. However, the rest of the other markets in the Group have no short-run effect on the stock market of South Africa.

Following the work of (Pesaran et al., 1996), A.R.D.L. Bound test is used to investigate the cointegration among the study variables. Moreover, F-statistics in the bound test is used as an indicator for the existence of cointegration or no cointegration. The rule to reject the null hypothesis that there is no cointegration among the study variables is possible when the U-Bound value becomes less than calculated F-stats.

Results from A.R.D.L. Bound Test. For cointegration, Panel-C shows that the U-Bound values are lesser than the calculated F-Stats, which rejects the null hypothesis. It means that cointegration with long-run relationship exists among the study variables.

Tab. 3. Long-tern & short-term estimates

Dependent Variables Coefficient / (p-value)						
Regressors	**Pakistan**	**Brazil**	**Russia**	**India**	**China**	**South Africa**
Lag Length	(4,0,4,0,1, 1,2)	(3,0,3,2, 2,4,2)	(4,2,2,1, 4,0,4)	(2,0,0,0,3, 0,0)	(4,2,0,0,0, 0,1)	(4,4,0,0,0, 0,0)
C	0.0004 (0.0124)	0.0029 (0.134)	0.0002 (0.321)	0.0003 (0.051)	0.0004 (0.443)	-0.0001 (0.730)
Pakistan	-	-0.026 (0.4040)	0.036 (0.281)	-0.034 (0.157)	0.0243 (0.188)	0.006 (0.566)
BRAZIL	0.034 (0.212)	-	0.006 (0.611)	-0.0011 (0.818)	-0.021 (0.233)	-0.0033 (0.633)
RUSSIA	0.032 (0.124)	0.063 (0.000)	-	0.054 (0.000)	-0.0042 (0.423)	0.006 (0.341)
INDIA	0.032 (0.216)	-0.053 (0.0223)	0.027 (0.308)	-	0.0487 (0.006)	-0.020 (0.227)
CHINA	0.012 (0.339)	0.021 (0.123)	0.061 (0.062)	0.052 (0.005)	-	0.037 (0.003)
SOUTH AFRICA	0.030 (0.042)	0.0663 (0.0039)	0.065 (0.0054)	-0.0087 (0.253)	0.0525 (0.000)	-
S&P500	0.0062 (0.744)	0.0184 (0.423)	0.055 (0.072)	-0.028 (0.210)	-0.0166 (0.341)	0.0042 (0.787)
Panel-B: Short-Term Estimates						
D(PAKISTAN)	-	0.034 (0.111)	0.038 (0.352)	-0.022 (0.206)	0.0221 (0.214)	0.014 (0.664)
D(BRAZIL)	0.017 (0.130)	-	0.109 (0.0006)	-0.001 (0.821)	0.023 (0.166)	0.029 (0.310)

D(RUSSIA)	0.005 (0.421)	0.0453 (0.000)	-	0.031 (0.012)	-0.0049 (0.613)	0.0055 (0.377)
D(INDIA)	-0.0139 (0.125)	-0.0017 (0.535)	0.081 (0.008)	-	0.0433 (0.006)	-0.019 (0.317)
D(CHINA)	0.018 (0.253)	0.0301 (0.1504)	-0.0051 (0.743)	0.032 (0.006)	-	0.058 -0.002
D(SOUTHAFRICA)	0.0031 (0.781)	0.0135 (0.219)	0.023 (0.297)	-0.006 (0.319)	0.0222 (0.003)	-
D(S&P500)	0.003 (0.911)	0.0311 (0.061)	0.062 (0.060)	-0.02 (0.199)	-0.0121 (0.441)	0.002 (0.995)
CointEq(-1)	-0.675 (0.000)	-1.022 (0.000)	-1.266 (0.000)	-0.921 (0.000)	-0.897 (0.000)	-1.171 (0.000)
Panel-C: A.R.D.L. Bound Test						
F-Stat	82.142	171.4	172.22	212.133	98.661	124.431
Upper Bound Critical Value	5.23	5.23	5.23	5.23	5.23	5.23

Moreover, a summarized view of A.R.D.L. tests is illustrated in Table 4 for the ease of reading, in which members among BRICS(P) group could have more chances to earn the portfolio diversification benefits in the long run and short run. Both Panels A and B explain that if the result of the coefficient is statistically negative, it does not matter whether it is significant or insignificant it does refer that investors of that member group may enjoy diversification benefits. Contrary, if the coefficients are statically positive and significant, then it means there is no space for investors to reap the portfolio diversification benefits.

Tab. 4. Summarized results of A.R.D.L. models

Investors from	Pakistan		Brazil		Russia		India		China		South Africa	
	LT	ST	LT	ST	LT	ST	LT	ST	LT	ST	LT	ST
Pakistan	-	-	Yes	Yes	Yes	Yes	Yes	Yes	Yes	Yes	Yes	Yes
Brazil	Yes	Yes	-	-	No	No	Yes	Yes	Yes	Yes	Yes	Yes
Russia	Yes	Yes	No	No	-	-	No	No	Yes	Yes	Yes	Yes
India	Yes	Yes	No	Yes	Yes	No	-	-	No	No	Yes	Yes
China	Yes	Yes	Yes	Yes	No	Yes	No	No	-	-	Yes	No
South Africa	Yes	Yes	No	Yes	No	Yes	Yes	Yes	No	No	-	-
S&P 500	Yes	Yes	Yes	No	No	No	Yes	Yes	Yes	Yes	Yes	Yes

Discussion

This study intends to investigate the benefits of international portfolio diversification, which can be reaped by the investors/speculators of BRICS(P) group. This study aims to examine the short and long-run investment benefits associated with the BRICS(P) Group. To achieve the oriented object of this study, we collected secondary data from Yahoo Finance, which is an authentic source to collect refined financial data of several stock indices. This study includes seven indices only. Linking the BRICS-(P) Group, we cover the sampled countries of Brazil, Russia, India, China, South Africa, and Pakistan, which is suitable to represent the concept of emerging economies at a global level (Rao & Padhi, 2020; Ahmed et al., 2018a). E.C.M. and A.R.D.L. model, respectively, test this study induced to collect Monthly data from November-2012 to October-2018 and short-run and long-run relationships. The given statistical techniques are very significant to investigate cointegration compared to traditional approaches. The long-run relationship among BRICS(P) shows that all investors belong from that Group may earn substantial benefits by diversifying their respective portfolio investments.

Moreover, this study result supports the past studies on benefits on portfolio investment diversification among evolving economies like (Opoku-Mensah et al., 2019; Zonouzi et al., 2014). One of the studies shows

that the economic volatility between the developed and developing world brings certain good factors for portfolio investors in diversifying their investment structures (Ahmed et al., 2018b; Sukumaran et al., 2015). This study also included the US S&P500, which is one of the leading global stock markets in the world. The reason to add US S&P500 is to investigate the dependency of the BRICS(P) group on this leading stock market. The study results regarding the US S&P500 refer that no longer run and short-run dependence occurs on the returns index of the US S&P500 except the Russian stock market (Bhoi, 2019). It is found that there is an uneven structure that leads the B.I.C.S.P. (Brazil, India, China, South African, and Pakistan) to cointegration without inducing the US S&P500. This study result supports the finding of Grubel (1968). Lastly, one of the significant implications of this study is to understand portfolio diversification benefits between two economies, which are highly cointegrated in the Group. The following members are Pakistan and India. There is a possibility of both long and short-run investment diversification benefits for investors of given economies. It is crucial for economists, policymakers, and speculators to understand the untapped mutual benefits between these two growing economies. It is observed that policymakers of both countries should make ease for investors to diversify their funds, and that would also lead to more prosperous and optimal economic conditions for both countries.

Conclusions

This study is motivated by the portfolio mechanism. The statement, "Portfolio risk is better than stand-alone risk," hors d'oeuvre for researchers to contribute their findings in fulfilment of portfolio concepts, and this study efforted to do the same. This study supports the context of portfolio diversification that it is better to diversify funds in the global emerging markets to reap maximum investment returns with minimal risk. Thou, this study had taken the BRICS(P) group to investigate whether the benefits of portfolio investment diversification exist or not. The outcomes of this study exposed that this emerging market has a high potential for investors so they can enjoy portfolio returns. It is the notion that investors who are willing and able to invest in the emerging market must consider associated risk factors like economic risk, political risk, social risk, etc. There should be a reconciliation between extreme volatility of emerging market and investment return. However, investment diversification has some significant advantages in that native investors hedged the investment by diversifying funds to other member countries in the Group, like the recession in the economy, devaluation of home currency, etc. This study recommends significant policy implications for investors as well as for policymakers. Firstly, it provides some implicit measures for investors to maximize their investment return and reduce the risk ratio by diversifying their investments. Thou, investors may reduce the risk bubble, and there would be ease in placing an optimal portfolio structure in BRICS(P) group. Secondly, it is directing to policymakers (Government) to reap benefits by diversifying their potential investment portfolios in this emerging market. However, that would help raise government funds to enhance the economic power and run better financial operations.

Moreover, the study result made an inference about the adequate investment diversification between two growing economies, Pakistan and India. Despite the economic risk and unmatched political situations between these two economies, it is investigated that investors may earn mutual investment returns. However, non-smoothness in political dialogues and negotiations reduced the optimization of co-investors, foreign investment is ignored where high political risk exists. However, the developing country investor tends to invest in a strong market where they could earn a suitable return. Still, owing to some uncertain domestic conditions, they could have faced loss. Though, it is felt that there is a need to make specific financial policies by which both economies (Pakistan & India) may diversify funds without hesitation. It is possible when both countries show their willingness to have a positive and constructive dialogue.

References

Ahmed, R. R., Vveinhardt, J., & Štreimikienė, D. (2018). Multivariate Granger Causality between oil and gold prices, and KSE100 index: Evidence from Johansen cointegration and G.A.R.C.H. approaches. *Acta Montanistica Slovaca*, *23*(2), 216-231. https://actamont.tuke.sk/pdf/2018/n2/10streimikiene.pdf

Ahmed, R. R., Vveinhardt, J., Štreimikienė, D., Ghauri, S. P., & Ashraf, M. (2018). Stock Returns, Volatility and Mean Reversion in Emerging and Developed Financial Markets. *Technological and Economic Development of Economy, 24*(3), 1149-1177. http://dx.doi.org/10.3846/20294913.2017.1323317

Bahlous, M., & Yusof, R. M. (2014). International diversification among Islamic investments: is there any benefit. *Managerial Finance*, *40*(6), 613-633. https://doi.org/10.1108/mf-08-2013-0225

Batareddy, M., Gopalaswamy, A. K., & Huang, C.-H. (2012). The stability of long-run relationships: A study on Asian emerging and developed stock markets (Japan and U.S.). *International Journal of Emerging Markets*, *7*(1), 31-48. https://doi.org/10.1108/17468801211197888

Bhoi, B. K. (2019). Can BRICS countries escape the middle-income trap? *Macroeconomics and Finance in Emerging Market Economies, 12*(3), 293-296. https://doi.org/10.1080/17520843.2019.1615970

Boubaker, S., & Jouini, J. (2014). Linkages between emerging and developed equity markets: Empirical evidence in the P.M.G. framework. *The North American Journal of Economics and Finance, 29*, 322-335. https://doi.org/10.1016/j.najef.2014.06.004

Cosset, J.-C., & Suret, J.-M. (1995). Political risk and the benefits of international portfolio diversification. *Journal of International Business Studies, 26*(2), 301-318. https://doi.org/10.1057/palgrave.jibs.8490175

Dhanaraj, S., Gopalaswamy, A. K., & Babu M, S. (2013). Dynamic interdependence between the U.S. and Asian markets: an empirical study. *Journal of Financial Economic Policy, 5*(2), 220-237. https://doi.org/10.1108/17576381311329670

Dunis, C., Sermpinis, G., & Ferenia Karampelia, M. (2013). Stock market linkages among new EMU members and the euro area: Implications for financial integration and portfolio diversification. *Studies in Economics and Finance, 30*(4), 370-388. https://doi.org/10.1108/sef-04-2012-0048

Fatima, Z., & Shamim, M. (2020). The Dynamic Nexus between G.D.P., Consumption and Exports of BRICS Countries: An A.R.D.L. Cointegration Analysis. *International Journal of Trade and Global Markets, 13*(3). https://doi.org/10.1504/ijtgm.2020.10021570

Ghauri, S. P., Ahmed, R. R., Arby, M. F., & Martinkute-Kauliene, R. (2020). Assessment of Effects of Relative Price Variability on Inflation. *Transformations in Business & Economics, 19*, No. 1 (49), 306-322. Available online http://www.transformations.knf.vu.lt/49/article/asse

Grubel, H. G. (1968). Internationally diversified portfolios: welfare gains and capital flows. *The American Economic Review, 58*(5), 1299-1314. https://doi.org/10.3386/w4340

Guidi, F., & Ugur, M. (2014). An analysis of South-Eastern European stock markets: Evidence on cointegration and portfolio diversification benefits. *Journal of International Financial Markets, Institutions, and Money, 30*, 119-136. https://doi.org/10.1016/j.intfin.2014.01.007

Hoque, H. A. A. B. (2007). Co-movement of Bangladesh stock market with other markets: Cointegration and error correction approach. *Managerial Finance, 33*(10), 810-820. https://doi.org/10.1108/03074350710779250

Huang, B., & Fang, X. (2019). Market Sentiment, Valuation Heterogeneity, and Corporate Investment: Evidence from China's A-Share Stock Market. *Emerging Markets Finance and Trade*. https://doi.org/10.1080/1540496x.2019.1672531

Huang, N., Huang, Z., & Wang, W. (2019). The Dynamic Extreme Co-Movement between Chinese Stock Market and Global Stock Markets. *Emerging Markets Finance and Trade, 55*(14), 3241-3257. https://doi.org/10.1080/1540496x.2018.1529559

Johnson, R., & Soenen, L. (2009). European economic integration and stock market comovement with Germany. *Multinational Business Review,17*(3),205-228. https://doi.org/10.1108/1525383x200900024

Laurenceson, J., & Chai, J. C. (2003). *Financial reform and economic development in China*: Edward Elgar Publishing. https://doi.org/10.4337/9781843767190

Lekovic, M. (2018). Investment diversification as a strategy for reducing investment risk. *Journal of Ekonomski horizonti, 20*(2), 173-187. https://doi.org/10.5937/ekonhor1802173l.

Levy, H., & Sarnat, M. (1970). Diversification, portfolio analysis, and the uneasy case for conglomerate mergers. *The Journal of Finance, 25*(4), 795-802. https://doi.org/10.1111/j.1540-6261.1970.tb00553.x

Li, K., Sarkar, A., & Wang, Z. (2003). Diversification benefits of emerging markets subject to portfolio constraints. *Journal of Empirical Finance, 10*(1-2), 57-80. https://doi.org/10.1016/s0927-5398(02)00027-0

Lintner, J. (1975). The valuation of risk assets and the selection of risky investments in stock portfolios and capital budgets *Stochastic Optimization Models in Finance* (pp. 131-155): Elsevier. https://doi.org/10.2307/1926735

Longin, F., & Solnik, B. (1995). Is the correlation in international equity returns constant: 1960–1990? *Journal of international money and finance, 14*(1), 3-26. https://doi.org/10.1016/0261-5606(94)00001-h

Markowitz, H. (1952). Portfolio selection. *The Journal of Finance, 7*(1), 77-91. https://doi.org/10.1111/j.1540-6261.1952.tb01525.x

Mei, G., & McNown, R. (2019). Dynamic causality between the U.S. stock market, the Chinese stock market and the global gold market: implications for individual investors' diversification strategies. *Applied Economics, 51*(43), 4742-4756. https://doi.org/10.1080/00036846.2019.1601156

Mobarek, A., & Li, M. (2014). Regional volatility: common or country-specific? Exploration of the international stock market. *Studies in Economics and Finance, 31*(4), 406-425. https://doi.org/10.1108/sef-04-2013-0051

Narayan, P. K., & Narayan, S. (2006). Savings behaviour in Fiji: an empirical assessment using the A.R.D.L. approach to cointegration. *International journal of social economics, 33*(7), 468-480. https://doi.org/10.1108/03068290610673243

Okwu, A. T., Oseni, I. O., & Obiakor, R. T. (2020). Does Foreign Direct Investment Enhance Economic Growth? Evidence from 30 Leading Global Economies. *Global Journal of Emerging Market Economies*. https://doi.org/10.1177/0974910120919042

Opoku-Mensah, E., Yin, Y., Sandra, A. A., & Tuffour, P. (2019). Mergers and Acquisitions Antecedents in BRICS. *Global Journal of Emerging Market Economies*, *11*(3), 202-214. https://doi.org/10.1177/0974910119887241

Ozturk, H., & Karabulut, T. A. (2020). Impact of financial ratios on technology and telecommunication stock returns: evidence from an emerging market. *Investment Management and Financial Innovations*, *17*(2), 76-87. https://doi.org/10.21511/imfi.17(2).2020.07

Parveen, S., Satti, Z. W., Subhan, Q. A., & Jamil, S. (2020). Exploring market overreaction, investors' sentiments and investment decisions in emerging stock market. *Borsa Istanbul Review*. https://doi.org/10.1016/j.bir.2020.02.002

Patev, P., Kanaryan, N., & Lyroudi, K. (2006). Stock market crises and portfolio diversification in Central and Eastern Europe. *Managerial Finance, 32*(5), 415-432. https://doi.org/10.1108/03074350610657436

Pesaran, M. H., Shin, Y., & Smith, R. J. (1996). *Testing for the existence of a Long-run Relationship*. https://doi.org/10.1016/0304-4076(94)01644-f

Rao, B. M., & Padhi, P. (2020). Macroeconomic costs of currency crises in BRICS: an empirical analysis. *Macroeconomics and Finance in Emerging Market Economies*. https://doi.org/10.1080/17520843.2020.1749103

Rua, A., & Nunes, L. C. (2009). International comovement of stock market returns A wavelet analysis. *Journal of Empirical Finance, 16*(4), 632-639. https://doi.org/10.1016/j.jempfin.2009.02.002

Salisu, A. A., & Oloko, T. F. (2015). Modelling spillovers between the stock market and F.X. market: evidence for Nigeria. *Journal of African Business, 16*(1-2), 84-108. https://doi.org/10.1080/15228916.2015.1061285

Sharpe, W. F. (1964). Capital asset prices: A theory of market equilibrium under conditions of risk. *The Journal of Finance, 19*(3), 425-442. https://doi.org/10.1111/j.1540-6261.1964.tb02865.x

Sivarethinamohan, R., & Sujatha, S. (2019). Econometric Modelling: Testing of Randomness,Volatility, Casualty and Cointegration of Emerging Stock Market Indices of India and MIST Countries. *International Journal of Innovative Technology and Exploring Engineering*, *9*(2), 1402-1417. https://doi.org/10.35940/ijitee.a4946.129219

Sukumaran, A., Gupta, R., & Jithendranathan, T. (2015). Looking at new markets for international diversification: frontier markets. *International Journal of Managerial Finance, 11*(1), 97-116. https://doi.org/10.1108/ijmf-05-2013-0057

Tsagkanos, A., Siriopoulos, C., & Vartholomatou, K. (2019). Foreign direct investment and stock market development. *Journal of Economic Studies*, *46*(1), 55-70. https://doi.org/10.1108/jes-06-2017-0154

Valadkhani, A., Chancharat, S., & Harvie, C. (2008). A factor analysis of international portfolio diversification. *Studies in Economics and Finance, 25*(3), 165-174. https://doi.org/10.1108/10867370810894693

Wang, L. (2019). Stock Market Valuation, Foreign Investment, and Cross-Country Arbitrage. *Global Finance Journal*, 40, 74-84. https://doi.org/10.1016/j.gfj.2018.01.004

Zonouzi, S. J. M., Mansourfar, G., & Azar, F. B. (2014). Benefits of international portfolio diversification: Implication of the Middle Eastern oil-producing countries. *International Journal of Islamic and Middle Eastern Finance and Management, 7*(4), 457-472. https://doi.org/10.1108/imefm-02-2014-0017

Acta Montanistica Slovaca
ISSN 1335-1788
actamont.tuke.sk

Determination of the Rational Number of Cutters on the Outer Cutting Drums of Geokhod

Alexey KHORESHOK[1,], Kirill ANANIEV[2], Alexander ERMAKOV[3], Dilshad KUZIEV[4] and Alexander BABARYKIN[5]*

Authors' affiliations and addresses:
[1]T.F. Gorbachev Kuzbass State Technical University, Mining machines Department, 650000 Kemerovo, 28 Vesennya st., Russian Federation
e-mail: haa.omit@kuzstu.ru

[2]T.F. Gorbachev Kuzbass State Technical University, Mining machines Department, 650000 Kemerovo, 28 Vesennya st., Russian Federation
e-mail: aka.kgmik@kuzstu.ru

[3]T.F. Gorbachev Kuzbass State Technical University, Mining machines Department, 650000 Kemerovo, 28 Vesennya st., Russian Federation
e-mail: ermakovan@kuzstu.ru

[4]National University of Science and Technology «MISiS», 119049 Moscow, 6 Leninskiy avenue, Russian Federation
e-mail: aka_black@list.ru

[5]T.F. Gorbachev Kuzbass State Technical University, Mining machines Department, 650000 Kemerovo, 28 Vesennya st., Russian Federation
e-mail: aleksandr_babarikin@mail.ru

***Correspondence:**
Alexey Khoreshok, 650000 Kemerovo, 28 Vesennya st., Russian Federation,
tel: +7(3842)396379
e-mail: haa.omit@kuzstu.ru

Funding information:
The research was sponsored by Grant of the President of the Russian Federation for state support of young Russian scientists MK-664.2018.8.

How to cite this article:
Khoreshok, A., Ananiev, K., Ermakov, A., Kuziev, D., and Babarykin, A. (2020). Determination of the Rational Number of Cutters on the Outer Cutting Drums of Geokhod. *Acta Montanistica Slovaca*, Volume 25 (1), 70-80

DOI:
https://doi.org/10.46544/AMS.v25i1.7

Abstract
The issue of substantiation and choice of a rational number of cutters on the outer cutting drums of the geokhod for the formation of grooves in medium strength rocks is considered in this article. It is established that the coefficient of variation of the torque must be taken into account while determining the number of cutters. It is established that the required feed velocities are realized with a crown-type outer cutting drum at one or two cutters in the cutting lines, and the coefficient of torque variation does not exceed 20% at any allowable number of cutters and equal lag angle. On the disk-type outer cutting drum required feed velocities are realized with the number of cutters in the cutting lines from 1 to 4. The minimum number of cutters providing a coefficient of variation of the torque on the disk-type outer cutting drum above the set depends on the angle of coverage and reduces with the increase of the angle of coverage. The example of schematic designs of OCD AR and OCD EP development is shown for a prototype model of geokhod (3.2 m diameter) using the obtained expressions to determine the basic geometric, kinematic, force, and structural parameters. The possibility of decision making of the type of OCD for geokhod and its creation is confirmed. The documentation design documents for production crown-type OCD for a prototype of geokhod were developed based on the conducted research.

Keywords
tunneling, geokhod, cutting drum, picks, cutting lines.

Introduction

The study of the underground space formation and the development of the subsoil are very important for the life of mankind and affect the development associated with the creation of new technologies for the construction of a network of underground transportation traffic, the construction of highways and railways at a considerable depth.

The construction of the underground mines, city highways, and subway tunnels is a laborious and expensive process. The most important tasks are increasing the rate of penetration, productivity, safety, and reduce the cost of work.

The traditional representation of excavation, as the process of cavity formation in rocks, has always defined and still determines the directions for improving the technologies for the construction of underground structures and the creation of tunneling equipment for the development of underground space. However, the well-known technologies of mining, developing along the path of increasing the power and metal consumption of equipment, have practically exhausted their possibilities in increasing productivity, ensuring the safety of workers, and expanding the scope.

Further development of work in the field of geotechnology and geotechnics can be performed in two directions:

- modernization of the existing mining equipment and its improvement by creating systems of a new technical level;
- search and creation of a fundamentally new, alternative toolkit (technologies and geotechnics) for the development of the subsoil and the formation of underground space.

In underground conditions, external propulsions are used to move the tunneling machines: tracked, wheeled, or wheel-rail. Propulsors which have proved themselves well working on the ground surface (at the contact of solid and air), are not adapted for movement in the geological environment.

From this circumstance, the main problems of modern technologies of mine workings follow:

- the impossibility of movement of the boring apparatus in any direction of the underground space;
- the impossibility of creating large pressure forces on the executive body for the destruction of hard rock.

As a result, to create sufficient pressure, the designers are forced to increase the weight of mining machines, which already reaches 80-100 tons. In addition, safety issues in the face zone continue to be acute.

In the course of work of the tunneling machine or shield, in order to create the force of thrust and pressure force on the cutting drum, the external media itself is not involved in any way, but only the solid surface of the excavation at the contact of the geo and air environments, or with the shield method of penetration - strong permanent support.

For a number of years in Russia, the team of authors has been working on the creation of a new type of mining technology. The idea of the work is based on the proposal to consider the excavation of mine workings initially as a process of movement of a solid body in the environment of the host rocks. At the same time, the rock is used as a supporting element, participating in the creation of the driving force of the tunneling machine and the pressure force on the cutting drums, as well as for performing the basic technological operations, including fixing the production of permanent support.

The principle of functional unification of the main movement (submission to the face) and the process of cutting rocks gave the name "geowinchester" technology for mining.

"Geowinchester technology" is a set of processes for the mechanized conduct of mine workings with the formation and use of a system of the boring screw and longitudinal grooves, where the processes for the development of the face, the cleaning of the rock, the fixation of the developed space, and the movement of the entire tunneling system to the face, are carried out in a combined mode. The involvement of the rock is achieved by introducing an additional technological operation - the formation of a system of outer grooves (Fig. 1).

On the basis of the functional-structural theory of the creation of mining systems, a prototype model of a tunneling unit was developed, the distinctive feature of which is the rotational-progressive movement to the face according to the principle of screwing. At present, this type of mining machines has been called the geokhod (Fig. 2).

As noted earlier, a characteristic feature of the technology of excavation using geokhods is the formation of grooves beyond the contours of the works. Screw grooves are involved in the conversion of transmission torque to the pressure force at the bottom. To stabilize the tail section, longitudinal grooves are formed. In the rocks of medium and high strength, the formation of grooves requires the use of active limiting executive bodies.

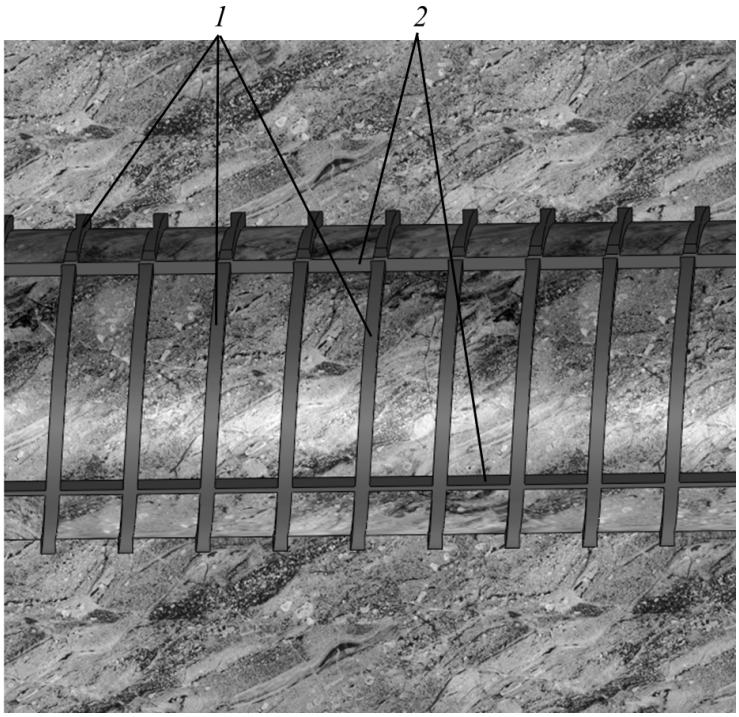

1 – screw grooves; 2 – longitudinal grooves

Fig. 1. Longitudinal cross-section of the mine with formed behind-contour grooves

The geokhod is a shield tunnel boring machine by which underground moves are carried out due to interaction with the geo-environment (Blashchuk et al., 2014; Chernukhin et al., 2015; Sadovets et al., 2015). In recent years, a team of authors is working on creating geokhod for work in rocks of medium strength (Figure 2) (Aksenov et al., 2015; Aksenov et al., 2019).

The main cutting drums of the geokhod for the formation of contours of heading has a number of prototypes in traditional mining machines (Jang et al., 2016). At the same time, the system for the grooves formation out of the contours of the heading was not previously used in such complexes. As options, two types of outer cutting drums (OCD) were proposed: disk-type and crown-type (Fig. 3).

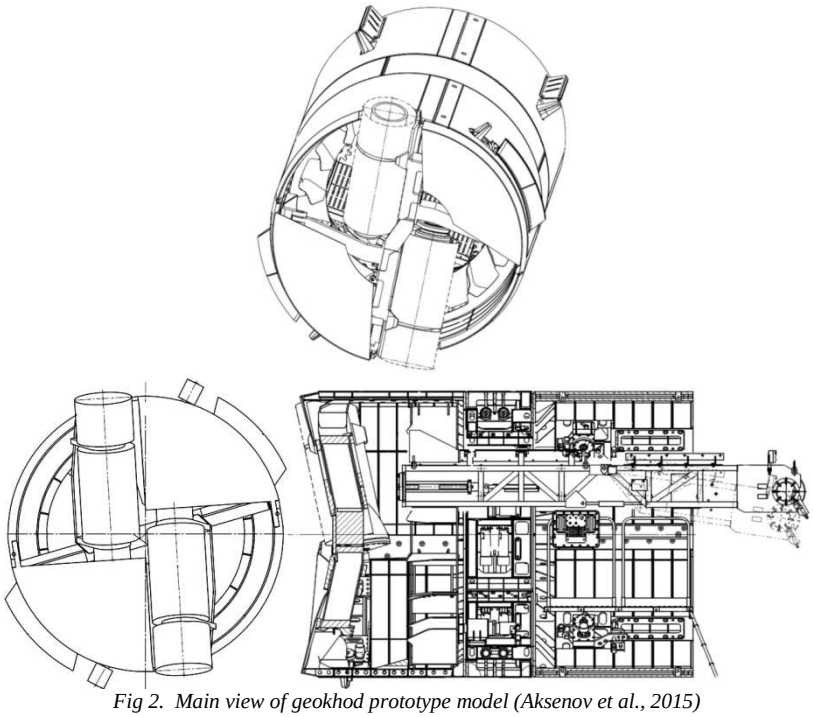

Fig 2. Main view of geokhod prototype model (Aksenov et al., 2015)

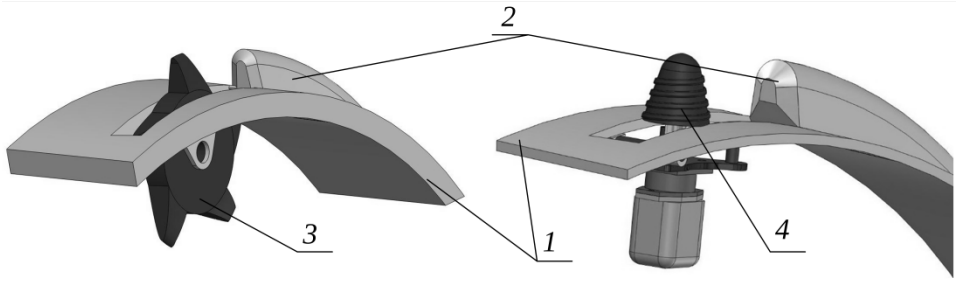

1 – geokhod's shield; 2 – screw blade; disk-type groove cutter; 4 – crown-type cutter
Fig 3. Schemes of the geokhod's OCDs

A comparison and evaluation of the proposed solutions require the algorithm for the arrangement of cutters on OCD. The task of the arrangement of the cutters is reduced to determining their rational number, taking into account the coefficients of variation (CV) loads, the characteristics of the rock, and the requirements for the specific energy of destruction (Balci, 2013; Hekimoglu and Fowell, 1991).

When choosing a scheme of the arrangement of the cutters, two conditions must be fulfilled: ensuring equal chip thickness and a minimum number of cutters. The first condition will ensure the possibility of comparing the results obtained with respect to the specific energy of destruction, and the second is a necessary condition for saving the most expensive part of the cutting drum (the hard alloy of the cutters).

Methods

The number of cutters on OCD regardless of type, can be defined as (Methodology. Shearers…,1984):

$$n_c = \sum_{i=1}^{n_{l.n}} n_{c.l.i} \quad . \tag{1}$$

In the type: nl.n stands for the number of cutting lines.

The number of cutters in the i-cutting line (Methodology. Shearers…,1984):

$$n_{c.l.i} = \frac{V_{FOCD}}{h_{\max} n_{OCD}} \quad . \tag{2}$$

In the type: V_{FOCD} stands for the feed velocity of OCD; h_{max} is the maximum cutting depth; n_{OCD} is OCD rotation frequency.

According to the recommendations (Baron et al., 1968) maximum cutting depth is set equal to 16 mm for the medium strength rocks. Larger values of the maximum cutting depth will lead to increased force on the cutting edges. At a small cutting depth values, the formation of the fissure collapse does not occur, which leads to a significant increase in the specific energy of destruction and increased tool wear (Wingquist and Hanson, 1987).

The feed velocity of OCD in the groove, on the one hand, is determined by the required feed rate of geokhod, and on the other depends on the number of cutters in the cutting line. The required feed velocity of OCD can be represented as:

$$V_{FOCD} = \sqrt{\left(\frac{V_{Fg}(D_g + 2h_g}{D_g \operatorname{tg}(\beta)}\right)^2 + V_{Fg}^2} \quad . \tag{3}$$

The explanations of the parameters and their values set for the study are presented in Table 1.

Table 1. The parameters of geokhod and OCD

Parameter	Designation	Value
Feed velocity of geokhod	VFg	7 [m/hr]
The outer diameter of geokhod	Dg	2,1 ÷ 5,6 [m]
The height of the outer groove formed by OCD	hg	0,1 ÷ 0,4 [m]
The helix angle of the screw blade	β	4 ÷ 20 [deg]

The OCD rotation frequency can be represented as a function of the cutting velocity

$$n_{OCD} = \frac{V_c}{\pi D_{OCD}} \quad . \tag{4}$$

In the type: V_c stands for the cutting velocity; D_{OCD} is the diameter of OCD by cutters.

The maximum acceptable cutting velocity can be set in accordance with the recommendations of the research (Chang et al., 2006; Dogruoz et al., 2015). At the high cutting velocity (more than 2.0 m/s), the intensive wear of the cutters occurs due to its overheating. In addition, in a number of experimental studies, the preferability of cutting of rocks with low cutting velocity was proved (Hurt and MacAndrew, 1985). The limitation of the cutting velocity is another condition that will lead to an increase in the number of cutters in the cutting lines in some schemes of the OCD.

Substituting into equation (2) equation (4) and expressing the feed velocity of OCD, we obtain an expression for determining the feed velocity of OCD with a given number of cutters in the cutting line (possible feed velocity of OCD).

$$V_{FOCD} = \frac{n_{c.l.i} V_c h_{\max}}{\pi D_g} \quad . \tag{5}$$

The number of cutting lines is determined by the distance between the adjacent cutting lines (so-called cutting step). Another feature of the geokhod's OCDs is the work in the groove, that is, in conditions typical for the peripheral parts of the cutting drums of coal mining and tunneling machines (Xuefeng et al., 2018). For the accepted cutting depth and tool width (b), the cutting step, t_{opt}, can be determined from the expression

$$t_{opt} = b + 1.3 h_{\max} \quad . \tag{6}$$

The number of cutting lines ($n_{l.n}$) for crown-type OCD is determined by the height of the groove, and for the disk-type OCD by the groove width:

$$n_{l.n} = \frac{h_{OCD}}{t_{opt}} \quad . \tag{7}$$

In the formula: h_{OCD} stands for the height of OCD.

The number of cutting lines for disk-type OCD and small groove width is equal to one that is not advisable since the cutter will be in the locked cut mode. Therefore, it is rational to take at least two cutting lines.

Relatively low values of feed velocity of OCD allow the use of schemes with a small number of cutters. At the same time, the values of torque CV can be much higher than CV of the traditional cutting drums. It is caused by a smaller number of cutters in contact with the rock and a significant fluctuation of this number (Li et al., 2013; Ermakov, 2016).

In accordance with (Ermakov, 2016) the torque CV is defined as

$$k_B = \frac{\sigma_M}{x_M} \quad , \tag{8}$$

$$\sigma_M = \sqrt{\frac{1}{n-1} \sum_{j=1}^{n} (x_j - x_M)^2} \quad , \tag{9}$$

$$x_M = \frac{1}{n} \sum_{j=1}^{n} x_j \quad , \tag{10}$$

In the formula: σ_M stands for the mean square deviation of torque on OCD; x_M is the expected value of torque on OCD; n is the number of observations in the sample; x_j is the current torque value; j is the number of the OCD considered position

The current torque value can be represented as

$$x_j = \frac{D_{OCD} \sum_{i=1}^{n_c} Pz_{ij}}{2} \quad . \tag{11}$$

Where Pz_{ij} is the cutting force on i-cutter in a j-position of OCD.

In accordance with (Baron, et al., 1968), the cutting force is determined by an expression that can be represented in a general form:

$$Pz_{ij} = f(h_{\max}, \varphi_{cov}, t_{opt}, f, F_r) \quad . \tag{12}$$

In the type: F_r are the parameters that characterize the geometry of the cutter (a type of cutter, a shape of the head of the holder, a width of the cutting edge, a shape of the front face, cutting angle and etc.), f is Protodyakonov rock strength.

Results and Discussion

Taking the number of cutters in the cutting line is discrete from one to four; the maximum possible feed velocities were determined from the expression (5). As the diameter of the OCD increases or the number of cutters in the cutting line decreases, the possible feed velocity of the OCD decreases (the cutting velocity is assumed constant). Figure 4 shows the joint graphs of the possible and necessary velocities of the submission of OCD.

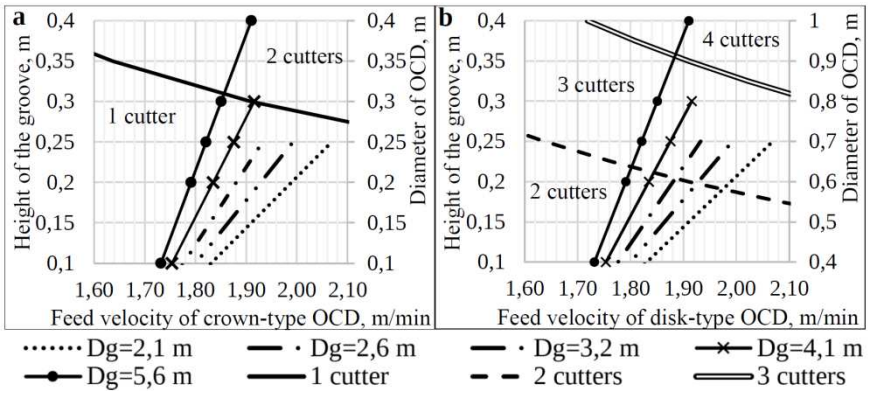

Fig 4. The diameter of the OCD and the height of the groove depending on the required and possible feed velocity

The curve "1 cutter" (Figure 4, a) shows the maximum feed velocity at one cutter in the cutting line and limits the area below which a single-cutter can work in the cutting line at the accepted cutting velocity and cutting depth. For disk-type OCD (Figure 4, b), the areas on the graph between the curves denoted by the number of cutters correspond to the maximum feed velocity with the number of cutters in the cutting line corresponding to the number of the curve bounding the area from above.

Based on the analysis of the graphs, it is established that for the crown-type OCD of any diameters and groove heights, the required feed velocity is achieved with one cutter in the cutting lines. Exceptions are the diameter of the geokhod 5.6 m, and the height of the groove is more than 0.31 m. In this case, two cutters in the cutting lines are required to realize the required feed velocity. The required feed velocity for the disk-type OCD is realized with the number of cutters from one to four for any diameter of the disk. In this case, four cutters in the cutting lines are required only for the groove height of more than 0.35 m and a diameter of the geokhod 5.6 m. In all other cases, one to three cutters in the cutting lines are sufficient.

For some of the schemes of cutters arrangement, the minimum required CV for the OCD is not provided. It is necessary to specify the minimum number of cutters for this condition. Since CV does not depend on absolute values of forces and torque, it is possible to evaluate it at the early stages of design when choosing the number of cutters. The CV was evaluated according to expressions (8) - (11) (OCD forms a groove of rectangular cross-section, the cutters are placed with the same angle lag, the number of cutters from 5 to 60). The cutting forces were determined by the simulation in the Matlab / Simulink environment. It has been established that the angle of coverage and the number of cutters on the OCD have the greatest influence on CV.

The CV obtained for crown-type OCD is acceptable and does not exceed 10% for any number of cutters, but it can be reduced by increasing the number of cutters. The increase in the total number of cutters is achieved by increasing the number of cutters in the cutting lines, and, therefore, occurs with a step equal to the number of cutting lines. It is not always rational to produce such an increase.

The coverage angle of the disk OCD determines the entry and exit points of the cutters from the contact with the rocks, which in turn affects the shape of the chips on the OCD and the nature of the torque variation on the OCD. Dependences of CV on disk-type OCD on the number of cutters at angles of coverage of 60 and 90 degrees are presented in Figure 5.

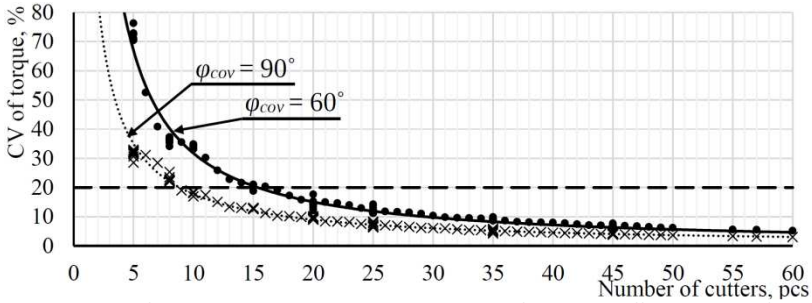

Fig 5. Dependence of CV on the disk-type OCD on the number of cutters at different angles of coverage

The points on the graph are approximated by power functions ($R^2 = 0.98$). CV values (unlike crown-type OCD) can significantly exceed the critical value (20% is indicated by a horizontal line). At a 90-degree angle of coverage, the CV exceeds 20% with 9 cutters, and at 60 degrees with 15 cutters, which is unacceptable. According to the graphs in Fig. 5, it is possible to determine the minimum number of cutters, at which CV does not exceed 20% for angles of coverage of 60 and 90 degrees. Similarly, for angles of coverage in the range of 60 to 90 degrees in 1-degree increments, the minimum cutter numbers were obtained to provide a CV of at least 10, 20, 30 and 40%. In Figure 6, the values obtained are presented graphically.

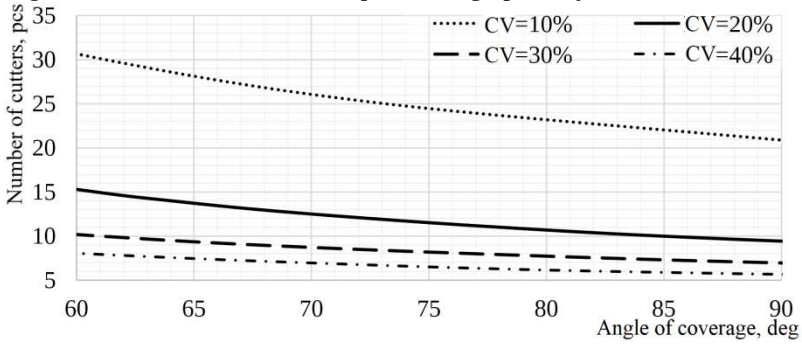

Fig 6. Dependence of the minimum number of cutters on the disk-type OCD on the angle of coverage

The curves limit from above the region in which the CV appears to be over the preset value. At a known coverage angle in accordance with Figure 6, the minimum number of cutters for a disk-type OCD can be determined by the condition of providing a given CV. To provide a CV comparable to a crown-type OCD, the total number of cutters on a disk-type OCD should exceed 20 pieces at a 90-degree coverage angle and 30 pieces at a coverage angle of 60 degrees.

As an example, the development of schemes and the determination of the main parameters of the OCD for a prototype of a geokhod 3.2 m in diameter are considered. The initial data for the calculation are presented in Table 2. The layout and the number of OCDs on the geokhod correspond to the scheme in Figure 2. For the initial ones presented in Table 2 of data, it is necessary to develop schemes both the disk and crown types of OCD of external propulsor (EP) and OCD of the anti-rotation elements (AR). It will make it possible to decide on the further constructive study of the options.

Table 2. The initial data for the development of OCD of geokhod

Parameter	**Value**		**Units**
The outer diameter of geokhod	3,2		[m]
Protodyakonov rock strength	5		[pcs]
The helix angle of the screw blade	4,55		[°]
Rotations per minute of geokhod	0,1		[rpm]
The lead of helix of the screw blade	0,8		[m]
	AR	EP	
The height of the outer groove	0,25	0,2	[m]
The width of the outer groove	0,2	0,2	[m]
The area of the outer groove	0,05	0,04	[m^2]

The results of the selection and determination of the main parameters of schemes are presented in Table 3. The cutting speed and depth of cut are adopted based on recommendations, as well as research results.

Table 3. The main parameters of schemes of OCDs

Parameter	Disk-type		Crown-type	
	OCD AR	OCD EP	OCD AR	OCD EP
The diameter of OCD, [m]	0,7	0,6	0,2	
The height, [m]	0,2		0,2	
The angle of coverage, [°]	74,1	71,5	180	
Minimum number of cutters on OCD to ensure the CV of at least 20%, [pcs]	12	13	1	
Number of cutters in cutting lines, [pcs]	1	2	1	
Number of cutting lines, [pcs]	7		9	7
Total number of cutters, [pcs]	7	9		
The total number of cutters taking into account the minimum CV, [pcs]	14			
Rotations per minute of OCD, [rpm]	2,51	35,43	5,01	70,86
Actual cutting speed, [m/s]	0,09	0,37	0,05	0,74

For a disk-type OCD AR, the number of cutters necessary in terms of productivity turned out to be insufficient under the condition of ensuring the CV. Therefore twice the number of cutters in the cutting lines is taken. So the total number of cutters for disk-type OCD AR and OCD EP is the same, despite different feed speeds.

The arrangement of the cutters should ensure uniformity of torque. Therefore, it is made with equal angular intervals of the cutters and cutting steps. Crown-type OCD EP and AR have different heights and patterns of arrangement of cutters. Thus, four designs of the OCDs are formed. The determination of the main parameters can be implemented using the obtained dependencies and using the developed computer model. Table 4 presents the results of determining the main parameters of the OCDs.

Table 4. The results of determining the main parameters of the OCDs

	OCD AR		OCD EP	
	Disk-type	Crown-type	Disk-type	Crown-type
Total friction path, [m/m]	207,27	164,72	157,03	131,78
Required torque, [N*m]	2879,54	1358,27	2303,63	1086,62
The specific power consumption on cutting, [kW*hr/m3]	3,14	2,96	3,14	2,96
Weight of OCD with a drive, [kg]	432,68	111,88	383,76	89,50
Cutting power, [kW]	0,76	0,71	8,55	8,06

Crown-type OCDs provide lower values of the total friction path, required torque, the specific power consumption on cutting, the weight of OCD with a drive, protrusion of OCD with a drive into the internal space of the geokhod, as well as permissible values of the resulting forces and torques. This led to the choice of crown-type OCD for the prototype model of geokhod at the stage of development of the design (Figure 7).

The constructive development of solutions required a number of changes to the design of the OCD:

a scheme with a cylindrical gearbox for OCD EP and OCD AR was adopted (Figure 7), the design of the mounting of the OCD drive at the same time provides access to the OCD for its maintenance and cutters replacement;

the design of the crowns was changed from cylindrical to conical due to change in the section of the blades to trapezoidal;

the number of cutters in the cutting lines was increased, the arrangement of the cutters was changed (four lag angles between the cutters, Figure 7).

The change in the number of cutters in the cutting lines is associated with the features of the prototype geokhod. OCD should ensure the formation of the groove during the operation of the starting device at the initial destruction. In an unsteady mode of operation, the feed of the OCD can significantly exceed the calculated ones, which can lead to damage of the cutting edges. Taking into account the changes introduced into the design of the OCD using a computer model, the main operating parameters were recalculated.

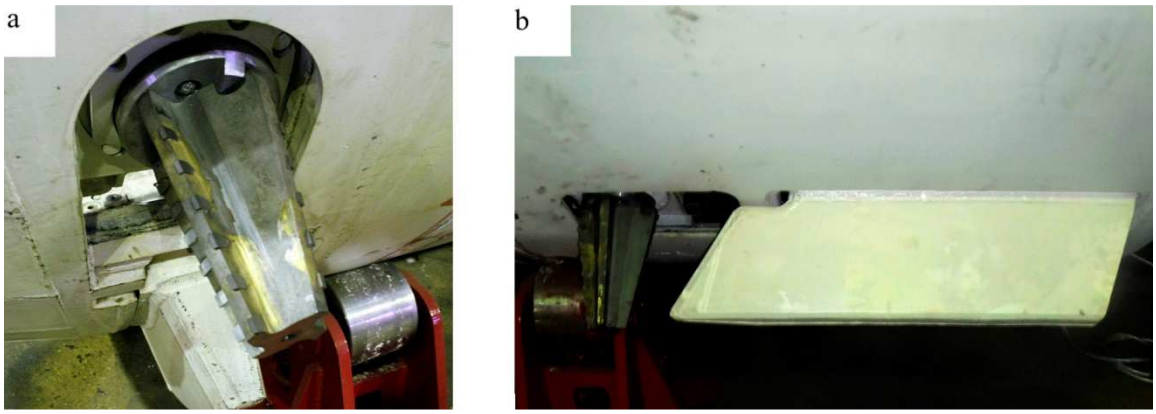

Fig 7. OCD EP (a) and OCD AR (b) of the prototype of geokhod

Based on the computations and studies, design documentation was developed for the production of OCDs of prototype geokhod. A general view of the prototype geokhod with a diameter of 3.2 m is presented in Figure 8.

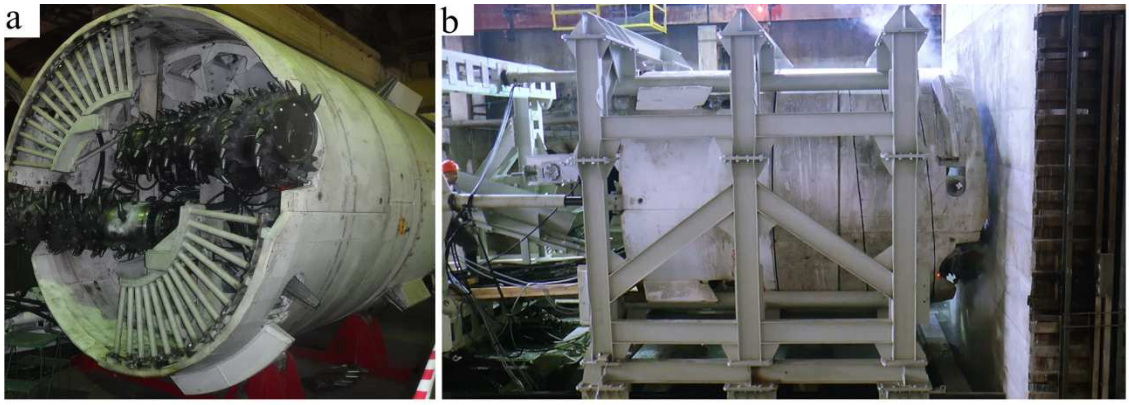

Fig 8. A general view of the prototype of geokhod (a) and test bench (b)

Conclusions

"Geowinchester technology" is a promising mining technology. The use of "Geowinchester technology" requires a significant amount of theoretical and experimental research. To conduct experimental research, a prototype geokhod 3.2 m in diameter was developed. When developing a prototype, the problem of choosing the OCD type was solved.

The number of cutters of OCD is determined by two factors: providing the required feed velocity and providing a torque CV of not higher than the preset value. At the crown-type OCD, the required feed velocities are realized with one or two cutters in the cutting lines, and the torque CV does not exceed 20% for any permissible number of cutters. On the disk-type OCD the required feed velocity is realized with the number of cutters in the cutting lines from one to four. The minimum number of cutters ensuring a torque CV on a disk-type OCD is not higher than the preset value, depends on the angle of coverage and decreases when it increases. Torque CV has lower values on the crown-type OCD than disk-type OCD under otherwise equal conditions. Also, it was established that the crown-type OCDs provide lower values of the total friction path, required torque, the specific power consumption on cutting, the weight of OCD with a drive, protrusion of OCD with a drive into the internal space of the geokhod, as well as permissible values of the resulting forces and torques.

The main directions for further research:

experimental full-scale studies of the operation of crown-type OCD on a prototype geokhod model;

the development of circuit solutions OCD combined types;

the study of the operation of the OCD of geokhod taking into account the stochastic mechanical properties of the rocks;

evaluation of the resulting efforts from the work of the OCD during the development through various geological disturbances.

References

Aksenov, V.V., Walter, A.V., Gordeyev, A.A., Kosovets, A.V., 2015. Classification of geokhod units and systems based on product cost analysis and estimation for a prototype model production. IOP Conference Series: Materials Science and Engineering 91, 012088. https://doi.org/10.1088/1757-899X/91/1/012088

Aksenov, V.V., Efremenkov, A.B., Dronov A.A., 2019. Development of a joint unit for sections of the geokhod. Journal of Mining and Geotechnical Engineering 4(7), 67-79. https://doi.org/10.26730/2618-7434-2019-4-67-79

Baranov, M.N., Božek, P., Prajová, V., Ivanova, T.N., Novokshonov, D.N., Korshunov, A.I., 2017. Constructing and calculating of multistage sucker rod string according to reduced stress. Acta Montanistica Slovaca 22.

Biały, W., 2014. Pomiar sił skrawania węgla z wykorzystaniem przyrządu POU-BW/01-WAP. Przegląd Górniczy 64-71.

Bialy, W., 2013. New devices used in determining and assessing mechanical characteristics of coal, in: SGEM2013 Conference Proceedings. Presented at the 13th SGEM GeoConference on Science and Technologies In Geology, Exploration and Mining, pp. 547–554.

Biały, W., Wedzicha, J., Nordin, V., 2018. Measurement of Forces During the Extraction Process. Multidisciplinary Aspects of Production Engineering 1, 117–128. https://doi.org/10.2478/mape-2018-0016

Bilgin, N., Copur, H., Balci, C., 2013. Mechanical excavation in mining and civil industries. CRC press.

Blashchuk, M.Yu., Kazantsev, A.A., Chernukhin, R.V., 2014. Capacity Calculation of Hydraulic Motors in geokhod Systems for Justification of Energy-Power Block Parameters. Applied Mechanics and Materials 418–425. https://doi.org/10.4028/www.scientific.net/AMM.682.418

Božek, P., 2014. Automated Detection Type Body and Shape Deformation for Robotic Welding Line, in: Swiątek, J., Grzech, A., Swiątek, P., Tomczak, J.M. (Eds.), Advances in Systems Science, Advances in Intelligent Systems and Computing. Springer International Publishing, Cham, pp. 229–240. https://doi.org/10.1007/978-3-319-01857-7_22

Cehlár, M., Rybár, P., Mihók, J., Engel, J., 2020. Analysis of investments in the mining industry. Journal of Mining and Geotechnical Engineering 1(8), 4–31. https://doi.org/10.26730/2618-7434-2020-1-4-31

Chang, S.-H., Choi, S.-W., Bae, G.-J., Jeon, S., 2006. Performance prediction of TBM disc cutting on granitic rock by the linear cutting test. Tunnelling and Underground Space Technology, Safety in the Underground Space - Proceedings of the ITA-AITES 2006 World Tunnel Congress and 32nd ITA General Assembly 21, 271. https://doi.org/10.1016/j.tust.2005.12.131

Chernukhin, R.V., Dronov, A.A., Blashchuk, M.Y., 2015. The application of the analytic hierarchy process when choosing layout schemes for a geokhod pumping station. IOP Conf. Ser.: Mater. Sci. Eng. 91, 012086. https://doi.org/10.1088/1757-899X/91/1/012086

Dogruoz, C., Bolukbasi, N., Rostami, J., Acar, C., 2016. An Experimental Study of Cutting Performances of Worn Picks. Rock Mech Rock Eng 49, 213–224. https://doi.org/10.1007/s00603-015-0734-x

Ermakov, A., n.d. Estimation of Coefficient of Variation of Torque of Geokhods out of Cross Section Cutting Drum. Mining equipment and electromechanics 8, 25–29.

Hekimoglu, O.Z., Fowell, R.J., 1991. Theoretical and practical aspects of circumferential pick spacing on boom tunnelling machine cutting heads. Mining Science and Technology 13, 257–270. https://doi.org/10.1016/0167-9031(91)90397-U

Hurt, K.G., MacAndrew, K.M., 1985. Cutting efficiency and life of rock-cutting picks. Mining Science and Technology 2, 139–151. https://doi.org/10.1016/S0167-9031(85)90357-3

Jang, J.-S., Yoo, W.-S., Kang, H., Cho, J.-W., Jeong, M.-S., Lee, S.-K., Cho, Y.-J., Lee, J.-W., Rostami, J., 2016. Cutting head attachment design for improving the performance by using multibody dynamic analysis. International Journal of Precision Engineering and Manufacturing 17, 371–377.

Jedliński, Ł., Gajewski, J., 2019. Optimal selection of signal features in the diagnostics of mining head tools condition. Tunnelling and Underground Space Technology 84, 451–460. https://doi.org/10.1016/j.tust.2018.11.042

Khoreshok, A., Aksenov, V.V., Ananiev, K.A., Ermakov, A.N., 2018. Study of the Rational Number of Cutters in the Cutting Lines of Cutting Drum of Geokhod, in: Proceedings of the 9th China-Russia Symposium

"Coal in the 21st Century: Mining, Intelligent Equipment and Environment Protection" https://doi.org/doi:10.2991/coal-18.2018.40

Khoreshok, A., Ananyev, K., Ermakov, A., Golikova, E., 2019. Application of Multi-Criteria Decision Analysis for Choice Geokhods Cutting Head. E3S Web Conf. 105, 03010. https://doi.org/10.1051/e3sconf/201910503010

Kim, Y., Bruland, A., 2015. A study on the establishment of Tunnel Contour Quality Index considering construction cost. Tunnelling and Underground Space Technology 50, 218–225. https://doi.org/10.1016/j.tust.2015.07.010

Li, X., Huang, B., Ma, G., Zeng, Q., 2013. Study on Roadheader Cutting Load at Different Properties of Coal and Rock. The Scientific World Journal 2013, 624512. https://doi.org/10.1155/2013/624512

Sadovets, V.Y., Beglyakov, V.Y., Aksenov, V.V., 2015. Development of math model of geokhod bladed working body interaction with geo-environment. IOP Conf. Ser.: Mater. Sci. Eng. 91, 012085. https://doi.org/10.1088/1757-899X/91/1/012085

Trofimov, V.A., Kubrin, S.S., Filippov, Y.A., Kharitonov, I.L., 2019. Numerical modeling of stress–strain state for host rock mass and thick gently dipping coal seam after mining completion in extraction panel. Mining Informational and Analytical Bulletin 2019, 42–56. https://doi.org/10.25018/0236-1493-2019-08-0-42-56

Wingquist, C.F., Hanson, B.D., 1987. Bit wear-flat temperature as a function of depth of cut and speed. US Department of the Interior, Bureau of Mines.

Xuefeng, L., Shibo, W., Shirong, G., Malekian, R., Zhixiong, L., 2018. Investigation on the influence mechanism of rock brittleness on rock fragmentation and cutting performance by discrete element method. Measurement 113, 120–130. https://doi.org/10.1016/j.measurement.2017.07.043

Acta Montanistica Slovaca
ISSN 1335-1788
actamont.tuke.sk

Interpretation of the results of mechanical rock properties testing with respect to mining methods

***Łukasz BOŁOZ*[1*]**

Authors' affiliations and addresses:
[1]AGH University of Science and Technology, Department of Machinery Engineering and Transport, A. Mickiewicza Av. 30, 30-059 Krakow, Poland
e-mail: e-mail boloz@agh.edu.pl

***Correspondence:**
Łukasz Bołoz, AGH University of Science and Technology, Department of Machinery Engineering and Transport, A. Mickiewicza Av. 30, 30-059 Krakow, Poland
e-mail: e-mail boloz@agh.edu.pl

Funding information:
AGH University of Science and Technology, Faculty of Mechanical Engineering and Robotics, 16.16.130.942

How to cite this article:
Bołoz, L. (2020). Interpretation of the results of mechanical rock properties testing with respect to mining methods. *Acta Montanistica Slovaca*, Volume 25 (1), 81-93

DOI:
https://doi.org/10.46544/AMS.v25i1.8

Abstract
The article is concerned with the influence of cutting direction on rock cutting resistance, which is a frequently neglected issue. Investigations into the mechanical properties of the unmined rock are carried out at the stage of works involving deposit identification or mining method selection. The most frequently performed tests include uniaxial compressive strength and, sometimes, mineability of the unmined rock. The results of these tests are strongly correlated with the direction in which they have been carried out. Additionally, depending on the method of mining (cutting, planning, drilling) and the site of sampling (sidewall, face), the direction of cutting is usually inconsistent with the direction of testing. In the article, the author has drawn attention to the commonly applied directions of cutting and presented recommendations on the direction of testing to be followed in underground mining plants in order to properly determine the unmined rock properties. The results of the author's research into a hard coal mine, rock salt and sandstones, shales and dolomites, conducted in three perpendicular directions have also been quoted. Furthermore, the subject literature in this field has been reviewed, and selected investigations presented. The research results confirm that depending on the cutting direction, there may be considerable, even fivefold differences in the value of mechanical properties. Knowing the planned cutting direction and the direction of testing is a necessary condition for interpreting the results in a proper way, choosing a suitable mining technique, the type of tools and process parameters, as well as achieving the projected efficiency and energy consumption.

Keywords
mechanical properties of rocks, selection of a mining method, rock anisotropy, mechanical cutting of rocks, cutting, planning, drilling

Introduction

The exploitation of useful minerals is accompanied by gangue mining. Both useful minerals and gangue can be mined by various methods. Useful minerals in underground mines most frequently include hard coal, ores of metals, in particular copper, iron, zinc and lead; rock and potassium salts; sulphur and others. Opencast mining also involves the mining of brown coal or building rock, such as marble or granite.

The simplest method, which is still applied on a small scale, is manual mining, for example with picks or hammers. However, the vast majority of mining processes are mechanized. The techniques used in underground mining machines are usually based on cutting, planning and drilling. Salts, as well as hard mineable and abrasive rocks, such as ores, are frequently mined with explosives. The winning efficiency, and, in consequence, the efficiency of exploitation, is mostly influenced by the mechanical properties of unmined rock, which are determined by a number of parameters. A parameter easy to determine and use is uniaxial compressive strength R_c, expressed in megapascals. This parameter does not describe the rock in a sufficient way, however. Knowing merely the value of compressive strength does not allow mining resistance to be determined (Biały, 2013), (Biały, 2014) (Biały and Fries, 2019). Rocks characterized by high compressive strength R_c can be easily mineable and vice versa; despite a relatively low value of R_c, the rock can be hard mineable. For this reason, rock mineability is frequently specified by determining mineability index A, which is expressed in newtons per centimetre, and by breakout angle ψ, expressed in degrees. All the three values enable selecting a method of winning, appropriate tools and head, as well as estimating the resistance of mining (Bołoz et al., 2018). It is of paramount importance, especially in the case of the most popular and efficient machines, i.e., mechanized longwall systems and roadheaders.

Compressive strength and rock mineability are usually determined in laboratory conditions. A sample subjected to tests can have a different direction in relation to that in the deposit. Investigations into rock properties conducted in laboratory conditions concern only one direction. Typical winning machines used in underground mining carry out the rock cutting process in a different way. An analysis of typical machines has revealed that mining resistance depends on various directions, which are most frequently inconsistent with the direction for which the mechanical properties of unmined rock have been determined. On the other hand, the results of mechanical properties tests conducted in three perpendicular directions indicate considerable differentiation in the obtained results, that is, rock anisotropy. Generally, anisotropy points to the influence of direction on rock properties. However, investigations conducted in three perpendicular directions are, in fact, research into orthotropy, which is a special case of anisotropy. For the analyzed problem, there is no need to determine directions in which properties are the most differentiated, as the directions are imposed by the directions of cutting and location in the deposit.

The direction for which mechanical rock properties will be determined should, therefore, be carefully determined while taking into account the exploitation method planned. Determination of the direction is vitally important, especially if there is a possibility of carrying out tests only in one, selected direction.

The article has been based on the results of laboratory research on rock properties obtained in numerous works in this field. Various rocks, such as brown coal, rock salt, sandstone, dolomite and shale, have been subjected to tests. The collected results have been subjected to analysis, and the observed correlations have been presented. Recommendations for selecting the direction of investigations into rock properties and their interpretation in relation to the specified mining method have been based on the theory of cutting as well as the experiences and analysis of cutting processes carried out with various machines.

Literature review

Information on anisotropy appears in publications devoted to mechanical properties of rocks, from the point of view of mining and geology as well as mining mechanization. It is a well-known and obvious subject. Below have been quoted selected research results and relevant conclusions.

The investigations quoted in the literature most frequently concern properties of particular rocks or the influence of various parameters (sample length/diameter ratio, humidity, weathering, etc.) on compressive strength (Agustawijaya, 2007). As early as several dozen years ago, it was found that rock anisotropy could cause differences in mechanical properties in 1:5 ratio (Muller and Pacher, 1965). The authors of those investigations emphasized that anisotropy was a typical phenomenon. The chart developed by the authors, which has been presented in Fig. 1a, concerns the case of stratified rocks.

In one of the publications (Nasseria et al., 2003), detailed results of research on a few types of shale for a full range of angles have been presented. The results of uniaxial compressive strength have revealed threefold differences in values, depending on the direction of shale layers during testing. Similar results were obtained for other materials, including shale (Fig. 1b), (Shuxin, 1992).

Sometimes the method of mining is chosen only on the basis of information on uniaxial compressive strength obtained as a result of investigations into core barrels at the stage of prospecting works. In such a case,

the only available data is the value of R_c in one direction (fig. 1c). In some investigations, attention has been drawn to differences in uniaxial compressive strength, reaching up to 50%, depending on the core barrel inclination angle (Majcherczyk and Niedbalski, 2004).

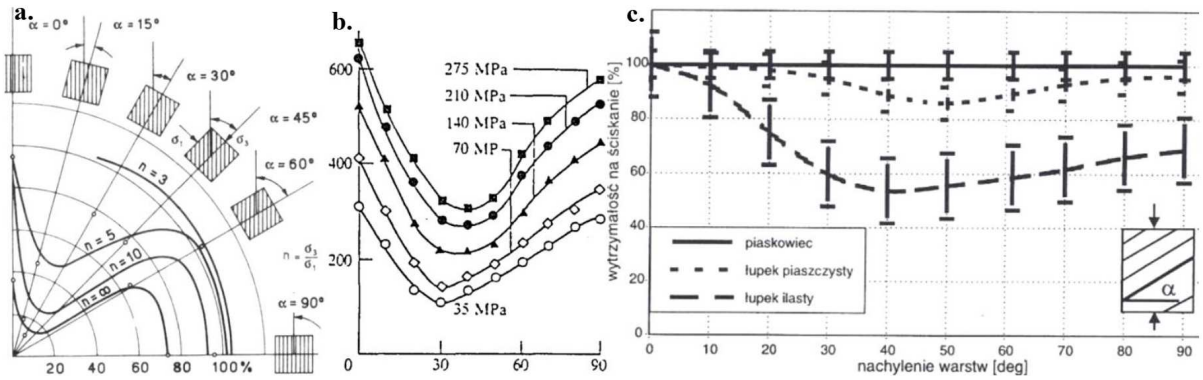

Fig. 1. Effect of stratified rocks anisotropy: a. on σ3 to σ1 strength ratio – shale (Muller and Pacher, 1965), b. on the variation of peak principal stress difference – slate (Shuxin, 1992), c. on compressive strength depending on strata inclination angle (Majcherczyk and Niedbalski, 2004)

In numerous works concerning the mechanical properties of rocks that have been published in recent years, attention has been drawn to anisotropy (Małkowski, 2015), (Ozcelik and Yilmazkaya, 2011), (Özbek et al., 2018), (Dinc et al., 2011). Apart from research into typical rocks mined in underground plants, it is worth quoting investigations into rocks from open-pit mines. Rocks subjected to testing included limestone, dolomite, claystone, marble (Hoek, 1980). There are reports in the subject literature indicating that the way rock is deposited in a rock mass influences the resistance of mining. However, these dependencies have not been presented, especially in relation to various methods of mining. An example is the analysis of the influence of travertine anisotropy on the efficiency of diamond line cutting (Ozcelik and Yilmazkaya, 2011). This study also contains an extensive review of works in the field of anisotropy of hard coal, diatomite, sandstone and other rocks. In one of the studies, the authors undertook to explain the effect of rock anisotropy on the drilling process by means of numerical analyses (Schormair et al., 2006). The study is only concerned with the analysis of results obtained for percussion drilling.

Mechanical cutting of rocks

The equipment that is most often used for mechanical cutting of rock raw materials includes cutting, planning or drilling machines. In this article, the focus has been placed on selected most popular machines. The recommendations presented in subsequent chapters also apply to the machines listed below (machine numbering is the same as in subsequent drawings)

1, 2. roadheaders (fig. 2b),
3. longwall shearers (fig. 2a),
4. coal ploughs (fig. 2c),
5. longwall shearers with vertical axes of rotation of the cutting heads (fig. 2d),
6. shearers drilling in Auger Mining System (fig. 2e),
7. continuous miners and machines for Continuous Highwall Mining (fig. 2f).

These machines are to various degree used all over the world. Roadheaders are widely applied in hard coal mines, but also in salt mines, ore mines, and the construction branch. Cutting shearers and coal ploughs are basic, and the most common cutter-loaders in mechanized longwall systems used to mine hard coal deposits. Similarly, longwall shearers with vertical axes of rotation of cutterheads are applied in the mining of hard coal deposits. Drilling machines are used in underground mines with thin and steeply sloped deposits, whereas continuous miners, similarly to roadheaders, work in various mines, such as ore, hard coal, rock salt mines (Bołoz, 2018a), (Bołoz, 2018b).

Working elements of mining machines are the subject of numerous studies and investigations in the field of design (Bołoz and Castaneda, 2018), (Bołoz and Midor, 2018), (Kotwica, 2018), (Gospodarczyk et al., 2013), (Gospodarczyk et al., 2016) as well as the selection, wear and renovation of mining tools (Bołoz, 2019), (Bołoz and Midor, 2019), (Prokopenko et al., 2018), (Ťavodová et al., 2016), (Hasilová and Gajewski, 2019). The cutterheads that have been schematically presented in subsequent drawings are usually equipped with conical picks or flat picks. Flat, non-rotary picks (radial and forward attach picks) are typically applied as plough head tools. Conical or flat picks are the most frequently applied in cutterheads of various kinds of shearers. An

exception is the shearer produced by Corum, which has been shown in the figure above. The most energy-consuming process carried out by these machines is the winning process, which "consumes" the most of machine power. Hence, a more precise estimate of power demand based on correctly determined and interpreted mechanical properties of unmined rock will result in a better selection of machines.

Fig. 2. Selected winning machines in underground mining: a. longwall shearer (MB12 320E TMachinery a. s.), b. roadheader (R-130 FAMUR S. A.), c. coal plough (PL 738V Ostroj a. s.), d. longwall shearer with vertical axes (KTB200 Corum Group), e. drilling shearer (VS-SEAL-625 z OKD Ostrava), f. continuous miner (CM210 CAT)

Investigations into mechanical properties of rocks

Physical and mechanical properties of rocks numerically describe their most important features. Physical parameters include absorbability as well as differently defined density and humidity. Among mechanical parameters, the following are listed: differently defined strength, internal friction angle, cohesion, Poisson ratio, mineability index, toughness index as well as abrasiveness and abrasibility. Parameters that are of huge importance for the mining process are mechanical properties. In practice, the most frequently determined is uniaxial compressive strength, but it is insufficient to select tools and estimate the resistance of mining. From the point of view of tools durability, an important parameter is rock abrasiveness (Mucha, 2019), which is a key issue in terms of pick replacement frequency, but it is not the subject of this article. The parameter which defines the resistance of unmined rock during the winning process is mineability. Uniaxial compressive strength is determined in accordance with standards concerning sample preparation (PN-G-04301) and strength determination (PN-G-04303), while rock mineability is defined by means of two values: cuttability index A and breakout angle ψ. According to the method developed by AGH University of Science and Technology, it is empirically determined by measuring the cutting force when making a straight cut of a specified depth, with a specified pick. The station for testing the planing process enables making a cut of a specified depth, width and length. During the cutting process, the values of signals from the system of sensors embedded in the holder with strain gauges are recorded, which allows for determining the value of the cutting, side and normal force. After making the cut, its real depth and width are measured. Knowing the cutting resistance, the depth of cutting and the values of relevant indexes, one can determine the cuttability, which is proportional to the force of cutting and inversely proportional to the depth of cutting (Krauze, 2000).

Anisotropy of mechanical rock properties on the basis of investigations

Anisotropy of rocks has been demonstrated in numerous investigations and publications. Below have been presented the results of laboratory tests conducted by the author or with his participation. The research was aimed at determining the mechanical properties of unmined rock in order to select the best mining method, so it concerned typical rocks that are mined mechanically, such as hard coal, rock salt, copper ores.

Investigations into hard coal were based on samples provided from two different locations, from mines in Ordos, China. Tests were carried out in order to determine the uniaxial compressive strength and cuttability index (Fig. 3). The strength was determined for three perpendicular directions. The cuttability index was measured on three perpendicular planes in two perpendicular directions.

Fig. 3. The investigation into hard coal: a. provided sample b. before R_c tests, c. after cuttability index tests

The results of tests for the coal from the first location have been given in Table 1. Differences between particular R_c values for different cutting directions are very big. The strength in the up-down direction accounts for more than 300% of the value for the right-left direction. It is similar in the case of cuttability index. Index *A* for the right longwall accounts for ca 175% of the index for the sidewall. A noticeable difference is also observed for two directions on one longwall. For example, the index on the right longwall in the up-down direction constitutes 150% of the value for the perpendicular direction, i.e., back sidewall. In consequence, the category of the tested coal mineability changes depending on the direction from well mineable to more than average mineable despite the fact that it concerns the same samples.

Tab. 1. Results of tests for the coal from the first location

No.	Rc direction	Rc [MPa]	Longwall	Direction A	A [N/cm]	ψ [°]	Category
1	up-down	14	sidewall	up-down	1 137	44	well mineable
				right-left	1 738	45	average mineable
2	right-left	5	up	back-sidewall	1 252	49	average mineable
				right-left	1 557	47	average mineable
3	sidewall-back	9	right	up-down	1 982	57	more than average mineable
				back-sidewall	1 347	47	average mineable

Similarly, for the coal from the other location, the results have been presented in Table 2. The strength in the up-down direction accounts for nearly 370% of the value for the right-left direction. The cuttability index *A* is different depending on the longwall and direction. Index A on the right longwall in the back-sidewall direction accounts for more than 125% of the value for the perpendicular direction, i.e. up-down. As a result, the category of the tested coal mineability ranges from more than average to hard mineable.

Tab. 2. Results of tests for the coal from the second location

No.	R_c direction	R_c [MPa]	Longwall	Direction A	A [N/cm]	ψ [°]	Category
1	up-down	19	sidewall	up-down	1 975	62	hard mineable
				right-left	2 367	57	*more than average mineable*
2	right-left	5	up	back-sidewall	2 113	59	*more than average mineable*
				right-left	2 292	57	*more than average mineable*
3	sidewall-back	6	right	up-down	1 889	59	*more than average mineable*
				back-sidewall	2 395	58	*more than average mineable*

One of the projects involved conducting comprehensive investigations into copper ores in the form of dolomites, sandstones and shales. An appropriate amount of rock was taken from the mine, and more than one hundred samples were prepared for strength and cuttability tests (Fig. 4, Fig. 5). Uniaxial compressive strength and cuttability in three directions were tested. Below have been presented maximum observed values determined on the basis of samples taken from one solid for each of the rocks (Tab. 3, Tab. 4, Tab. 5).

Fig. 4. Investigations into R_c of copper ores: a. sample preparation, b. shale during R_c testing, c. a scrap of shale, sandstone and dolomite after tests

Fig. 5. Copper ores cuttability tests: a. dolomite, b. sandstone, c. shale

The results of compressive strength tests for sandstone indicate high differentiation of values for all three directions. The biggest – 4, 5-fold differences can be observed between the up-down and back-sidewall directions. The value of one of the remaining combinations of directions is twice higher than that of the other combination. Similarly, the cuttability index for the back-sidewall direction is twice lower than the value for the remaining directions. Due to high values irrespective of the direction, this sandstone has been classified as particularly hard mineable. It should be noted, however, that the applied classification does not have a separate category for values higher than those described with the term of "particularly hard mineable", although they can be four times higher.

Tab. 3. Results of tests for sandstone

No.	Rc direction	Rc [MPa]	Direction A	A [N/cm]	ψ [°]	Category
1	up-down	16	up-down	22 886	39	particularly hard mineable
2	right-left	72	back-sidewall	11 716	65	particularly hard mineable
3	sidewall-back	37	up-down	20 610	49	particularly hard mineable

For dolomite strength results, the relative differences are not so big. The largest difference between the sidewall-back and up-down direction is slightly more than 40%, which, however, with high strength values reaches almost 40 MPa. On the other hand, there is a significant difference in the cuttability index, the values of which are twice higher. Hence, there is a difference in the mineability category between the up-down and the remaining directions.

Tab. 4. Results of tests for dolomite

No.	R_c direction	R_c [MPa]	Direction A	A [N/cm]	ψ [°]	Category
1	up-down	89	up-down	2 559	71	hard mineable
2	right-left	104	back-sidewall	5 252	61	particularly hard mineable
3	sidewall-back	127	up-down	5 303	75	particularly hard mineable

Shale tests revealed differences in uniaxial compressive strength, the level of which was more than twice higher for one of the values. A considerably lower strength in the sidewall-back direction and the characteristic shale structure caused that the sample was destroyed during cuttability tests in the up-down direction. The results of the cuttability index for the remaining directions differ by nearly 35%. An interesting finding is more than a triple difference in the value of breakout angle ψ. This, however, is a typical characteristic of shale.

Tab. 5. Results of tests for shale

No.	R_c direction	R_c [MPa]	Direction A	A [N/cm]	ψ [°]	Category
1	up-down	63	sample was destroyed			
2	right-left	61	back-sidewall	6 097	22	particularly hard mineable
3	sidewall-back	27	up-down	4 549	71	particularly hard mineable

In recent years, single investigations have often been carried out to determine the uniaxial compressive strength of various types of rock in three directions. It should be emphasized that depending on the type and homogeneity of the rock, the results even for one direction may vary several times. For example, dolomite was characterized by significant differences; in the case of single samples tested in one direction, more than a threefold difference in results was observed (158 MPa and 46 MPa). However, individual, much lower than other values are not important for the estimation of energy consumption of the process and for the choice of the mining method. One should be guided by the maximum values. Differences in the results of tests for various samples of dolomite and sandstone reached up to approximately 50%, depending on the compression direction, for example, 113 MPa and 77 MPa for two perpendicular directions of compression.

Rock salt is an example of a mineral that, from the point of view of mechanical cutting, has several interesting properties (Mansouri and Ajalloeian 2018), (He et al., 2019). Salt is not very abrasive, which means that it causes the wear of tools only to a small extent. Salt is characterized by quite high cutting resistance and frequently - by high cutting indexes. Samples of rock salt from the Polish mines were subjected to tests (Fig. 6).

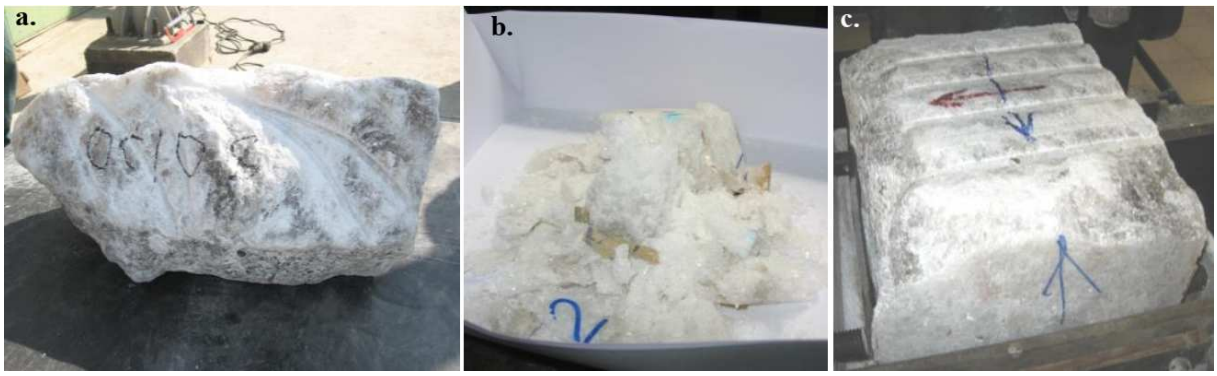

Fig. 6. Rock salt tests: a. provided sample b. after R_c tests, c. after cuttability index tests

Investigations into the mechanical properties of salts in three directions have revealed that the obtained values of uniaxial compression strength depend on the direction to a lesser extent. The value of uniaxial compressive strength determined for perpendicular directions was 35 MPa, 33 MPa and 34 MPa, respectively, which means that the differences do not exceed 6%. In some extreme cases, the differences for individual samples reached ca 17%. Due to the specificity of the mining process and the scope of the order, the cuttability tests were carried out only for two perpendicular directions. The average cuttability index A was 5 083 N/cm and 5 860 N/cm, respectively. The difference reaches over 15%, with maximum differences of nearly 35%.

The direction of mechanical properties determination with respect to the mining method

In order to determine the mechanical properties of unmined rock, its cuttability index, breakout angle, toughness or uniaxial compressive strength are tested. Tests are usually performed for samples taken from the excavated workings. Taking a sample for tests enables determining its properties in any direction in laboratory conditions. It should be noted that toughness is an energy indicator and does not depend on the direction. A sample can be taken from working to be mined by means of various previously mentioned machines. For the diagram shown in Fig. 7, the sample can be taken from excavations marked A, B or C. For a popular longwall system, sample P3 can be taken from the longwall (excavation C), sample P2 from the top road (excavation B) or sample P1 from the bottom road (excavation A). Typically, the use of roadheader (1, 2) was considered for roadway excavations and the use of longwall shearer (3) and coal plough (4) for the longwall. At the same time, it was assumed that, apart from classic longwall shearers, also cutting shearers with vertical axes of rotation of the heads could be used (5). The diagram also includes a boring machine in the Auger Mining system (6) and a cutterhead for the Continuous Highwall Mining system (7). The last two systems are not used in typical longwall excavations. However, in this situation, samples marked as P1 and P2 can be taken from previously made holes or headings described as excavations A and B, so the cutting direction system remains the same. The situation is similar for the room and pillar mining system, where the continuous miner is used. The interpretation for such a shearer is identical as for the cutting head (7).

The presented layout of sampling locations in specific excavations can also be generalized for other mining excavations and machines used, for example for borer miners, such as Ural-360, Marietta, Xcel Miners 4-Rotor or for cutting machines. Then, the direction of cutting and the corresponding direction of determining the mechanical properties of the sample should be analyzed using the method presented below.

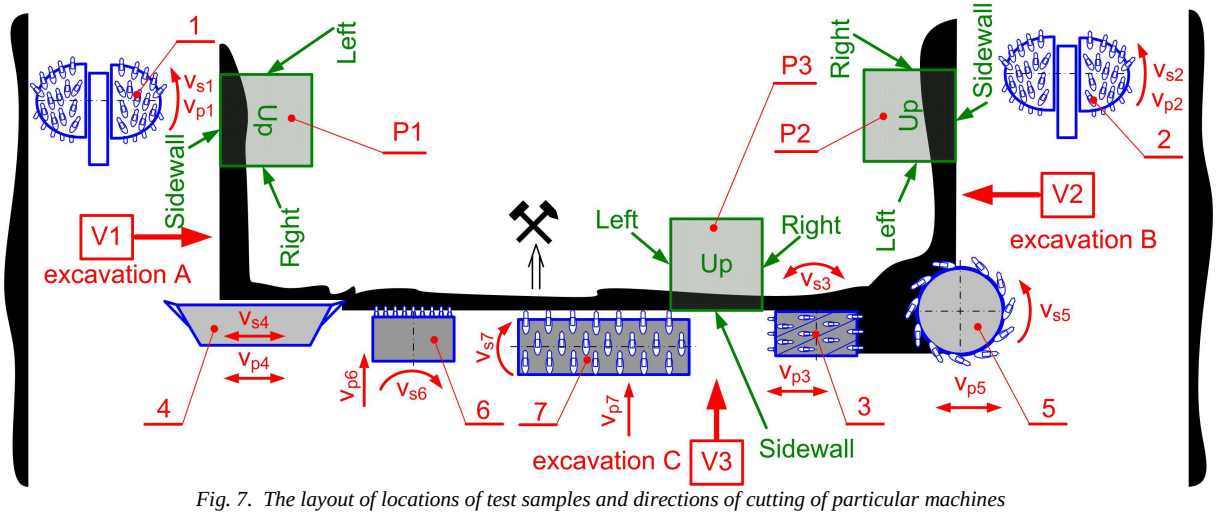

Fig. 7. The layout of locations of test samples and directions of cutting of particular machines

Markings in Fig. 7:

P1 – sample located in excavation A,
P2 – sample located in excavation B,
P3 – sample located in excavation C,
1 – roadheader in excavation A,
2 – roadheader in excavation B,
3 – classic longwall shearer,
4 – coal plough,
5 – longwall shearer with vertical axes of cutterheads,
6 – tunnel boring machine in Auger Mining System (AM),
7 – shearer in Continuous Highwall Mining System (CMH),
v_p –vector of cutting head travelling speed for each of the machines (1-7),
v_s – vector of the cutterhead cutting speed for each of the machines (1-7),
V1 – view of unmined rock in excavation A,
V2 – view of unmined rock in excavation B,
V3 – view of unmined rock in excavation C.

The place of cutting and the type of cutting machine determine the cutting direction and, in consequence, the direction in which mechanical properties of the unmined rock should be determined. Therefore, diagrams have been prepared for all excavations (A, B, C) from which the sample may come (P1, P2, P3) so as to assign

the direction of determining the mechanical properties of the sample taken to the type of mining machine used. The diagrams present the sample in three projections as well as the cutting heads. The cutting heads were correlated with a specific view of the sample. The drawings were made so as to enable an analysis of the cutting direction and the direction in which the mechanical properties of the sample should be determined. Three cases were analyzed as follows:

- sample P1 – a sample taken from excavation A – fig. 8,
- sample P2 – a sample taken from excavation B –
- fig. 9,
- sample P3 – a sample taken from excavation C – fig. 10.

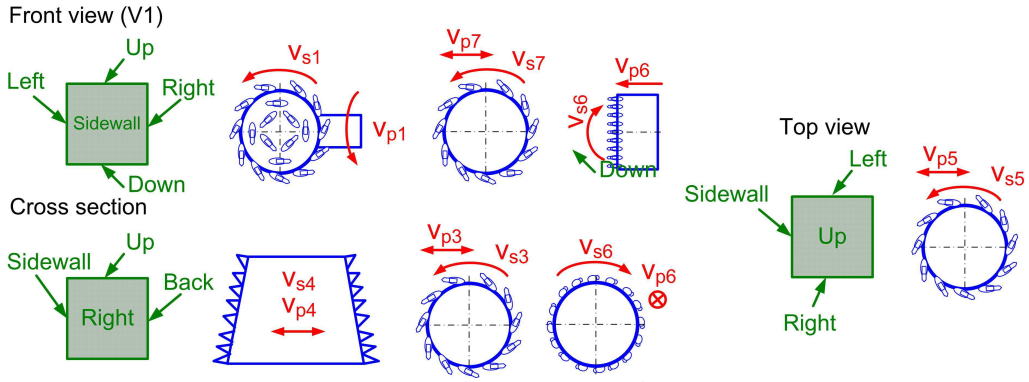

Fig. 8. Cutting directions for sample P1 taken from excavation A

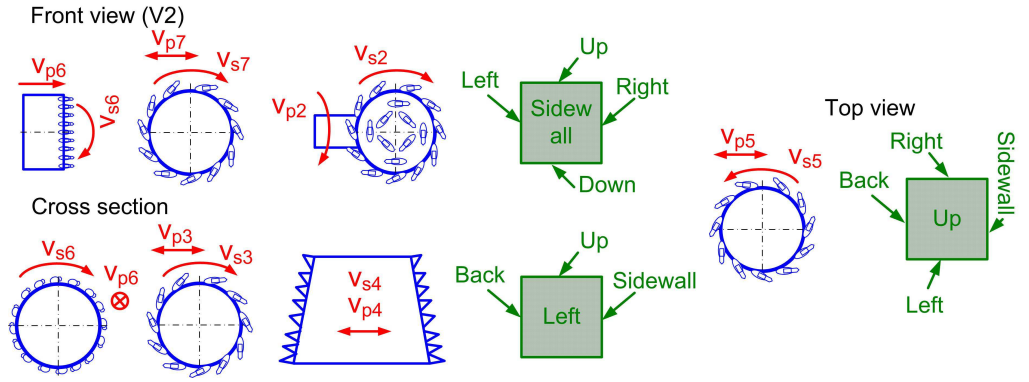

Fig. 9. Cutting directions for sample P2 taken from excavation B

In each of the presented situations, the mining method depends on the direction in which the mechanical properties of the sample should be determined. The direction that most strongly influences the cutting resistance was determined for the analyzed cutting heads. The direction is understood as the direction in which the mechanical properties of the sample were determined. Uniaxial compressive strength can be determined for the sample in three perpendicular directions. Cuttability tests can also be carried out in three perpendicular directions on six available sample surfaces. The adopted names of sample surfaces were marked symbolically: up (U), down (D), right (R), left (L), sidewall (S), back (B), so there are three directions for uniaxial compressive strength: U-D, R-L, S-B. Cuttability tests can be done in two perpendicular directions on each of the longwalls, for example on the sidewall surface in U-D and R-L direction. In addition, cuttability tests can be performed for two orientations in each direction, for example, U-D and D-U. Until present, the impact of cutting orientation on the obtained results of cuttability tests has not been comprehensively studied. Based on the research results, it can be concluded that orientation does have an impact, especially if the surface prepared for cutting is not perpendicular or parallel to the cleavage plane. Recommended planes, directions and orientations have been given below. If the mining method is known, the rock properties should be determined in accordance with the provided recommendations. In the case of coal ploughs and longwall shearers, the direction of the cutting speed vector changes with a change in the direction of machine movement in the longwall.

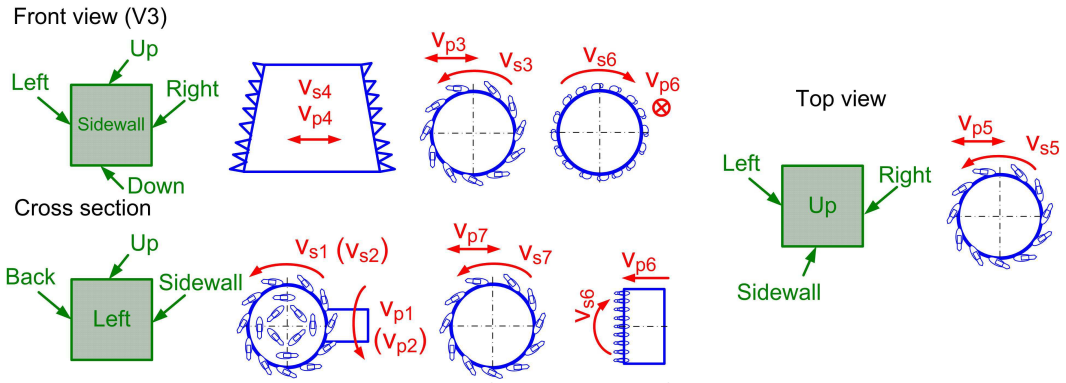

Fig. 10. Cutting directions for sample P3 taken from excavation C

In the case of sample P1 taken from excavation A (Fig. 8), the following dependencies are observed:

- mining with roadheader (1) and CHM (7):
  - uniaxial compressive strength in U-D direction,
  - cuttability on R surface, U-D orientation,
- mining with longwall shearer (3):
  - uniaxial compressive strength in U-D direction,
  - cuttability on B or S surface, U-D or D-U orientation,
- mining with plough head (4):
  - uniaxial compressive strength in S-B direction,
  - cuttability on R surface, S-B and B-S orientation,
- mining with longwall shearer with vertical axes (5):
  - uniaxial compressive strength in R-L direction,
  - cuttability on B or S surface, L-R orientation
- mining with a boring head (6):
  - uniaxial compressive strength in R-L direction,
  - drillability in R-L drilling direction.

In the case of sample P2 taken from excavation B (Fig. 9), the following dependencies are observed:

- mining with roadheader (2) and CHM (7):
  - uniaxial compressive strength in U-D direction,
  - cuttability on L surface, U-D orientation,
- mining with longwall shearer (3):
  - uniaxial compressive strength in U-D direction,
  - cuttability on B or S surface, U-D and, possibly, D-U orientation,
- mining with plough head (4):
  - uniaxial compressive strength in S-B direction,
  - cuttability on surface L, S-B and B-S orientation,
- mining with longwall shearer with vertical axes (5):
  - uniaxial compressive strength in R-L direction,
  - cuttability on B or S surface, R-L orientation.
- mining with drilling head (6):
  - uniaxial compressive strength in R-L direction,
  - drillability in L-R drilling direction.

In the case of sample P3, taken from excavation C (Fig. 10), the following dependencies can be observed

- mining with roadheader (1, 2) and CHM (7):
  - uniaxial compressive strength in U-D direction,
  - cuttability on S surface, U-D orientation,
- mining with longwall shearer (3):
  - uniaxial compressive strength in U-D direction,
  - cuttability on R or L surface, U-D and, possibly, D-U orientation,
- mining with plough head (4):
  - uniaxial compressive strength in R-L direction,
  - cuttability on S surface, R-L and L-R orientation,
- mining with longwall shearer with vertical axes (5):

- uniaxial compressive strength in S-B direction,
- cuttability on R or L surface, B-S orientation,

- mining with drilling head (6):
  - uniaxial compressive strength in S-B direction,
  - drillability in S-B drilling direction.

The two-way classic longwall shearer is equipped with two cutting heads, which cut in opposite directions. The front head usually cuts downward, while the back one - upward. The front cutterhead cuts with its entire diameter, hence the most important thing is to determine the U-D cuttability, whereas the back head cuts the remained coal towards the free surface, hence the mining resistance is lower, and there is no need to determine the D-U cuttability.

Longwall shearers with vertical axes are equipped with two cutting heads, which cut in the same direction, i.e. towards the free surface, regardless of the direction of the shearer's movement. The cutting direction in the coal plough is identical with the direction of the head's movement. However, in the case of other machines (1, 2, 6, 7) there is no change in the direction of cutting.

In the case of drilling with a head (6) equipped with conical picks, the picks cut the unmined rock in a plane perpendicular to the direction of drilling. Each pick is in contact with unmined rock at all times. This type of cutting necessitates the determination of the value of uniaxial compressive strength in three directions and the value of cuttability on four planes. To simplify the determination of unmined rock properties for drilling, it is recommended that drillability should be determined in accordance with the drilling direction and uniaxial compressive strength in the same direction.

Samples P1 and P2 can also be taken from the face of excavation A and B; in such a case, the analysis in question also applies. On the other hand, samples P1 and P2 can be taken from the sidewall of the gallery, which is opposite to the one indicated in the drawing. In this case, appropriate directions should be taken into account in the analysis, according to the presented methodology. Sample P3 can be taken from the drift face; in such a case, the interpretation of directions will remain unchanged.

Summary

The presented test results do not allow for approaching the problem in a comprehensive way but provide sufficient evidence pointing to the existence of significant discrepancies, depending on the direction of determining the mechanical properties of rocks. In some cases, the differences reach 500%. It should be emphasized that there is no need to perform tests in three directions. However, it is crucial to analyze all the potential mining methods and take them into consideration when determining the mechanical properties of rocks. Knowing the sample orientation in the deposit and using the presented methodology, it is possible to specify the way of determining mechanical properties so that the results are adjusted to the planned method of mining to the largest extent possible. In the event various techniques or machines are considered, testing may be required in more than one direction.

If the mining technique is well known, for example, if it is a very common method of mining with a longwall shearer, the only problem comes down to choosing the direction of determining the mechanical properties, as shown above. So obtained results will allow for a more accurate estimate of the cutterheads' power demand.

The investigations, the results of which are quoted in the article, have revealed the need for further research so as to determine unambiguous dependences, especially with respect to the effect of the cutting orientation during cuttability tests on the obtained test results. The tests conducted in different directions and in perpendicular orientations give only a general view on this issue, indicating differences in the results.

The most important conclusion and recommendation is to carefully select the direction of determining rock properties depending on the method planned. To facilitate the interpretation of results and sproperly choose this direction, the methodology presented in the article should be applied.

The literature review has revealed numerous reports of the rock anisotropy problem. Researchers draw attention to the impact of properties determination direction in relation to the deposition or stratification of rock samples on the obtained results. However, until the present, this issue has not been described comprehensively in terms of mechanical mining. The problem presented in the article, together with recommendations regarding the choice of direction for determining rock properties and their interpretation in the case of selecting the method of exploitation is the first such study.

References

Agustawijaya, D. S. (2007). The Uniaxial Compressive Strength of Soft Rock. Civil Engineering Dimension. 9(1), pp. 9-14

Biały, W. (2013) New devices used in determining and assessing mechanical characteristics of coal. 13th SGEM GeoConference on Science and Technologies in Geology, Exploration and Mining, SGEM2013 Conference Proceedings, June 16-22, 2013, Vol. 1, BUŁGARIA ISBN 978-954-91818-7-6/ISSN 1314-2704. pp. 547-554.

Biały, W. (2014). Coal cutting force measurement systems - (CCFM). 14th SGEM GeoConference on Science and Technologies In Geology. Exploration and Mining. SGEM2014 Conference Proceedings, Vol. III, pp. 91-98.

Biały, W. and Fries, J. (2019). Computer Systems Supporting the Management of Machines/Equipment in Hard Coal Mines. Case Study. Management Systems in Production Engineering, Volume 27 issue 3/2019. pp. 138-143. ISSN 2299_0461. DOI 10.1515/mspe-2019-0022

Bołoz, Ł. (2018). Longwall shearers for exploiting thin coal seams as well as thin and highly inclined coal seams, "Mining – Informatics, Automation and Electrical Engineering", 2(534), pp. 59-65.

Bołoz, Ł. (2018). Mining of thin coal seams using surface-underground methods, "Mining – Informatics, Automation and Electrical Engineering", 3(535), pp. 59-73.

Bołoz, Ł. (2019). Directions for increasing conical picks' durability, In: New trends in production engineering, Sciendo, 2(1), pp. 277-285.

Bołoz, Ł., Krauze, K. and Kubin, T. (2018). Mechanization of longwall extraction of hard and abrasive rocks. Multidisciplinary Aspects of Production Engineering. Sciendo, 1(1), pp. 331-337.

Bołoz, Ł. and Leonel, F. Castañeda, (2018). Computer-aided support for the rapid creation of parametric models of milling units for longwall shearers. Management Systems in Production Engineering, 26(4), pp. 193-199.

Bołoz, Ł. and Midor, K. (2018). Process innovations in mining industry and effects of their implementation presented on example of longwall milling heads. Acta Montanistica Slovaca, 23(3), pp. 282-292.

Bołoz, Ł. and Midor, K. (2019). The procedure of choosing an optimal offer for a conical pick as an element of realizing the sustainable development concept in mining enterprises. Acta Montanistica Slovaca, 24(2), pp. 140-150.

Dinc, O., Sonmez H., Tunusluoglu C. and Kasapoglu K.E. (2011). A new general empirical approach for the prediction of rock mass strengths of soft to hard rock masses, International Journal of Rock Mechanics and Mining Sciences, 48, pp. 650-665.

Gospodarczyk, P., Kotwica, K. and Stopka, G. (2013). A new generation mining head with disc tool of complex trajectory, Archives of Mining Sciences, 58(4), pp. 985–1006.

Gospodarczyk, P., Kotwica, K., Mendyka, P. and Stopka, G. (2016). Innovative roadheader mining head with asymmetrical disc tools, Exploration and mining, mineral processing. International Multidisciplinary Scientific GeoConference SGEM, 2, pp. 489–496.

Hasilová, K. and Gajewski, J. (2019). The use of kernel density estimates for classification of ripping tool wear, Tunnelling and Underground Space Technology, 88, pp. 29-34.

He M., Li N., Zhu C., Chen Y. and Wua H. (2019). Experimental investigation and damage modeling of salt rock subjected to fatigue loading, International Journal of Rock Mechanics and Mining Sciences, 114, pp. 17-23.

Hoek, E. and Brown, E.T. (1980). Empirical Strength Criterion for Rock Masses. Journal of Geotechnical and Geoenvironmental Engineering, 106, pp. 1013-1035.

Kotwica, K. (2018). Atypical and innovative tool, holder and mining head designed for roadheaders used to tunnel and gallery drilling in hard rock. Tunnelling and Underground Space Technology, 82, pp. 493-503.

Krauze, K. (2000). Urabianie skał kombajnami ścianowymi. Wydawnictwo naukowe „Śląsk", Katowice,

Majcherczyk, T. and Niedbalski, Z. (2004). Wpływ nachylenia otworów badawczych na zmianę parametrów wytrzymałościowych skał, XXVII Zimowa szkoła mechaniki górotworu, Kraków, pp. 898-907.

Małkowski, P. (2015). The impact of the physical model selection and rock mass stratification on the results of numerical calculations of the state of rock mass deformation around the roadways, Tunnelling and Underground Space Technology, 50, pp. 365-375.

Mansouri, H. and Ajalloeian, R. (2018). Mechanical behavior of salt rock under uniaxial compression and creep tests, International Journal of Rock Mechanics and Mining Sciences, 110, pp. 19-27.

Mucha, K. (2019). The new method for assessing rock abrasivity in terms of wear od conical picks. In: New Trends in Production Engineering, Sciendo, 2(1), pp. 186-194.

Muller, L. and Pacher, F. (1965). Modellversuche zur Klarung der Bruchgefahr geklufteter Medien, Felsmech. u. Ing. Geol., Suppl. II, pp. 7-24.

Nasseria, M.H.B., Raob K.S. and Ramamurthyb T. (2003). Anisotropic strength and deformational behavior of Himalayan schists, International Journal of Rock Mechanics & Mining Sciences, 48, pp. 626-636.

Ozcelik, Y. and Yilmazkaya E. (2011). The effect of the rock anisotropy on the efficiency of diamond wire cutting machines, International Journal of Rock Mechanics & Mining Sciences, 40, pp 3-23.

Özbek, A., Gül, M., Karacan, E. and Alca, Ö. (2018). Anisotropy effect on strengths of metamorphic rocks, Journal of Rock Mechanics and Geotechnical Engineering, 10, pp. 165-175.

Prokopenko, S. A., Vorobiev, A. V., Lyudmila, A. and Janocko, J. (2018). Waste Cutters Utilization in Underground Coal Mining, Acta Montanistica Slovaca, 23(1), pp. 81-89.

Schormair, N., Thuro, K. and Plinninger, R. (2006). The influence of anisotropy on hard rock drilling and cutting, The Geological Society of London, IAEG, Paper 491, pp. 1-11.

Shuxin, W. (1992). Fundamental studies of the deformability and strength of jointed rock masses at three-dimensional level, dissertation, The University of Arizona (http://hdl.handle.net/10150/185923).

Ťavodová, M., Kalincová, D., Hnilicová, M. and Hnilica R. (2016). The influence of heat treatment on tool properties mulcher, Manufacturing technology, 16(5), pp. 1169-1173.

Acta Montanistica Slovaca
ISSN 1335-1788
actamont.tuke.sk

Laboratory research on the influence of selected technological parameters on cutting forces during hard rock mining with asymmetric disc tools

Grzegorz STOPKA[1*]

Authors' affiliations and addresses:
[1]AGH University of Science and Technology, Department of Machinery Engineering and Transport, A. Mickiewicza Av. 30, 30-059 Krakow, Poland
e-mail: stopka@agh.edu.pl

***Correspondence:**
Grzegorz Stopka, AGH University of Science and Technology, Department of Machinery Engineering and Transport, A. Mickiewicza Av. 30, 30-059 Krakow, Poland
e-mail: stopka@agh.edu.pl

Funding information:
AGH University of Science and Technology, Faculty of Mechanical Engineering and Robotics

How to cite this article:
Stopka, G. (2020). Laboratory research on the influence of selected technological parameters on cutting forces during hard rock mining with asymmetric disc tools. *Acta Montanistica Slovaca*, Volume 25 (1), 94-104

DOI:
https://doi.org/10.46544/AMS.v25i1.9

Abstract
One of the most prospective developments of hard rock mechanical excavation methods is the possibility of the disc tools usage in new constructions of mining machinery. For many years, such research on the excavation using both symmetrical and asymmetrical disc tools has been conducted in the Department of Mining, Dressing and Transporting Machines in the AGH University in Cracow. The primary effect of these tests is an innovative solution of a mining head with complex motion trajectory asymmetrical disc tools. The concept of the disc head assumes the mining of rock stone by chipping as a result of a complex trajectory of disc tools. To develop such innovative construction of roadheader head, determination of work principles and guidelines based on laboratory tests was necessary. The article presents the methodology, course, and results of the disc tools mining tests. Those studies included quasi-static and dynamic experiments of excavation using disc tools. In this paper constructions of specially prepared laboratory stands for the examination of disc tools of complex trajectory were presented. Each trial has been performed for different physical properties of rock samples and different excavation technology. The conducted research significantly broadens the scope of knowledge in the field of mining with asymmetrical disc tools. The results of tests described in the paper could be used in the construction of innovative machines and devices for mechanical hard rock mining, in opposition to classical mining methods involving explosive materials.

Keywords
disc tools, hard rock mining, undercutting, roadheader

Introduction

Rock excavation using disc tools is one of the most promising directions for the development of mechanical hard rock mining. The use of disc tools for this purpose allows, compared to the standard milling method, reducing the energy consumption of the mining process and leads to the reduction of dust generation associated with mining. The fragmentation of rock output is also reduced. Due to the significant reduction of friction forces in the rock mining process, the durability of the tools also increases. Two basic techniques of mechanical rock mining can be distinguished by means of disc tools, namely excavation with static pressure and by undercutting. The above advantages of using disc tools, especially in the case of mining hard rocks, resulted that the interest in the industrial application of the rear undercutting technique has recently increased. Attempts are made to apply disc tools not only on conceptual (prototype) machines but also in industrial ones that have used the standard mining tools (picks, teeth) (Acaroglu et al., 2017; Asbury et al., 1998; Manfred, 2005; Gospodarczyk et al., 2015a; Kotwica et al., 2003). However, this type of actions requires the use of proven calculation procedures to verify the reliability of such new solutions for mining systems.

The essence of destroying the cohesion of rocks by disc tool in a simplified way can be illustrated using the example of penetration of the wedge profile into rock half-space. A characteristic feature of this process is the relatively small size of the so-called compression zone, and therefore the foremost part of the excavated material during the disc mining is the volume of side fragments. The course of penetration of the wedge profile into a half-space is characterized by dynamic variability, which directly affects the value of the P_d pressing force during mining. The consequence of this fact is the difficulty of formulating a full mathematical description of the process of disc's blade penetration into the rock body. In connection with the above, models specifying the mining resistance forces assume simplifications and allow only for an approximate estimation of forces acting on the tool during rock excavation. It should be emphasized that the computational models of different authors are most often the result of their experimental research, and so they are valid in the area of restrictions that were considered during the experiment. Also, the analytical formulas for describing the resistance forces of disc mining assume simple kinematics of the mining system (most often rectilinear). The use of analytical formulas for calculation of disc tool loads is often insufficient, and it is possible to generate errors when defining boundary conditions for new and innovative types of mining machinery (Stopka, 2011).

The dominant group of disc mining models is the one describing the load of symmetric disc tools. A standard feature of these models is the assumption of proportionality of forces generated on the disc's blade during operation to the size of the surface area of the imprint. An example of such a model is the description proposed by Roxborough and Philips (Roxborough, 1975). According to this model (Fig.1), the pressing force P_d is described by the formula:

$$P_d = 4 \cdot 10^{-3} \cdot R_C \cdot tg\beta \cdot \sqrt{D \cdot h^3 - h^4} \qquad (1)$$

Where:
R_c – uniaxial compression rock strength (UCS),
h – cutting depth of the disc,
D, β – geometric parameters of the disc.

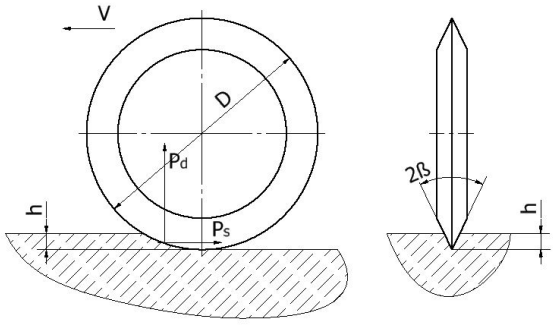

Fig.1. Diagram of forces affecting disc tool (Roxborough, 1975)

The assumption described above which characterizes the symmetrical disc mining models is a reasonable approximation of the symmetrical discs mining process in the case of simple mining kinematics (mining with static pressure). A different situation occurs in the case of the undercutting technique, where the disc moves on a complex track, and the asymmetric disc during penetration into the rock body and at the time of complete dehiscence of the rock fragment generates strongly variable lateral forces. In the case of the undercutting technique, a significant problem is the lack of a model basis allowing to predict loads of asymmetrical disc tools,

which in effect makes the correct selection of construction parameters of mining machines difficult. The estimation of loads of specific disc tools is most often performed empirically, assuming simplified mining kinematics (Kotwica et al., 2010; Kotwica, 2011). The inadequacy of analytical methods is the reason why simulation methods have been used to analyze such problems (Gajewski et al., 2008; Gospodarczyk et al., 2015b; Jonak et al., 2012; Labra et al., 2017; Rojek, 2007; Xiaohuo et al., 2012, Xia et al., 2017).

Currently, many research and development centres attempt to use asymmetrical disc tools in the working bodies of mobile mining machines. The issues of modelling and research of prototype mining machinery solutions are one of the primary research directions implemented at the Department of Mining, Dressing and Transport Machines at AGH in Krakow, Poland (Bołoz, 2013) (Bołoz et al., 2018) (Gospodarczyk et al., 2015a). An example of this type of work is an attempt to develop and implement a new generation of disc head dedicated for use in the construction of roadheaders (Gospodarczyk et al., 2013; Gospodarczyk et al., 2016; Mendyka, 2016). The concept of the disc head assumes the mining of rock stone by chipping as a result of a complex trajectory of disc tools, presented in Figs. 2 and 3. The elaborated mining unit consists of independently propelled body and mounted in it propelled discs with asymmetrical disc tools. The unit body 1 is propelled by an external drive shaft 2. In the body, in seats 3 drive shafts 6 are mounted with plates 4, on which in bearing seats 10 disc tools 5 are installed. The most favourable number of tools should be 6 to 8 pieces. The drive shafts 6 are propelled by an internal drive shaft 7 independent from the external drive shaft 2 and a set of bevel gears 8 and 9 or alternative ones.

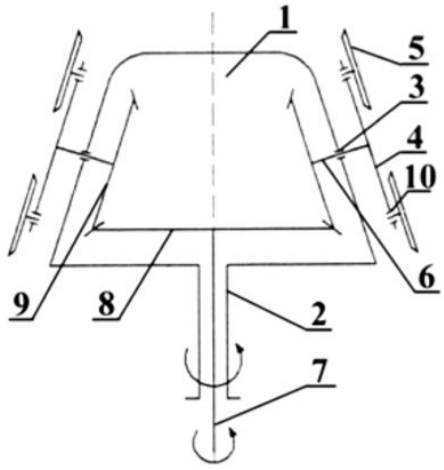

Fig.2. The conception of a unit equipped with disc tools of a complex motion trajectory

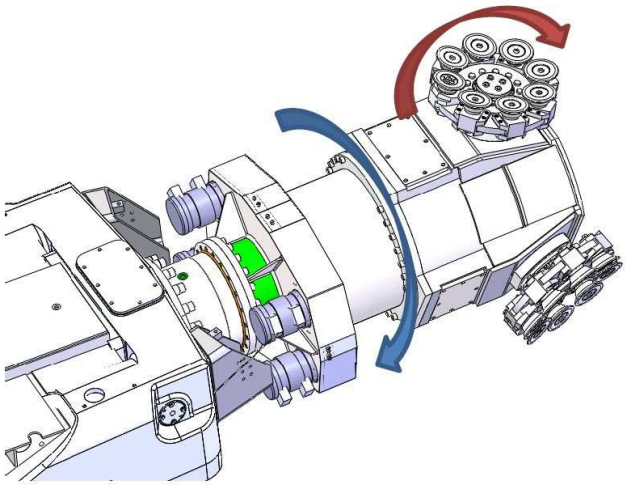

Fig.3. 3D model of the new head solution

Due to the lack of theoretical and experimental basis that would allow defining boundary conditions for the construction of a new disc head, it was decided to carry out laboratory research on asymmetrical disc tools. The primary goal of this research was to identify the impact of geometric parameters of discs and selected mining process parameters on the value of resistance forces during mining using a single disc tool and disc plate.

Testing methodology

Research on the mining process with asymmetrical disc tools has been divided into two phases. As part of the first issue, research was conducted on the impact of geometric parameters of disc tools on the values of loads generated by pushing a tool into a rock sample. The second research problem was the assessment of the impact of selected mining process parameters, i.e., the penetration depth and cut spacing on loads of a single disc in the similar to real working conditions.

Static tests consisted of pushing the disc into a rock at a given distance from the sample edge until the material was detached entirely (Fig. 4). The following geometric and process parameters were adopted as independent variables for the tests:

- the diameter and a tip angle of the disc tool (D, α),
- cut spacing (t),
- physical and mechanical properties of the rock sample (R_c) (Biały, 2013; Biały, 2014).

Based on the literature analysis of the subject as well as previous author experiences in the field of industrial application of disc tools, it has been determined that the tests will be carried out for disc tools with D = 150, 160 and 170 mm diameter and blade angles α = 35 °, 40 °, and 45 °. Fig. 5 shows disc tools used for pressing (rock penetration) tests. During the conducted research, the P_d pressure force and displacement of the disc tool were measured and recorded.

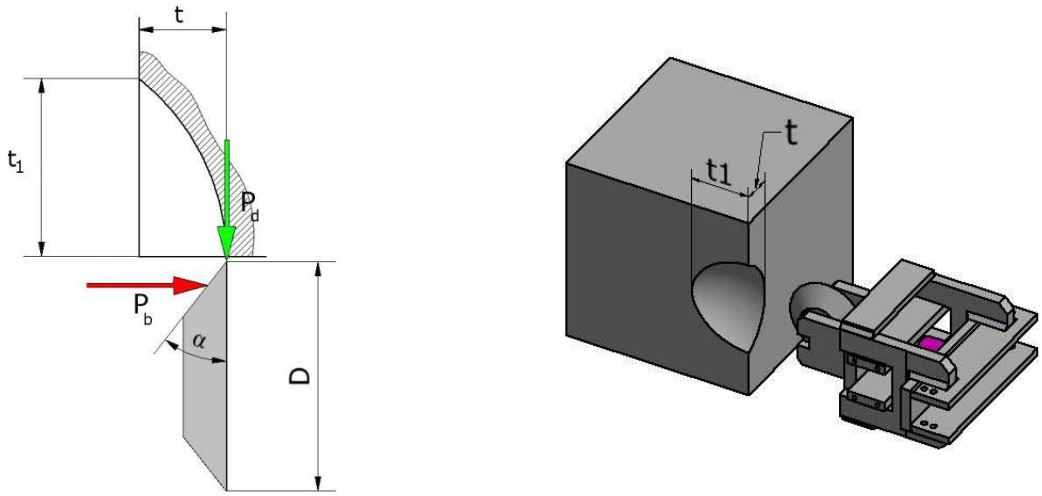

Fig.4. Measured parameters during mining tests with single disc tool

Fig.5. Tested disc tools

As part of the second phase of the research, mining tests using a plate armed with six-disc tools were performed (Fig. 6). Those tests were conducted for one type of disc geometry. Individual excavation attempts consisted of a series of cuts in the vertical plane with a given cutting depth and spacing. To reduce the number of independent variables, the measurements were made at the constant values of the plate rotational velocity and its feed rate (vp), established during the pilot tests. The individual components of the cutting resistance forces (P_d, P_s) were indirectly identified on the basis of pressure values in the feed cylinder of the stand and the disc plate hydraulic drive. The physical model of the disc plate load and the method of carrying out the tests are shown in the figure below.

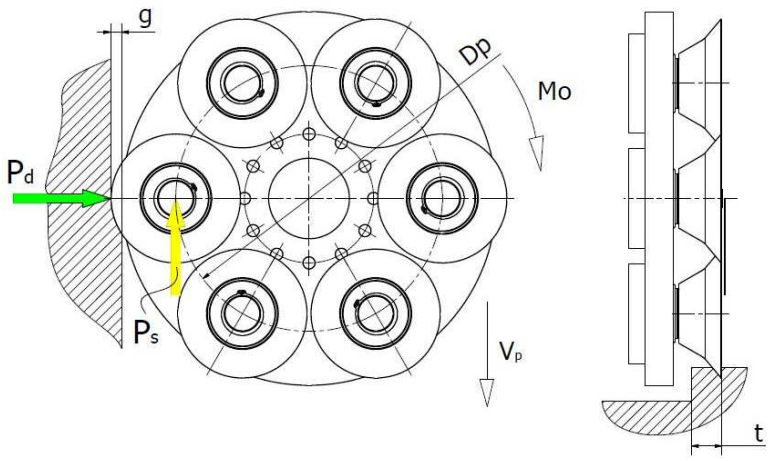

Fig.6. Diagram of vertical mining of the sample by the plate with disc tools

Research on the disc mining process was performed for concrete samples with different mechanical properties. The research with a single disc tool was carried out on concrete samples with uniaxial compressive strength of 25 MPa and sandstone samples with uniaxial compressive strength of 79 MPa. However, disc plate mining tests were performed on a concrete sample with compressive strength R_c = 25 MPa. Laboratory tests were carried out on a dedicated laboratory stand, which consists of two primary components (modules). These modules are shown in Figs. 7 and 8. Each operation on the stand is carried out using hydraulic actuators (cylinders or motors). Fig. 5 shows a measuring system for testing the static process of pressing disc tools into a rock sample. Presented stand allows to attach the disc tool in the holder; the construction of this holder permits to change the position of the disc relative to the sample, and thus gives the opportunity to set the right cut spacing. The system is equipped with a strain gauge force sensor that allows measuring the pressure force in the range of 0 ÷ 200 kN and a transformer displacement sensor with a measuring range of 0 ÷ 300 mm. The disc tool is pressed through the feed system of the station into a rock sample in the form of a 400 x 400 x 400 mm block. The sample is fastened to the construction of the station using a special metal frame. The second module is the disc plate arm, mounted on a movable table (Fig. 8). The design of this module is described in detail in several publications (Kotwica et al., 2010). The displacement of the disc plate in the horizontal and vertical plane is due to two hydraulic cylinders. An additional movement is the table feed, along with the arm and disc plate. The angular displacement of the arm allows the plate to mine an artificial rock specimen measuring 1650 mm x 1200 mm x 1000 mm (~ 2 m^3). The tests used a disc with a pitch diameter D_p = 444 mm. The drive unit of the disc is the OMTS 250 hydraulic motor by Sauer Danfoss and the RR5 / OMC planetary gear. The used disc plate drive allows obtaining the nominal torque of 3650 Nm.

Fig.7. Lab stand for testing mining process of single disc tools

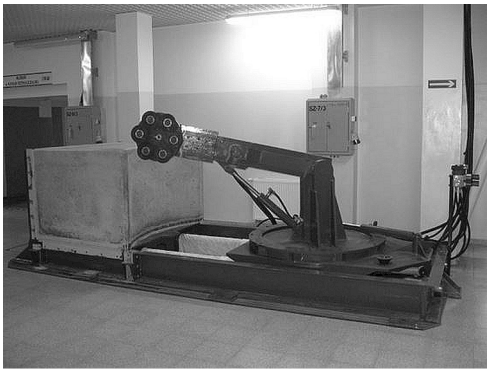

Fig.8. Lab stand for testing mining process of the plate with disc tools

Laboratory tests

The first stage of the research was a series of tests of disc tools static insertion into samples made of concrete with different uniaxial compression strength. Each of the mining tests consisted of setting an appropriate cut spacing by the appropriate aligning and locking of the handle together with the disc tool. In the next step, the disc insertion was made close to the edge of the rectangular rock sample until the material was entirely de-bonded. The tests were carried out for three cut spacing values, namely for the parameter t (Fig. 4) equal to 15, 25 and 35 mm. After each of the tests, the extent of the destruction zone was measured. Performing another attempt required moving the holder towards the opposite, intact edge of the sample and rotating the disc tool so that the cutting was obtained by the conical surface of the disc. Each of the trials for a given configuration of the geometric disc parameters and the determined scale pitch was repeated at least three times. Based on the observations made during the tests, there was a negligible share of the compression zone in the process of destroying the consistency of the sample. The vast majority of tests were completed by chip separation, whose dimensions (height, depth) were multiple times higher of the assumed cut spacing.

Exemplary results of static insertion of disc tools are presented in the following figures. Fig. 9 shows exemplary forms of destruction of samples mined with disc tools 150 mm in diameter. In contrast, Fig. 10 shows a form of spoil being the result of mining discs with diameters Ø 160 and 170 mm for different graduations.

Fig.9. A view of the sandstone block after the mining test (R_c = 79 MPa) - disc Ø 150/40°, t = 15 mm

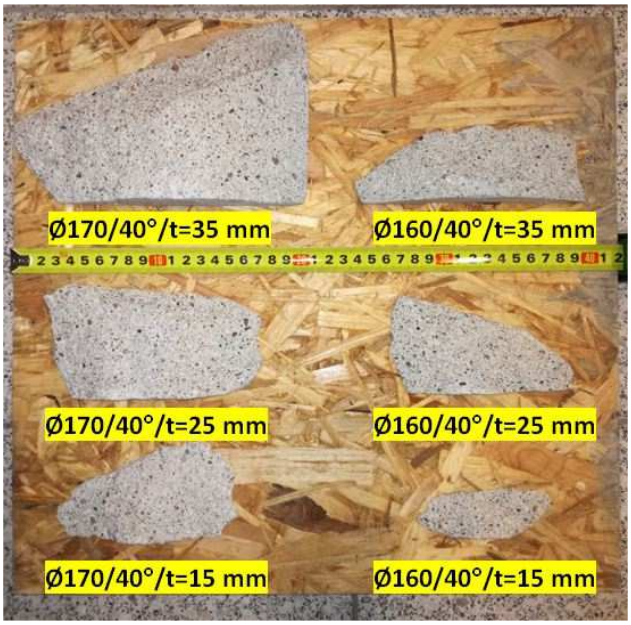

Fig.10. Graining of the output obtained during the mining tests with single disc tool (R_c=25 MPa)

The second part or research included mining tests with disc plate. The test was, in a sense, analogous to the static pressing one and consisted of the task of setting an appropriate cutting depth and spacing of disc plate mining and then performing the vertical cutting. Specification of the above parameters of the mining process was carried out by appropriate positioning of the arm and table of the station using hydraulic cylinders. As in the case of static tests, the detachment of the sample material followed the conical surface of the disc. As a result of preliminary pilot tests, kinematic parameters of the disc plate during the mining process were determined. It has been assumed that the tests will be carried out for the disc plate rotational speed of 60 rpm. It was the minimum value of this parameter which allowed to carry out the mining process in a smooth way. On the basis of pilot tests, it was assumed that individual mining attempt would be carried out for a depth of cut of g = 15, 20 and 25 mm and a cut spacing t = 20, 30, 40 and 60 mm. As a result of the tests, it was observed that in the case of the t = 60 mm scale the sample material was not completely crushed. For the remaining mining scales, a full exploration of the sample material was obtained for the full range of cutting depth. The form of output obtained in individual samples was characterized by a large number of platelet grains. This form of output testifies to the relatively low energy consumption of the mining process. Exemplary results of disc plate excavation research are shown in the figures below. Fig. 11 shows the moment of making the cut by plate disc, while in Fig. 12 the concrete block surface after a few series of mining tests was presented.

Fig.11. A view of the cut after one of the mining test

Fig.12. A view of the concrete block surface after completing the mining test

Test results

The laboratory tests allowed to identify the impact of geometrical parameters of disc tools, as well as cutting process parameters on the resistance forces of both a single disc tool and plate disc. Due to the limited number of tests carried out in this publication, only exemplary research results are provided. Static attempts to push the disc tool made it possible to quantitatively compare the influence of a number of geometric parameters of the discs on the value of the pressure force. Fig. 13 shows selected force waveforms for various configurations of process parameters and physical properties of rock samples for disc 150 mm. The recorded waveforms are characterized by the variability typical for the processes of rock centre destruction by a tool similar in profile to the wedge. Relevant information is not only the value of the maximum destructive force but also the limit value of the disc's depth. Depending on the configuration of the geometric parameters tested, and the properties of the sample, the disc penetration causing the sample to be destroyed was 2 to 10 mm.

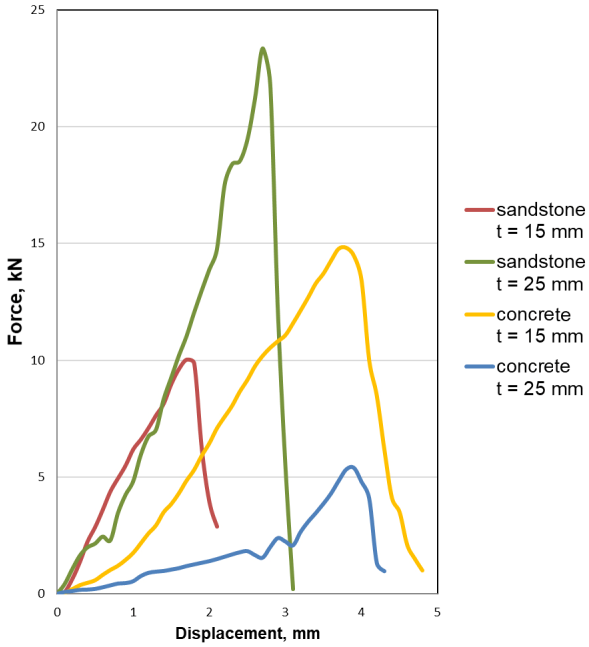

Fig.13. Exemplary courses of press force as a function of displacement for disc ø 150 mm

Fig. 14÷17 are examples of graphs of the impact of selected geometric parameters of disc tools and cutting spacing on the value of press force. Mean values of maximum press forces were calculated on the basis of at least three measurements. Based on the results of the research, it can be concluded that the increase in the value of individual independent variables caused an increase in the generated downforce. On the other hand, the dynamics of the changes of the press forces values varied depending on the variable adopted as the input parameter for the tests. The most significant increases in the pressing force were observed in relation to the cutting spacing. The change of such parameters as the diameter of the disc or the angle of the disc's blade caused a smaller increase of the pressure force as in the case of the cutting spacing. As part of the research, the influence of the strength of the sample on the value of the pressing force of the disc tool was also checked. On the basis of the tests carried out, it can be concluded that the increase in the strength of the sample caused a proportional increase in the registered press force.

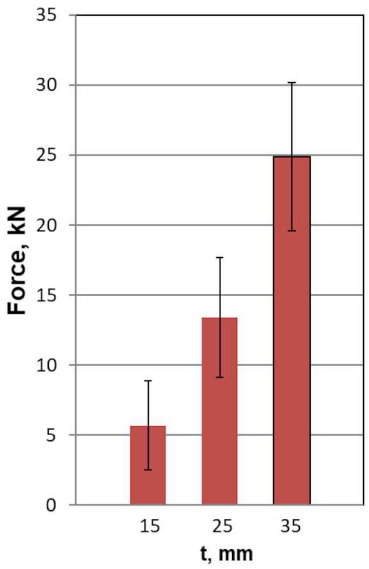

Fig.14. Mean values of maksimum press forces (D = 160 mm, R_c = 25 MPa)

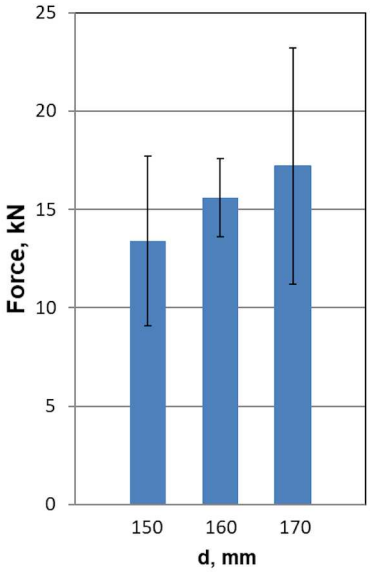

Fig.15. Mean values of maksimum press forces (t =25 mm, α = 40°, R_c = 25 MPa)

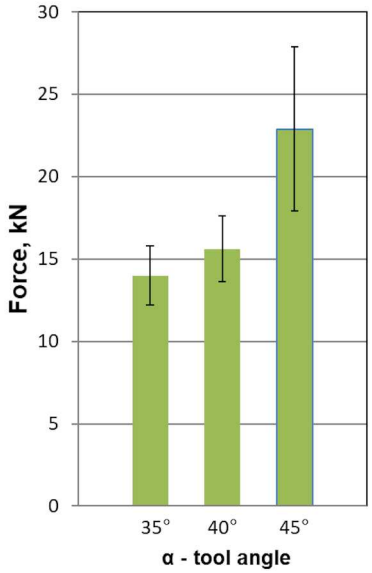

Fig.16. Mean values of maximum press forces (D = 160 mm t = 25 mm, R_c = 25 MPa)

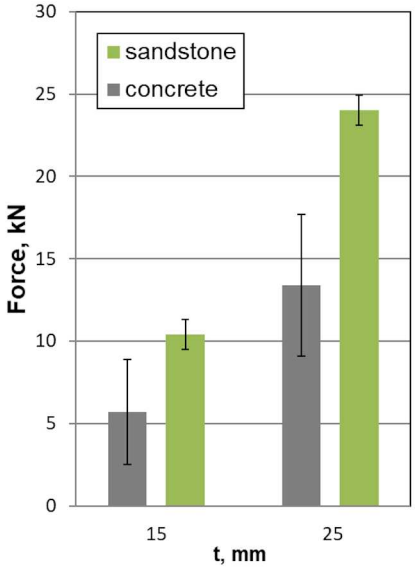

Fig.17. Mean values of maximum press forces (D = 150 mm, R_c = 25 and 79 MPa)

In the second phase of research, disc plate mining tests were carried out, equipped with discs of a diameter of 160 mm and a 40 ° blade angle. Fig. 18 shows an example measurement of a dynamic torque on the shaft of a disc drive motor for one of the mining tests. Based on the momentary force waveforms in the feed cylinders and the torque on the drive shaft of the disc plate drive, the average values of the individual components of the cutting resistance force were calculated for each of the tests. The exemplary test results are shown in Fig. 19 and 20. The charts show both data in a discrete form (average value) and approximations of the test results using

curves. The conducted disc mining excavation research shows that the dominant component of the resistance force for the disc plate is the pressing force. The conducted research allowed to identify the influence of depth and cutting spacing on the value of press force and cutting disc plate. In the case of cutting force (tangential to the disc), it should be stated that the value of this force is determined primarily by the cutting depth.

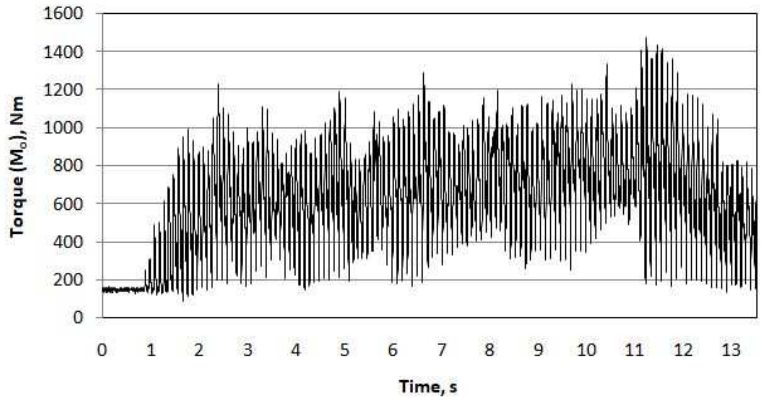

Fig.18. Graph of torque during sample vertical mining by the plate with disc tools (g = 25 mm, t = 20 mm, v_p = 0,05 m/s)

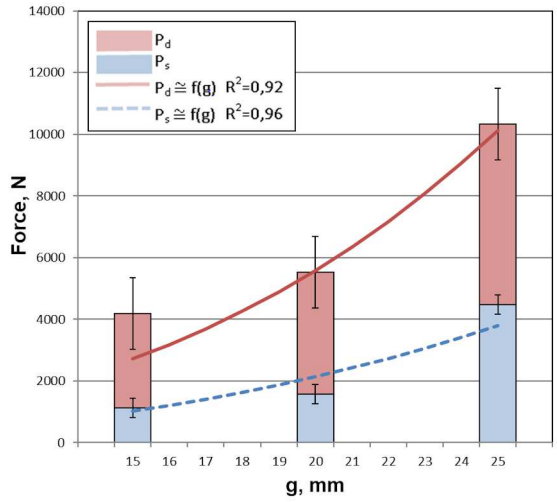

Fig.19. Mining forces as a result of the mining tests with the plate with disc tools (t = 20 mm)

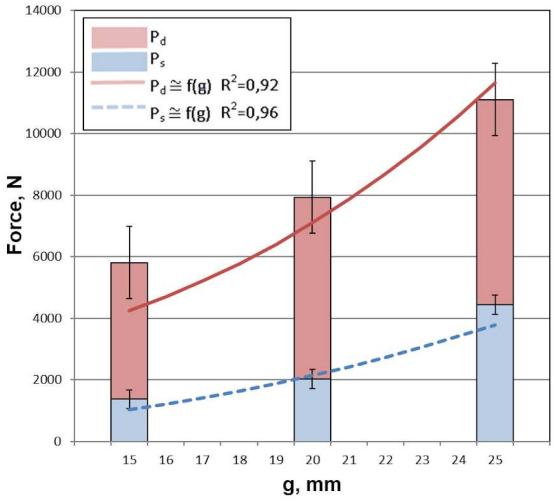

Fig.20. Mining forces as a result of the mining tests with the plate with disc tools (t = 40 mm)

Selected aspects of the test results usefulness

The conducted research significantly broadens the scope of knowledge in the field of mining with asymmetrical disc tools. The practical (utilitarian) aspect of described laboratory research out involves the use of test results for the selection of kinematic and dynamic parameters of a new type of roadheader disc head. The construction of such a head is shown in Fig. 21. The results of the research conducted on the prototype disc head confirmed the validity of the methodology used for testing with a single disc plate. In turn, the cognitive goal of the completed research was achieved by identifying the correlation between a number of geometrical parameters of disc and process tools and the values of mining resistance forces. Quantitative and qualitative assessment of the impact of selected independent variables on the formation of resistance to mining using asymmetrical disc tools is key information for the validation of analytical and simulation models of the mining process. An example simulation of pushing a disc tool into a rock sample is shown in Fig. 22 (D = 160 mm, t = 25 mm, R_c = 25 MPa).Taking into account the cost of manufacturing and researching prototype solutions of mining machines, it should be stated that the development of elementary models of rock cutting using asymmetrical discs will be an important factor determining the development of this type of construction.

Fig.21. The new generation mining head with disc tools during field tests

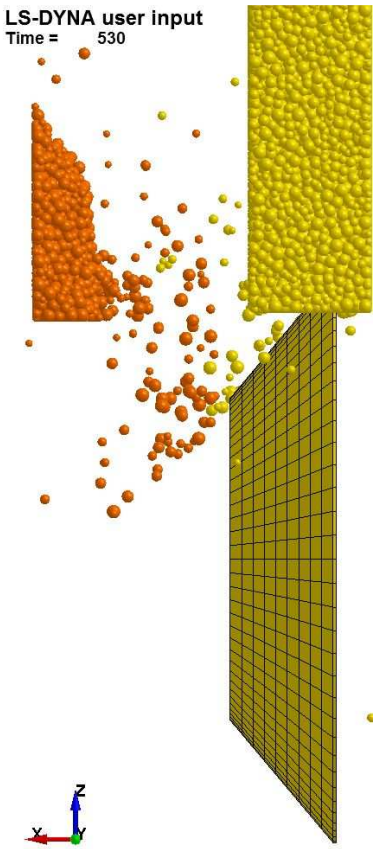

Fig.22. Simulation of rock cutting in LS-Dyna (Discrete Element Method)

Conclusions

The use of asymmetrical disc tools for the mining of hard and very hard rocks is a promising direction for the development of mechanical mining methods. Several industrial research has confirmed the possibilities of a significant reduction in the energy consumption of the mining process, and thus minimization of the size and weight of the mining machine (Biały, 2017). Also, research on the disc mining process that has been carried out so far confirmed the prospective character of the development of unconventional mining techniques based on disc tools.

One of the fundamental problems of application of asymmetrical disc tools in mining machine heads is the issues of forecasting their loads. Currently, there are no model foundations that would allow evaluating a load of disc tools, especially in the conditions of complex mining kinematics. The development of computer simulation tools gives hope for the development of efficient mining models due to the required accuracy and acceptable time-consumption of each test.

The results of laboratory tests presented in the described study constitute unique information regarding the impact of geometric parameters of disc tools and mining process parameters on the reaction force generated during mining. From a practical point of view, the presented test results can be input data for design purposes and can be used to select the necessary parameters of dynamic mining heads (Stopka, 2019). The relations between the individual geometric parameters of the discs and the mining process and the reaction forces, identified as a result of the conducted research, can be used to validate analytical and simulation mining models.

References

Acaroglu O., Erdogan, C. (2017). Stability analysis of roadheaders with mini-disc, Tunneling and Underground Space Technology, vol 68. s.187-195.

Asbury B., Ozdemir L. and Rostami J.(1998). Mini Disc Equipped Technology for Hard Rock Minig. SME 1998, Orlando, USA

Biały W. (2013). New devices used in determining and assessing mechanical characteristics of coal. 13th SGEM GeoConference on Science and Technologies in Geology, Exploration and Mining, SGEM2013

Conference Proceedings, June 16-22, 2013, Vol. 1, BUŁGARIA ISBN 978-954-91818-7-6/ISSN 1314-2704. pp. 547-554.

Biały W. (2014). Coal cutting force measurement systems - (CCFM). 14th SGEM GeoConference on Science and Technologies In Geology. Exploration and Mining. SGEM2014 Conference Proceedings, Vol. III, pp. 91-98.

Biały W. (2017). Application of quality management tools for evaluating the failure frequency of cutter-loader and plough mining systems. Archives of Minning Sciences, Volume 62, issue 2, 2017. pp. 243-252. ISSN 0860-7001. DOI 10.1515/amsc-2017-0018.

Bołoz Ł. (2018). Model Tests of Longwall Shearer with String Feed System, Archives of Mining Sciences, 63(1), pp. 61-74.

Bołoz Ł., Leonel F. Castañeda (2018). Computer-aided support for the rapid creation of parametric models of milling units for longwall shearers, Management Systems in Production Engineering, 26(4), pp. 193-199.

Gajewski J., Podgórski J., Jonak J. and Szkudlarek Z. (2008). Numerical simulation of brittle rock loosening during mining process, Computational Materials Science, vol. 43.

Gospodarczyk P., Kotwica K. and Stopka G. (2013). A new generation mining head with disc tool of complex trajectory, Archives of Mining Sciences 2013 vol. 58 no. 4, s. 985–1006.

Gospodarczyk P, Kotwica K., Mendyka P. and Stopka G. (2016). Innovative roadheader mining head with asymmetrical disc tools, Exploration and mining, mineral processing. International Multidisciplinary Scientific GeoConference SGEM, vol.2, Sofia 2016, s. 489–496.

Gospodarczyk P., Kotwica K., Mendyka P. and Stopka G. (2015). Innovative solution of the roadheader mining head with disc tools of complex motion trajectory, Maschinen und Verfahren fur den Bergbau und Spezialtiefbau, Freiberg 2015/a, s. 53-63.

Gospodarczyk P., Mendyka P. and Stopka G. et al. (2015). Wybrane zagadnienia modelowania procesów urabiania, ładowania i odstawy w kompleksach ścianowych. Wydawnictwa AGH, Krakow 2015/b.

Huiyun Li, Erxia Du (2016). Simulation of rock fragmentation induced by a tunnel boring machine disk cutter, Advances in Mechanical Engineering, 2016, Vol. 8(6) 1–11

Kotwica K. (2003). Modelowanie urabiania skał zwięzłych narzędziami dyskowymi ze wspomaganiem wysokociśnieniowymi strugami wody. Archives of Mining Sciences, Vol. 43, Issue 1, 1998, s. 147 – 184

Kotwica K., Gospodarczyk P. (2003). Hard Rock Mining with use of New Cutting Tools. Journal of Mining Sciences. Vol. 39, No. 4 2003. s. 387-393.

Kotwica K. (2011). The influence of water assistance on the character and degree of wear of cutting tools applied in roadheaders. Archives of Mining Sciences. Vol. 56, 3/2011. s. 353-374

Kotwica K., Gospodarczyk P., Stopka G. and Kalukiewicz A. (2010). Projektowanie i badania stanowiskowe nowego rozwiązania głowicy z narzędziami dyskowymi o złożonej trajektorii ruchu do urabiania skał zwięzłych, Mechanics and Control, 3/2010

Labra C., Rojek J. and Oñate E. (2017). Discrete/Finite Element Modelling of Rock Cutting with a TBM Disc Cutte, Rock Mechanics and Rock Engineering, March 2017, Volume 50, Issue 3, pp 621–638

Manfred V. (2015). Maschinentechnische Herausforderung zur Umsetzung des Konzeptes Hinterschneidtechni, Symposium Tunnelbau, Zurich 2005.

Jonak J. and Podgórski J. (2012). Numeryczne badania skrawania skał anizotropowych dyskiem asymetrycznym, Politechnika Lubelska, 2012

Mendyka P. (2017). Laboratory stand tests of mining asymmetrical disc tools, Exploration and mining, mineral processing. International Multidisciplinary Scientific GeoConference SGEM, vol.17, Sofia 2017, s. 487–494.

Stopka G. (2011). Badania procesu urabiania narzędziami dyskowymi. Doctoral Thesis. AGH w Krakowie, Kraków 2011.

Stopka G. (2019). Numerical simulation in design process of the new generation mining head with disc tools. Systemy Wspomagania w Inżynierii Produkcji: ISSN 2391-9361. — 2019 vol. 8 iss. 1 Górnictwo - perspektywy i zagrożenia, s. 164–172.

Rojek J. (2007). Discrete element modeling of rock cutting, CompMethod Mater Sci 2007; 7: 224–230.

Roxborough F.F., Phillips H.R. (1975). Rock Excavation by Disc Cutter. Int. Journal of Rock Mech. and Min. Sci., Vol. 12, 1975.

Xiaohuo Li, Wei Du, Zhilong Huang and Weili Fu (2012). Simulation of Disc Cutter Loads Based on ANSYS/LS-DYNA, Applied Mechanics and Materials Vol. 127 (2012) pp 385-389

Xia Y.M., Guo B., Cong G.Q. and Zeng G.Y. (2017). Numerical simulation of rock fragmentation induced by a single TBM disc cutter close to a side free surface, International Journal of Rock Mechanics and Mining Sciences, Volume 91, January 2017, Pages 40-48

Acta Montanistica Slovaca
ISSN 1335-1788
actamont.tuke.sk

Legislative instruments and their use in the management of raw materials in the Slovak Republic

***Lucia BEDNÁROVÁ*[1]*, *Jana DŽUKOVÁ*[2], *Roland GROSOŠ*[3], *Marián GOMORY*[4]** *and* ***Miloš PETRÁŠ*[5]**

Authors' affiliations and addresses:
[1]Faculty of Mining, Ecology, Process Control and Geotechnologies Technical University of Kosice, PK 19, 042 00 Košice, Slovak Republic
e-mail: lucia.bednarova@tuke.sk

[2]Faculty of Mining, Ecology, Process Control and Geotechnologies Technical University of Kosice, PK 19, 042 00 Košice, Slovak Republic
e-mail: janka.dzukova@gmail.com

[3]Faculty of Mining, Ecology, Process Control and Geotechnologies Technical University of Kosice, PK 19, 042 00 Košice, Slovak Republic
e-mail: roland.grosos@tuke.sk

[4]Faculty of Mining, Ecology, Process Control and Geotechnologies Technical University of Kosice, PK 19, 042 00 Košice, Slovak Republic
e-mail: marian.gomory@tuke.sk

[5]Faculty of Mining, Ecology, Process Control and Geotechnologies Technical University of Kosice, PK 19, 042 00 Košice, Slovak Republic
e-mail: milos.petras@tuke.sk

***Correspondence:**
Lucia Bednárová, Faculty of Mining, Ecology, Process Control and Geotechnologies Technical University of Kosice, PK 19, 042 00 Košice, Slovak Republic
tel: +421903357959
e-mail: lucia.bednarova@tuke.sk:

Acknowledgement:
This paper was supported by the Scientific Grant Agency od the Ministry of Education of Slovak republic under grant VEGA 1/0651/2018 - Research of institutional environment influence to the corporate social responsibility, consumers satisfaction and performance of the company.

How to cite this article:
Bednárová, L., Džuková, J., Grosoš, R., Gomory, M. and Petráš, M. (2020). Legislative instruments and their use in the management of raw materials in the Slovak Republic. *Acta Montanistica Slovaca*, Volume 25 (1), 105-115

DOI:
https://doi.org/10.46544/AMS.v25i1.10

Abstract
Mineral resources are an integral part of society's life and affect many sectors of society's economy. None of the production sectors of the economy and social life can exist without securing a sufficient amount of minerals. In this article, we deal with the analysis of the raw materials policy of the Slovak Republic. A necessary condition for the creation of the raw material policy of the territory is the knowledge of the raw material base and the raw material needs of the given territory. Without this knowledge, raw materials policy-making is impossible. We made an analysis of the legal environment on the basis of which we created a set of critical areas of the Slovak Republic raw materials policy. We have drafted a recommendation to be incorporated into the legislative proposals with regard to raw materials policy. The proposed recommendation could ensure the sustainability of the country's mining industry as well as streamlining mining fees.

Keywords
raw material policy, mining, legislative, mining fee.

Introduction

Global change and especially the global environmental crisis pose a serious challenge to the available control systems, including the legal system. We already know what has to be done: the demand for an “effective state” and for “effective low" is the central axis around which political and administrative reform must be attempted in our age. The law that has adopted the new, systemic decision-making methods has been put forward as the most flexible.

Raw materials are essential for the sustainable functioning of modern societies. Access to and affordability of mineral raw materials are crucial for the sound functioning of the EU's economy. Sectors such as construction, chemicals, automotive, aerospace, machinery and equipment sectors which provide a total value added of € 1 324 billion and employment for some 30 million people all depend on access to raw materials.

The starting point of this article is the need to implement the Raw Materials Initiative, in particular its second pillar, which relates to fostering a sustainable supply of raw materials within the European Union from domestic resources. This is also taking place in the framework of the implementation phase of the Strategic Implementation Plan (SIP) of the European Innovation Partnership on Raw Materials. The latter plan identifies a number of particular actions, under Action areas "II.1 Minerals Policy Framework"; and "II.2 Access to Mineral Potential in the EU", which relate to the challenges of "policy and legal framework, information framework, land-use planning and permitting”.

Action area "II.1 Minerals Policy Framework" aims to "strengthen the exchange of best practices in the area of mineral policies and related regulation among the Member States, that may lead to streamlining the permitting procedure along the whole chain of extractive activities (prospecting, exploration, extraction, processing, closure, post-closure activities) with regard to the time frame, the regulatory co-authority regime, the financial and administrative conditions, and ensure stable, predictive environment." "Another objective is to increase transparency on raw materials availability in the EU (Straka et al., 2016). Information on exploration, mineral production, trade, reserves and resources should be standardized and systematically reported by the EU and the Members States, when information is available and without breaching competition rules."

The goal of raw material policy should be to define priorities for Slovakian raw material industry from the view of the need to provide sustainable development of national economy and society, as well as to define measurements and tools for providing of stable development of single raw material industry and its competitiveness in international level in the measure, adequate to created conditions (Cavender, 1992). The goal of the presented contribution is, therefore, to make a system for raw material legislative policy in particular conditions of the country. The larger the system, the greater the number of factors, decisions, constraints, and risks it involves (Straka et al., 2018). Knowledge of these factors is very important not only for the development of relevant policy concepts in the country but also for the national and international benchmarking (Khouri et al., 2017).

The mineral wealth of the Slovak Republic is the property of the state, and thus the state itself allows the use of this wealth to individual organizations, which are obliged to pay fees for this use if the specified legal conditions are met. The legislative framework for the use of the state's mineral wealth is determined by laws, decrees, government regulations and other generally legally binding acts. Mineral wealth is exploited in many industries, and some industries would not exist without minerals. Strategic intentions and directions in the use of the state's mineral wealth are defined in the Raw Materials Policy, from which subsequent generally binding legal acts should be derived. These strategic intentions need to be updated on the basis of geopolitical developments but also on the basis of scientific and technical progress, new knowledge and other factors.

The role of the state is to protect mineral wealth, but also to create suitable conditions for its rational use.

Literature review

Many countries in the world run their economies with minerals in various forms, be it mining, importing or exporting minerals. The more developed a country is the more it uses modern raw materials and materials, which until recently were considered unnecessary waste, and the less the country has its own resources of minerals, the more important it is for it to approach the raw materials policy. One of the important criteria in formulating rules and principles on securing the country with minerals is the maturity of the country.

Today we know full well that, for example, it is clearly futile to monitor the cleanliness of the atmosphere, waters and soils, if you do not at the same time curb those who pollute them. There must at least be understanding of the simple systemic rule "think globally and act locally", which is addressed to every responsible citizen in our age and stresses the interdependence of the many factors that stem from man’s intervention in the environment (Bednárová et al., 2018). However, the decision-makers must also recognize that sustainable development, which imposes the incorporation of criteria for the protection of natural, cultural and social capital in every policy whether public or private, is nothing more than the necessary and delayed application of systemic thinking in making decisions of all kinds. However, although that is how things stand in

the new science of sustainable development, the same need to implement systemic methodology also exists for the Law of Sustainable Development (Decleris, 2000).

The mining industry can be critical to a nation's economic well-being. Impacts may be felt on a national or regional level, with their significance dependent in part on the resources under development as well as existing government policies. The changing character of mining is today opening up new opportunities for foreign investment and technology assistance (Dorian et al., 1994).

Mining activities divide communities and countries (Gray, 2018) due to different geological, legislation, political, social, and economic conditions. Therefore, analysis of mining activities must be regarded from the view of the growth economy, encouraged by government tools – together with ecological integrity (Gentry&Neil, 1984).

Openness, transparency, and public participation of the state is a longstanding issue. The state must adopt such decision to public participation with the aim to prevent mining activities from harmful impact to environment, society, and economy. Therefore, also in areas of mining principles of corporate, social responsibility must be regarded (Curran, 2017).

The new Circular Economy package contains a combination of both legislative and non-legislative elements, such as new and revised legislative proposals on waste, clear targets for waste reduction – such as the common EU target for recycling 65 per cent of municipal waste by 2030 – and proposed actions to "close the loop" and tackle all phases in the lifecycle of a product: from production and consumption to waste management and the market for secondary raw materials. It also contains a list of proposed actions that will target market barriers in specific sectors or material streams, such as critical raw materials, as well as horizontal measures in the areas of innovation and investment.

Critical Raw Materials have also been identified as a priority area in the new package. According to the European Commission, existing EU legislation encourages the recycling of electronic waste, including through mandatory targets; but only high-quality recycling can ensure the recovery of critical raw materials. As a result, the EU is focusing on improving the economic viability of the recycling process and encouraging member states to promote the recycling of critical raw materials in its revised proposals on waste. As a result, the Commission is taking a series of actions to encourage the recovery of critical raw materials, including producing a report on best practices and options for further action mention in critical raw materials from 2018.

Developed countries use different strategies to meet the needs of minerals. On the one hand, it is a slowdown in the extraction of domestic resources and a significant import of minerals, in order to ensure the needs of the country in the event of poorer availability of resources. On the other hand, it is mutually beneficial international cooperation, which includes: geological exploration, and mining in a developing country, and the establishment of joint enterprises for the processing of minerals, including the training and employment of workers in developing countries. Japan is one example of this strategy, which it has been pursuing for a long time and successfully.

The efficient use of domestic mineral resources is interfered with by internal and external factors. Internal factors interfere with the quality and volume of proven geological reserves, the maturity of the industrial infrastructure in the mining zone, the mining conditions. External factors that interfere with the usability of domestic mineral resources are mainly based on the liberalization of the market for commodities of mineral origin, world market prices. Also, in terms of availability and contingency, offset them from a domestic source, including secondary raw materials. From the point of view of socio-political intentions declared in the Constitution of the Slovak Republic and the course of integration into the EU, raw materials policy must seriously have the social and ecological focus of market policy in mining and processing of minerals, it also takes into account the careful use of natural resources. The EU's dependence on imports of energy minerals is highly critical, where the EU's dependence on imports is up to 54%.

Based on this, it is absolutely crucial to:

- diversify sources of supply of energy commodities, especially from the point of view of suppliers,
- reduce energy intensity in all spheres of life,
- increase the share of the use of renewable energy sources (biomass, wind, water, sun),
- save their own energy resources (41 regions in 13 EU countries mine coal),
- support the search for new deposits of mineral energy commodities (uranium, shale gas),
- support science and research in the development of new types of fuels (hydrogen and others).

The current legislation should be replaced after consultation of individual regions and strengthened national responsibility, as well as the encouragement of information exchange between countries. Relations present various supplier-consumer, legislative, property, personal, economic, political, and other relations in the frame of the system, as well as relations with its surroundings. System of "Slovakian raw material industry" presents a subset in the vertical level of European and worldwide raw material industry. In horizontal level, it presents part of the Slovakian national economy.

Methodology

Minerals policies are sometimes not clear and effective enough because they are either dispersed among other policies or have no public and implementation support. Coordination and implementation of minerals policies at different levels (EU, Member States regional, local) and horizontally with other sectorial policies is often not straightforward and therefore, in some cases, contradictory and time-consuming.

Even in the cases where Member States (MS) have recently issued a modern minerals policy strategy, adapted to the needs of society and the economy, this could prove to be ineffective if this policy is not strongly linked with other national policies such as an appropriate land use planning policy, environment policy including biodiversity and mine waste management and also with a common understanding and categorization of mineral deposits of local, regional, national and EU importance.

Legislation should facilitate innovation. Competition is vital to the flourishing industry in Europe and should remain a top priority. In addition, it must be ensured that competition law allows the establishment and development of research partnerships.

Policy and legislative processes need to underpin the competitiveness of industry when it comes to access to and trading in raw materials, by means of harmonization and bottom-up orientation. A cumulative impact assessment, which evaluates the impact of multiple policies, should form the basis for a comprehensive EU industrial policy which coordinates the individual policies and ensures a level playing field. This will only be possible with a consolidated vision across Europe, and a clear understanding of the needs and capacities of each member state and region, as well as the synergies they bring to the EU's internal market. This might require more institutionalized consultation processes with the European Economic and Social Committee (EESC) mention in Strategic implementation plan for the European innovation partnership on raw materials.

The raw materials policy deals not only with renewable resources but also with fuel, energy, ore and non-ore and construction raw materials from primary as well as secondary sources. Secondary resources form an important part of raw materials policy, not only in terms of saving primary resources but also in terms of saving costs and energy for the treatment and processing of primary raw materials. It follows that raw materials policy is not only directly linked to energy policy but is closely linked to it. Few countries have so many types of minerals to cover their domestic consumption, so they are dependent on imports. Conversely, many countries are dependent on the export of minerals to other countries, whether raw or already processed. Therefore, an integral part of raw materials policy is the issue of import and export of minerals.

The environmental activities are carried out in the legislative frameworks, which also create a platform for setting up regulatory and stabilization mechanisms in the area of environmental, economic and social policies. Our goal is to harmonize the legislation of the Slovak Republic and propose changes in the case of direct payments from mining in the most affected areas. In many permitting procedure segments, especially at the local/regional level, qualified personnel may be missing or be insufficiently trained. Transparency regarding the permitting procedures as well as the level of permitting fees, royalties, etc., is not always sufficient. The permitting procedure would be enhanced if the EU mineral potential were considered in the design of national mineral and land use planning policies. Rational use of mineral wealth means that we will allow applicants to use mineral wealth in accordance with laws and regulations, permits and restrictions that will be defined, during the permitting process. Rational means reasonable, i.e., so that everyone can benefit from this process. State in the form of fees and taxes, employees in the form of wages for work performed, employers in the form of profits. Customers who obtain primary raw materials for their purposes. Intervention into the rock environment must be thoughtful, systematic, the most modern methods and approaches must be used to make the intervention as considerate as possible. The state should support such use of mineral wealth, i.e. it must create such conditions that mineral wealth can be used rationally.

There are several examples where rational use can be spoken of only partially or not at all. From the systematic view, there is possible to consider the Slovakian raw material industry as a single system. Elements of the system present all research, mining, processing, metallurgical, recycling, education, environmental organizations, as well as state and administration institutions. Relations present various supplier consumer, legislative, property, personal, economic, political, and other relations in the frame of the system, as well as relations with its surroundings. The classification of the sectors was based on the SK NACE Rev. 2, which represents the classification used in the conditions of the Slovak Republic, formerly referred to as OKEČ (Sectoral Classification of Economic Activities). According to this classification, we have selected sector mining and quarrying for our use. For further processing of economic parameters, we performed a financial analysis within selected companies as well as an analysis of financial flows, on the basis of which we can compile an overview of fees for mining space.

In the contribution, we will deal with the description of individual system elements interests, for example, miners, applicators of raw materials, consumers, environmentalists, politicians, etc. However, from the systematic point of view, there is necessary to underline that all such interests together present one set of interest that has its very complex structure, in which some interests contradict each other, others are in antagonistic

relation, some have only objective or only subjective characteristics, some are short term or long-term, resp. permanently applied.

Results

Payments for the use of earth resources in Slovak republic compering the other V4 countries

A major problem at the legislative level is the various authorization procedures, which are lengthy in time and the information required for authorizations is ambiguous. The permitting procedure is often lengthy and involves many authorities with potentially overlapping and even conflicting requirements. Thus, the whole permitting chain sometimes does not have a clear course since various, and sometimes repetitive requirements are requested based on different pieces of legislation. Some of the required information is frequently not available to investors at the time of permit application on the one hand, and on the other permit applications frequently lack the required information, which should be provided by investors.

In the case of Slovak legislation, we deal with several problems. Each organization that has a designated mining area is, according to par. 32a of Act 44/1988 Coll. Mining Act, as amended, obliged to pay a fee for the mining area. The fee is 663.88 EUR for each km^2 started. As mentioned before, 20% of the fee is the revenue of the state budget, and 80% is the revenue of the municipality or municipalities in whose cadastral territories the relevant mining area is located.

Another fee is the fee from the extracted mineral. The method of calculation as well as the fee rate is determined by Government Regulation 50/2002 Coll. on payment for mining area, payment for extracted minerals and on payment for storage of gases or liquids. Reimbursement for extracted minerals is calculated for each quarter of the calendar year as the product of the ratio of the costs of mining the minerals to the total costs of making products from the extracted minerals, revenues from sold products made from the extracted minerals and the reimbursement rate. What we need to mention is, so the payment is the income of the Environmental Fund.

The obligation to pay compensation for extracted mineral has been in our legal system since 1991. If we compare the system of fees for extracted mineral with neighbouring countries, we will find that the system is the same in the Czech Republic. Rates are higher, for some minerals up to several times. However, the system of fees in Hungary is different and is based on determining the value of extracted mineral (Government Regulation) and the percentage rate, which is 5% for surface mining, if we compare these fees with fees in the Slovak Republic, we find that for some commodities fees are several times higher as in SR. In the Polish system, however, there is a significant difference in the fact that in the Geological and Mining Act, the rate of the fee is directly determined, and the fee is the product of the extracted amount of mineral and the rate of the fee. However, what is also different is who is the recipient of this fee. The distribution of the fee according to the recipients is given in Tab. 1.

Table. 1. Distribution of fees according to V4 countries

State	% payment share	Recipient of charge
Slovak Republic	100%	Environmental fund
Czech Republic	25%	National budget
	75%	Municipality according to the cadaster of the mining area
Hungary	100%	Office of Mining and Geology
Poland	40%	National fund for environmental protection
	60%	Municipality according to the cadaster of the mining area

source: XV. Odborný seminár SZVK; Zborník prednášok str. 31 - 42; Atrium hotel, Nový Smokovec 42; Vysoké Tatry; 24. – 25.10.2013

It follows from the above that the recipient is the state only in Hungary and Slovakia. In Slovakia, the fees are the lowest. The highest share, up to 75% of the fee for extracted mineral, will be obtained by the municipality in which the mining area (MA) in the Czech Republic is located. In this context, it is important to say that the immediate environment is in the immediate vicinity of mineral extraction. These loads are mainly noise, dust, vibration, soil and water pollution as well as loads caused by traffic services. However, as for direct payments in the Slovak Republic, the municipality in which the mining area (MA) is located will receive only 80% of the fee for the mining area, which is in most cases 531.10 EUR / year, because most of the mining area has a size of up to 1 km2. Tab. 19 presents the distribution of recipients of fees for mining space and extracted mineral in selected DPs of the company LBK PERLIT, Ltd. and LB MINERALS SK, Ltd. for 2017.

Table .2. distribution of fees LB MINERALS SK, Ltd. and LBK PERLIT, Ltd.

Mining area	Comp	any Payment for MA	Fees for extracted mineral	Total fee	Village	State
Lehôtka pod Brehmi	LBK PERLIT, Ltd.	664 €	7 045 €	7 709 €	531 €	7 178 €
					7%	93%
Šaštín	LB MINERALS SK, Ltd.	1 328 €	6 223 €	7 551 €	1 062 €	6 489 €
					14%	86%
Tomášovce	LB MINERALS SK, Ltd.	664 €	5 014 €	5 678 €	531 €	5 147 €
					9%	91%
Rudník	LB MINERALS SK, Ltd.	664 €	8 377 €	9 041 €	531 €	8 510 €
					6%	94%
Rudník II	LB MINERALS SK, Ltd.	664 €	2 155 €	2 819 €	531 €	2 288 €
					19%	81%
Michaľany	LB MINERALS SK, Ltd.	664 €	14 245 €	14 909 €	531 €	14 378 €
					4%	96%
Ťahanovce	LB MINERALS SK, Ltd.	664 €	2 304 €	2 968 €	531 €	2437 €
					8%	82%

source: LB MINERALS SK, Ltd., LBK PERLIT, Ltd. (Mendel, 2019)

As can be seen from Table 2, the distribution of income from fees for mining activities is divided so that the municipality that bears the most burdens due to mining activities, obtains by direct payments from fees from 4% in the case of MA Michaľany to 19% in the case of MA Rudník II. Paradoxically, the more the mining company benefits, the relatively lower the share of direct payments from fees for the municipality. System set up in this way the distribution of income from payments for mining activities appears to be unfair and makes it significantly more difficult for mining companies to negotiate in the mining licensing process. Municipalities usually no longer agree with mining activities. Why should they also, when 100% of negative consequences are borne by municipalities, but they have from 4% to 19% of the fees in the case of the MAs listed in the table. The municipality, as a participant in the procedure for a mining activity permit, mostly on the basis of requests from citizens, proposes various measures to eliminate these negative impacts, which are many times intractable or difficult to solve and highly costly. They propose restrictions on production and transport service time, construction of bypass roads, prohibition or restriction of blasting works, various environmental measures even beyond the relevant laws. Mining companies, on the other hand, try to eliminate these negative consequences of mining activities with various concessions or services for the benefit of the municipality. We believe that the state in politics charges is failing and should change this policy. A municipality that is affected by mining activities must feel that, in order to bear these negative consequences, they have advantages that distinguish them from other municipalities, for example, lower taxes, free transport, free kindergarten, a significantly higher share of fees for mining activities and others. They must be positively discriminated against compared to other municipalities that do not feel these negative consequences of mining activities.

The position of the mining industry in Slovak society

The extractive industry occupies a special position among industries, as it provides raw materials for other industries. So, in that industrial chain, the industry is at the very beginning. Only metallurgy has a similar special position from the point of view of industries, i.e., metallurgical primary production, which is in the second place in the chain. The importance of the extractive industry is assessed from two basic perspectives:

- economic - its share in the gross domestic product,
- nation economic.

No extractive industry can be characterized only in terms of economic inputs and outputs, because the extractive industry requires significant investment inputs and produces outputs with very low added value (0 added value) (Mendel, 2019). It serves primarily as a supporting type of industry for other downstream industries. The share of the value of mining is very low in individual countries in relation to gross domestic product. Globally, this ratio is around 5%. In different European countries, this share of value manifests itself differently and depends on the value of mining in a given country and the structure of industries. The position of

the mining industry in comparison with other industrial and industrial areas in the Slovak Republic is shown in Table 3.

Table .3. SK NACE rev. 2 - selected indicators 2016

SK NACE	Gross production		Employment	
	mil. EUR	%	number	%
Sum	197 075,7	100	2 321 049	100
Mining and quarrying	535,6	0,27	6 525	0,28
Manufacturing	76 640,3	38,89	508 814	21,92
Construction	14 646,6	7,43	166 132	7,16
Other	105 253	53,41	1 639 578	70,64

source: own processing form SK NACE selected information

As shown by the data in Table 3, mining and quarrying are of only marginal importance for the national economy of the Slovak Republic in terms of GDP and employment. This can also be attributed to the low political influence in negotiations with partners, as well as the weak enforcement of bills that would protect or support the extraction and processing of minerals. For example, 134,483 employees work in healthcare (21 times more than in mining and quarrying) or 171,875 employees in education (26 times more than in mining and quarrying). However, we dare say that these statistics (SK NACE rev 2.) have certain shortcomings and inaccuracies in terms of interpreting the share of mining and quarrying in total gross output as well as employment. For example, the production of cement, lime, concrete or magnesite is carried out under industry and not undermining and quarrying, which can significantly distort these statistics to the detriment of mining and quarrying.

Mining and quarrying are closely linked to other industries such as the chemical industry, the petrochemical industry, the energy industry, the rubber industry, the metallurgical industry, the construction industry, the automotive industry, the glass and ceramics industry, but also the electrical engineering industry. Without the minerals that are the inputs to these industries, these industries could not exist. What would it mean for the Slovak economy if we immediately stopped mining, for example, building materials such as gravel, sand or building stone, or non-metallic raw materials such as limestone (cement and lime production) and we would be completely dependent on the import of these raw materials from abroad. The prices of these commodities would become several times more expensive because the price of these commodities would be significantly affected by the purchase price but especially the transport of these commodities. 30 € / t. This increase would be reflected in the price of building stone products such as concrete, mortar or bituminous mixtures, and this, in turn, would affect the realizable price of the buildings. There would also be a deterioration of the environment, which would be enormously burdened by increased traffic, there would be more significant wear and tear on the transport infrastructure, which we would have to rehabilitate from public resources. This means that the mining industry is much more important for the economy and life of the Slovak Republic than is presented in the statistical data. It is certainly necessary to think about redefining the minerals for which fees are levied. Many mining activities, in particular gravel mining or building stone mining, which are not reserved for minerals but have a high environmental impact on the environment, should also be included among the minerals for which fees will be paid. On the one hand, a certain injustice would be eliminated, whereas, for strategic reasons, certain deposits of building stone or gravel have been classified as reserved deposits. Regarding the number of fees, as mentioned above, in comparison with neighbouring countries, the fees in Slovakia are lower and a certain adjustment upwards, in the event that the redistribution of recipients of fees is adjusted, such as, for example, in the Czech Republic, would certainly improve the permitting process for mining activities. The calculation of the fee for the extracted mineral, which gives room for certain creativity of accountants in mining companies, is also questionable, and the state mining administration, which controls these calculations, does not have enough professionally qualified inspectors to detect these tricks. The fee system in place in Poland or Hungary is certainly clearer and less sensitive to manipulation by mining companies.

Raw material security and rational use of mineral wealth

The role of the state is not only to protect the mineral deposit but should create the conditions for such deposits not to be speculatively blocked because then the state loses the benefits that it could obtain by actively using such deposits. Application of the concept of mineral deposits of public importance as to facilitate investment in similar way as for hydrocarbons but ensuring that mineral property rights are sufficiently protected. Slovakia is also relatively well geologically researched in comparison with the most developed countries in the world, and we do not expect to discover any deposit of world importance here. But the occurrences of some elements, which were included among the critical elements defined by the EC, we could

find here. In the past, these elements were not as important as they are today and were considered a pollutant rather than a useful mineral. Today, geological exploration is funded almost exclusively from private sources, but many investors are discouraged by the unstable legislative environment. Some changes in the law affect the significance of the results of geological work. As an example, we can mention the already mentioned Kurišková deposit or the gold deposit near Detva or Kremnica. We are of the opinion that the state, as the owner of mineral wealth, should care to have thorough information about mineral wealth and how it could benefit from it. The state should finance the geological survey from the state budget. The survey should focus on those critical raw materials defined by the EC. It should certainly be invested in a survey focused on the use of energy in the earth's core, where the Slovak Republic has great and hitherto untapped potential**.** All the above information has one common denominator, and thus there is insufficient legislation in the field of mining activities as well as fees associated with it**.** The update of the raw materials policy as of 31 December 2003 and the evaluation of the fulfilment of the objectives of this update as of 31 December 2018, i.e., after 15 years, brought conclusions that lead to the following conclusions.

The main objectives of the raw materials policy were the following:

• Liberalization and organization of the mineral market

Status: In 2003, there were no market barriers to the sale of mineral commodities.

• Coordination of the use of minerals in terms of their lifespan

Status: There is no legislation coordinating the use of minerals for their lifetime.

• Sustainable development of the company while at the same time the efficient use of domestic resources of mineral resources

Status: Declarative task, not implemented in any legislation.

• Reassessment of the methodology for classifying mineral resources according to the UN methodology.

Condition: Not implemented.

• Evaluation of mineral deposits, so-called feasibility study before their use, which will determine the value of the deposit for the investor as well as the state.

Condition: Not implemented.

• Stabilization of the workforce in regions with developed mining.

Status: Declarative task.

• Attenuation programs for unpromising mining industries.

Status: No attenuation program was adopted after 31.12.2003. A decline in mining activity and liquidation of the Baňa Dolina a.s.Veľký Krtíš (Government Resolution No. 1037/2001).

This evaluation of the main objectives of raw materials policy (as amended in 2003) shows that the objectives have not been met after 15 years. The objectives of the raw materials policy did not reach the implementation and realization through generally legally binding acts of the Slovak Republic. This suggests that such an understanding of raw materials policy is vague and legally ineffective. Raw materials policy is rather just an academic work that has no or almost no impact on minerals in the Slovak Republic. Even some of the measures that have been taken are at odds with raw materials policy, such as radioactive minerals. There is no mention of radioactive minerals in the raw materials policy or in its 2003 update. Nevertheless, an amendment to the Geological Act was adopted in 2013, where paragraph 24 a) was inserted. Unless raw materials policy becomes an integral part of the legal system of the state, its creation or updating is only an academic work, which has only a marginal influence on the real activity of the state, mining companies and the public. We dare say that whether or not we have a raw materials policy will not change in reality. In no legal Act of the Slovak Republic is the phrase Raw materials policy, no legal regulation refers to raw materials policy. In the Czech Republic, the Mining Act is in the comment procedure, which will directly refer to the raw materials policy. Such anchoring of our raw materials policy would certainly increase the seriousness of such a work, and politicians could no longer ignore it as it is now.

As we have already stated in the previous points, the last update of the raw materials policy is from 2004 as of 31.12.2003. This means that for 15 years no update has been made, resp. issued a new raw materials policy. This condition is definitely incorrect and has several reasons. Greater efforts were expected by the Ministry of Economy of the Slovak Republic, which is the creator and guarantor of previous raw materials policies. It was probably not enough political will to act more forcefully in this matter, which is certainly caused by the weak political influence of the miners, resp. excessive influence of conservation associations. Indeed, there could be a real risk that the raw materials policy, as part of the inter-ministerial commentary, would be subject to measures that would not be aimed at protecting and promoting the use of raw materials. Greater efforts should also be made by the professional public; if the state is not active in this matter, then the initiative should be taken by the one who is least satisfied with this situation. There are several professional organizations such as the Slovak Mining Company, the Slovak Association of Aggregate Producers or the Association of Metallurgy, Mining and Geology, which have the support of mining in Slovakia in their statutes. We also had stronger expectations from the academic community, which knew this situation and have enough experts to create a raw materials policy

model. Table 4 contains findings that are, in our view, critical for the raw materials policy of the Slovak Republic and the EU. Since we most areas in previous paragraphs devoted in the table to individual findings, adding the draft measures to eliminate the negative impact on the investigated area. We consider the solution of these areas to be key within the solution of the issue of mineral resources in the Slovak Republic. We are of the opinion that if these findings are not satisfactorily addressed, the situation with regard to minerals will not improve; on the contrary, the situation will worsen. Of these areas, we consider the following to be absolutely most important

- fees,
- energy raw materials.

If the fee policy does not change, the company's view on mining and mineral processing will not change either. Both the Slovak Republic and the EU have a high and even poorly diversified import dependence on energy minerals, which could have fatal consequences for our and the EU economy in the event of geopolitical tensions.

Table. 4. Critical areas of the raw materials policy of the Slovak Republic

Area	Detection	Proposal for measures
Binding nature of the raw material policy	The raw materials policy is not enshrined in any legally binding one document of the Slovak Republic if we do not consider the Resolution to be legally binding of the Government of the SR. Experience as shown that such legal force is for binding. Insufficient raw materials DO lies.	Secure the raw materials policy in the legal order of the Slovak Republic, for example, in the Mining Act, which would refer to the Raw Materials Policy.
Raw materials policy update	The raw materials policy has not been updated since 2003.	Continuous updating of the raw material policy as proposed by the National technology platform for research, development and innovation in the field minerals. Strategic goals they must have such legal force that they change will only be subject to broad society-wide professional discussion. To avoid frequent changes strategic objectives of the raw material policy, we propose its approval in parliament by a constitutional majority.
The long - term sustainable raw materials policy	Change in the laws that concerned minerals such as gold or radioactive minerals are not consistent with the current one raw materials policy. Laws protecting the environment they make it difficult but impossible to all objectives of raw materials policy.	To prepare a wide society discussion on the consensus between the use of the raw material potential of the state and environmental protection. Establish the agreement in the legislation of the state.
Energy resources	Currently, except the coal, there are almost no usable energy sources in Slovakia. Geothermal energy is a one of possible source, but under current conditions it has no legislative support or its use is hindered by trade agreements.	Reduce import dependence on energy raw materials by support renewable energy sources as well as rational use of their own raw- material resources such as uranium or geothermal energy. Brown coal as the only one currently in existence to protect the raw-material energy source as a strategic reserve.
Fee	Present policy fees settings for the use of the mineral wealth of the Slovak Republic is not optimal. From point of view of the negative consequences, which mining, processing, transportation serviceability during mining and processing minerals brings, are very low.	Simplify usage calculation mineral wealth and eliminate a differentiated approach to reserved and non-reserved the mineral. Amount of fees for mining areas as well as for extracted minerals is too low to be a more significant resource income. Recipients of fees should be above all those who are mining, and processing of minerals and with it associated traffic load, noise and dust loads and other negative factors the most load.
The position of the mining industry in society	The mining industry consists only negligible share in the GDP of the Slovak Republic. However, the importance of raw materials as a primary source for industries is underestimated. The public considers it their natural right to have access to raw materials. The problem is that they do not even think about the impact of mineral extraction on the environment.	It is essential to raise awareness to laic public about the importance of minerals for everyday life in modern society. How would the abandonment of the use of minerals affect the lives of every inhabitant of the Slovak Republic or the EU.

Rational use of mineral resources	The state protects mineral wealth through the Institute of Protected Deposit territory and the Mining Area. The state does not create an enough stable legislative environment for investors, which would be able invest to the geological survey. The state does not have effective tools to take away mining areas to organizations, which block them from speculative reasons..	The state should not only protect minerals wealth but also create appropriate conditions so that we can use mineral wealth rationally, of which would benefit all involved social groups. The state should invest m your own geological survey to have knowledge of raw- materials potentials that he would know then appropriately and in line with strategic interests of the Slovak Republic.

source: own processing

Conclusion

Raw materials policy must be a general consensus among all stakeholders involved in its creation. It must be a compromise between environmental protection and the need to secure minerals for the proper functioning of the state. The state, the people of the state and all participants in this process must benefit from this process. The safest access (safe raw materials) is to the raw materials that we can find in our territory, they are of sufficient quality, and we have enough of them. In the conditions of the Slovak Republic, limestone, dolomite, magnesite and building materials can certainly be considered safe minerals. The most dangerous (critical) approach is to raw materials that we do not have, but they are necessary for the functioning of society, and without these raw materials, we could not exist. In the conditions of the Slovak Republic, it can be said with certainty that all energy raw materials such as oil, natural gas, coal or uranium can be considered as these. The Slovak Republic is very vulnerable in terms of the need for these raw materials, without which life in Slovakia would have stopped and due to the fact that we import almost all these raw materials from Russia. Any political tension can cause the cessation of these supplies, and the Slovak Republic would, in the long run, find it very difficult to find a replacement for these supplies. By application of new legislative, we should also improve the transparency of information on raw materials through public reporting. This will allow prudent use of existing and future mineral deposits, as well as former mining site to be re-opened if appropriate and to contribute to developing monitoring systems on raw materials, flows and early warning systems on EU dependency on certain raw materials.

References

Aktualizácia surovinovej politiky SR; MH SR, http://www.economy.gov.sk/surovinova-politika-5672/127357s

Bednárová, L., Chovancová, J., Pacana, A., Ulewicz, R. (2018). The Analysis of Success Factors in Terms of Adaptation of Expatriates to Work in International Organizations. - Registrovaný: Web of Science, Registrovaný: Scopus. In PolishJournal of Management Studie. - Czestochowa : Faculty of Management, CzestochowaUniversity of Technology. ISSN 2081-7452, 2018, vol. 17, no. 1, pp. 59-66

Bednárová, L. et al. The Life cycle assessment of selected production in SimanPro V.7. - Registrovaný: Web of Science. In Geoconference on ecology, economics, education and legislation SGEM 2014. international multidisciplinary scientific geoconference. Geoconference on ecology, economics, education and legislation SGEM 2014: 14th international multidisciplinary scientific geoconference, 17-26 june 2014, Albena, Bulgaria. - Sofia: STEF92 Technology Ltd., 2014. ISBN 978-619-7105-19-3, pp. 479-484.

Cavender, B. (1992). Determination of the optimum lifetime of a mining project using discounted cash-flow and option pricing techniques. Mining Engineering, New York, 1992

Communication from the Commission to the European parliament, the council the European economic and social committee and the committee of the regions tackling the challenges in commodity markets and raw material, Brussels, 2.2.2011, Retrieved from https://eur-lex.europa.eu/legal-content/SK/TXT/HTML/?uri=CELEX:52011DC0025&from=EN

Critical raw materials, Critical Raw Materials Alliance c/o Ridens Public Affairs | Rue Belliard 40, 1040, September 2018, Brussels , Retrieved from https://www.crmalliance.eu/circular-economy-environment

Colving, R.M., Witt, G.B., Lacey, J. (2015) The social identity approach to understanding socio-political conflict in environmental and natural resources management. Global Environmental Change, vol. 34, p. 237-246

Decleris, M. (2000). The law of sustainable development , General priciples, Luxembourg: Office for Official Publications of the European Communities, 2000 ISBN 92-828-9287-5https://www.pik-potsdam.de/avec/peyresq2003/talks/0917/sillence/background_literature/sustlaw.pdf

Dorian. J.P., Humphreys, H.B. (1994). Economic impacts of mining A changing role in the transitional economies, https://doi.org/10.1111/j.1477-8947.1994.tb00869.x

Gentry, D.W., O'Neil, T.J. (1984). Mine Investment analysis. Soc. of Min. Engineers of. Am. Inst. of Min., Metall., and Petroleum Engineers. New York 1984, p. 502

Gray, J. (2018). A global update on the ambit of unconventional gasmining and analternative framework for mediating energy demands. Ecological Integrity, Law and Governance, p. 119-128.

Grincova, A., Andrejiova, M., Marasova, D., Khouri, S. (2019). Measurement and determination of the absorbed impact energy for conveyor belts of various structures under impact loading, Volume: 131, Pages: 362-371, DOI: 10.1016/j.measurement.2018.09.003, JAN 2019

Hajduová, Z., Lacko, R., Mildeová, S., Stričík, M. (2015) Case study in the field of innovation in selected companies in Slovak Republic. In: Scientific annals of the Alexandru Ioan Cuza University of Iasi: Economic sciences. - Poland : De Gruyter, 2015. ISSN 2068-8717, vol. 62, no. 1, pp. 103-199 online.

Jurkasova, Z., Cehlar, M., Khouri, S. (2016). Tools for organizational changes managing in companies with high qualified employees, Pages: 409-412, CRC PRESS-TAYLOR & FRANCIS GROUP, 6000 BROKEN SOUND PARKWAY NW, STE 300, BOCA RATON, FL 33487-2742 USA,

Khouri, S., Cehlar, M., Horansky, K., Sandorova, K. (2017). Expected life expectancy and its determinants in selected European countries. Transformation in Business and Economics, vol.16, No 2B, p. 638-655.

Kúšik, D., Mižák, J., Šoltes, S. (2017). Nerastné suroviny SR. Slovak minerals yearbook 2017; © Štátny geologický ústav Dionýza Štúra 2018. ISBN 978-80-8174-037-4

Mendel, J., (2019): Stratégia využívania zemských zdrojov SR z pohľadu Surovinovej politiky EÚ v rámci, Dissertation thesis

Natura (2000). Legislation. Available at: http://www.sopsr.sk/natura/index1.php?p=3&lang=sk

Pelaudeix, C., Basse, E.M., Loukacheva, N. (2017) Openness, transparency and public participation in the governance of uranium mining in Greenland: A legal and political track record. Polar Record, vol.53, No 6, p. 603-616.

Pickett, S. and McDonnell, M. (2017). The art and science of writing a publishable article. Journal of Urban Ecology, 3(1).

Rybár, P, Cehlár, M., Engel, J., Mihok, J. (2005) Evaluation of mineral deposits, AMS, FBERG, TU Košice, 2005

Straka, M., Lenort, R., Khouri, S., Feliks, J. (2018). Design of large-scale logistics systems using computer simulation hierarchic structure. International Journal of Simulation Modelling, vol.17, No 1, p.105-118

Straka, M., Cehlar, M., Khouri, S., Trebuna, P., Rosova, A., Malindzakova, M. (2016). Asbestos exposure and minimization of risks at its disposal by applying the principles of logistics, Przemysl Chemiczny in 2016. vol 95., issue 5, p.n963-970doi.org/10.15199/62.2016.5.13

Šimková, Z., Očenášová, M., Tudoš, D., Róth, B. (2019). The political frame of the European Union formining of non-energetic raw materials, Acta Montanistica Slovaca Volume 24, number 1, 35-43 ISSN 1335-1788

Surovinová politika ČR v oblasti nerostných surovin a jejich zdroju, Ministerstvo průmyslu a obchodu ČR; http://www.ospzv-aso.cz/addons/114%20RHSD/2014-11-21-Surovinova-politika.pdf

Strategic implementation plan for the European innovation partnership on raw materials, part II –priority areas, action area and actions 18/09/2013 Retrieved from https://ec.europa.eu/growth/sites/growth/files/eip-sip-part-2.pdf

Strategic Dialogue on Sustainable Raw Materials for Europe, STRADE November 2018, Retrieved from https://www.stradeproject.eu/index.php?id=3

Study on the review of the list of critical raw materials. Critical raw materials facts sheets. Written by deloitte sustainability, British geological survey, Bureau de rechercheséologigues et miniéres, Netherlands organization for applied scientific research, June 2017; ISBN 978-92-79-72119-9. © EÚropeanUnion

Trade, Growth and World Affairs: Trade Policy as a Core Component of the EU's 2020 Strategy; European Commission, 2010, 8

Zimon, D., Gajewska, T., Bednarová, L. (2016). An Influence of quality management system for improvement of logistics distribution. - Registrovaný: Scopus. In Quality - Access to Success. - Bucharest: Society for Quality Assurance - SRAC, 2016. ISSN 1582-2559, 2016, vol. 17, no. 155, pp. 60-672017

XV. Odborný seminár SZVK; Zborník prednášok; str. 31 - 42; Atrium hotel, Nový Smokovec 42; Vysoké Tatry; 24. – 25.10.2013

Acta Montanistica Slovaca
ISSN 1335-1788
actamont.tuke.sk

Examples of secondary online data for raising awareness about geo and mining heritage

Csaba SIDOR[1], Branislav KRŠÁK[2], Ľubomír ŠTRBA[3], Ján GAJDOŠ[4], Adriana ŠEBEŠOVÁ[5] and Jana KOLAČKOVSKÁ[6]*

Authors' affiliations and addresses:
[1,2,3,4,5,6]Department of Geo and Mining Tourism, Institute of Earth Resources, Faculty BERG, Technical University of Košice,
Letná 9, 042 00 Košice, Slovakia
e-mail : csaba.sidor@tuke.sk[1]
e-mail : branislav.krsak@tuke.sk[2]
e-mail : lubomir.strba@tuke.sk[3]
e-mail : jan.gajdos@t-systems.com[4]
e-mail : adriana.sebesova@vucke.sk[5]
e-mail : jana.kolackovska@tuke.sk[6]

***Correspondence:**
Csaba Sidor, Department of Geo and Mining Tourism, Institute of Earth Resources, Faculty BERG, Technical University of Košice, Letná 9, 042 00 Košice, Slovakia,
Tel.: +421 55 602 3298
e-mail : csaba.sidor@tuke.sk

Acknowledgement:
This work was supported by the Slovak Research and Development Agency under contract no. APVV-14-0797.

How to cite this article:
Sidor, C., Kršák, B., Štrba, Ľ., Gajdoš, J., Šebešová, A. and Kolačkovska, J. (2020). Examples of secondary online data for raising awareness about geo and mining heritage. *Acta Montanistica Slovaca*, Volume 25 (1), 116-126

DOI:
https://doi.org/10.46544/AMS.v25i1.11

Abstract
The paper analyzes the potential of secondary spatial data and online user-generated content. Special focus is dedicated to social networks and travel platforms, respectively their open application programming interfaces as tools for using third party platforms with the combination of open machine-readable data for raising awareness about geo and mining heritage. Existing good practise within harvesting of open access machine-readable data from the social network Facebook, the hybrid map service Google Places and the travelers' application Foursquare was used for constructing the current partial online image of the Zemplín geopark as a selected example area with a higher density of geosites and objects of mining heritage. Subsequently, based on the pilot results, the harvested data's suitability was analyzed for both tourism services' consumers' satisfaction and geosites' visitors' experiences' monitoring, and the creation of feedback for selected geological and mining heritage points of interest. Even though the current volumes of records representing geosites and mining heritage within the analyzed platforms are low, the results could help to strengthen the relationship between tourism service providers and geosites as an essential part of primary resources within the shared online communication environment.

Keywords
Geosites, geotourism, open-access data, machine-readable data.

Introduction

The necessity to integrate continuous collection and analysis of own, open and big data into destination management organizations' planning and decision-making processes for establishing destination knowledge structures has been in the scope of several types of research (Ritchie and Ritchie, 2001; Baggio and Caporarello, 2005; Ritchie and Ritchie, 2001; Chang and Liao,2010; Baggio and Cooper, 2010; Fuchs et al.,2011; Xiang et al., 2014; Fuchs et al., 2014; Sabou et al.,2016). In general knowledge infrastructures were defined by Edwards et al. (2010) as *"robust networks of people, artefacts, and institutions that generate, share, and maintain specific knowledge about the human and natural worlds"*. In terms of tourism knowledge structures, data may be considered as a central asset in destination management (Pesonen and Lampi, 2016).

The European Commission (2011) based on the Digital Britain report, acknowledged data as the knowledge economy's currency. The role of data in tourism knowledge management has been recognized for several years. The issue of monitoring tourism and its sustainability has been a topic for over two decades. Fuchs's et al. (2014) pointed out the fact that for a long-time, sustainable tourism used to be misused as a political catchphrase with several definitions but remaining a blurred concept. Delaney and MacFeely (2014) and many other emphasizes that consumption and expenditure in tourism are dispersed across a wide range of industries: transport, accommodation, catering, entertainment, culture, sports, and other related services. Not only at the destination level, but in general, tourism statistics have become consequently difficult to compare with other economic sectors (Delaney and MacFeely, 2014). Ionescu (2014) pointed out another issue that there are cases of inappropriate use of tourism indicators or without combinations of related indicators. Thus, the results of the analysis are put out to the danger of inconsistency. Quantifiable data has become an essential asset not only in destination management but also in the processes of conducting evidence-based policies impacting tourism. Already in 1995, concepts of Tourism Satellite Accounts were designed to increase and improve knowledge of tourism's relationship to overall economic activities at the level of member states (UNWTO, 2008). At present, national partial tourism data, data from related industries, data about related social a demography aspects of EU member countries are open and accessible at Nomenclature of Territorial Units for Statistics (hereinafter NUTS) levels 1 - 3 level (European Union, 2017). For local destinations represented by destination management organizations (hereinafter DMO) uniting local public and private stakeholders operating at district (hereinafter LAU 2) levels, this data is only partially usable. There have been efforts with the aim of building knowledge structures based on down to top principals using information and communication technologies (hereinafter ICT) and data mining methods to fill the gaps at local destination management. Examples of tourism intelligence systems may be identified all across Europe. The Swedish DMIS for advanced observation of destination Åre, the TourMIS Austrian marketing information system for tourism managers, European Travel commission's dashboard demonstrate the power of reliable data in destination management (Fuchs et al., 2015; Sabou et al.,2016; ETC, 2017).

Due to tourisms' nature, most of the related industries' products cannot be tested (for example, accommodation, meal, ride in an amusement park etc.), online feedback has become one of the main factors within potential visitors' decision making. With 2.6 billion active monthly users, the social network Facebook may be considered as the global environment for creating user-generated content (Clement, 2020). The Google search engine covering more than 60 % of all monthly desktop searches worldwide, is the global leader for online information distributing (Netmarketshare, 2020). For the above mentioned, Google and Facebook may be considered the essential platforms for the monitoring of customers' level of satisfaction and other points of interests' visitors' experiences. Service providers within tourism are capable of communicating the content of their products via their own or secondary communication channels. Without active marketing of geo and mining heritage carried out by local administrators as destination managements organizations, protected areas' management organizations, museology institutions or local governments, the content of these objects is primarily distributed by visitors communicating their experience within their communities or via online user-generated content (hereinafter UGC) concentrated on social media, and travel & tourism related platforms. While orally communicated experiences of visitors are recorded by the person receiving the information, open access UGC may be used for continuous monitoring of both tourism services' consumers and visitors of geo a mining heritage points of interest. Tourism service providers are dependent on primary tourism resources, which, to a large extent, comprise of geological heritage and state of the landscape. In terms of Slovakia's mining history and its anthropogenic results, objects of mining heritage contribute to the total value and potential of primary tourism resources in several local areas. For the relationship between the tourism industry and primary resources to result in natural and sustainable tourism development, it is necessary to work with both local economy data and data related to geo and mining heritage (Newsome and Dowling, 2018).

The global aim of the paper is to analyze the usability of open governmental data with the combination of social media and travel & tourism related web applications' data accessible via open application programming interfaces (hereinafter open API) for raising awareness about and monitoring of points of interests related to geosites and objects of mining heritage.

Materials and Methods

The protection and preservation of natural objects or landscapes and their attributes as geological structures or relief form as parts of global heritage are essential for future generations' opportunity to study planet Earth's geological history and admire nature's astonishing beauties (Štrba a Rybár, 2015). Covering several aspects of this issue, as geology, geomorphology, tourism, management, and economy, the most complex approach may be found in the concept of Geotourism (Štrba a Rybár, 2015). In terms of Geotourism, an object with a certain potential for Geotourism is referred to as a geosite (Reynard, 2008; Bujdosó a kol., 2015; Štrba a Rybár, 2015). More specifically, Štrba & Rybár (2015) define geosites as geological or geomorphological objects, that have achieved scientific, cultural, historical, esthetic, or social-economic value due to human perception or use.

Mining tourism resources connect aspects of industrial, technological, cultural, and ethnographic heritage into a cognitive educational and experiential form of tourism (Rybár, 2013). Różycki & Dryglas (2017) indicate a missing unified agreement within the academic community, whether mining tourism is identical to industrial tourism. While industrial tourism mainly relates to the industrial nature of the visited object or area, mining tourism covers several aspects related to the mining industry (Różycki & Dryglas, 2017). According to Rybár (2013), the variety of mining heritage relevant within mining tourism are objects and phenomena that provide to see and get to know:

- mining technologies,
- processes explaining mining and raw material processing,
- historic mining objects,
- stories of historical personas with a significant impact on the mining industry,
- mining traditions (Rybár, 2013).

Mihalič (2013) focusing on environmental resources' performance in destinations has identified several approaches and perspectives of tourism resources' categorization. Some authors emphasize environmental attractions and attractors as primary resources and tourism services as supportive resources; some distinguish primary resources as non-reproducible and secondary as reproducible (Tisdell, 1991; Ritchie and Crouch, 2003). From these perspectives, among primary tourism potential may be included natural preconditions and socio-cultural results of anthropogenic activities (Mihalič, 2013). In terms of tourism resource categorization, both geo and mining heritage may be placed among primary resources. Geological heritage objects can be classified as natural tourism resources, and geological processes as primary preconditions (climatic, geomorphological, hydrogeological). Objects of mining heritage may be assigned to anthropogenic sources (technical and industrial objects, museums) and intangible aspects related to the traditions of mining to cultural and social events.

Štrba et al. (2018) within their comparison of nine methods of assessing geosites identified intersections among indicators binding to objects' uniqueness, conservation status, economic potential, added anthropogenic and cultural value, accessibility, added functional value, representativeness, vulnerability, ecological value, level of protection and observation conditions. While the above-mentioned indicators were identified in more than half of the methods, less than half of the methods used indicators related to information availability, distance from tourist centres, nature of the surrounding country, visiting rates, marketing, road infrastructure, traffic capacity, and educational value. One of the methods within the comparison, constructed by Štrba and Rybár (2015), focuses comprehensively on the evaluation of geosites both in terms of scientific value and in terms of tourism (in the form of geotourism) and its marketing. Within their method, one object is evaluated in ten categories, but the maximum value of the criteria in individual categories is identical. This way, the maximum value of criteria such as physical accessibility, availability of information, relevance for tourism, the value of the services provided is in balance with the criteria tending more to scientific and environmental value.

For geoheritage conservation, education, and geotourism in an area a geopark may be established. The United Nations Educational, Scientific, and Cultural Organization (hereinafter UNESCO) defines geoparks as a nationally-protected area containing many geological heritage sites of particular importance, rarity or aesthetic appeal, that operates as an integrated concept of protection, education and sustainable development (UNESCO, 2006).

Based on the report of the Office Government of the Slovak Republic (2016) about the Zemplín area's potential of inclusion among geoparks, the Zemplín Geopark is located in the southwest of the Trebišov district. In the core of the area arises from the Tokaj wine region in Tokaj hills. In the southern part and the western part, the geopark borders the Hungarian part of the Tokaj wine region, and in the north, it borders the Zemplín Hills (see Figure 1). In the eastern sector, the river Ondava flows into the river Bodrog, which further flows across the southern sector of the territory (see Figure 1). Within the scope of the paper, the report's third annexe containing the area's passport from the perspective is essential. The passport contains 80 localities comprising from 3 archaeological sites, 22 geosites, 19 mining heritage objects, 5 historical and 10 cultural-historical landmarks, 4 recreation zones, and 7 objects related to viticulture. All of the objects may be considered as points of interest. Most of the objects are in the core of the geopark in the Tokaj Wine Region. On the other hand, almost half of

the geosites are located on the outskirts of the geopark in the village of Brehov. According to Kršák et al. (2017), the essential density of water elements in the form of 4 rivers, numerous wetlands, abandoned meanders and other water structures, resources of water tourism could become in the case of meaningful cooperation between the geopark, officials and local stakeholders the areas' future building block of sustainable tourism development. From their perspective, the Somotor channel comes as an interesting potential waterway connection between the core and east part of the theoretically extended geopark (Kršák et al., 2017).

Several examples of online UGC's use within tourism research may be found from all around the world. Dolan et al. (2019) used the Qantas airline's reviews at Facebook for identifying, categorizing, and analyzing patterns in customers complaining practices from the perspective of a brand's co-creation and co-destruction. Within a combination of textual and feedback and user demographics extracted from data related to check-ins via Facebook at points of interest, Kerson et al. (2017) created personalized itineraries. Based on UGC and check-ins data from Foursquare, Aliandu (2015) used Naive Bayes probabilistic classifiers for analyzing sentimental values of visitors' feedback Kupang, Indonesia. Chorley et al. (2013) analyzed the visitors' personas from the perspective of conscientiousness, extraversion, friendliness, and neuroticism on a sample of 173 globally active Foursquare users. De Vries (2013) used live user data recorded by Google Places for identifying and monitoring user hotspots. Other authors focus on web data scraping techniques from tourism-related platforms without and open application programming interface as Booking and TripAdvisor. Silva et al. (2018) identified spatiotemporal patterns in the Hospitality based on ad-hoc routines for web data extraction over aggregations of point-based grids. The Python-based Scrapy framework was used for extracting user feedback from Booking and TripAdvisor with the aim of conducting sentimental analysis over textual user comments (Martin-Fuentes et al., 2018)

Since data representing points of interest at social media and travel & tourism platforms are registered mostly by tourism service providers for marketing purposes or by visitors sharing online their experience, the availability of open access governmental data related to geo a mining heritage is essential. In the case of Slovakia, the most complex in the field is the State Geological Institute of Dyonýz Štúr's (hereinafter ŠGÚDŠ) web services accessing data mapping significant geological localities, old mining sites, and geomorphological areas.

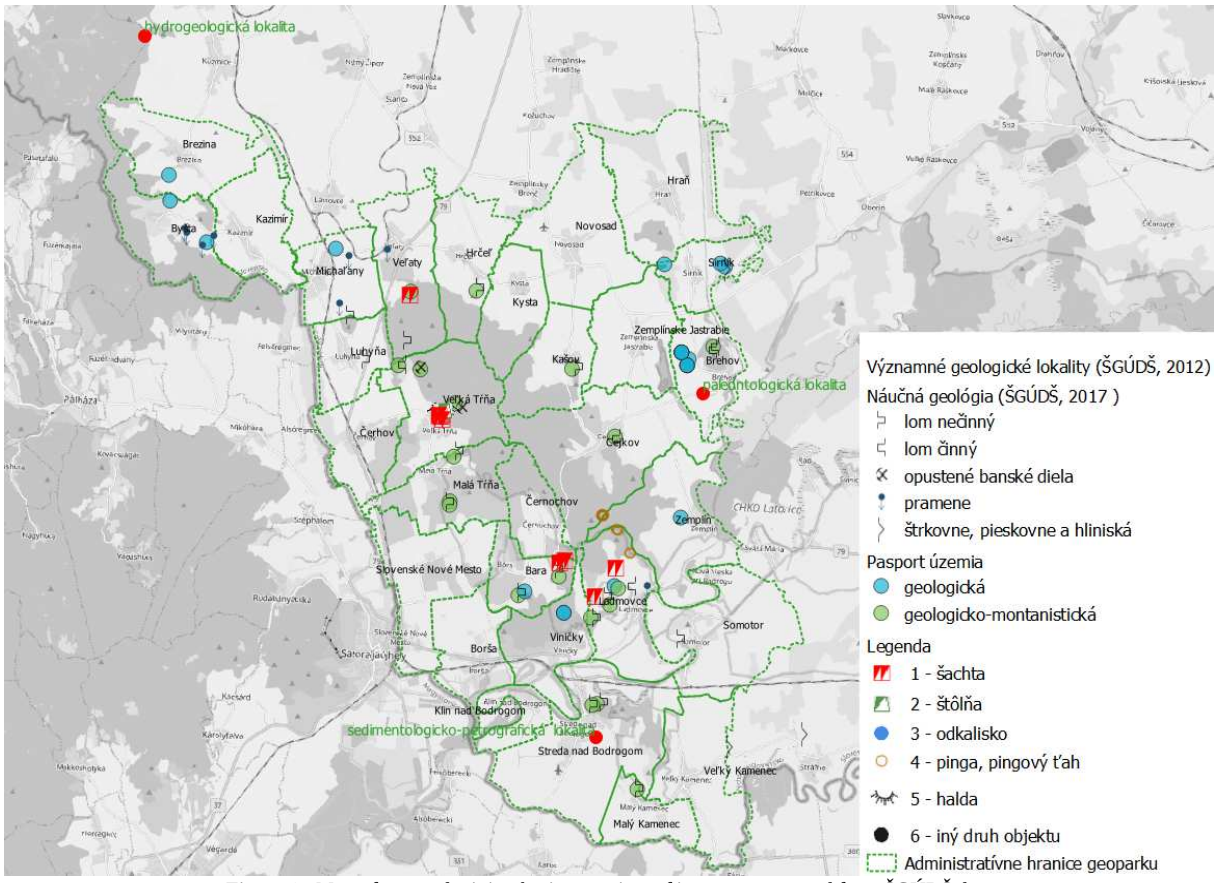

Figure 1. Map of geo and mining heritage points of interests extracted from ŠGÚDŠ data

ŠGÚDŠ's datasets were used as professionally selected input data for spatial representation of geological and mining heritage from experts the point of view (See Figure 1). Besides the above mention report's passport

wast processed into a structured format projection via vector layers (See Figure 1). Most of the mentioned and other related research used third party applications as Ncapture, Netvizz, LikeAlyze a Karma for extracting UGC, which has limits in terms of geographical coverage. Sidor et al. (2019) within their effort to identify service providers with an obligation towards local occupancy taxes created a simple reusable way to extract data from Airbnb, Booking, Facebook Places, Foursquare, Google Places, and TripAdvisor.

For the paper's aim, the Sidor et al. (2019) method was used to create a radial grid layer (1 point per 1000 meter) over the area of the Zemplín geopark (See Figure 2). The points of the layer were further used for making extraction calls to Facebook Places Graph API, Google Places API, and Foursquare Venue API. For the purposes of semi-automatic data extraction, a simple radial based loop in Python connected to the relevant APIs was used. Afterwards, according to the data providers category and type identifiers, records relating to primary natural and anthropogenic tourism resources were separated and aggregated from the users' interactions. Afterwards, the walking accessibility of the geosites and objects of mining heritage enlisted within the above-mentioned passport, from a sample of Points of interest with a higher volume of interactions was tested in the environment of the Google Distance Matrix API.

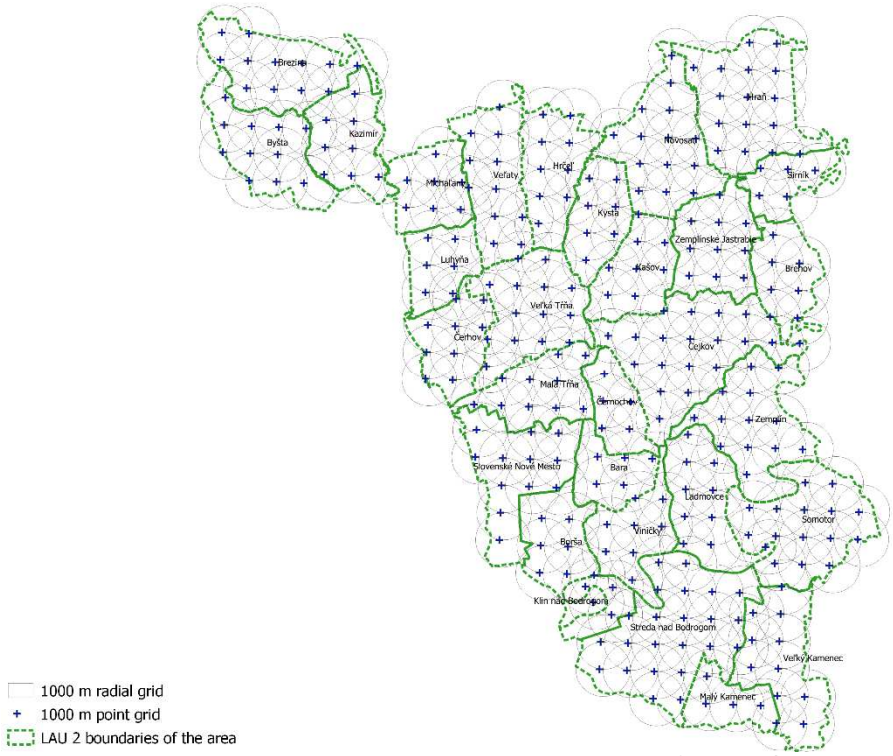

Figure 2. Radial grid layer over the boundaries of the Zemplín geopark

Results and Discussion

Within the examination of ŠGÚDŠ's map service, additional records of geo a mining heritage were identified (See Figure 1). The data set named *Significant geological localities* contained one object representing a paleontological locality in the Brehov municipality and a sedimentological and petrographic locality in the municipality of Streda nad Bodrogom. Within the ŠGÚDŠ map server, a data set named *Educational geology – Zemplín hill also* containing records of geosites (8 springs, 2 gravel pits - sand pits - clay pits) and mining heritage (5 active quarries, 2 abandoned mining works, 14 idle quarries) with the are of the geopark was identified. Most objects are concentrated in the municipalities Ladmovce (4), Byšta (4), Michaľany (3), Veľká Tŕňa (3). Other municipalities contain two objects (Veľaty, Brehov, Streda nad Bodrogom, Malá Tŕňa, Bara or one (Sirník, Kašov, Somotor, Malý Kamenec, Veľký Kamenec, Hrčeľ, Cejkov). In another data set of the institute named *Old mining sites*, 29 objects were identified, comprising ping moves (15), shafts (10), tunnels (2), and heaps (2). Most objects are concentrated in the municipality of Cejkov (10), followed by the municipalities of Veľká Tŕňa (9), Ladmovce (7), Bara (2) and Veľaty (1). Based on the attributes of the objects, it can be stated that none of the objects needs to be physically remediated.

From the 324 extracted objects within the area of the geopark, extracted from Facebook Places Graph API, 104 records contained actual rating, with an average of 11 ratings per object and an average rating of 4.65. In terms of tourism resources categorizing, 38 objects had a category identifier belonging to Hospitality, 27 of them contained an actual rating with an average of 26 per object and a 4.75 average rating. While most objects are

highly rated, only two of them have more than 100 ratings. In the case of natural and anthropogenic tourism resources, 28 objects were identified, from which only 3 were rated. One of the objects, the complex of tuff wine cellars in Malá Tŕňa may be considered as an object of mining heritage (See Figure 3).

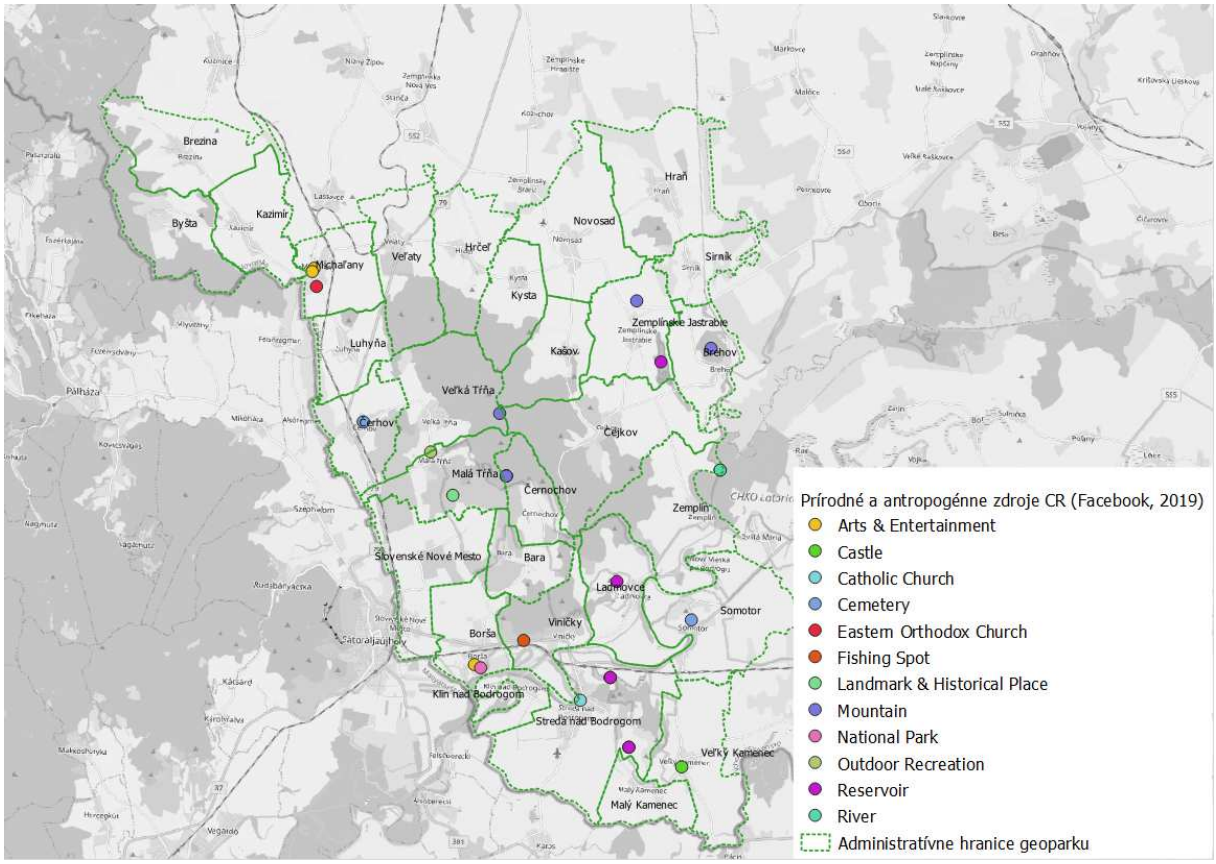

Figure 3. Map of natural and anthropogenic POIs extracted from Facebook Places Graph API

From the perspective of user check-ins, 186 objects elicited a user reaction, with an average of check-ins pre objects. Logically, most check-ins contained records of municipalities. Tourism service providers average 422 check-ins per object, most of them were recorded at cafes, lodging and restaurants as Espresso Bodrog (3192), Zlatá Putňa Restaurant & Pension (2448), TOKAJ MACIK WINERY (2188), Chateau GRAND BARI (1377), Korona Étterem (1274), Penzion Aqua Maria (1240). Objects of natural and anthropogenic resources average 195 check-ins per record. Concerning the number of "likes" and check-ins (See Figure 4), the best results were achieved by the Tokaj Lookout Tower, an unnamed point in the village of Hraň, Rákoczi castle in Borša and the castle in Veľký Kamenec.

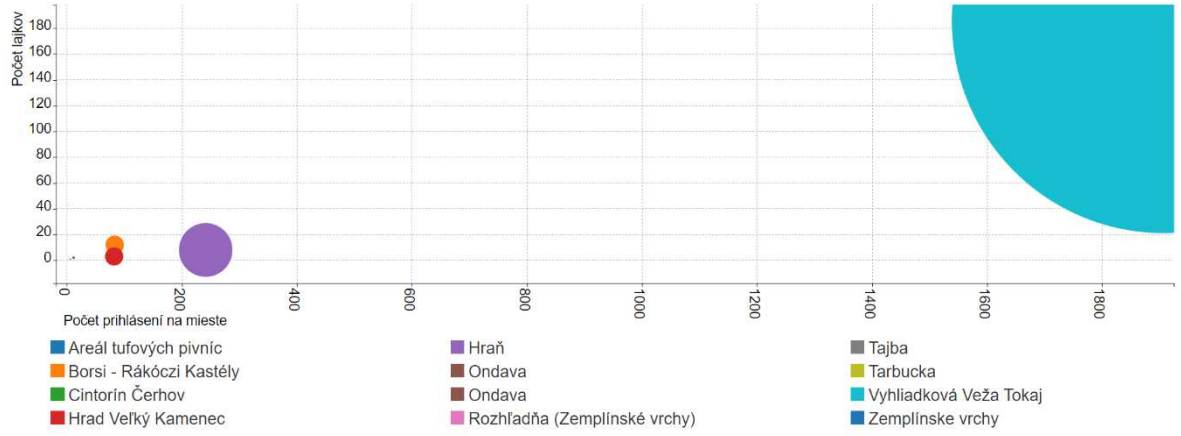

Figure 4. The ratio of the number of check-ins and likes of natural and anthropogenic objects within Facebook Places Graph API

Of the 305 Google Places objects identified in the geopark, 120 had an actual rating, on average 14 ratings per object, and an average rating of 4.2. From the total number of objects, it was possible to unambiguously assign 17 records to tourism service providers, of which 12 had an actual rating, with an average of 89 ratings per object and an average rating of 4.4 points. While most objects have a high average rating, only 2 objects have more than 100 ratings, namely Zlatá Putňa - Restaurant & Pension (540.0) and Korona Restaurant (315.0). Within natural and anthropogenic tourism resources, it was possible to unambiguously identify 14 points of interest according (See Figure 5), of which 8 were rated (average of 121 ratings with an average rating of 4.65). One object represents geological or montane heritage (Mineral spring in the municipality of Ladmovce with one 1 rating). In terms of the ratio of the number of ratings, the criteria above 100 ratings, were met by three identical objects as in the case of Facebook Places Graph API, namely the Observation tower Tokaj (572.0), Mansion F. Rakoczi II. (213.0) and Veľký Kamenec Castle (173.0) (See Figure 6). Other evaluated objects reached below the number of five ratings.

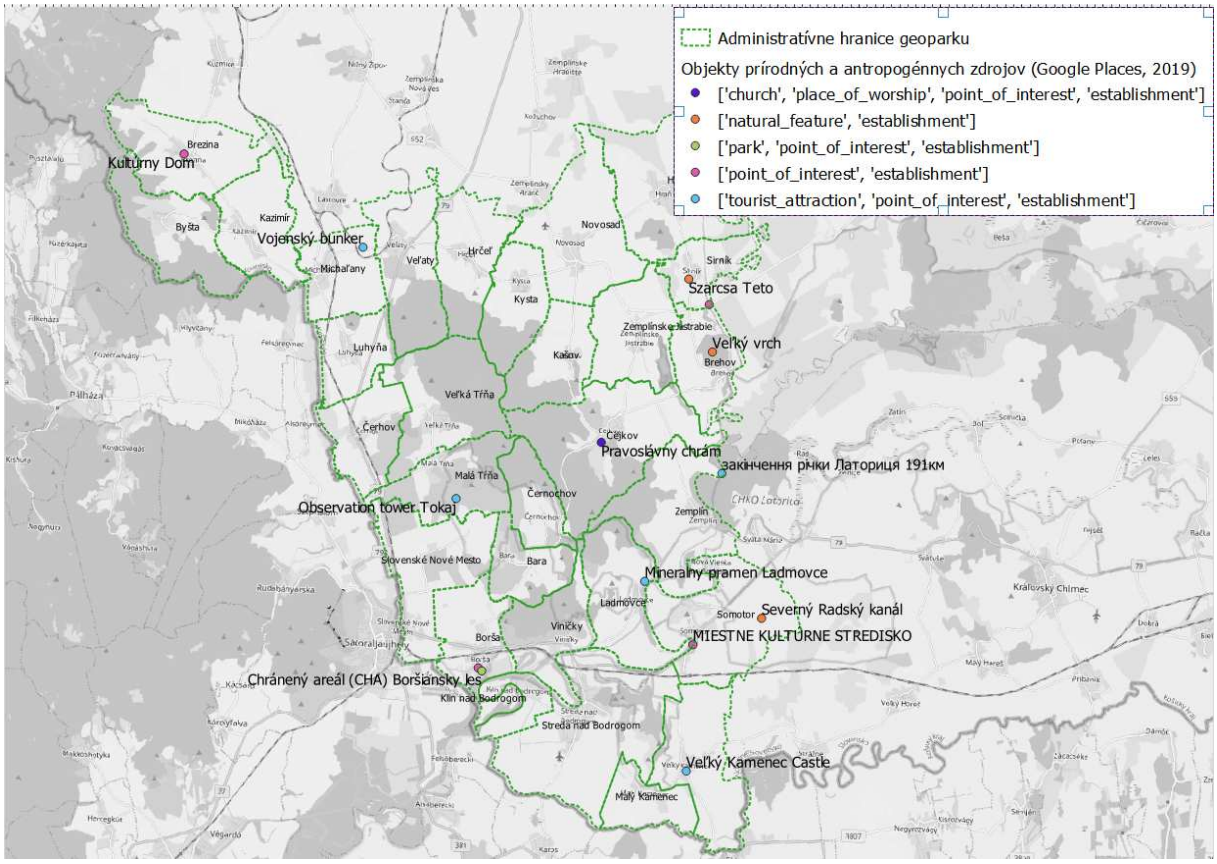

Figure 5. Map of natural and anthropogenic POIs extracted from Google API

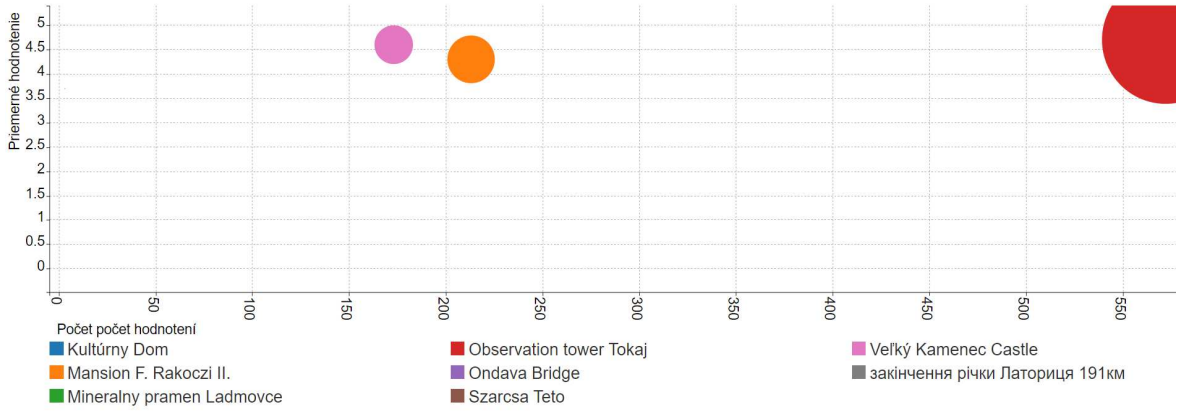

Figure 6. The ratio of the number and average evaluation of natural and anthropogenic objects within Google Places API

Within the Foursquare Venue API, only 35 objects were identified in the area, of which 18 objects could be assigned to tourism service and only 7 objects related to natural and anthropogenic tourism resources (See Figure

7). In both cases, the objects showed mostly zero feedback values or very low values. One facility within the Hospitality sector generated 19 on-site check-ins (Tokaj Macik Winery) with a high average rating (8.1 out of 10), and the area's dominant in the form of the Lookout Tower achieved 7 on-site check-ins with a rating of 7.8 points.

Foursquare is actively used by almost 15 million travellers globally each month. The low level of feedback on the platform may be subjectively caused by the use of the Foursquare application mainly by users from countries that cannot be objectively included among the main markets of inbound tourism in the Košice region, except the United Kingdom with a 2.2% share of the application.

Figure 7. Map of natural and anthropogenic POIs extracted from Foursquare Venue API

Due to a higher concentration of user-generated content (check-ins, ratings) at the social network Facebook, the top 5 objects, in terms of check-ins on the spot were selected for pilot testing (See Table 1). Three of the five objects are accommodation services providers, and all five are part of the Hospitality sector. Thus, it may be assumed that their main target groups consist of tourists and one day visitors. Since the database of the Google Distance Matrix currently does not contain walking routes (cycling or hiking trails, sidewalks) between the selected objects of geo & mining heritage and the pilot set of objects representing Hospitality stakeholders, generalized road routes within 5 km distance were used.

The basic results (See Table 1) of the distance test indicate that three of the Hospitality stakeholders are relevant in terms of geo and mining heritage objects' density and user interactions at Facebook. The Espresso Bodrog café with over 1000 check-ins is situated near 2 geosites (visible structures of Perlit and volcanic glass) and 5 mining heritage (abandoned quarries and quarries used as wine cellars) POIs with an average distance of 3.43 km. However, the disparity between a higher number of check-ins and a low number of ratings (0.01 rating per check-in) may indicate that café is a hotspot for local communities. The highest density of geo & mining heritage POIs within 5 km was identified at the Zlatá Putňa Restaurant & Pension in the municipality of Viničky. The restaurant (0.08 rating per check-in) is situated within the limit to 5 mining POIs (4 quarries and unmined perlite bearing) and 2 geosites (sites of volcanic glass and obsidian). The Tokaj Macik Winery providing also accommodation services (0.04 rating per check-in) is situated within the limit to 5 abandoned quarries. The winery itself has an underground system of historic wine cellars in its immediate vicinity, which may also be considered as an object of mining heritage, and also is closest to the geopark's iconic watchtower. The other tested objects did not achieve relevant results.

Table 1. Basic results of the distance test of Facebook POIs and geo & mining heritage

Name	Municipality	Number of check-ins	Number of ratings	Average rating	Number of geo & mining POIs in 5 km	Average distance (km)
Espresso Bodrog	Streda nad Bodrogom	3192	20	4.8	7	3.43
Zlatá Putňa Restaurant & Pension	Viničky	2448	207	4.8	8	3.75
TOKAJ MACIK WINERY	Veľká Tŕňa	2188	78	4.9	5	2.28
Chateau GRAND BARI	Slovenské Nové Mesto	1377	23	4.8	3	2.63
Korona Étterem	Veľký Kamenec	1274	108	4.9	1	2.8

Conclusions

Overall the largest volume of objects was identified at Google Places (500) and Facebook Places (456). In terms of user interactions, with an overall average of 200 check-ins per object, Facebook Places may be considered the most suitable for pilot communication of the 80 points of the interest from the geopark's passport. Additionally, the 29 objects identified within ŠGÚDŠ's dataset on old mines are for consideration of further examination as suitable points of interest.

Due to the landscape of the area (large areas of vineyards and meadows), most walkable trails to objects of geo & mining heritage is not recorded by web map applications as Google Maps or Apple Maps. This may lower the overall experience of a visitor or a geotourist, in order to not to flood the geopark's online environment with geo and mining heritage objects at once. The first reasonable step should be to assess the objects from the geopark's passport by the methodology developed by Štrba & Rybár (2015). Afterwards, the paths to most relevant objects' should be at least uploaded to Google Maps. For both practical and research purposes, the objects of geo a mining heritage within the passport of the area should be updated as points of interest in all three platforms. Firstly, to raise awareness about their existence and accessibility among users of the examined platforms. Secondly, to generate a critical mass of user-generated content and feedback that could reach a wider online audience. Thirdly, to create an opportunity for administrators of both the Tokaj Wine Region destination and Zemplín geopark to monitor both tourists and geotourists satisfaction and feedback. If the objects related to geo and mining heritage were to be registered under the account of one of the administrators of the area, additionally all textual feedback (users' written review) at the platforms could be extracted for implementing methods of sentimental analysis.

The possible issue of visitors in environmentally vulnerable areas and their irresponsible presence in private vineyards must be addressed by the public authorities and local administrators. Even though the areas are publicly accessible via officially marked trails, continuous on-site informing of visitors about correct behaviour towards the local environment, communities and their properties is an essential part of developing sustainable forms geotourism.

Since none of the platforms' categorization of objects contains identifiers as geosite or mining heritage, the use of appropriate combinations should be reasonable. For Google Places, it could be suitable to use a unified list of identifiers *["tourist_attraction", "point_of_interets", "natural_feature"]*, but with different keywords as geosite, mining, spring etc. For Facebook Places Graph API the identifier *"TOURS_SIGHTSEEING*" and for Foursquare Venue API the list *["Nature Preserve", "Scenic Lookout", "Other Great Outdoors"]* could be sufficient enough for the initial registration of the objects.

Even though data and feedback on geo and mining heritage sites in the examined area of Zemplín geopark were significantly absent, the results prove that monitoring of both satisfaction in the tourism sector and monitoring of experiences from visiting geo and mining heritage points of interest is possible by methods of continuous machine extraction of data from the social network Facebook, web application Google Places and travel platform Foursquare.

References

Baggio, R., Caporarello, L. (2005). Decision Support Systems in a Tourism Destination: Literature Survey and Model Building. In Proceedings of itAIS 2005, 2nd Conference of the Italian Chapter of AIS. Available at http://www.iby.it/turismo/papers/baggio-dss-tourism.pdf (Accessed December 31, 2019)

Baggio, R., Cooper, C. (2010). Knowledge transfer in a tourism destination: The effects of a network structure. In The Service Industries Journal 30(10). https://doi.org/10.1080/02642060903580649

Bujdosó, Z.; Dávid, L.; Wéber, Z.; Tenk, A. (2015). Utilization of Geoheritage in Tourism Development. Social and Behavioral Sciences, 188(14). https://doi.org/10.1016/j.sbspro.2015.03.400.

Clement, J, (2020). Number of monthly active Facebook users worldwide as of 1st quarter 2020. Available at: https://www.statista.com/statistics/264810/number-of-monthly-active-facebook-users-worldwide/ (Acessed 15 March 2020)

Delaney, J.; MacFeely S. (2014). Extending supply side statistics for the tourism sector: A new approach based on Linked-Administrative data. In Journal of the Statistical and Social Inquiry Society of Ireland 43 (14)

de Vries, S.; Buijs, A. E.; Langers, F.; Farjon, H.; van Hinsberg, A.; Sijtsma, F. J. (2013). Measuring the attractiveness of Dutch landscapes: Identifying national hotspots of highly valued places using Google Maps. Applied Geography, 45. https://doi.org/10.1016/j.apgeog.2013.09.017

Dolan, R.; Seo, Y; Kemper, J. (2019). Complaining practices on social media in tourism: A value co-creation and co-destruction perspective. Tourism Management, 73. https://doi.org/10.1016/j.tourman.2019.01.017

Edwards, P. N., Jackson, S. J., Chalmers, M. K., Bowker, G. C., Borgman, C. L., Ribes, D., Burton, M., & Calvert, S. (2013) Knowledge Infrastructures: Intellectual Frameworks and Research Challenges. Available at: https://deepblue.lib.umich.edu/handle/2027.42/97552 (Accessed 5 March 2020)

European Commission (2011). Open data, an egine for innovation, growth and transparent governance. Available at: https://eur-lex.europa.eu/LexUriServ/LexUriServ.do?uri=COM:2011:0882:FIN:EN:PDF (Accessed 10 January 2020)

European Travel Commission (2017). ETC DASHBOARD. Available at: http://etc-dashboard.org/data-partners/ (Accessed: 25 January 10, 2020)

European Union (2017). Tourism in a nutshell. Available at: http://ec.europa.eu/eurostat/web/tourism (Accessed 15 January 2020)

Fuchs, M. (2011). K&K project: Engineering the knowledge destination. Available at: https://www.miun.se/siteassets/forskning/center-och-institut/etour/publikationer/kk-project-2pdf (Accessed, 5 Ferbruary 2020)

Fuchs, M., Höpkenb, W., Lexhagena, M. (2014). Big data analytics for knowledge generation in tourism destinations – A case from Sweden. Journal of Destination Marketing & Management 3 (4). https://doi.org/10.1016/j.jdmm.2014.08.002

Kesorn, K.; Juraphanthong, W.; Salaiwarakul, A. (2015). Personalized Attraction Recommendation System for Tourists Through Check-In Data. IEEE ACCESS 2017, 5. https://ieeexplore.ieee.org/document/8123926

Kršák, B.; Sidor, C.; Štrba, Ľ. (2017). Expanding Zemplín area's (Slovakia) potential of inclusion among geoparks from the perspective of open data. In Journal of Landscape Management 8 (1)

Ionescu, V. (2014) Are the tourism indicators able to quantify the regional disparities across the European Union? In Romanian Society of Statistics. Available at: https://www.researchgate.net/publication/308468493 (Acessed 15 March 2019)

Chang Y., Liao, M. Y. (2010). A Seasonal ARIMA Model of Tourism Forecasting: The Case of Taiwan. In Asian Pacific Journal of Tourism Research 15 (2). https://doi.org/10.1080/10941661003630001

Chorley, M. J.; Colombo, G. B.; Allen, S. M.; Whitaker, R. M. (2013). Visiting Patterns and Personality of Foursquare Users. 2013 IEEE 3rd International Conference on Cloud and Green Computing 2013. https://ieeexplore.ieee.org/document/6686042

Newsome, D.; Dowling, R. (2018). Geoheritage and Geotourism. Geoheritage - Assessment, Protection and Management. https://doi.org/10.1016/B978-0-12-809531-7.00017-4

Netmarkeshare (2020). Search Engine Market Share. Available at: https://www.netmarketshare.com/ (Acessed 30 March 2020)

Martin-Fuentes, E.; Mateu, C.; Fernandez, C. (2018) Does verifying uses influence rankings? Analyzing Booking. com and Tripadvisor. In Tourism Analysis 23 (1). https://doi.org/10.3727/108354218X15143857349459

Mihalič, T. (2013). Performance of Environmental Resources of a Tourist Destination. Journal of Travel Research 52 (5). doi:10.1177/0047287513478505

Personen, J., Lampi, M. (2016). Utilizing open data in tourism. In Enter 2016 Available at: https://www.researchgate.net/publication/298788688 (Accessed 15 March 2020)

Reynard, E. (2008). Scientific research of tourist promotion of geomorphological heritage. Geografia Fisica e Dinamica Quaternaria 31(2). https://serval.unil.ch/resource/serval:BIB_9448D137D568.P001/REF.pdf.

Ritchie, J. B. R; Ritchie, J. R. B. (2002). A framework for an industry supported destination marketing information system. In Tourism Management 23 (5). https://doi.org/10.1016/S0261-5177(02)00007-9

Ritchie, J. R., & Crouch, G. I. (2011). The competitive destination: a sustainable tourism perspective. Wallingford (UK): CABI Publishing.

Różycki, P.; Dryglas, D. (2017). Mining tourism, sacral and other forms of tourism practiced in antique mines - analysis of the results. Acta Montanistica Slovaca, 22 (1). https://actamont.tuke.sk/pdf/2017/n1/6rozycki.pdf

Rybár, P.: Banský turizmus (Mining tourism). Technical University of Košice, vol. 1, p. 90, ISBN: 978- 80-553-1362-7, 2013

Sabou, M., Onder, I., Brasoveanu, A., Scharl, A. (2016). Towards cross-domain data analytics in tourism: A linked data based approach. Information Technology & Tourism, 16, 71–101 (2016). https://doi.org/10.1007/s40558-015-0049-5

Sidor, C.; Kršák, B.; Štrba Ľ., Cehlár, M.; Khouri, S.; Stričík, M.; Dugas, J.; Gajdoš, J. Bolechová, B. (2019).Can Location-Based Social Media and Online Reservation Services Tell More about Local Accommodation Industries than Open Governmental Data?. Sustainability 11(21). https://doi.org/10.3390/su11215926

Silva, F.B.E.; Herrera, M.A.M.; Rosina, K.; Barranco, R.R.; Freire, S.; Schiavina, M. (2018). Analyzing spatiotemporal patterns of tourism in Europe at high-resolution with conventional and big data sources. In Tourism Managament 68. https://doi.org/10.1016/j.tourman.2018.02.020

Štátny geologický ústav Dionýza Štúra (2020). Mapy a dáta. In Register geofondu. Available at: https://www.geology.sk/sluzby-inspire (accessed 12 December, 2019).

Štrba, Ľ.; Kršák, B.; Sidor, C. (2018). Some Comments to Geosite Assessment, Visitors, and Geotourism Sustainability. Sustainability, 10(8). https://doi.org/10.3390/su10082589.

Štrba, Ľ.; Rybár, P. (2015). Revision of the "Assessment of attractiveness (value) of geotouristic objects". Acta Geoturistica, 6 (1).

Tisdell, C. A. (1991). Economics of Environmental Conservation: Economics for Environmental & Ecological Management(Ser. 1). Amsterdam: Elsevier Science Pub. Co.

UNESCO. 2006. Global geoparks network. UNESCO Division of Ecological and Earth Sciences Global Earth Observation Section Geoparks Secretariat. Available at http://unesdoc.unesco. org/images/0015/001500/150007e.pdf (accessed 12 December, 2019).

UNWTO (2008). The Tourism Satelite Account (TSA): Recommended Methodological Framework. Available at: https://unstats.un.org/unsd/publication/Seriesf/SeriesF_80rev1e.pdf (Accessed 10 January 2020)

Xiang, Z, Schwartz, Z., Gerds, J. H., Muzaffer, U. (2015). What can big data and text analytics experience tell us about hotel and satisfaction?. In International Journal of Hospitality Management 44. https://doi.org/10.1016/j.ijhm.2014.10.013

Acta Montanistica Slovaca
ISSN 1335-1788
actamont.tuke.sk

Small UAV Camera Gimbal Stabilization Using Digital Filters and Enhanced Control Algorithms for Aerial Survey and Monitoring

Miroslav LAŠŠÁK[1], Katarína DRAGANOVÁ*[2], Monika BLIŠŤANOVÁ[3], Gabriel KALAPOŠ[4] *and* ***Juraj MIKLOŠ[5]***

Authors' affiliations and addresses:
[1] Flight Management and Control, CoE, Honeywell International, Inc., Turanka 100, 627 00 Brno, Czech Republic
e-mail: miroslav.lassak@honeywell.com

[2, 3, 4] Technical University of Košice, Faculty of Aeronautics, Rampová 7, 041 21 Košice, Slovakia
e-mail : katarina.draganova@tuke.sk
e-mail : monika.blistanova@tuke.sk
e-mail : gabriel.kalapos.1@gmail.com

[5] MiklosTech Contracting Inc., 435 New Brighton Place SE, Calgary, T2Z4W5, Alberta Canada
e-mail : miklos.juraj.ml@gmail.com

***Correspondence:**
Katarína Draganová, Technical University of Košice, Faculty of Aeronautics, Rampová 7, 041 21 Košice, Slovakia
tel: +421 55 602 6153
e-mail: katarina.draganova@tuke.sk

Funding information:
Slovak Research and Development Agency
Grant Number APVV-18-0248 and APVV-17-0184
Cultural and Educational Grant Agency
Grant Number KEGA 052TUKE 4/2018, 058TUKE-4/2018
Research Agency
Grant Number 019/2019/1.1.3/OPVaI/DP, ITMS code 313011T557.

Acknowledgment:
This work was supported by the APVV-18-0248, APVV-17-0184, KEGA 052TUKE 4/2018, 058TUKE-4/2018 and the VA No. 019/2019/1.1.3/OPVaI/DP with the ITMS code 313011T557 projects.

How to cite this article:
Laššák, M., Draganová, K., Blišťanová, M., Kalapoš, G. and Mikloš, J. (2020). Small UAV Camera Gimbal Stabilization Using Digital Filters and Enhanced Control Algorithms for Aerial Survey and Monitoring. *Acta Montanistica Slovaca*, Volume 25 (1), 127-137

DOI:
https://doi.org/10.46544/AMS.v25i1.12

Abstract
Aerial photography, monitoring and survey using small Unmanned Aerial Vehicles (UAVs) is a modern, cheap, simple, helpful and still developing and improving area. For these purposes the ongoing research is focused mainly on the cameras and image processing methods and software. However, as it was confirmed in the article, a stabilized camera gimbal is also very necessary to obtain quality and bright pictures or video records and to allow the operator or the tracking computer to track the camera's line of sight to the point of an interest. Because the camera stabilization is a key factor influencing the quality of the pictures or videos and considering the application on the UAVs performing the flights in the low altitudes and often also in the mountain terrain, the wind conditions, turbulences, wind shears, which can vary in their magnitudes and directions significantly, the convenient stabilization of the camera gimbal can have a significant influence on the quality of the obtained results, which are very important for the creation of the precise 2D or 3D models. Furthermore, to increase the UAV payload, it is important to use lightweight solutions. Due to the onboard electronics of small UAVs, regarding the limited memory and computational performance, a small microcontroller including a convenient, simple, and still fast enough control algorithm needs to be designed and implemented. In order to stabilize a camera gimbal, it is needed to design a model of the actuators as well as the gearings, to propose an effective control algorithm and to implement the control algorithms into the on-board microcontrollers. This article deals with the modelling of the actuator, conventional commercial servomotor used for a camera gimbal stabilization and with the design and verification of the improved control algorithm based on the inverse characteristics of the actuator model. Due to the requirement of the high-quality images, where the fast stabilization is needed, a dynamic correction feedback was implemented. And as the gyroscopes are very sensitive to the UAVs vibrations, the vibrations of the camera gimbal were eliminated by the digital low pass filter. The theoretical background was experimentally verified by the geological survey of the stone pits in Sedlice, Vechec and Klatov in the Eastern Slovakia.

Keywords
unmanned aerial vehicle (UAV), camera gimbal, stabilization, monitoring, photogrammetry, mining areas.

Introduction

Unmanned aerial vehicles (UAVs) have been recently used in various applications. From the monitoring and survey applications in regard to the mining areas (Ren, et al., 2019) as for example, object monitoring, dump, surface subsidence, coal gangue heap, open pit, mining pit or industrial site monitoring can be mentioned. In the terrain surveying and 3D modelling the topographic changes are monitored, earthwork computations are perfomed, dynamic surveys of mine reserves are performed, or soil erosion is estimated. From the ecological and environment monitoring and land damage assessment applications the tasks involving analysis of crop yield decrease is very important, but also surface subsidence, accumulated water, or soil destruction can be monitored (Blistan, et al., 2016). In the case of geological or other disasters, UAVs can be used for pollution monitoring, gas monitoring, coal fire monitoring etc. UAVs also find their applications in the land reclamation and ecological restoration assessment; they can be used, for example, for the monitoring of the vegetation coverage changes, for surveying of the land use or vegetation classification (Ren, et al., 2019). Monitoring of the geological environment of mines is crucial to improving mine environment and reducing and mitigating damage caused by exploitation (Li, et al., 2015).

For all of the above mentioned applications, aerial photogrammetry, surveillance, and monitoring, including the geological survey, monitoring of Earth resources, of the mining areas, monitoring of the ecological purposes, followed many times with the creation of the 2D and 3D models, the utilization of a camera system is necessary (Blistan, et al., 2019), (Blistan and Kovanic, 2017) and (Lucieer, et al., 2014).

The accurate terrain data are not only the basis of the 3D modeling, but they are also important for the geological risk prediction, due to the fact that the mining exploitation also causes serious damage to the both land and the ecological environment (Ren, et al., 2019), (Xiang, et al., 2018), (Fernández-Lozano, et al., 2018). The framework of UAV applications in the mining activities is presented in the Fig. 1.

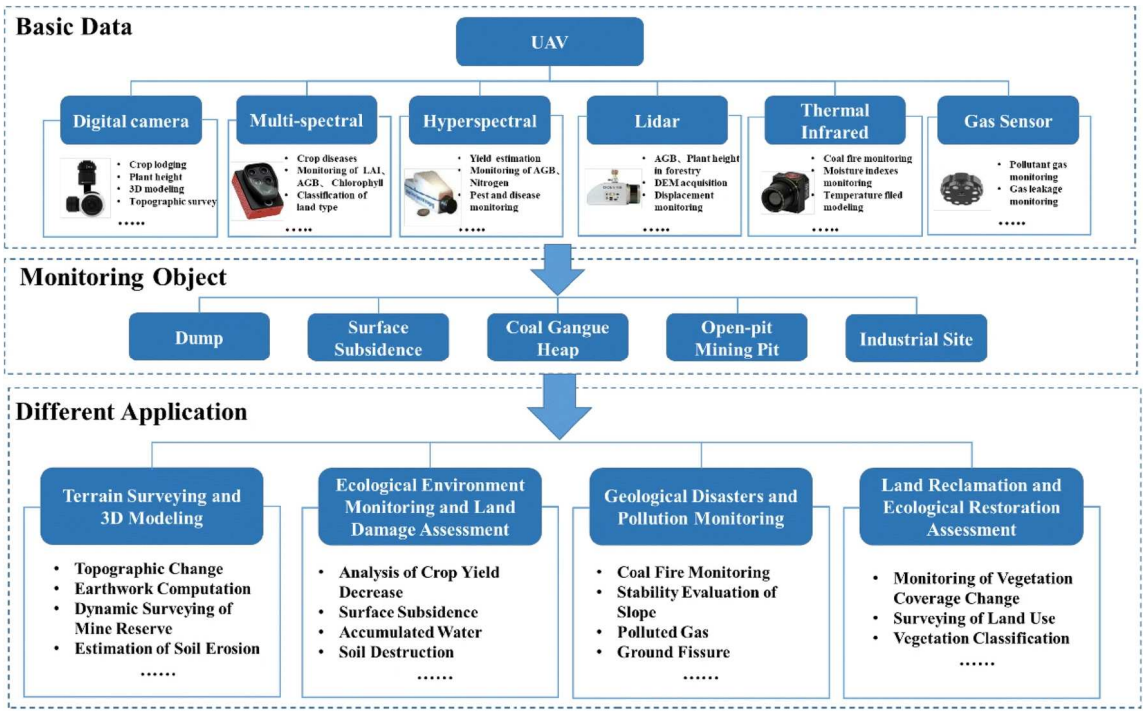

Fig.1. The framework of UAV applications in the mining activities (Ren, et al., 2019 - modified by authors)

The research in the above mentioned areas is mainly focused on the camera design and development and related image or video processing methods and software (Kršák, et al., 2016). The importance of the proper camera gimbal stabilization is often forgotten, although it can have a significant influence on the quality of the resulting camera image or video.

It has to be also mentioned that the category of the small UAVs has in comparison to the conventionally used airborne systems many particularities (Čižmár and Jalovecký, 2010), as for example operator demands (Lipovsky, et al., 2019), dimensions, weight, computational demands and last but not least price of the used systems, due to which a new interesting task has arisen: construction of a camera gimbal platform together with the stabilizing and tracking control algorithms fulfilling these requirements. Because without the convenient camera stabilization the UAV itself, the flight manouvers and meteorological conditions, particularly the wind

and turbulences in the mountain areas and during the flight performed in the low altitudes above ground level, the quality of the images or videos can be decreased significantly.

Recently multiple techniques for the camera gimbal stabilization have been developed. Some of them are based on the PID controllers and on the enhancement of their parameters applying, for example, a feedback loop and steering parameters calculated from quaternion transformation angular velocities received from gyroscopes (Zych, et al., 2015) or evolutionary algorithms such as PSO, GA (Rajesh and Kavitha, 2016) or on the gain scheduling approach with the gimbal model identified in the close loop manner by the PEM algorithm (Golmohammad, et al., 2007) to reduce disturbances and provide better performance and accuracy in the system response due to their effectiveness, simplicity and feasibility. As an alternative approach, the artificial neural networks can provide a more accurate model of the gimbal system based on their non-linear mapping to model the inertial characteristics gyro-stabilized multi-gimbal system (Layshot and Yu, X.-H., 2011). Other approach applicable for the micro and mini UAV category is based on the DC servo motor control and a novel robust control strategy employing the technique of uncertainty and disturbance estimator (UDE) (Kori, Ananda and Chandar, 2016). Other approach uses piezo motors (Karasikov, et al., 2016) instead of the more common servo motors characterized by the higher bandwidth, fast response and direct drive.

For the UAVs of mini and micro categories also gimbals in the role of mechanical video camera stabilizers represent unacceptable payload, thus approaches based on the video stabilization using the computer vision techniques, software image stabilization (Wiriyaprasat and Ruchanurucks, 2015), (Windau. and Itti, 2011), (Pieniązek, 2003) and video smoothing methodologies (Vazquez and Chang, 2009) have been developed.

Our approach of the camera gimbal stabilization uses a commercial servomotor and the improved control algorithm based on the inverse characteristics of the actuator model with the dynamic correction feedback applying the angular rate signals from the gyroscopes. And thanks to stabilization, better input data in the form of the photos or videos can be achieved, and more precise terrain models can be created.

Materials and Methods

Unmanned Aerial Vehicles

Nowadays, on the market, there are available many types of small UAVs. For the monitoring purposes, the mostly preferred are flying vehicles from the category of rotary wings, so-called “multirotors“. They differ mainly in the number of rotors (starting from three rotors –”tricopter”). The usage payload is slightly increasing with the number of rotors, the stability is also better when comparing ie. tricopter versus hexacopter with 6 rotors or octocopter comprising of 8 rotors. Flying time of octocopter OktoXL with installed 10 000 mAh batteries and an additional payload of 1000 grams reaches still more than 15 minutes, what is enough for monitoring of a small area. An advantage of modular construction of small UAVs is in the possibility of swapping batteries by a spare (fully charged) in several seconds what gives us the ability to continue in the flight mission / survey. In Fig.2 octocopter predefined for carrying of the camera with the raised landing gear is shown. In the Fig. 2 with the number 1 protective hood is marked, 2 is motor with a 12” propeller, 3 is a rigger, 4 is a landing gear, 5 is a battery holder and finally, as 6 a camera gimbal is labeled.

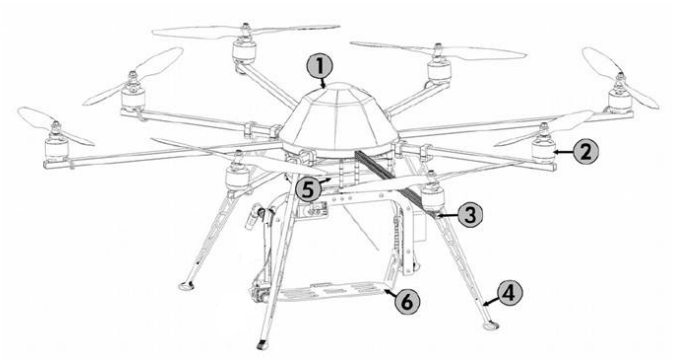

Fig. 2. Octocopter OktoXL (source: https://www.mobilexcopter.com/files/ARF-OktoXL-Manual_%28en%29.pdf)

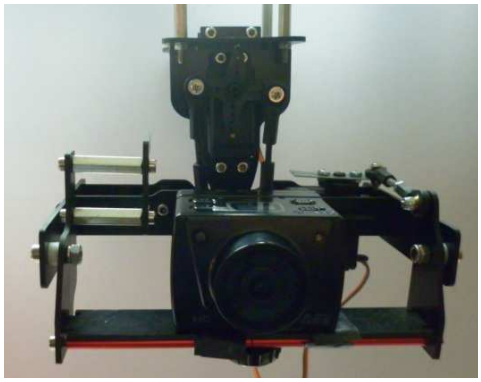

Fig.3. Camera gimbal with the GoPro camera

Camera Gimbal

Camera gimbals allow us to rotate the camera around each axis, so it is possible to track an object of interest and to have it still in the line of sight (Lozano, 2010). There are many types of camera gimbals used around the world. After the precise analyses of their parameters, cost, weight, and our requirements, the camera gimbal with two degrees of freedom was chosen (Fig. 3). In order to reach the highest precision in the positioning and

smooth movement, the servomotors with the high number of steps have been used (resulting in the angle resolution less than 0.1°).

Considering the multi rotor application, the gimbal will be used to compensate the roll and pitch angles. If the heading needs to be changed, a multi rotor vehicle can rotate around its *z* axis, meaning that the third gimbal axis is not necessary. As a camera, the high-quality GoPro camera MagiCam SD21 was chosen. This camera is predefined for such applications, as it can make excellent and sharp images even if small vibrations occur.

To give the ground station operator the ability to see online pictures from the flying UAV, the vehicle was equipped with the wireless video transmitter TS 351 (operating at the 5.8 GHz frequency), and in the ground station, the receiver RC 305 was used.

Onboard Sensorics

To determine the UAV position and the camera gimbal position in the real time, the camera gimbal platform was equipped with the IMU 9 DOF stick (inertial measurement unit with 9 degrees of freedom), the 66 channels GPS receiver Locosys LS20031 and the barometric pressure sensor BMP 102, the data of which were processed by the mbed microcontroller. The used inertial measurement unit includes a 3 axes accelerometer (providing linear acceleration data), a 3 axes gyroscope (providing angular rate data) and a 3 axes magnetomer (needed for the heading computation). All data were onboard stored to a micro SD card. To obtain a better position determination and positioning precision and to eliminate the noise and errors of the used sensors, the complementary filter was used for the INS and GPS data fusion.

Servomotor Simulation Model

As a servo motor, we used the high-quality Power HD 1209TH servomotor (with the titanium gearings) that allows us to rotate the camera gimbal in the range from –30° to +30°. It's dimensions are 40.3 mm x 20.2 mm x 37.2 mm, its weight is just 57 grams, and the maximum angular rate is up to the 750°/s. As it is well known, a servomotor is a complex and nonlinear electromechanical system. We didn't study servomotor's internal construction and gearing, but we modeled it as a "black box" only according to the servomotor's transition characteristics measured using a special workstation. The servomotor was installed on a workstation connected to the external rotational angle sensor (rotational potentiometer), which output data were sampled using the mbed NXP LPC1768 microcontroller at the 10 kHz rate. As soon as the primary measured data were analyzed, the transport delay of 20 ms was determined. At this moment, we were aware of the difficulties that we will face during the control algorithm design process (the instability when the regulator is fast, long regulation time). After additional precise analyses were completed, the simulation model was designed and also simplified using the Mason's gain formula. The simplified simulation model of the Power HD 1209TH Servomotor in the Matlab Simulink is shown in the Fig. 4.

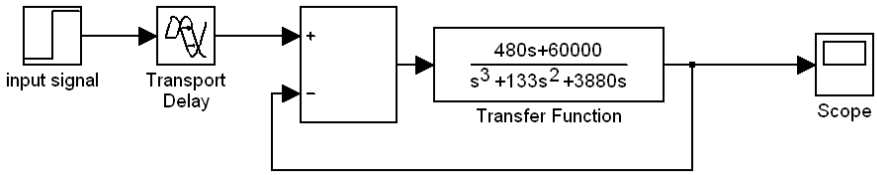

Fig. 4. Simplified simulation scheme of the POWER HD 1209 TH servomotor

The obtained simulation results were compared with the real measured data from the servomotor, and the correctness of the proposed model was confirmed. As it is clear from the Fig. 5, where the results from the step responses are displayed, the simulation model is precise enough.

For the quantitative evaluation of the proposed model, the following statistical values were calculated: maximum absolute average error (MAAE), mean absolute average error (MAE), mean absolute percentage error (MAPE) and quadratic integral error (QIE):

MAAE = 2.916°

MAE = 1.284°

MAPE = 0.0469 %

QIE = $9.1406.10^{-4}$

After the successful servomotor simulation model design, the complex model of the whole gimbal was developed, considering the camera gimbal's gearing in the roll and pitch axis, too.

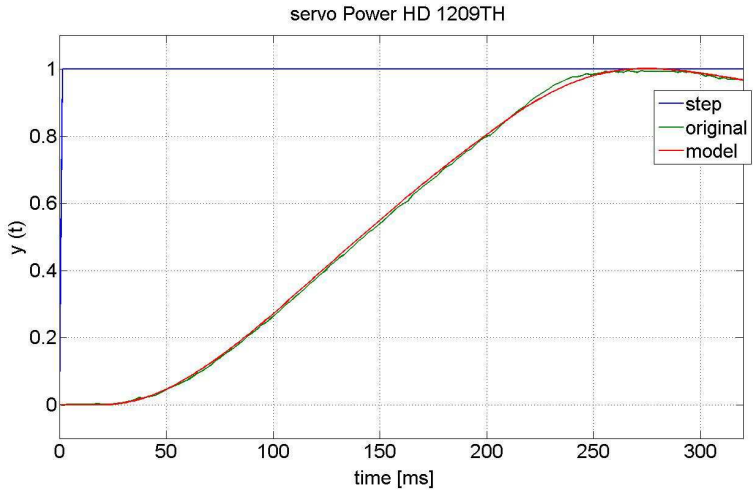

Fig. 5. Verification of the proposed POWER HD 1209 TH simulation model.

Results and Discussion

As it was mentioned earlier, used servomotors have the transport delay that makes the control algorithm design quite difficult. There are many robust control algorithms primary designed for the systems with the transport delay, but usually, they are slow and have high computational demands. Considering the onboard microcontroller that will be used for the camera gimbal stabilization, our goal was to use as simple algorithm as possible, obviously with the satisfactory results. Firstly we decided for an open-loop control algorithm based on an inverse function of the mathematical model. For the transport delay elimination, the corrective element was used. Based on the theory (Bakshi and Bakshi, 2009), the dynamic parameters of the controlled object can be modified via a closed-loop corrective element. The main principle of the corrective element is to add a closed loop, which needs to guarantee the stability and quality, and to add an additional signal, initially not used in the control algorithm, that improves the controlling process (Madarász, et al., 2009). In our application, the dynamic correction was performed; the angular rate signals from gyroscopes were added to the actuating signal u_r computed by the inverse model controller (IMC) as it is illustrated in the Fig. 6.

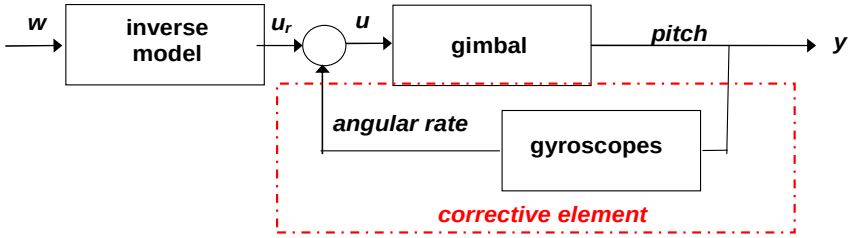

Fig. 6. Block scheme of the inverse model control loop with the dynamic correction.

From the control algorithms theory, for the stability purposes, only the middle frequency asymptote is important (it has to have the "–1" slope) (Bakshi and Bakshi, 2009). The gyroscopes, as the angular rate sensors, can be considered as a source of a high-frequency signal – as they sense fast changes in the direction. For the reduction of the possible high frequency (disturbing) noise (noise dynamics is considerably higher than the servomotors dynamics), the low pass filter was applied for the gyroscopes' data. The low pass filter transfer function is:

$$F(s) = \frac{1}{T_1 s + 1} \tag{1}$$

where T_1 is the filter time constant.

As the control algorithm was implemented in the mbed microcontroller, the necessity of the digital filtering algorithms creation and implementation in the microcontroller arose. Due to the high demands on the dynamics and the lowest possible delay, the IIR (Infinite Impulse Response) filter was chosen (Vaispacher, Andoga, Bréda, Adamčík, 2015).

IIR Filter

The low pass filter, needed for the angular rate data filtering, with the window size of 2 samples, was designed based on (Steven, 1997). The advantage of the IIR filters in comparison with the FIR (Finite Impulse Response) filters lies in the better filtering ability and the lower time delay. The main disadvantage of IIR filters is the possibility to be unstable.

IIR filter design approach: Consider the data that has to be filtered as an input signal for the filter, in our application, the angular rate, x_{IIR}. The output data from the filter are marked as y_{IIR}. In the discrete-time domain, the input data is one column vector (with the length of L), with samples numbered as 1, 2, 3, ... L. Simple, the IIR filter principle is based on the iterative algorithm. The output signal is computed from the actual input data $x(n)$, previous input data ($x(n–1)$, $x(n–2)$, ...), and also the previous output data ($y(n–1)$, $y(n–2$), ...).

In general, the formula for such IIR filter is known as a recursive equation:

$$y_{IIR}(k) = a_0 x_{IIR}(k) + a_1 x_{IIR}(k-1) + a_2 x_{IIR}(k-2) + \\ +a_3 x_{IIR}(k-3) + \cdots + b_1 y_{IIR}(k-1) + b_2 y_{IIR}(k-2) + b_3 y_{IIR}(k-3) + \cdots \quad (2)$$

where y_{IIR} is the output filter data, x_{IIR} are input filter data (raw data), k represents the number of samples, $a_0 \ldots a_3$ are coefficients, which the input filter data are multiplied by and $b_1 \ldots b_3$ are coefficients, which the output filter data are multiplied by.

The design of the used low pass IIR filter can be explained on a simple example, where one output sample and two input samples will be used. For a sample frequency f_s and a cut-off frequency f_c the following relationship can be written:

$$z = e^{-2\Pi fc / fs} \quad (3)$$

where the criterion f_c/f_s falls into the interval (0, 0.5).

For the low pass filter, the coefficients can be computed as:

$$a_0 = 1 - z; b_1 = z \quad (4)$$

In our application, the sampling frequency f_s = 100 Hz was used. Based on the experiments and analyses of the gimbal dynamics, the cut-off frequency was set to f_c = 1/6 rad.s^{-1} ~ 1 Hz. When the input signal is at the frequency of f = 20 Hz (f/f_s = 0.2), the attenuation of –9 dB occurs.

The filtering ability verification of the designed IIR filter applied to the real measured angular rate data can be seen in the Fig. 7.

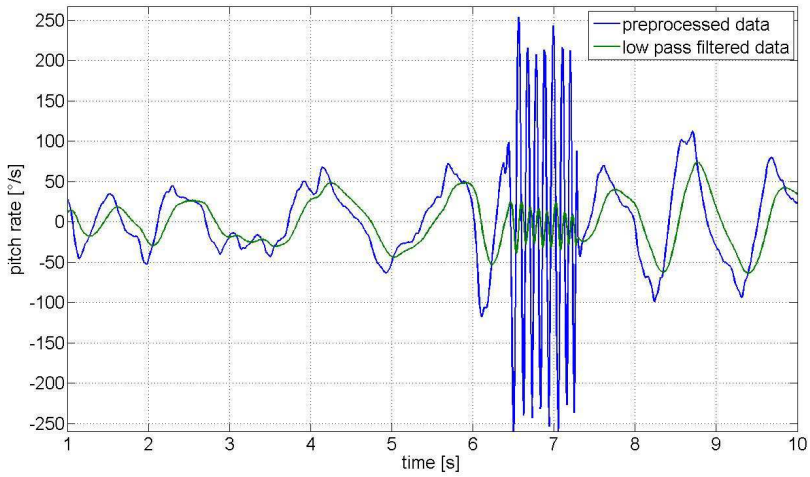

Fig. 7. IIR low pass filter verification (angular rate data as the input)

As it can be seen from the Fig. 7, the IIR filter filters out the high frequency „noise“, vibrations that occurred at the time between 6–7 seconds. When the multi-rotor realized a smooth movement, the IIR filter passed the input data without any attenuation (Vaispacher, Bréda, Madarász, 2015).

Inverse Model Controller

Based on the aforementioned analyses, the inverse model controller with the dynamic correction was designed and simulated with the gimbal simulation model in the control loop (see Fig. 8).

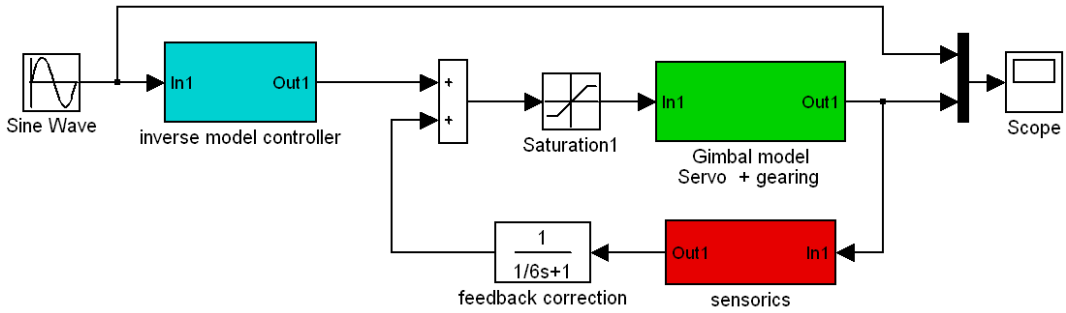

Fig. 8. The simulation scheme of the inverse model controller with the dynamic correction

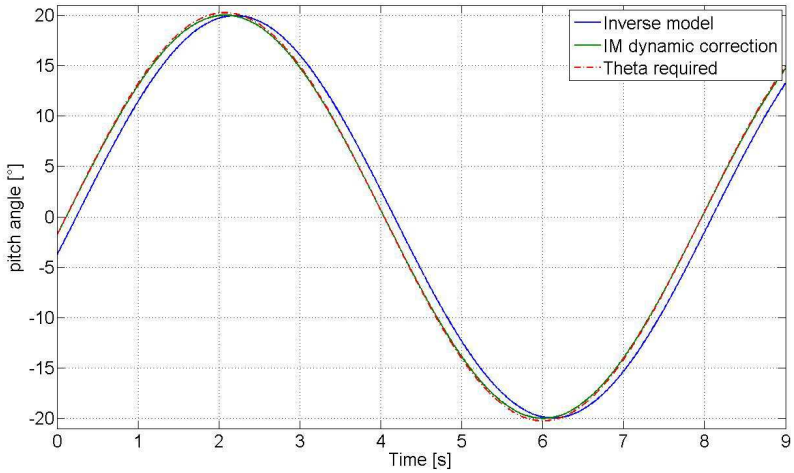

Fig. 9. The inverse model controller simulation verification

Running plenty of simulations of the designed camera gimbal control algorithms with a variety of input signals, the maximum time delay between the command and measured gimbal output of 13 ms (without the dynamic correction), and only 1 ms with the dynamic correction was determined. Running the simulation with the steps input signal, the maximum steady-state error of 0.04° in the pitch and 0.06° in the roll angle was determined.

The correct inverse model controller behaviour was confirmed by the Fig. 9. A significant improvement in the performance of the inverse model controller with the dynamic feedback correction against the conventional inverse model controller, especially in the regulation time, can be seen from the the Fig. 9. During the inverse model controller simulation, the sinusoidal signal as the input signal (simulating continuously changing pitch angle with the amplitude of 20°) was used. For the regulator verification, only the sine wave signal is presented, as the sine wave signals represent the possible movement of the UAV during manoeuver, climbing, descending, rotation around z-axes, or movement due to the wind. However, better results in the regulation time, due to angular rate signals used by the control law, were reached for all input signals (step, ramp, etc.).

Tab. 1. Statistical errors for the controller verification

	IMC without the dynamic correction	*IMC with the dynamic correction*
MAAE [°]	*2.0497*	*0.2523*
MAE [°]	*1.3916*	*0.1510*
MAPE [%]	*0.6611*	*0.0180*
QIE [-]	*2.3200*	*0.0280*

From the Tab. 1 with overviewed statistical errors can be seen that in the case of the inverse model controller with the dynamic correction, the decrease in the achieved statistical errors, which means an increase in the quality of the control process, is obvious.

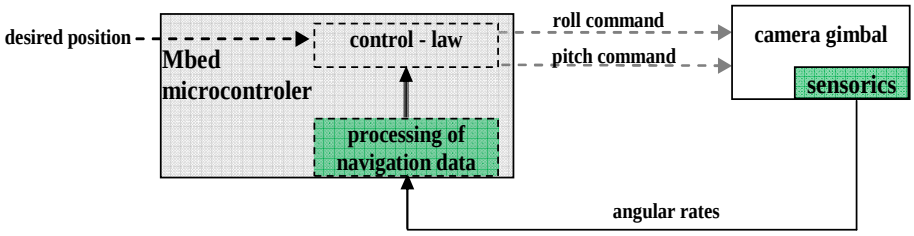

Fig. 10. Hardware implementation

As the proposed inverse model controller was successfully verified by the simulation, it was implemented into the onboard mbed microcontroller (Fig. 10.) and successfully tested on the real camera gimbal for the UAV with the satisfactory results.

Geological Monitoring and Photogrammetry

When flying with the small and lightweight UAVs, even a small gust of wind can significantly affect their flight, and the UAV has to compensate these disturbances continuously via changing the pitch and roll (or yaw angle) and position itself. To obtain high quality images and videos, the camera gimbal is compensating for the UAV movements (position angles) as well as tracking the object of an interest.

The proposed above-mentioned methodology was also tested experimentally. A geological survey was performed using the UAV - Mikrokopter Okto XL in cooperation with the Future Fly company that is an owner of the Aerial Work Operator Certificate No. SK/096, in the stone, pits Sedlice shown in the Fig. 11., Vechec (Fig. 12) and Klatov (Fig. 13) in the Eastern Slovakia. Based on the dimensions of the monitored area, photos were taken from the height of approximately 500 meters. The camera gimbal stabilization and precise positioning are extremely important as just small vibrations caused by the UAV's rotors, the noise of inertial sensors used for the stabilization, or noise of positioning servo motors have a significant influence on the image quality. Taken into account the 500 m height, vibrations in the camera line of sight with the amplitude of just 0.1 degrees will result in the error of ±0.9 meters and accordingly blurred photos.

Image shown in the Fig. 13 was taken in the Klatov area from the height 150 m above ground level, and subsequently, they were processed into the 3D model using the Agisoft PhotoScan software, as can be seen in the Fig. 14. In this area, the first set of testing pictures were taken without the enhanced stabilization of the camera gimbal (Fig. 15 and Fig. 16), and these pictures were then compared to the images taken with the active camera gimbal stabilization (Fig. 17 and Fig. 18). As can be clearly seen from the pictures, the proposed and tested stabilization of the camera gimbal lead to the higher sharpness of the image and minimal noise.

Fig. 11. Aerial survey of the open pit mine Sedlice.

Fig. 12. Aerial survey of the open pit mine Vechec.

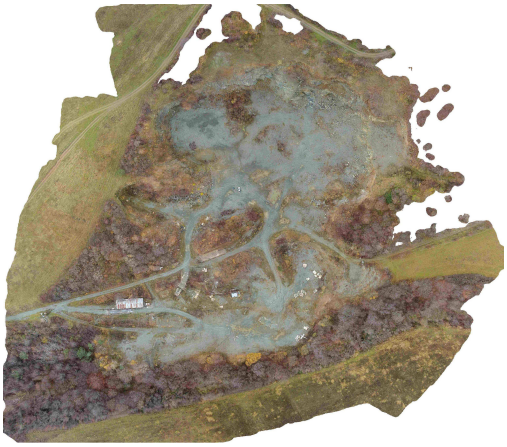

Fig. 13. Aerial survey of the open pit mine Klatov.

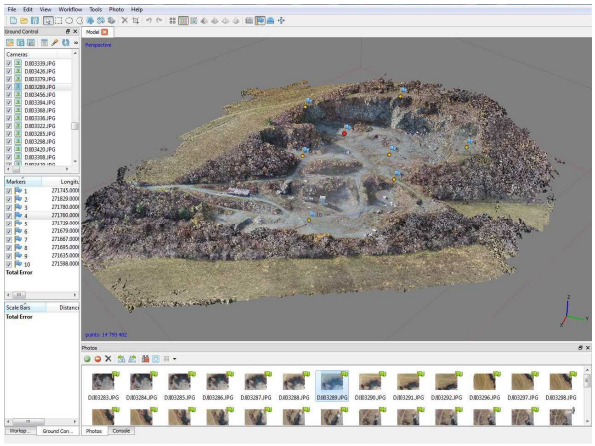

Fig. 14. Image processing using the PhotoScan software.

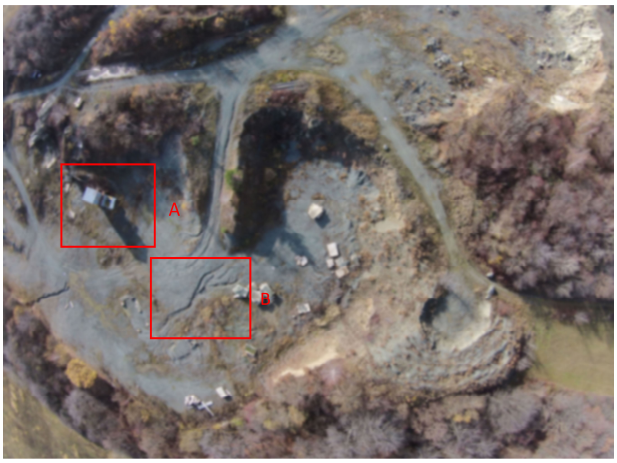

Fig. 15. Photos taken without the enhanced camera gimbal stabilization (A – building, B – grooved terrain).

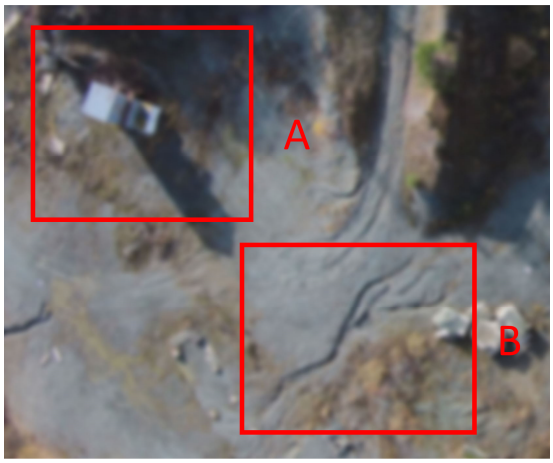

Fig. 16. Detail of the objects of interest without the enhanced camera gimbal (A – building, B – grooved terrain).

Fig. 17. Photos taken with the enhanced camera gimbal stabilization (A – building, B – grooved terrain).

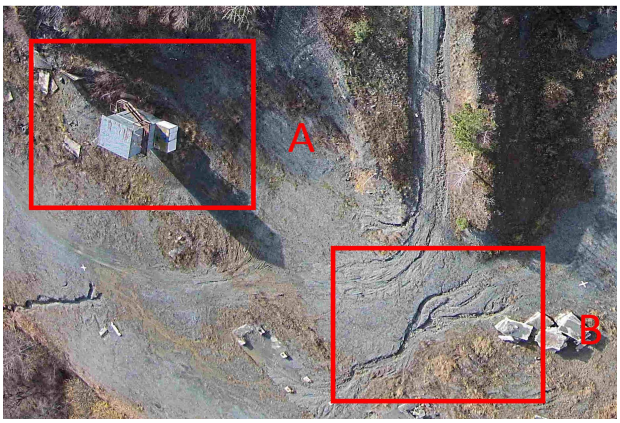

Fig. 18. Detail of the objects of interest without the enhanced camera gimbal (A – building, B – grooved terrain).

In addition to the obviously seen functionality of the proposed camera gimbal stabilization from the photos shown in Fig. 15 – Fig. 18., the correctness of the theoretical principles together with their implementation and practical realization on the UAV was also proved by the fact that the resulting error of the image resolution per pixel was reduced in compliance with the theoretical assumptions almost ten times.

Conclusion

Aerial survey and monitoring using small Unmanned Aerial Vehicles (UAVs) are modern, cheap and still rapidly developing and improving the area, which can be used for a wide band of various applications, such for example aerial photography, photogrammetry, surveillance, and monitoring, including geological survey, monitoring of Earth resources, of the mining areas, monitoring of the ecological purposes, natural disasters, etc., for which utilization of a camera system is required. For these purposes, a stabilized camera gimbal is necessary to obtain quality and bright pictures and to allow the operator or the tracking computer to track the camera's line of sight to the point of interest. Considering these applications, a very challenging task is to design a properly stabilized camera gimbal, which can compensate the vibrations caused by the UAV construction and operation itself, which is able to whitstand also the performed maneuvers and also which is resistant to the wind conditions, that can cause significant problems with the stabilization, especially considering the UAV utilization in the low altitudes and in the mountain terrain. In order to stabilize the camera gimbal, it is needed to design a model of the actuators as well as the gearings, to propose an effective control algorithm and to implement the control algorithms into the onboard microcontrollers. As the payload of the used vehicle is important, the small and lightweight single cheap microcontrollers have to be used. Due to the limited memory and computational power of the small microcontroller, a convenient, simple, and still fast enough control algorithm needs to be designed and implemented. This article deals with the modeling of the actuator, conventional commercial servomotor, used for the camera gimbal stabilization, and with the design and verification of the improved control algorithm based on the inverse characteristics of the actuator model. As for the high-quality images, the fast stabilization is needed, dynamic correction feedback based on the angular rates signals from the gyroscopes to the computed command was added. Considering the fact that gyroscopes measure fast rotational movements, they are very sensitive to the UAVs rotor vibrations, are noisy, and so the elimination of the undesirable vibrations of the camera gimbal applying the digital low pass filter for the angular rates signal is needed. As the microcontroller is working in the discrete-time domain, a discrete digital filter was designed.

UAVs nowadays are inexpensive and have wide applicability also in the mining applications. The correctness of the proper inertial sensors data fusion, data filtering, and fast camera gimbal stabilization was therefore proven experimentally in the geological survey of the stone pits, using the UAV of the octocopter configuration, where bright pictures were obtained. As UAVs are able to scan the terrain rapidly and cheaply, also other experimental flights were performed in the stone pit area. In this case, the images obtained from the UAV during the test flight without the enhanced camera gimbal stabilization were compared to the photos taken with the proposed camera gimbal stabilization. The results of the further image processing confirmed the theory and approximately ten times better results were achieved.

The further research will be focused mainly on the optimization of the control algorithm also in connection to the fast-developing onboard sensors that can be used for the camera gimbal stabilization, which will significantly improve the quality of the images, which is determining for the further postprocessing in software used in the photogrammetry, for the texture information in the topography and mainly for the creation of the 3D terrain models in the areas, where the changes and variations are monitored and evaluated.

References

Bakshi, U.A, Bakshi, V.U. (2009). Automatic Control Systems. Technical Publications.

Blistan, P.; Kovanič, Ľ.; Zelizňaková, V.; Palková, J. (2016) Using UAV photogrammetry to document rock outcrops. *Acta Montanistica Slovaca, 21 (2).*

Blistan, P., Kovanic, L. (2017). Verification of usability of low-cost UAV photogrammetry in comparison with close-range photogrammetry in the context of documentation of Earth's surface. *Geographic Information Systems Conference and Exhibition* (GIS ODYSSEY 2017).

Blistan, P, Kovanic, L., Patera, M., Hurcik, T. (2019). Evaluation quality parameters of DEM generated with low-cost UAV photogrammetry and Structure-from-Motion (SfM) approach for topographic surveying of small areas. *Acta Montanistica Slovaca*, 24 (3).

Čižmár, J., Jalovecký, R. (2010). Design of an Inertial Reference Unit with the mixed gravitational and magnetic correction of gyroscopic drift. *Transport Means* - Proceedings of the International Conference (2010).

Fernández-Lozano, J., González-Díez, A., Gutiérrez-Alonso, G., Carrasco, R.M., Pedraza, J., García-Talegón, J., Alonso-Gavilán, G., Remondo, J., Bonachea, J., Morellón, M. (2018). New Perspectives for UAV-Based Modelling the Roman Gold Mining Infrastructure in NW Spain. *Minerals* , 8 (11).

Golmohammad, H., Homaei, A., Saadat, S. (2007). Design and implimentation of an adaptive PI controller for a two axis gimbal system. *IFAC Proceedings Volumes (IFAC-PapersOnline)*, 17, Part 1.

Karasikov, N., Peled, G., Yasinov, R., Yetkariov, R. (2016). Piezo-based miniature high resolution stabilized gimbal. *Proceedings of SPIE - The International Society for Optical Engineering 9828*. DOI: 10.1117/12.2225623.

Kori, A.S., Ananda, C.M., Chandar, T.S. (2016). Robust control of single axis gimbal platform for micro air vehicles based on uncertainty and disturbance estimation. *Proceedings of 2016 7th International Conference on Mechanical and Aerospace Engineering*. DOI: 10.1109/ICMAE.2016.7549588.

Kršák, B., Blišťan, P., Pauliková, A., Puškárová, P., Kovanič, Ľ., Palková, J., Zelizňaková, V (2016). Use of low-cost UAV photogrammetry to analyze the accuracy of a digital elevation model in a case study. *Measurement*, 91.

Layshot, N., Yu, X.-H. (2011). Modeling of a gyro-stabilized helicopter camera system using artificial neural networks. *2011 IEEE International Conference on Information and Automation, ICIA*. DOI: 10.1109/ICINFA.2011.5949035.

Li, Y., Zhao, H. and Fan, J., (2015). Application of remote sensing technology in mine environment monitoring. *MATEC Web of Conferences 22*, DOI: 10.1051/matecconf/20152204008

Lipovsky, P., Szoke, Z., Moucha, V., Jurc, R., Novotnak, J. (2019). Data acquisition system for uav autopilot and operator evaluation. MOSATT 2019 - Modern Safety Technologies in Transportation International Scientific Conference, Proceedings. DOI: 10.1109/MOSATT48908.2019.8944105

Lozano, R. (2010). Unmanned aerial vehicles : Embedded control. Wiley.

Lucieer, A., Jong, S.M.D., Turner, D. (2014). Mapping landslide displacements using Structure from Motion (SfM) and image correlation of multi-temporal UAV photography. *Progress in Physical Geography*, 38 (1).

Madarász, L., Andoga, R., Főző, L., Lazar, T. (2009) Situational control, modeling and diagnostics of large scale systems. *Studies in Computational Intelligence*, 243. DOI: 10.1007/978-3-642-03737-5_11.

Pieniązek, J. (2003). Software-based camera stabilisation on unmanned aircraft. *Aircraft Engineering and Aerospace Technology*, 75 (6). DOI: 10.1108/00022660310503048.

Rajesh, R.J., Kavitha, P. (2016). Camera gimbal stabilization using conventional PID controller and evolutionary algorithms. *IEEE International Conference on Computer Communication and Control*, IC4 2015. DOI: 10.1109/IC4.2015.7375580.

Ren, H., Zhao, Y., Xiao, W., Hu, Z. (2019). A review of UAV monitoring in mining areas: current status and future perspectives. *International Journal of Coal Science & Technology*, 6. DOI :10.1007/s40789-019-00264-5.

Steven, W. S. (1997). The Scientist and Engineer's Guide to Digital Signal Processing Recursive Filters. 2nd edition. California Technical Publishing.

Vaispacher, T., Andoga, R., Bréda, R., Adamčík, F. (2015). Application of linearized Kalman filter in integration of navigation systems. *CINTI 2015 - 16th IEEE International Symposium on Computational Intelligence and Informatics, Proceedings*. DOI: 10.1109/CINTI.2015.7382898.

Vaispacher, T., Bréda, R., Madarász, L. (2015). Integration architectures of navigation systems for unmanned vehicles. *SAMI 2015 - IEEE 13th International Symposium on Applied Machine Intelligence and Informatics, Proceedings*. DOI: 10.1109/SAMI.2015.7061854.

Vazquez, M., Chang, C. (2009). Real-time video smoothing for small RC helicopters. *Conference Proceedings - IEEE International Conference on Systems, Man and Cybernetics*. DOI: 10.1109/ICSMC.2009.5346659.

Windau, J., Itti, L. (2011). Multilayer real-time video image stabilization. *IEEE International Conference on Intelligent Robots and Systems*.DOI: 10.1109/IROS.2011.6048344.

Wiriyaprasat, K., Ruchanurucks, M. (2015). Realtime VDO stabilizer for small UAVs using a modified homography method. *Proceedings 2015 International Conference on Science and Technology, TICST*. DOI: 10.1109/TICST.2015.7369337.

Zych, C., Wrońska-Zych, A., Dudczyk, J., Kawalec, A. (2015). A correction in feedback loop applied to two-axis gimbal stabilization. *Bulletin of the Polish Academy of Sciences: Technical Sciences*, 63 (1). DOI: 10.1515/bpasts-2015-0025.

Xiang, J., Chen, JP., Sofia, G., Tian, Y., Tarolli, P. (2018). Open-pit mine geomorphic changes analysis using multi-temporal UAV survey. *Environmental Earth Sciences*, 77 (6).